NASA TECHNICAL MEMORANDUM

NASA TM X-3372

NASA TM X-3372

EFFECT OF KRÜGER NOSE FLAPS ON THE EXPERIMENTAL FORCE AND MOMENT CHARACTERISTICS OF AN OBLIQUE WING

Edward J. Hopkins and George H. Lovette

Ames Research Center
Moffett Field, Calif. 94035

NATIONAL AERONAUTICS AND SPACE ADMINISTRATION • WASHINGTON, D. C. • JULY 1976

1. Report No.	2. Government Accession No.	3. Recipient's Catalog No.
NASA TM X-3372		

4. Title and Subtitle	5. Report Date
EFFECT OF KRÜGER NOSE FLAPS ON THE EXPERIMENTAL FORCE AND MOMENT CHARACTERISTICS OF AN OBLIQUE WING	July 1976
	6. Performing Organization Code

7. Author(s)	8. Performing Organization Report No.
Edward J. Hopkins and George H. Lovette*	A-6362
	10. Work Unit No.
9. Performing Organization Name and Address	505-11-12
Ames Research Center Moffett Field, Calif. 94035	11. Contract or Grant No.
	13. Type of Report and Period Covered
12. Sponsoring Agency Name and Address	Technical Memorandum
National Aeronautics and Space Administration Washington, D.C. 20546	14. Sponsoring Agency Code

15. Supplementary Notes

*Project Engineer, ARO, Inc., Moffett Field, Calif. 94035

16. Abstract

Six-component experimental force and moment data are presented for an oblique wing mounted on a body of revolution and equipped with Krüger type nose flaps. The effectiveness of these flaps in making the moment curves more linear by controlling the flow separation on the downstream wing panel at high lift coefficients was determined. The investigation of the effects of the Krüger flaps covered two cases: (1) use of the flaps on the downstream wing panel only and (2) use of the flaps on both wing panels. For part of the tests, the Krüger flaps were mounted on nose flaps that were drooped either 5° or 10°. The wing was elliptical in planform, had an aspect ratio of 6.0 (based on the unswept span) and was tested at sweep angles of 0, 45°, and 50°. The Mach-number range covered was from 0.25 to 0.95.

It was found that the most effective arrangement of the Krüger flaps for making the pitching-, rolling-, and yawing-moment curves more linear at high lift coefficients was having the Krüger flaps mounted on the nose flaps drooped 5° and only on the downstream wing panel.

17. Key Words (Suggested by Author(s))	18. Distribution Statement
Wings, oblique Leading-edge flaps, Krüger Wings, flow separation	Unlimited Star Category – 08

19. Security Classif. (of this report)	20. Security Classif. (of this page)	21. No. of Pages	22. Price*
Unclassified	Unclassified	204	$7.25

For sale by the National Technical Information Service, Springfield, Virginia 22161

NOMENCLATURE

The axes systems and sign conventions are presented in figure 1. Lift and drag are presented about the wind axes; side force, pitching moments, rolling moments, and yawing moments are presented about the body axes.

b	wing span
C_D	drag coefficient, $\frac{\text{drag}}{qS}$
C_l	rolling-moment coefficient about the body axes, $\frac{\text{rolling moment}}{qSb}$
C_L	lift coefficient, $\frac{\text{lift}}{qS}$
C_m	pitching-moment coefficient (see fig. 2(a) for moment-center location), $\frac{\text{pitching moment}}{qS\bar{c}}$
C_n	yawing-moment coefficient about the body axes, $\frac{\text{yawing moment}}{qSb}$
C_Y	side-force coefficient about the body axes, $\frac{\text{side force}}{qS}$
c	wing chord
c_{aft}	portion of wing chord aft of the $0.25c$ line
c_{fwd}	portion of wing chord forward of the $0.25c$ line
c_{root}	wing root chord
$\bar{c}$	wing mean aerodynamic chord
H	vertical distance from wing reference plane to base line (see fig. 2(b))
M	Mach number
q	free-stream dynamic pressure
RN/L	unit Reynolds number per meter times 10^{-6}
r	body radius
S	wing area
$(t/c)_{max}$	maximum thickness-to-chord ratio
x	chordwise distance along airfoil

x_1 axial distance along body from the 57.45 cm longitudinal station

Y distance along wing span (see fig. 2(b))

z vertical distance above the wing chord plane

α angle of attack, deg

Λ sweep angle measured between a perpendicular to the body axis and the $0.25c$ line of the wing in a horizontal plane (the right wing tip is forward for positive Λ's), deg

EFFECT OF KRÜGER NOSE FLAPS ON THE EXPERIMENTAL FORCE AND MOMENT CHARACTERISTICS OF AN OBLIQUE WING

Edward J. Hopkins and George H. Lovette*

Ames Research Center

SUMMARY

Six-component experimental force and moment data are presented for an oblique wing mounted on a body of revolution and equipped with Krüger type nose flaps. The effectiveness of these flaps in making the moment curves more linear by controlling the flow separation on the downstream wing panel at high lift coefficients was determined. The investigation of the effects of the Krüger flaps covered two cases: (1) use of the flaps on the downstream wing panel only and (2) use of the flaps on both wing panels. For part of the tests, the Krüger flaps were mounted on nose flaps that were drooped either 5° or 10°. The wing was elliptical in planform, had an aspect ratio of 6.0 (based on the unswept span), and was tested at sweep angles of 0, 45°, and 50°. The Mach number range covered was from 0.25 to 0.95.

It was found that the most effective arrangement of the Krüger flaps for making the pitching-, rolling-, and yawing-moment curves more linear at high lift coefficients was to mount them on the nose flaps drooped 5° and only on the downstream wing panel.

INTRODUCTION

It has been shown experimentally in references 1 through 4 that a low aspect-ratio oblique wing-body combination (suitable as a highly maneuverable vehicle) has higher maximum lift-to-drag ratios at transonic Mach numbers than a conventional swept wing-body combination. At moderate to high lift coefficients, however, the trailing wing panel of a swept oblique wing incurs flow separation that leads to large changes in the rolling-, pitching-, and yawing-moment coefficients. In references 2 and 4, an attempt was made to create a more uniform spanwise wing stall at high lift coefficients by bending the wing panels upward, thereby producing washout on the trailing wing panel and washin on the leading wing panel. Results from that study indicated that the amount of upward bending required to linearize the moment curves would lead to an impractical wing pivot location to reduce the rolling moments to zero at small lift coefficients.

The present wind-tunnel investigation was undertaken, therefore, to explore the possibility of delaying the wing stall on the trailing wing panel by using Krüger nose flaps. With the wing swept either 45° or 50°, these flaps were successively tested on both wing panels, on the downstream wing panel, and on nose flaps drooped either 5° or 10° to determine the optimum arrangement.

---

*Project Engineer, ARO, Inc., Moffett Field, Calif. 94035

Consideration was given primarily to the resultant linearity of the moment curves at transonic Mach numbers. With the wing in the unswept position for low-speed flight (Mach numbers ≤ 0.6), the Krüger flaps were tested only on both wing panels.

CONFIGURATION CODE

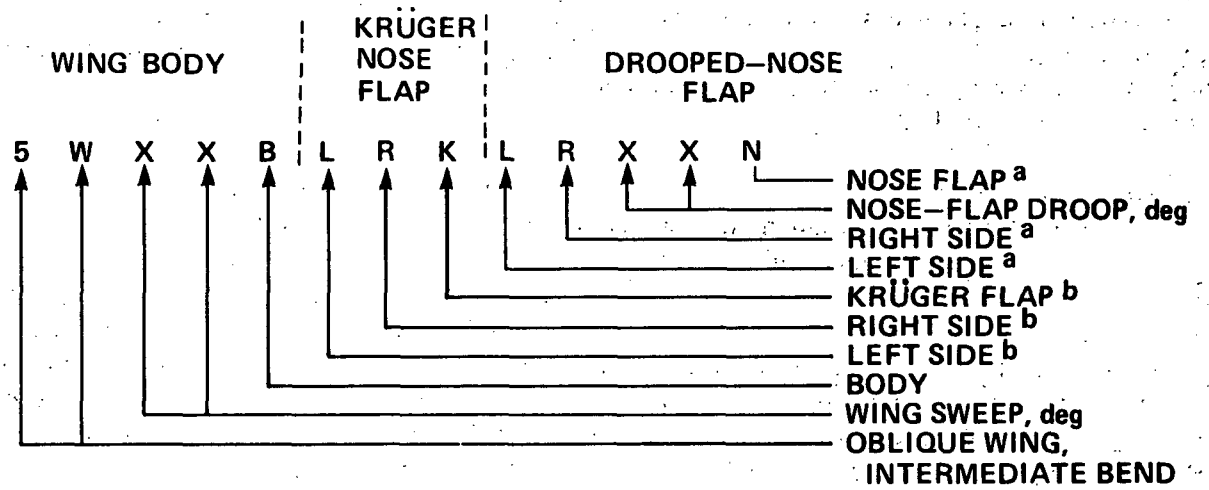

[a]WHEN SYMBOL IS DELETED, DROOPED-NOSE FLAP IS UNDEFLECTED

[b]WHEN SYMBOL IS DELETED, KRÜGER NOSE FLAP IS REMOVED

TEST FACILITY

The Ames 6- by 6-Foot Wind Tunnel is a variable pressure, continuous flow, closed return-type facility. The nozzle ahead of the test section consists of an asymmetric sliding block that permits a continuous variation of Mach number from 0.25 to 2.3. The test section has a perforated floor and ceiling for boundary-layer removal to permit transonic testing.

MODEL DESCRIPTION

The model consisted of an oblique wing mounted on top of a Sears-Haack body of revolution designed to have minimum wave drag for a given length and volume. By installing different fairing blocks under the wing, as indicated in figure 2(a), the wing could be swept 0, 45°, and 50°. (Details of the body and of the fairing blocks are given in table 3 of reference 1.) Note in figure 2(a) that the wing pivot point and the moment center are located at 0.40 c_{root} ($\Lambda = 0$). The wing planform consisted of two semi-ellipses having the same major axis but different minor axes in the ratio of 3:1 so that the major axis is the quarter chord line. Geometric twist was accomplished by bending the wing panels upward so that the chord lines perpendicular to the quarter chord line remain in

horizontal planes. This type of bending results in wing twist when the oblique wing is swept; that is, washout on the downstream panel and washin on the upstream panel. Equations for the bend line of the wing with the so-called "intermediate bend" of the present investigation and the wing planform are shown in figure 2(b). Additional geometric wing and body details are presented in table 1.

A subcritical Garabedian profile (designed for a lift coefficient of 1.3 for a maximum $t/c = 0.1016$ at a Mach number of 0.6) was used perpendicular to the quarter chord line. This profile, shown in figure 2(c), varied in maximum thickness from $0.11c$ at the wing root to $0.06c$ at the wing tip according to the elliptical equation given in figure 2(b). Coordinates for the Garabedian profile are given in table 2.

The model was equipped with leading-edge Krüger flaps which have a span 62.6 percent of that of the wing. These flaps were segmented as shown in figure 2(d). For part of the test, when the wing was swept, these flaps were used only on the downstream wing panel. The flaps had a constant nose diameter along the wing span of 0.4572 cm, resulting in a variation of the ratio of nose diameter to Krüger flap chord of 25 to 80 percent. A constant percent camber of 9.2 percent of the Krüger flap chord was built into the upper surface of these flaps by a radius fairing. The chords of the Krüger flaps were nominally 10 percent of the wing chords, but varied slightly from this value because of the leading-edge curvature of the wing (each Krüger flap segment has a straight leading edge). Only one Krüger flap deflection was tested, that of 135° relative to the chord line of the wing nose; however, for part of the test, nose flaps upon which the Krüger flaps were mounted were drooped either 5° or 10°. The nose flaps were pivoted about an axis located on the lower surface of the wing at about 15 percent of the wing chord behind the leading edge. All gaps around the drooped-nose and Krüger flaps were sealed.

DATA REDUCTION AND TEST PROCEDURE

The model was sting-supported through the base of the model on a six-component electrical strain-gage balance as shown in figure 3. Measured drag forces were corrected to a condition corresponding to that of having the free-stream static pressure on the base of the fuselage. Moment data are presented about a moment center located on the body axis at $0.4\,c_{root}$ ($\Lambda = 0$) (see fig. 2(a)). Reference lengths and the wing area used in the reduction of the data are given in table 1.

Boundary-layer transition strips (0.1905 cm wide) consisting of a random distribution of 0.01905-cm glass spheres were placed on the upper and lower surface of the wing, on the upper surface of the Krüger flap (0.762 cm downstream of the leading edge), and on the body 2.54 cm behind its tip. Sublimation studies made on the plain wing at wing sweep angles of 0 and 45° indicate that the boundary layer was tripped by the 0.01905-cm spheres near the roughness strips at $\alpha = 0$ and 10° and at Mach numbers of 0.6 and 0.9.

The unit Reynolds number was held constant at 8.2×10^6/m except when the Mach number was 0.25; in the latter case the unit Reynolds number was reduced to 5.6×10^6/m because of the dynamic overload restrictions of the balance. The model was mounted on a sting that was bent 10° to increase the maximum angle of attack; the resulting range was from −3° to 28°. With the wing

swept 45° and 50°, data were obtained at Mach numbers of 0.25, 0.4, 0.6, 0.8, 0.9, and 0.95. With the wing unswept, the Mach number range was reduced to a maximum Mach number of 0.8. Angle of attack was indicated by an electrical dangleometer mounted in the support located downstream of the sting. Corrections were applied to the indicated angle of attack for balance and sting deflections.

RESULTS AND DISCUSSION

Experimental results for the oblique wing equipped with Krüger flaps on both wing panels are presented in figures 4–9 for a wing sweep-angle of 45°, in figures 10–15 for a sweep angle of 50°, and in figures 16–19 for a sweep angle of 0. Results for the case in which Krüger flaps were used on both wings and with a nose-flap droop of 5° are shown in figures 20–25 for a sweep angle of 45° and in figures 26–29 for a sweep angle of 0. For the case in which Krüger flaps were used on the downstream wing panel only and with a nose-flap droop of 5°, the results are shown in figures 30–35; the results for a nose-flap droop angle of 10° are shown in figures 36–41. In each of the above figures, comparisons are shown between the results for the plain wing and the wing equipped with Krüger flaps at Mach numbers between 0.6 and 0.95 inclusive. For Mach numbers of 0.25 and 0.40, such comparisons were made only for the unswept case without nose-flap droop (figs. 16 and 17), and for the unswept case with 5° of nose-flap droop (figs. 26 and 27), because data for the plain wing for the other configurations were not obtained.

Krüger Flaps on Both Wing Panels

With the oblique wing swept either 45° or 50°, the linearity of the pitching-, rolling-, and yawing-moment curves at high lift and high Mach numbers was improved only slightly by adding the Krüger flaps to both wing panels (see figs. 6–9 and 12–15). A nose-flap droop of 5° in conjunction with the Krüger flaps on both wing panels slightly improved the linearity of the pitching-moment curve, but had little effect on the rolling- or yawing-moment curves (compare figs. 9 and 25). With the oblique wing unswept at a Mach number of 0.4, the Krüger flaps on both wing panels provided increments in maximum lift coefficient of about 0.2 to 0.3 with nose-flap droop angles of 0 and 5°, respectively (see figs. 17(a) and 27(a)).

Krüger Flaps on the Downstream Wing Panel

At high Mach numbers with the Krüger flap mounted on the nose flap with a droop of 5° and only on the downstream wing panel, the linearity of the yawing-moment curves was improved considerably and the linearity of the pitching- and rolling-moment curves was somewhat improved over the curves for the wing with Krüger flaps on both wing panels (compare figs. 35 and 25). Increasing the nose-flap droop to 10° produced moment curves which were less linear than for a droop of 5° (compare figs. 41 and 35).

Further improvements in linearizing the moment curves could probably be realized by increasing the Krüger flap span on the downstream wing panel up to the wing-body intersection when the wing is swept.

In reference 4 it was shown that increasing the upward spanwise bend of the oblique wing from small to intermediate (the same bend as used for the present investigation) had a very small effect on making the moment curves more linear at high lift coefficients. Therefore, little or no bend would probably be used for the final design of an oblique-wing and the aerodynamic moments caused by bending would be negligible or eliminated.

CONCLUDING REMARKS

It was shown that Krüger flaps mounted on the nose flaps drooped 5° on the downstream panel of an oblique wing swept 45° or 50° was the most effective arrangement for making the pitching-, rolling-, and yawing-moment curves more linear. It appears that a full-span Krüger flap on the downstream wing panel of a highly swept oblique wing might be even more effective in linearizing the moment curves.

Ames Research Center
National Aeronautics and Space Administration
Moffett Field, Calif. 94035, January 20, 1976

REFERENCES

1. Hopkins, Edward J.; Meriwether, Frank D.; and Pena, Douglas F.: Experimental Aerodynamic Characteristics of Low Aspect Ratio Swept and Oblique Wings at Mach Numbers Between 0.6 and 1.4. NASA TM X-62,317, Nov. 1973.

2. Hopkins, Edward J.; and Levin, Alan D.: An Experimental and Theoretical Study of Low-Aspect Ratio Swept and Oblique Wings at Mach Numbers Between 0.6 and 1.4. AIAA Preprint 74-771, AIAA Mechanics and Control of Flight Conference, Anaheim, Calif., Aug. 6–9, 1974.

3. Hopkins, Edward J.; and Nelson, Edgar R.: Effect of Wing Bend on the Experimental Force and Moment Characteristics of an Oblique Wing. NASA TM X-3343, 1976.

4. Hopkins, Edward J.: Effects of Wing Bend on the Aerodynamic Characteristics of a Low Aspect Ratio Oblique Wing. AIAA Preprint 75-995, AIAA Aircraft Systems and Technology Meeting, Los Angeles, Calif., Aug. 4–7, 1975.

TABLE 1.– MODEL GEOMETRY

Body	
Radius	$r = 3.856[1 - (1 - 2x_1/114.94)^2]^{3/4}$ cm
Length	
Closed	114.94 cm
Cutoff	91.44 cm
Maximum diameter	7.71 cm
Wing	
Planform ellipticity about 0.25 c line	4.7:1
Span	90.51 cm
Span (reference)	71.12 cm
Area (reference)	1365.09 cm^2
Mean aerodynamic chord (reference), $\bar{c}$	20.88 cm
Root chord	19.20 cm
Aspect ratio ($\Lambda = 0$)	6.0
Aspect ratio ($\Lambda = 45°$)	3.2
Incidence relative to body centerline	0
Profile perpendicular to 0.25 c line	Garabedian, subcritical (see table 2)

TABLE 2.– COORDINATES FOR GARABEDIAN PROFILE

[$(t/c)_{max}$ = 0.1016, design lift coefficient = 1.3 at M = 0.6]

x/c	z/c	x/c	z/c
0	0	0	0
−.00045	.00079	.00048	−.00058
−.00073	.00146	.00104	−.00120
−.00086	.00191	.00165	−.00176
−.00097	.00244	.00257	−.00249
−.00103	.00290	.00343	−.00308
−.00106	.00345	.00467	−.00382
−.00104	.00403	.00592	−.00445
−.00098	.00463	.00674	−.00481
−.00077	.00572	.00774	−.00519
−.00052	.00653	.00943	−.00570
−.00021	.00732	.01149	−.00620
.00026	.00830	.01539	−.00694
.00073	.00909	.02583	−.00837
.00163	.01033	.03967	−.00970
.00276	.01161	.06022	−.01116
.00464	.01340	.09339	−.01288
.00709	.01538	.13965	−.01462
.01197	.01878	.19880	−.01601
.02179	.02443	.25034	−.01684
.03187	.02928	.31761	−.01738
.04250	.03373	.38597	−.01735
.06373	.04113	.45495	−.01657
.09353	.04969	.50010	−.01568
.13389	.05882	.54359	−.01456
.17545	.06597	.57465	−.01363
.22415	.07249	.61351	−.01232
.28227	.07822	.65330	−.01090
.34741	.08236	.68122	−.00988
.41444	.08434	.71655	−.00865
.48168	.08406	.74682	−.00771
.55738	.08094	.77611	−.00702
.62052	.07591	.82243	−.00642
.68276	.06852	.87054	−.00698
.72012	.06288	.89717	−.00810
.75413	.05684	.91595	−.00941
.82318	.04227	.94348	−.01235
.85663	.03370	.96854	−.01674
.89115	.02388	.98615	−.02126
.92448	.01327	.99596	−.02434
.95410	.00145	1.00000	−.02600
.97175	−.00538		
.99163	−.01450		
1.00000	−.01900		

Page Intentionally Left Blank

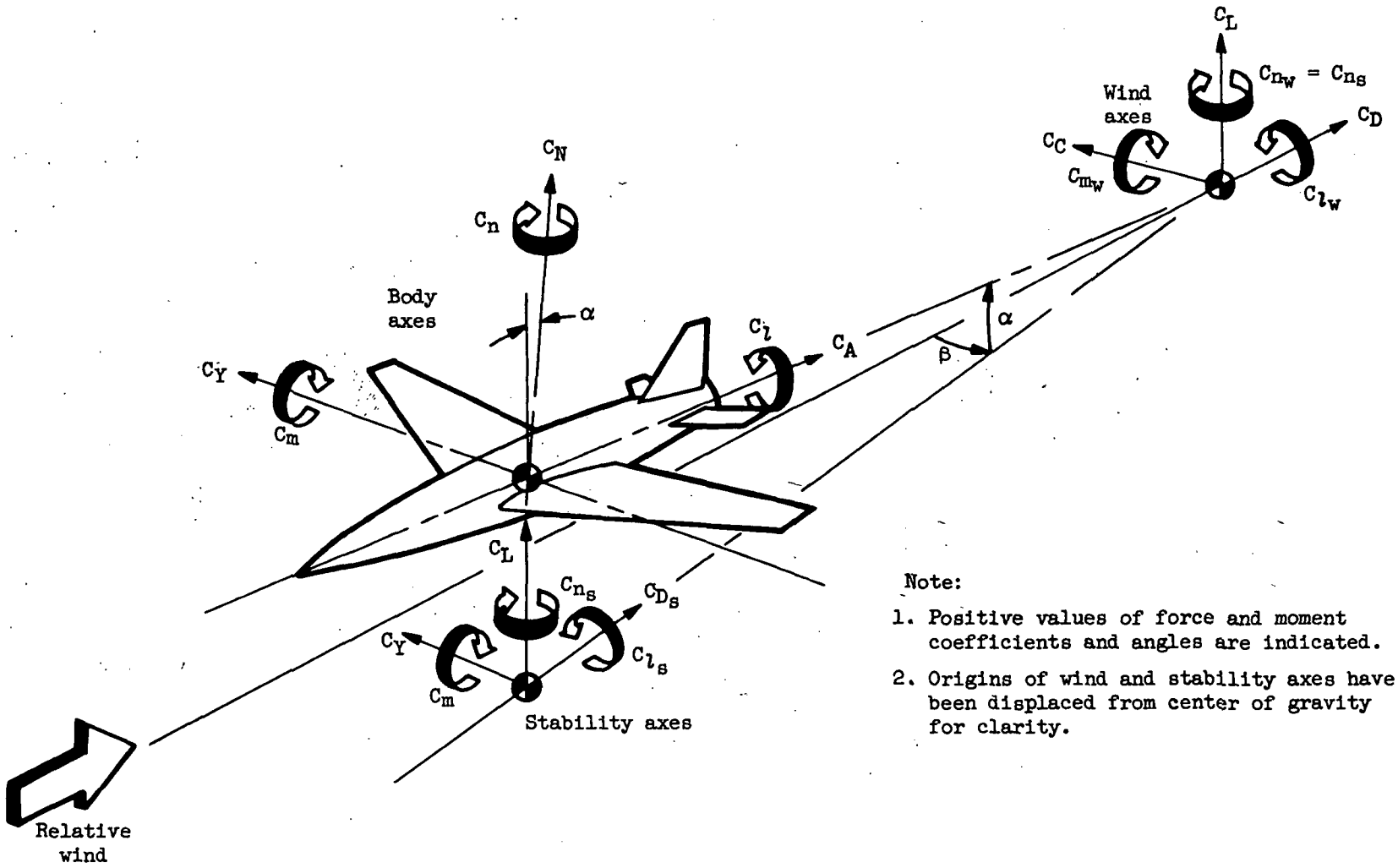

Figure 1.– Orientation of force and moment coefficients about body, wind, and stability axes.

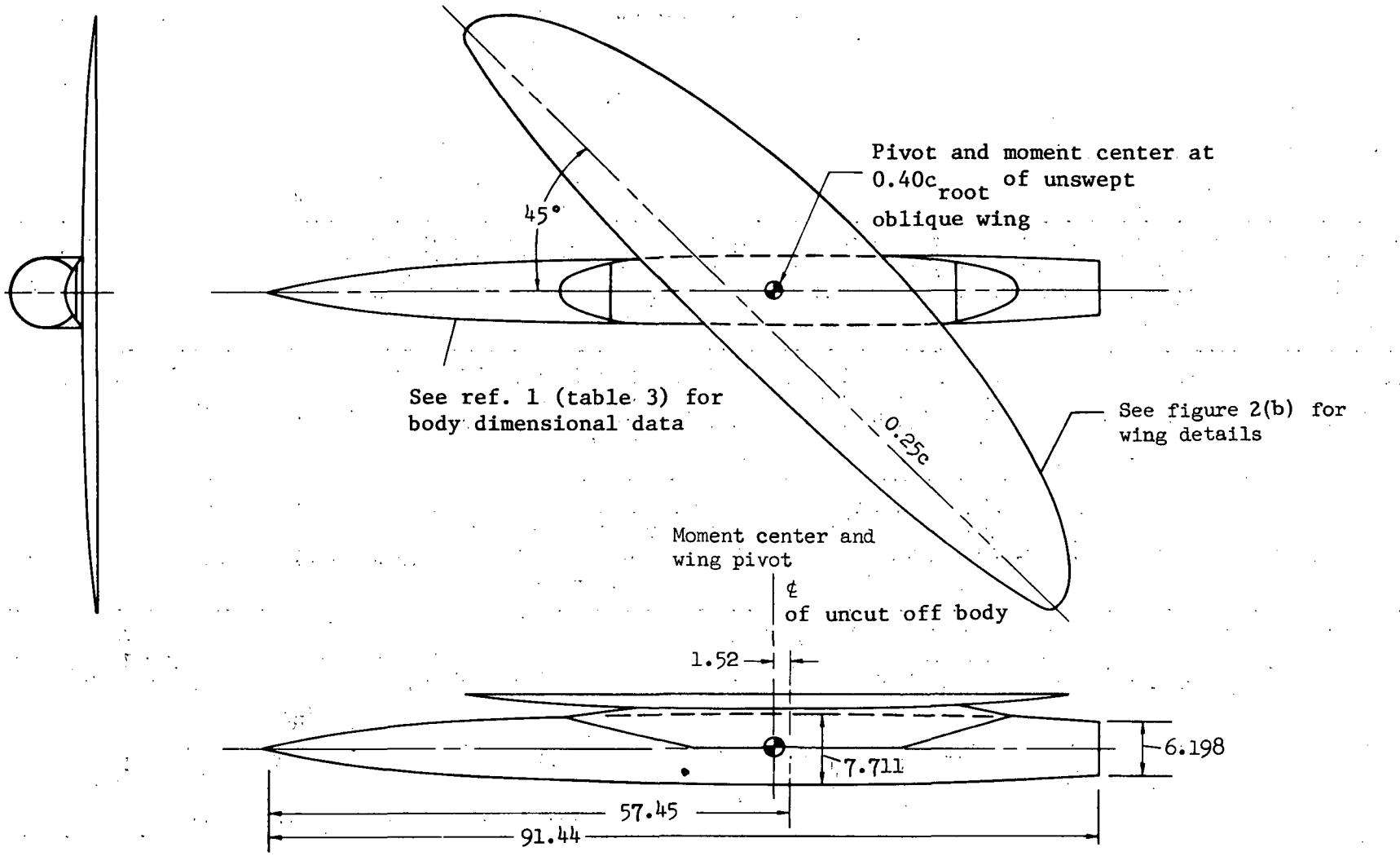

(a) Moment-center and wing pivot location.

Figure 2.– Oblique wing-body details.

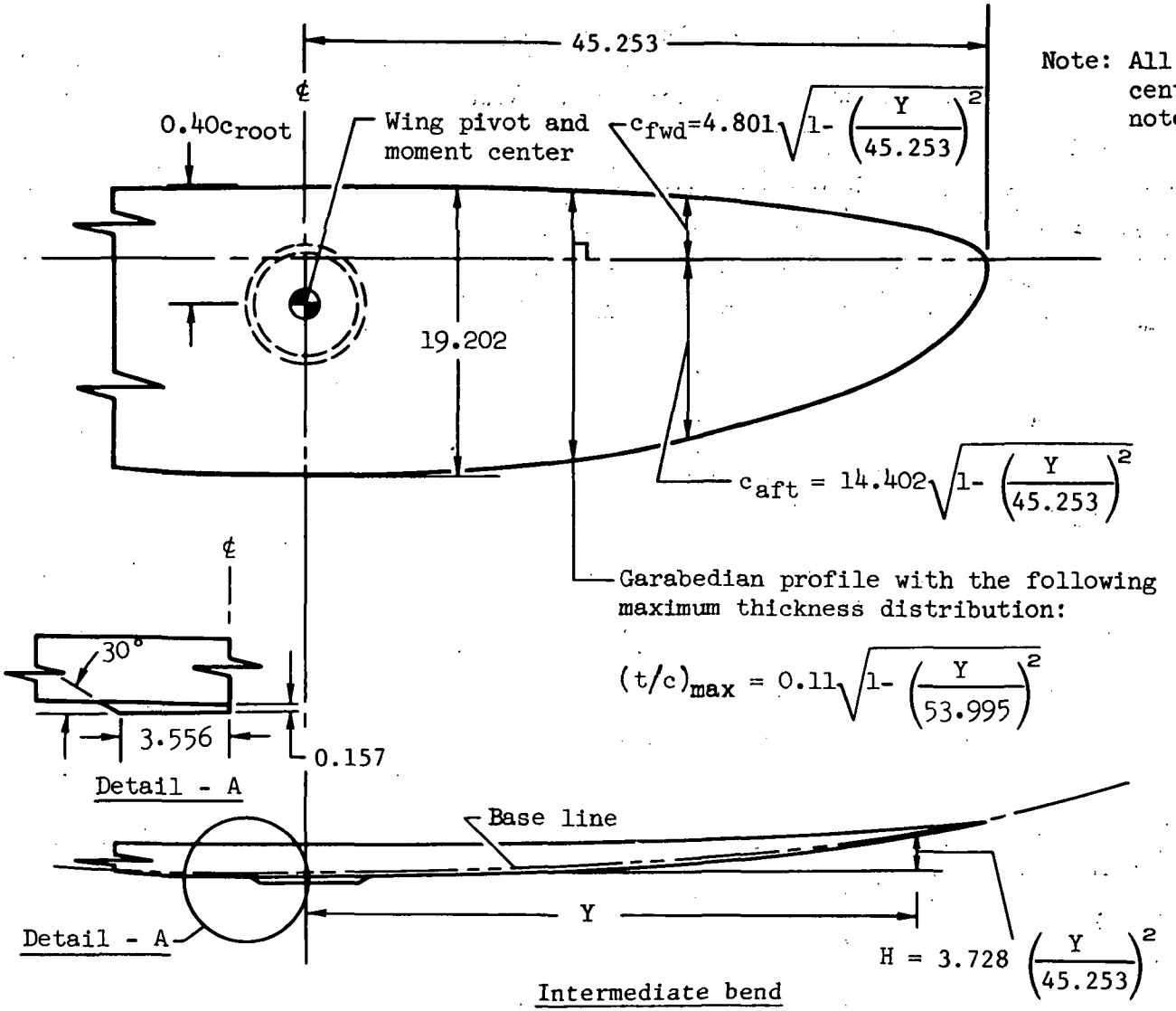

(b) Wing dimensional details.

Figure 2.– Continued.

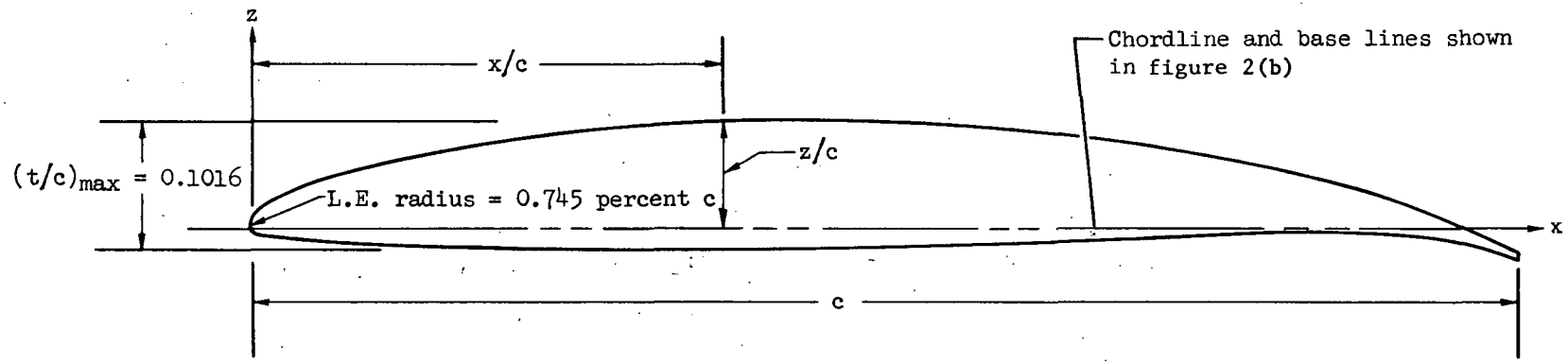

(c) Garabedian profiles (M_{Des} = 0.6 at $(C_L)_{Des}$ = 1.3).

Figure 2.– Continued.

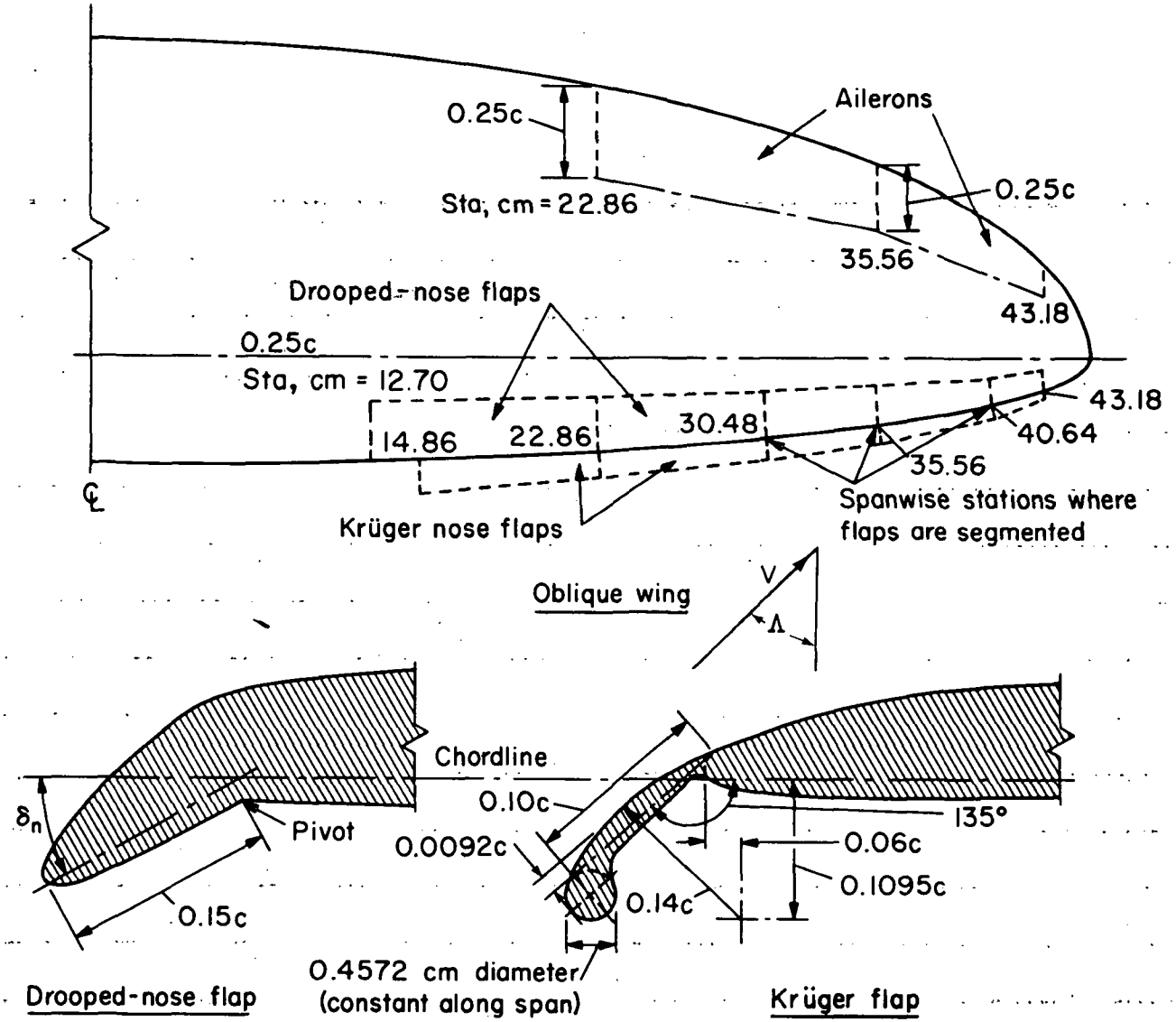

(d) Drooped-nose and Krüger flap details.

Figure 2.– Concluded.

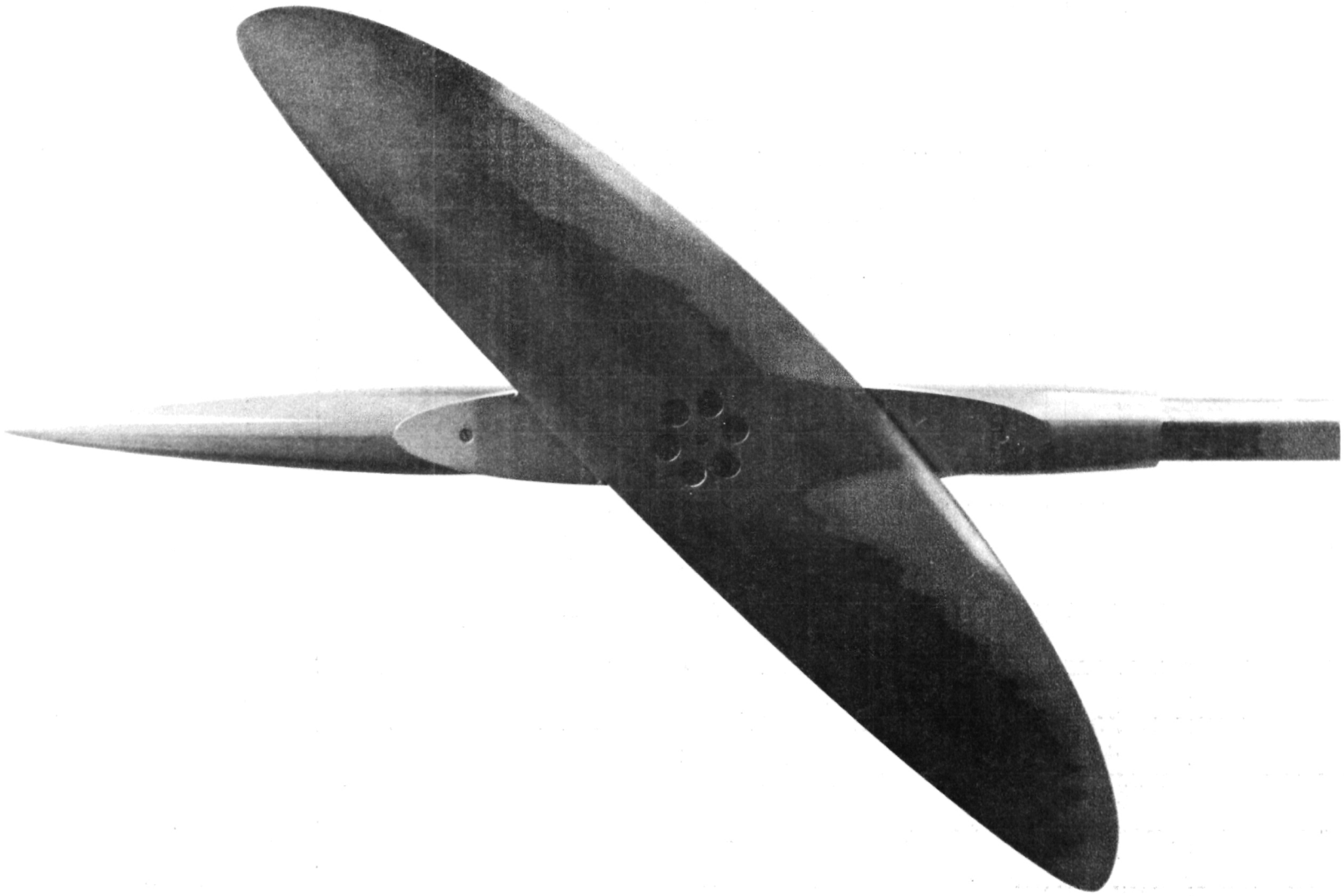

Figure 3.– Oblique wing-body combination ($\Lambda = 45°$).

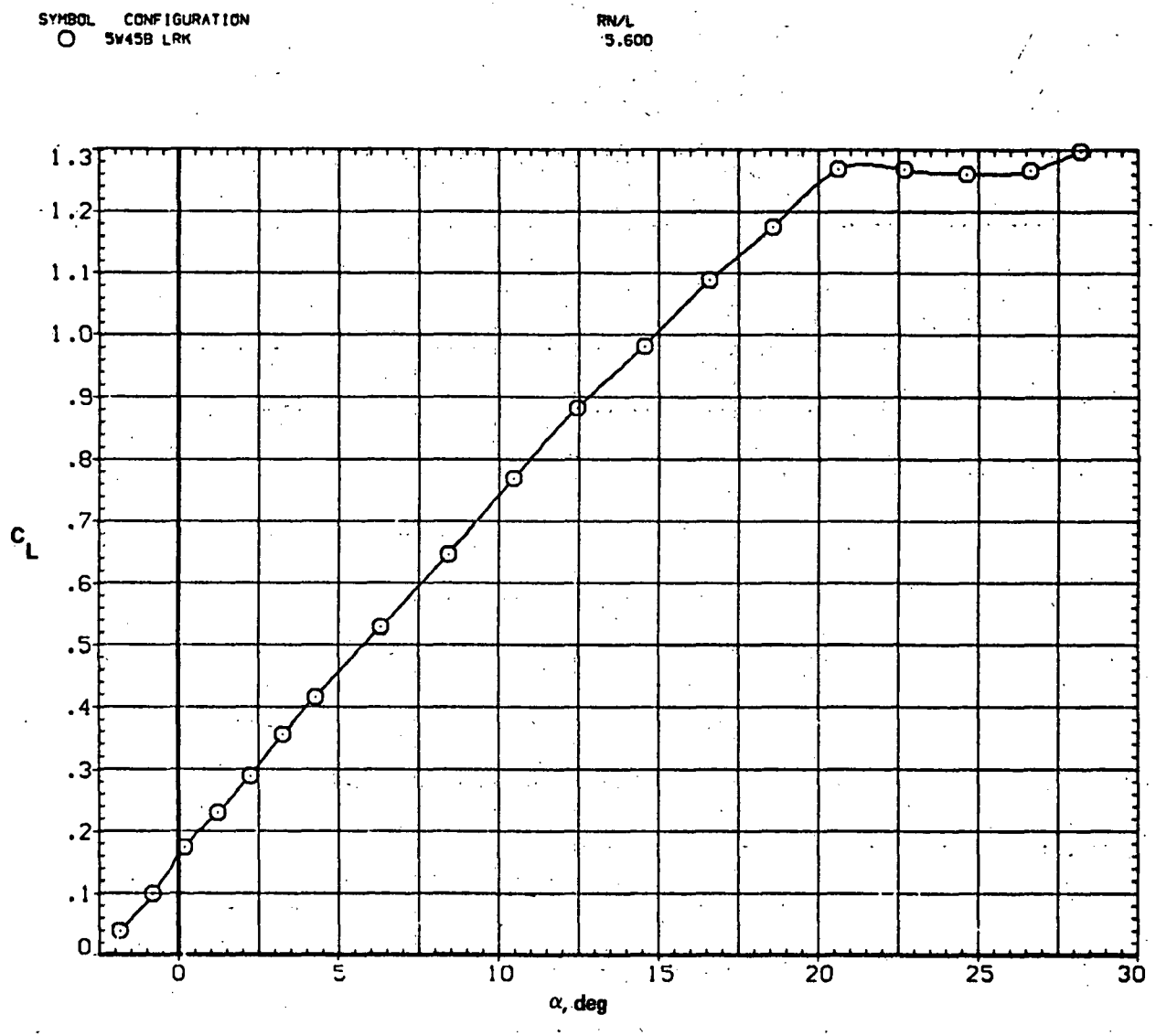

(a) C_L vs α

Figure 4.– Effect of having Krüger flaps on both wing panels on the static longitudinal characteristics of an oblique wing: $\Lambda = 45°, M = 0.25$.

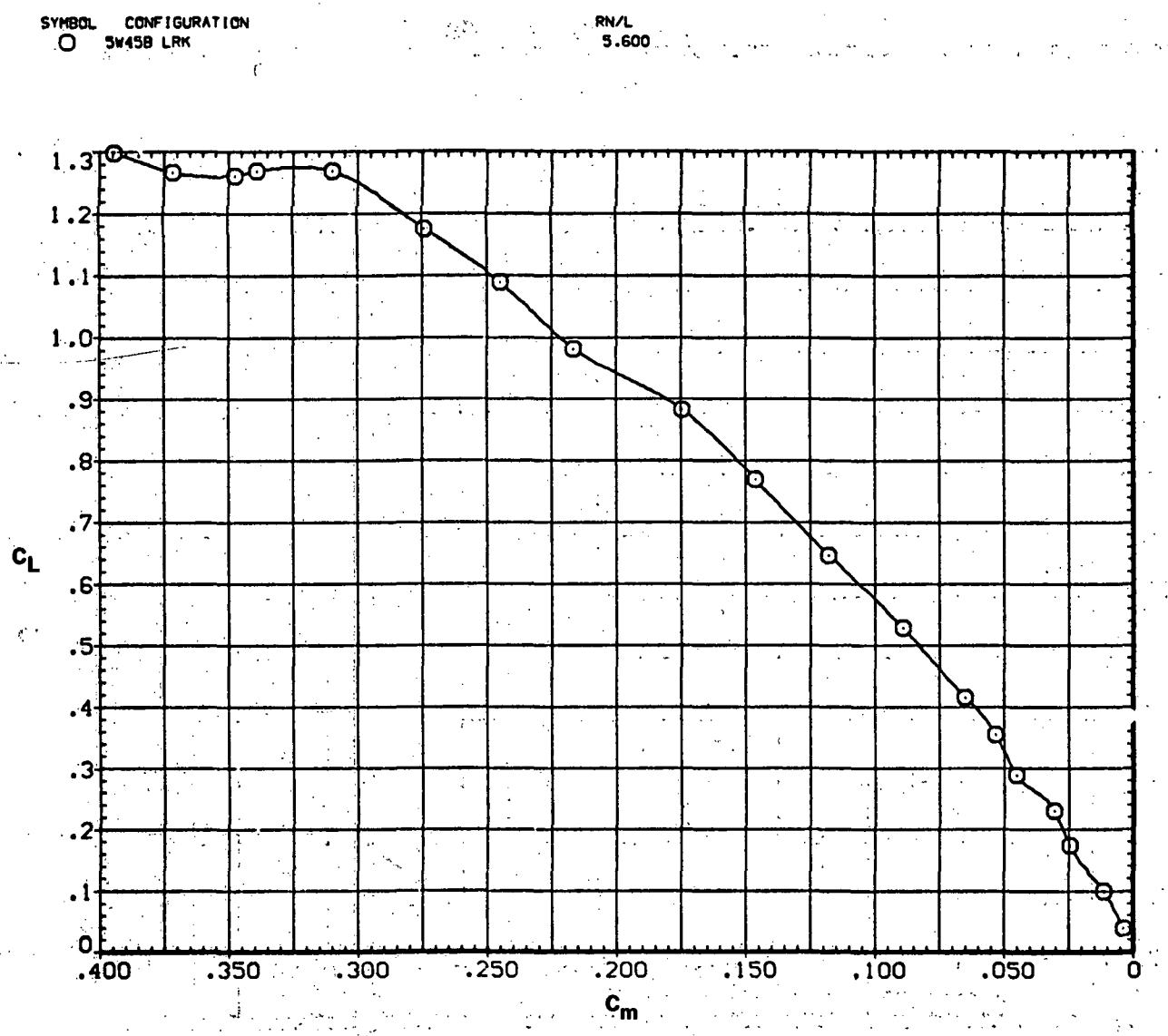

(b) C_L vs C_m

Figure 4.– Continued.

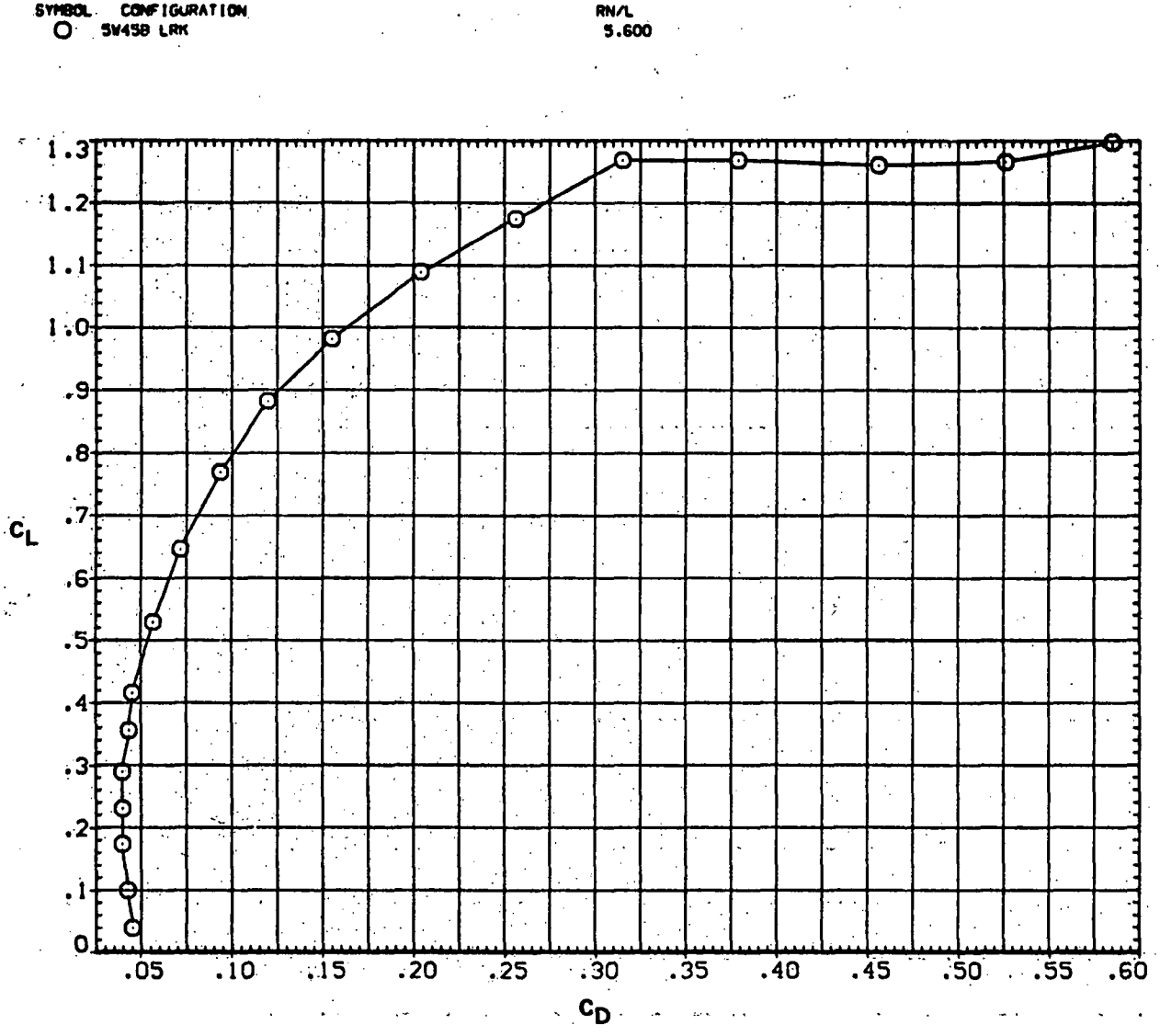

(c) C_L vs C_D

Figure 4.– Continued.

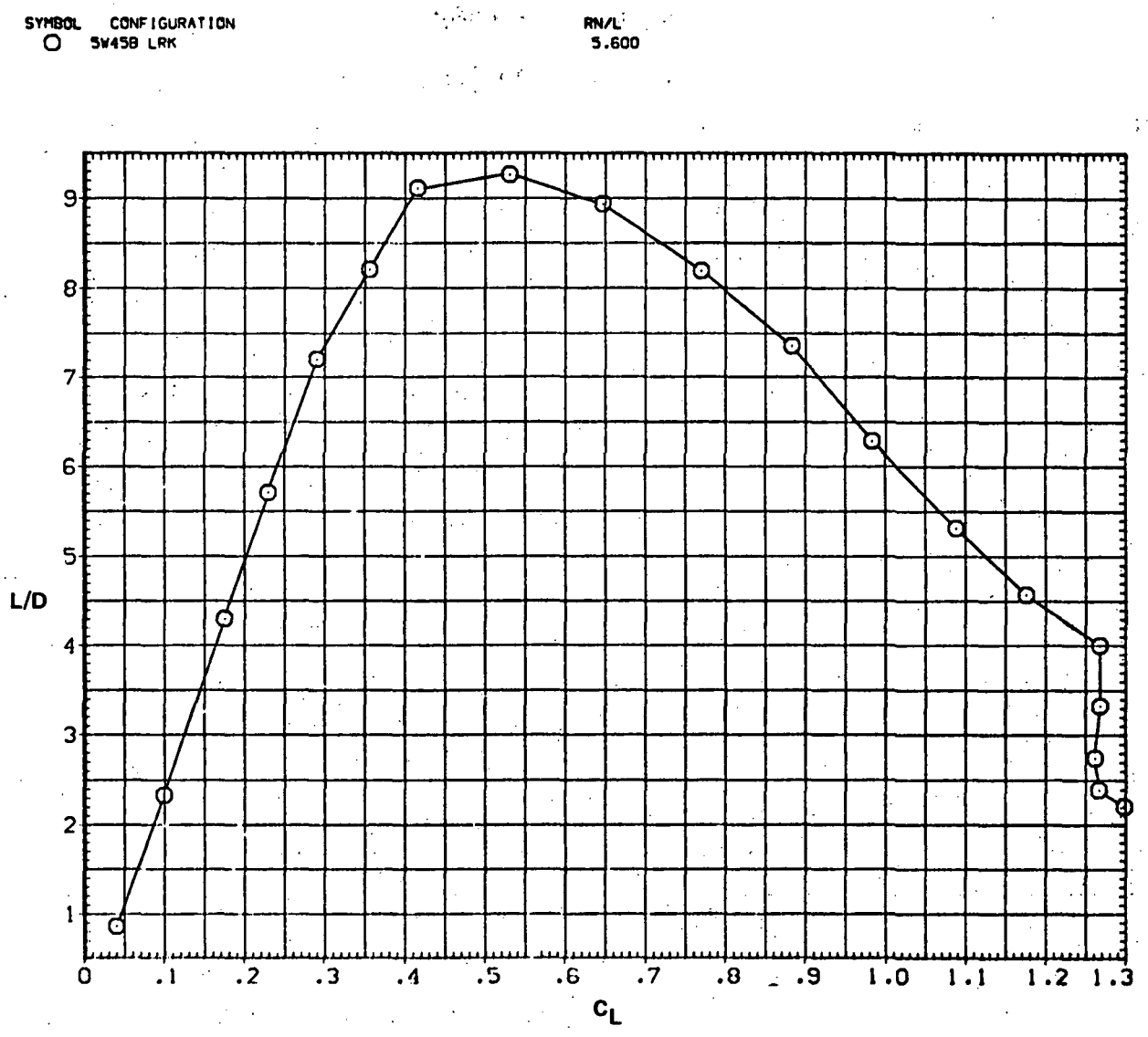

(d) L/D vs C_L

Figure 4.– Continued.

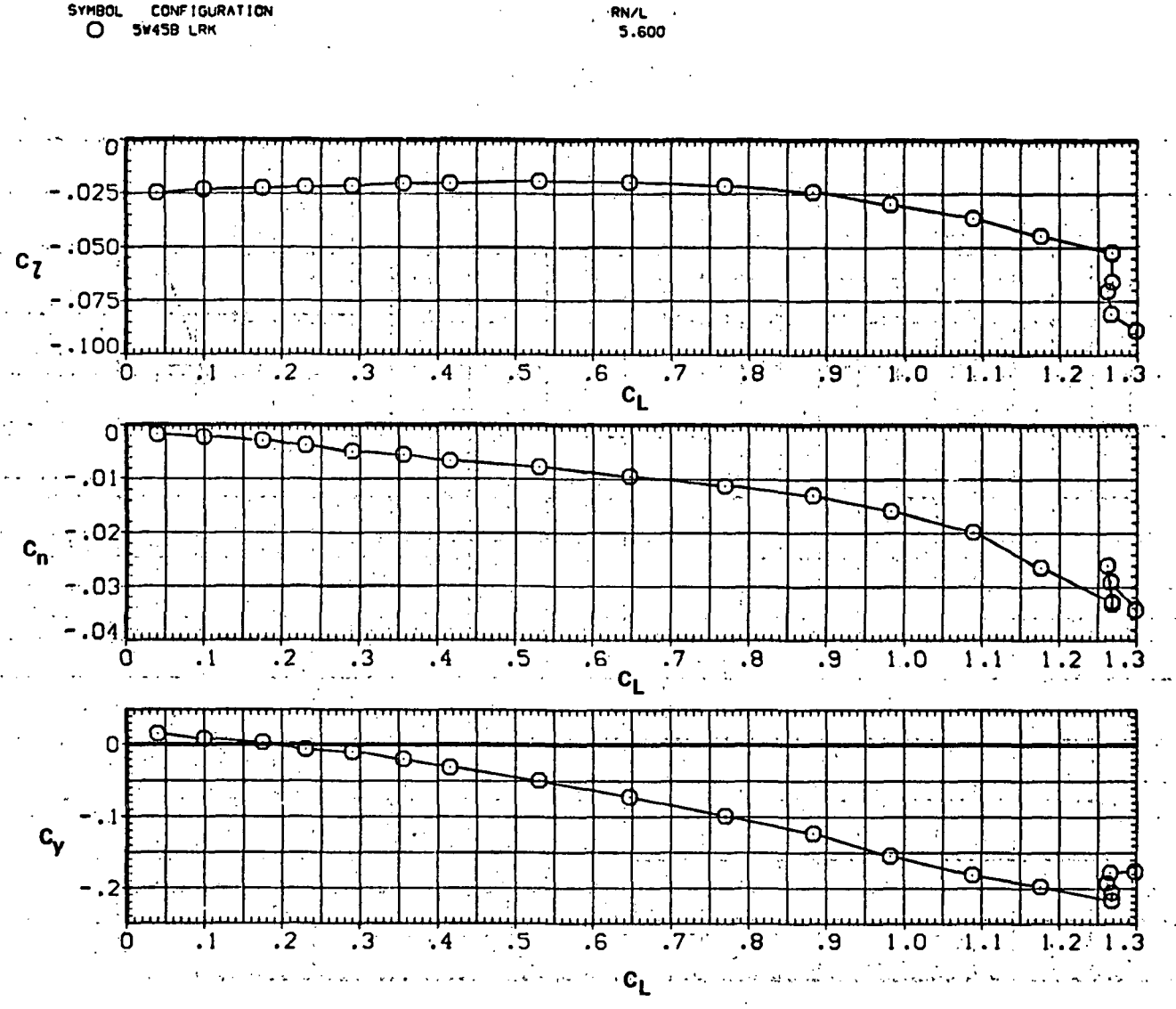

(e) C_l, C_n, and C_Y vs C_L

Figure 4.– Concluded.

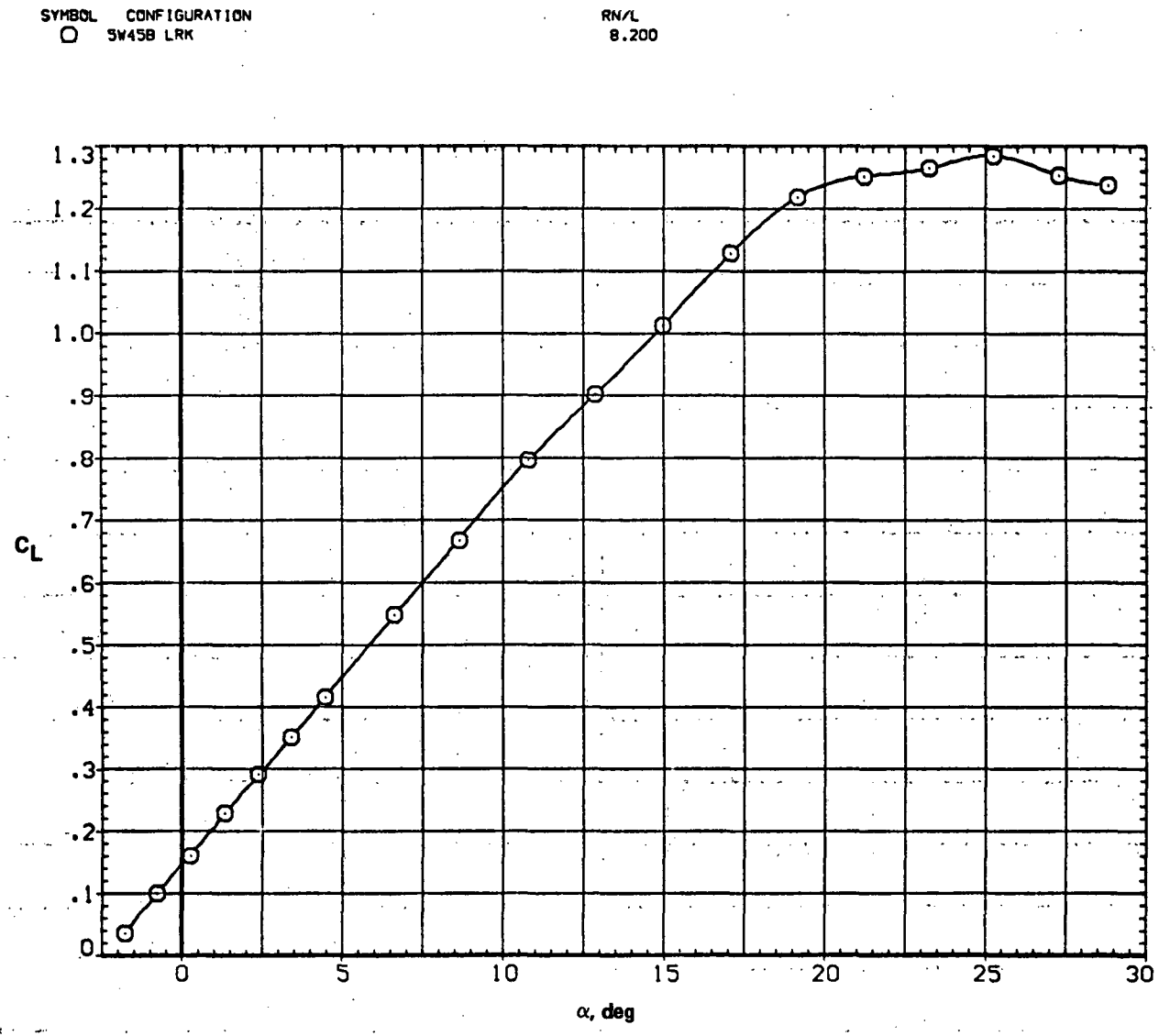

(a) C_L vs α

Figure 5.– Effect of having Krüger flaps on both wing panels on the static longitudinal characteristics of an oblique wing: $\Lambda = 45°$, $M = 0.40$.

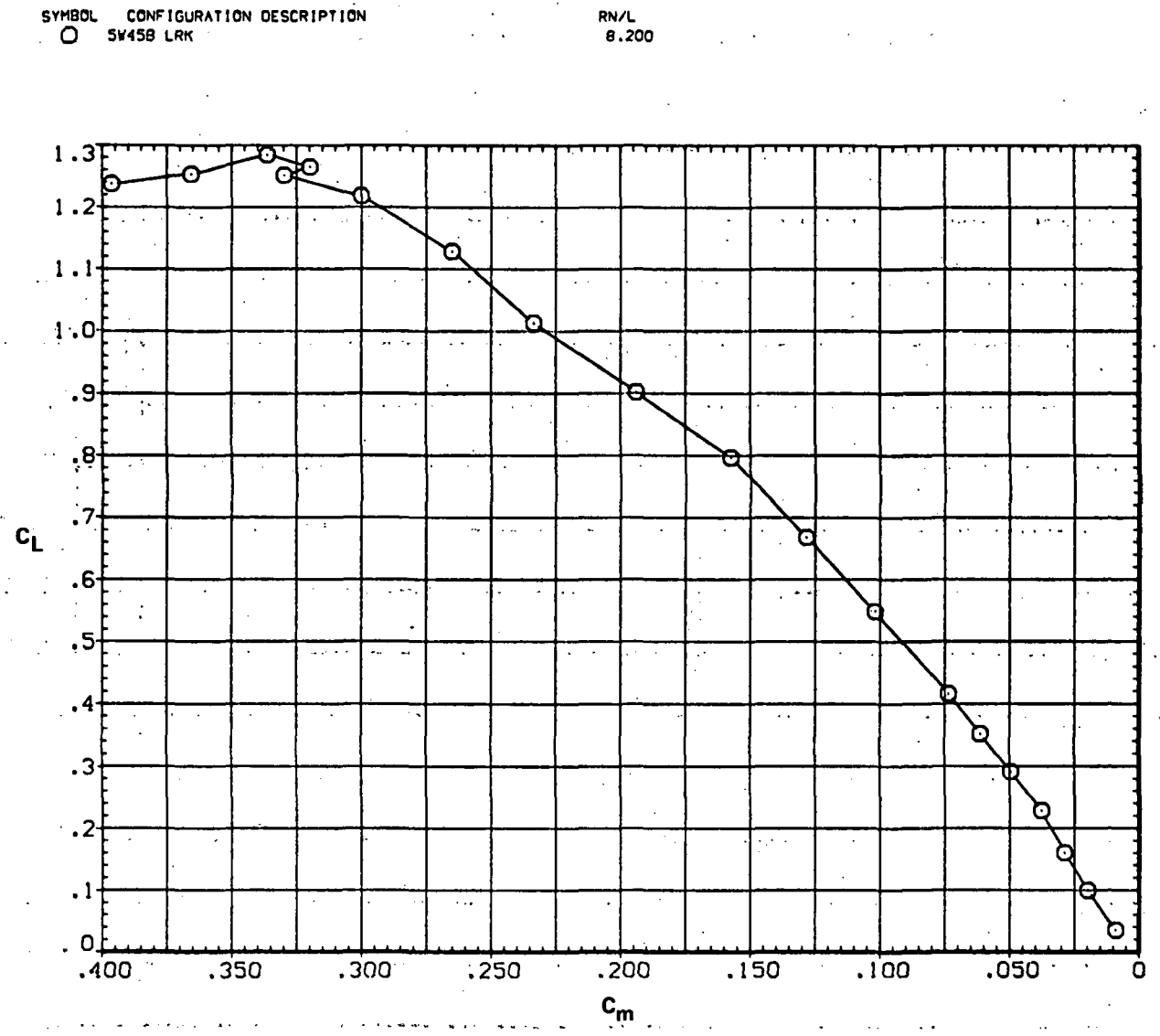

(b) C_L vs C_m

Figure 5.– Continued.

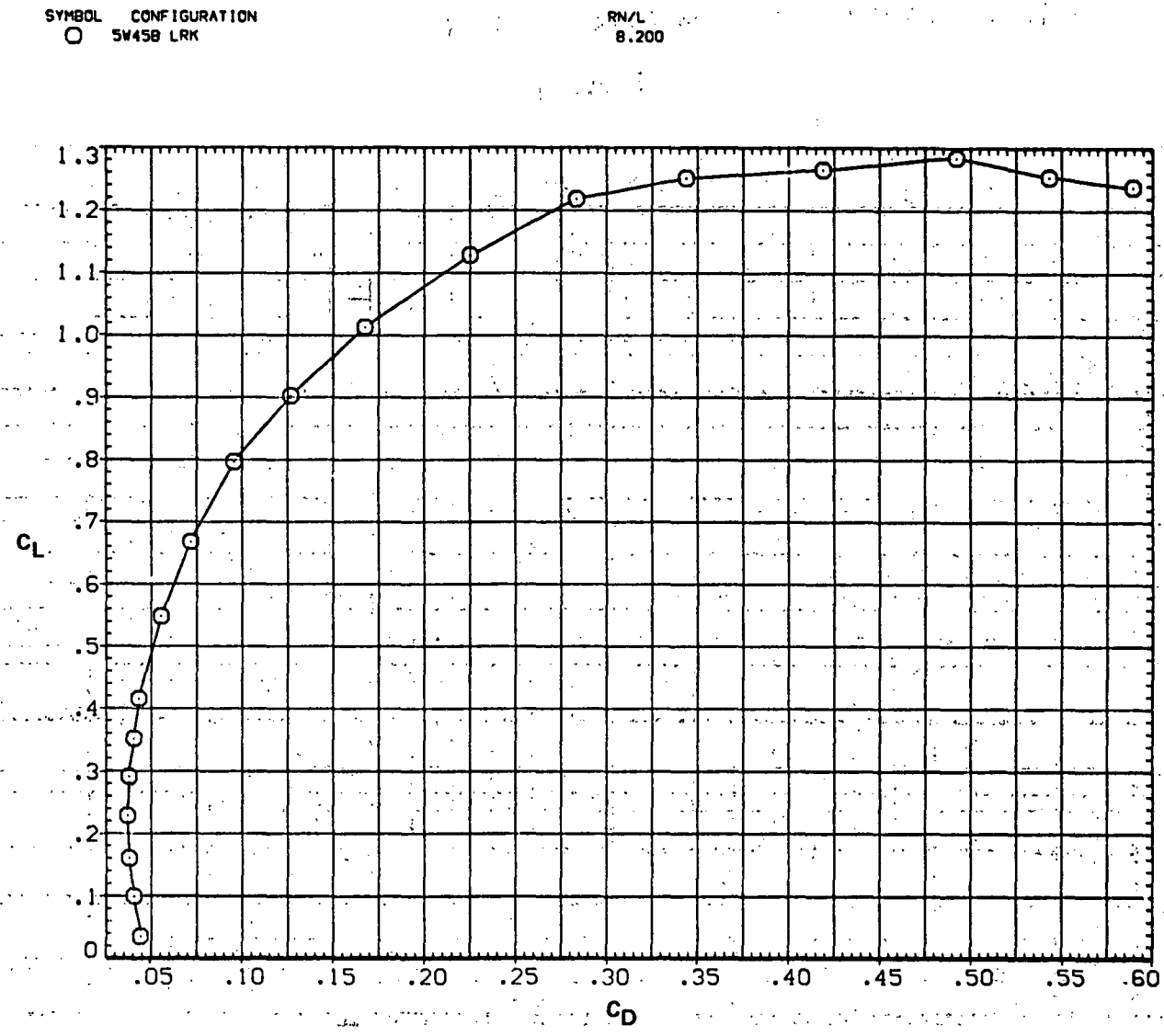

(c) C_L vs C_D

Figure 5.– Continued.

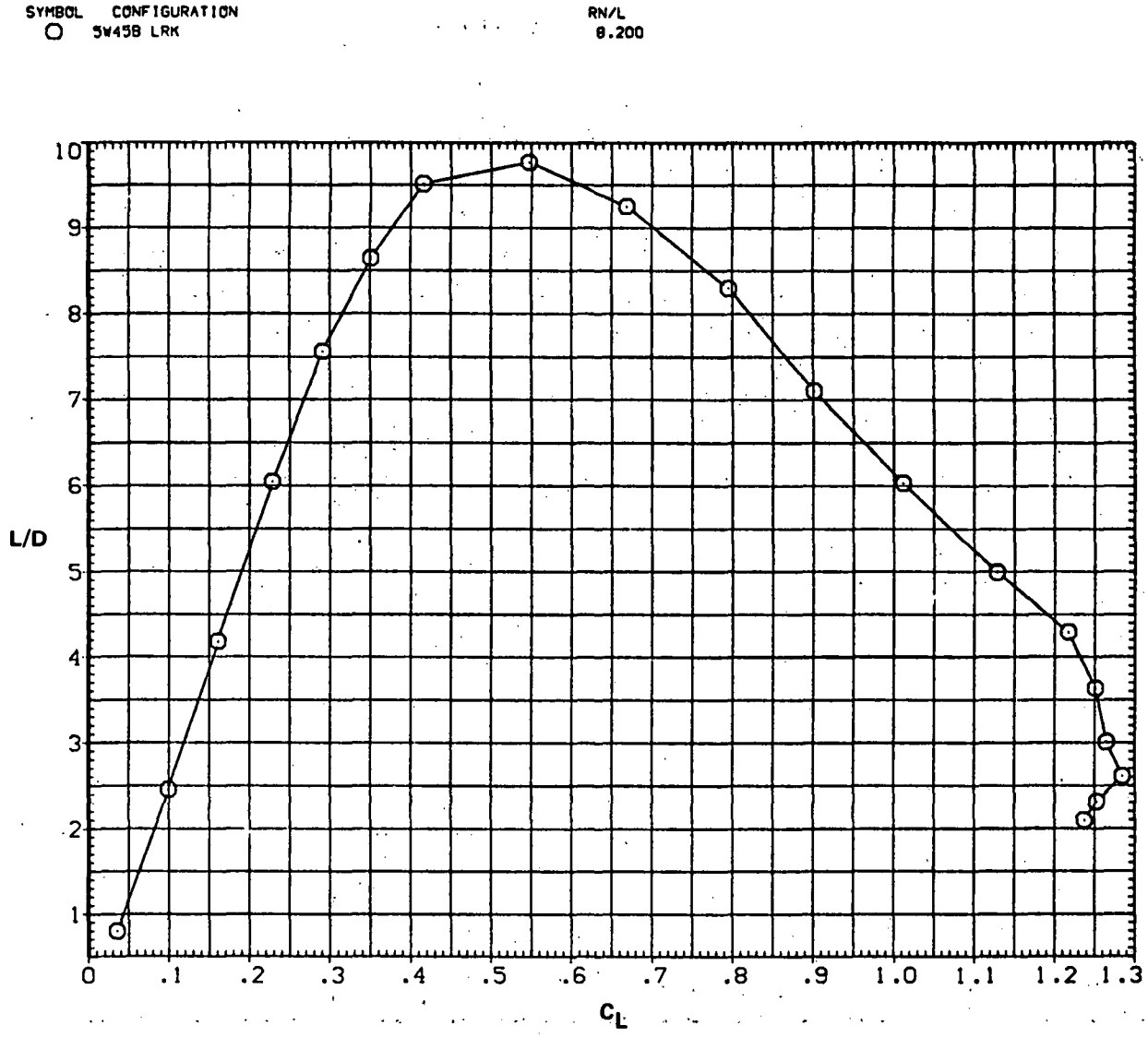

(d) L/D vs C_L

Figure 5.– Continued.

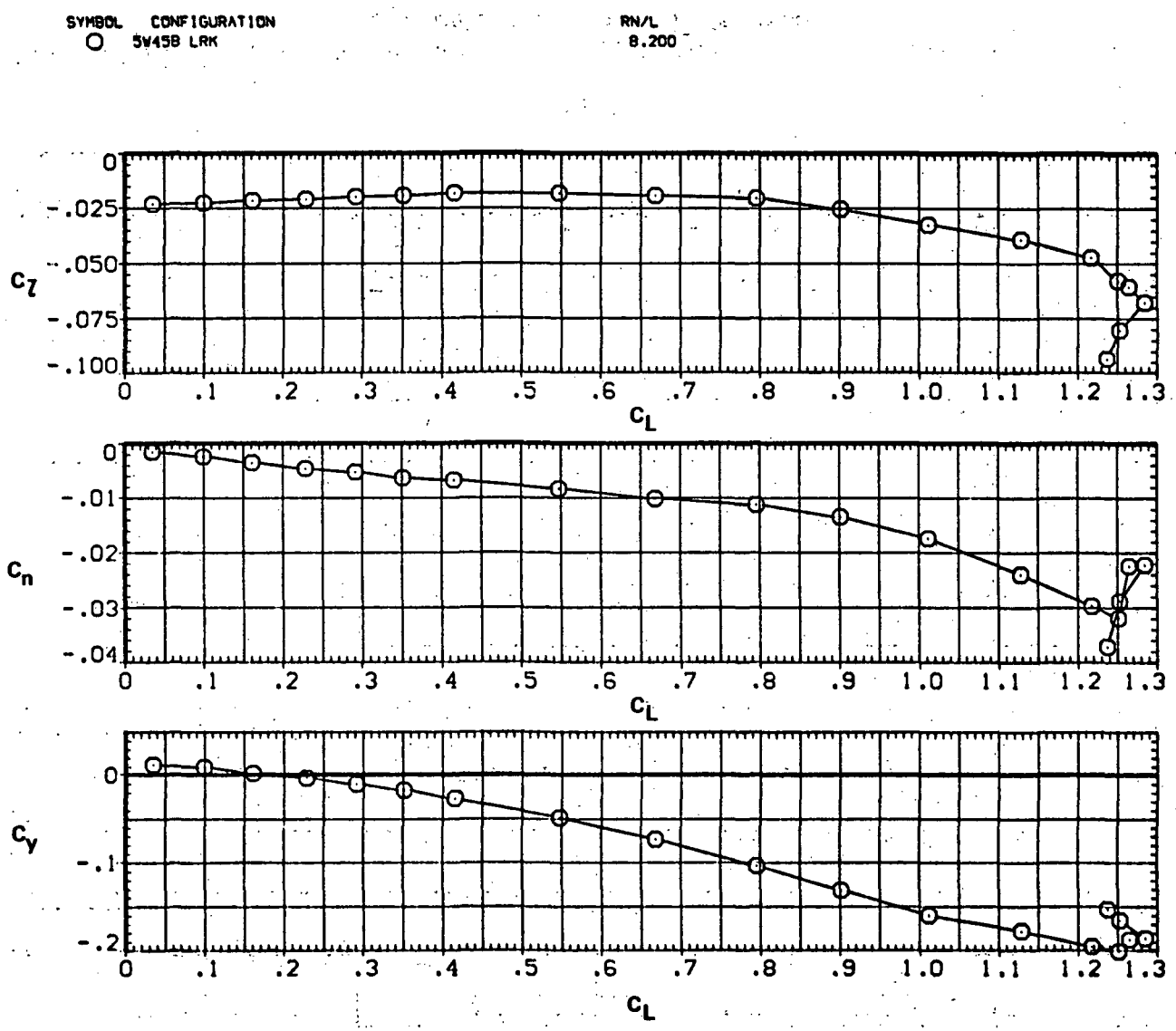

(e) C_l, C_n, and C_Y vs C_L

Figure 5.– Concluded.

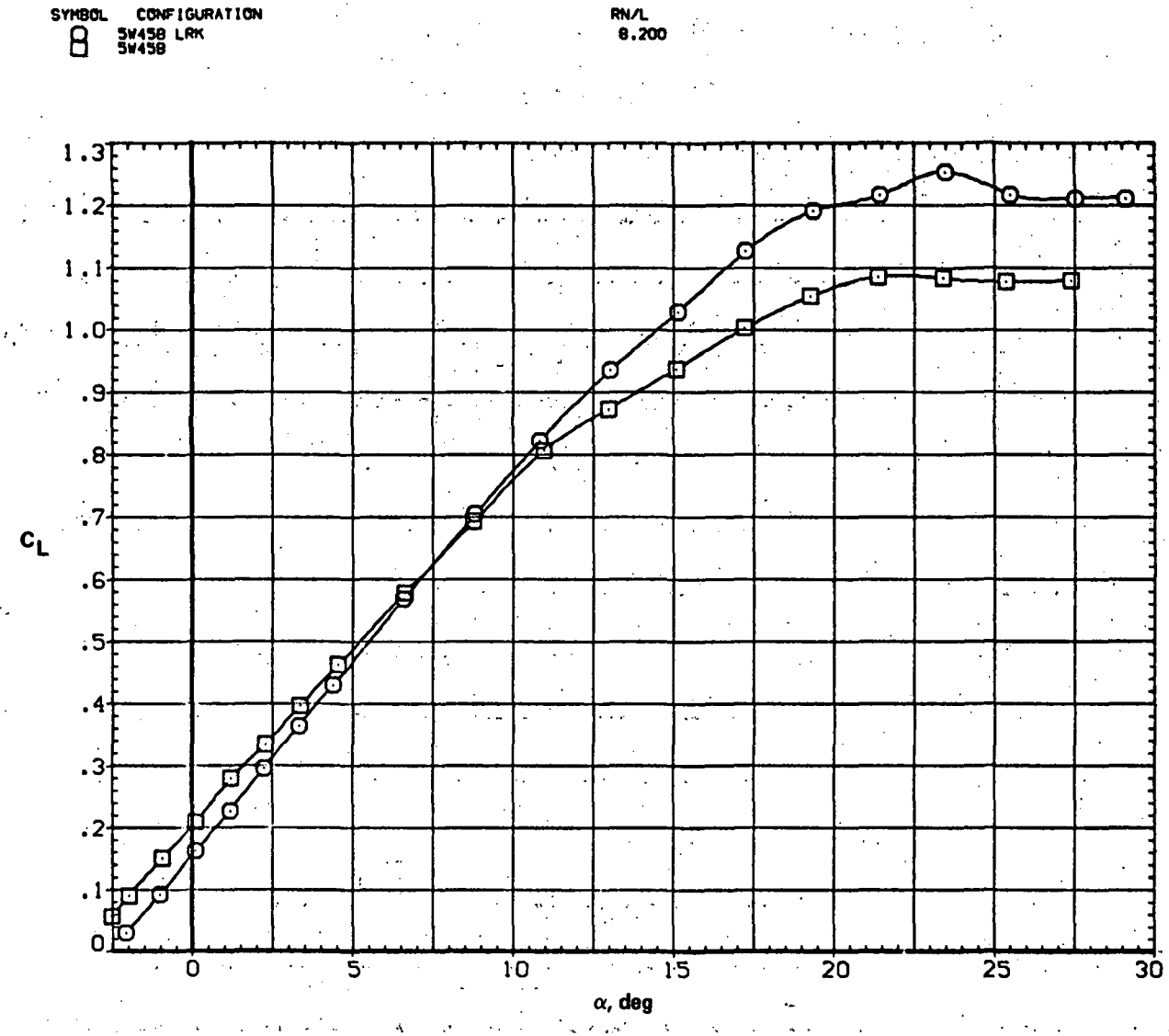

(a) C_L vs α

Figure 6.– Effect of having Krüger flaps on both wing panels on the static longitudinal characteristics of an oblique wing: $\Lambda = 45°$, $M = 0.60$.

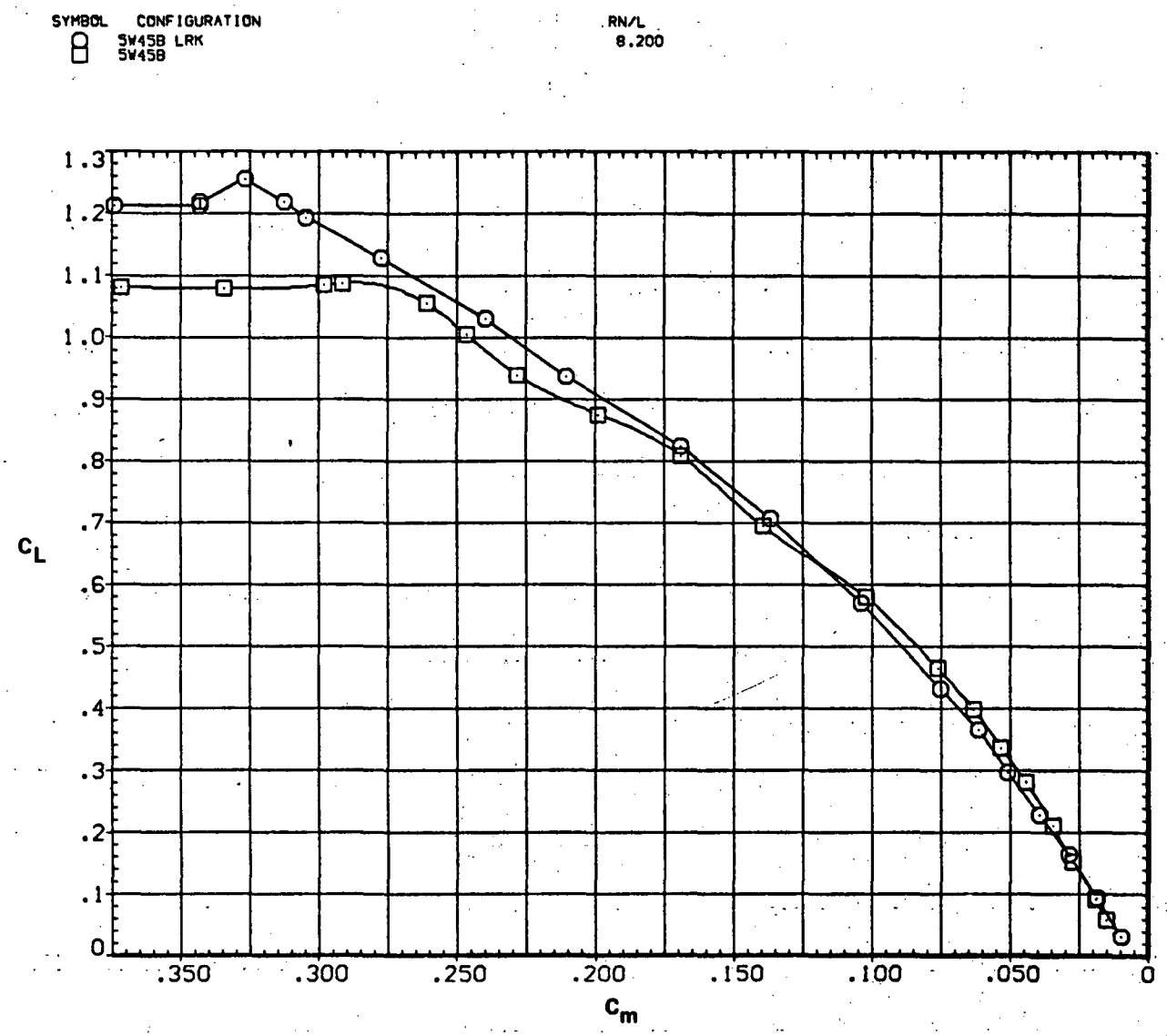

(b) C_L vs C_m

Figure 6.– Continued.

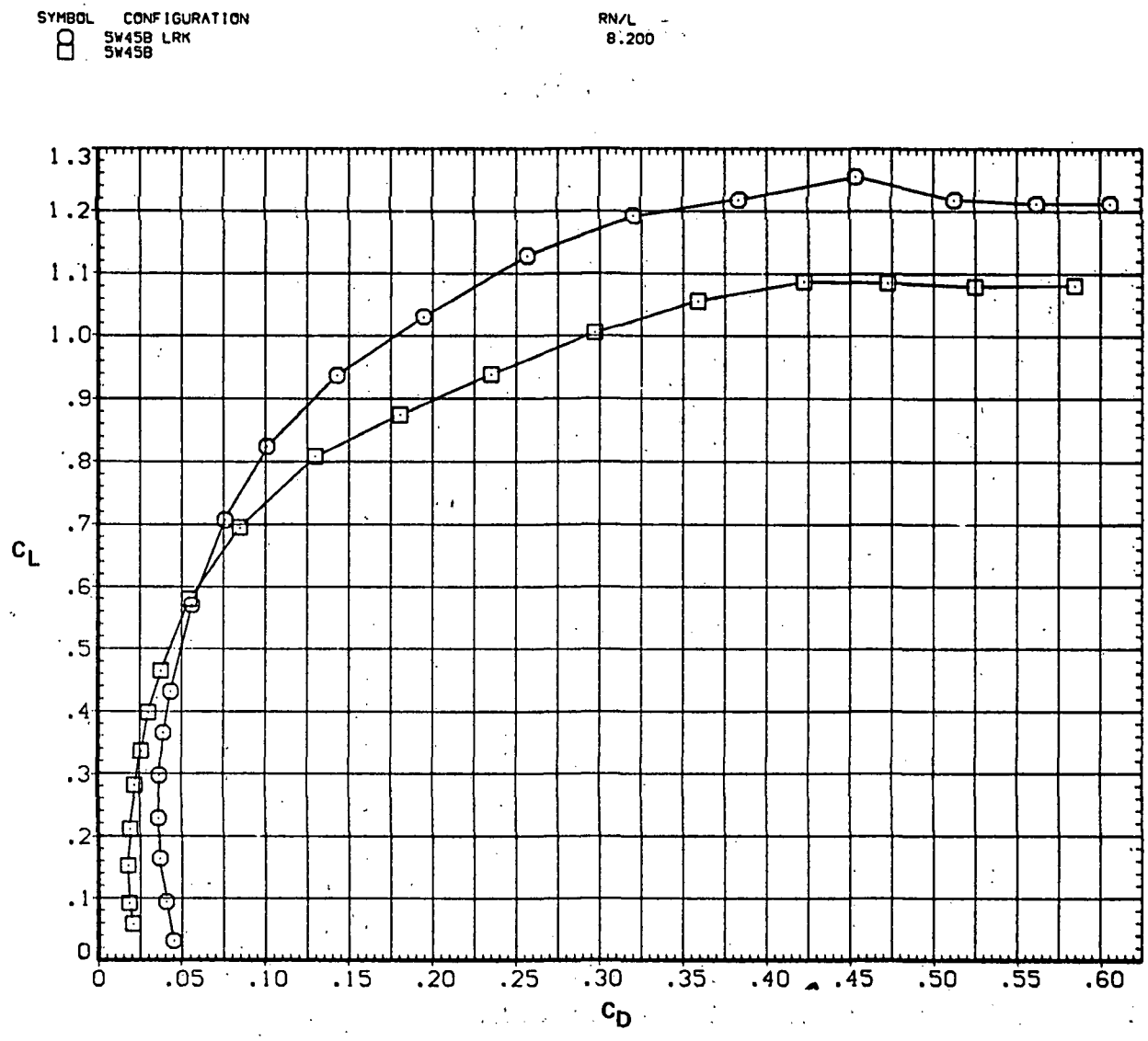

(c) C_L vs C_D

Figure 6.– Continued.

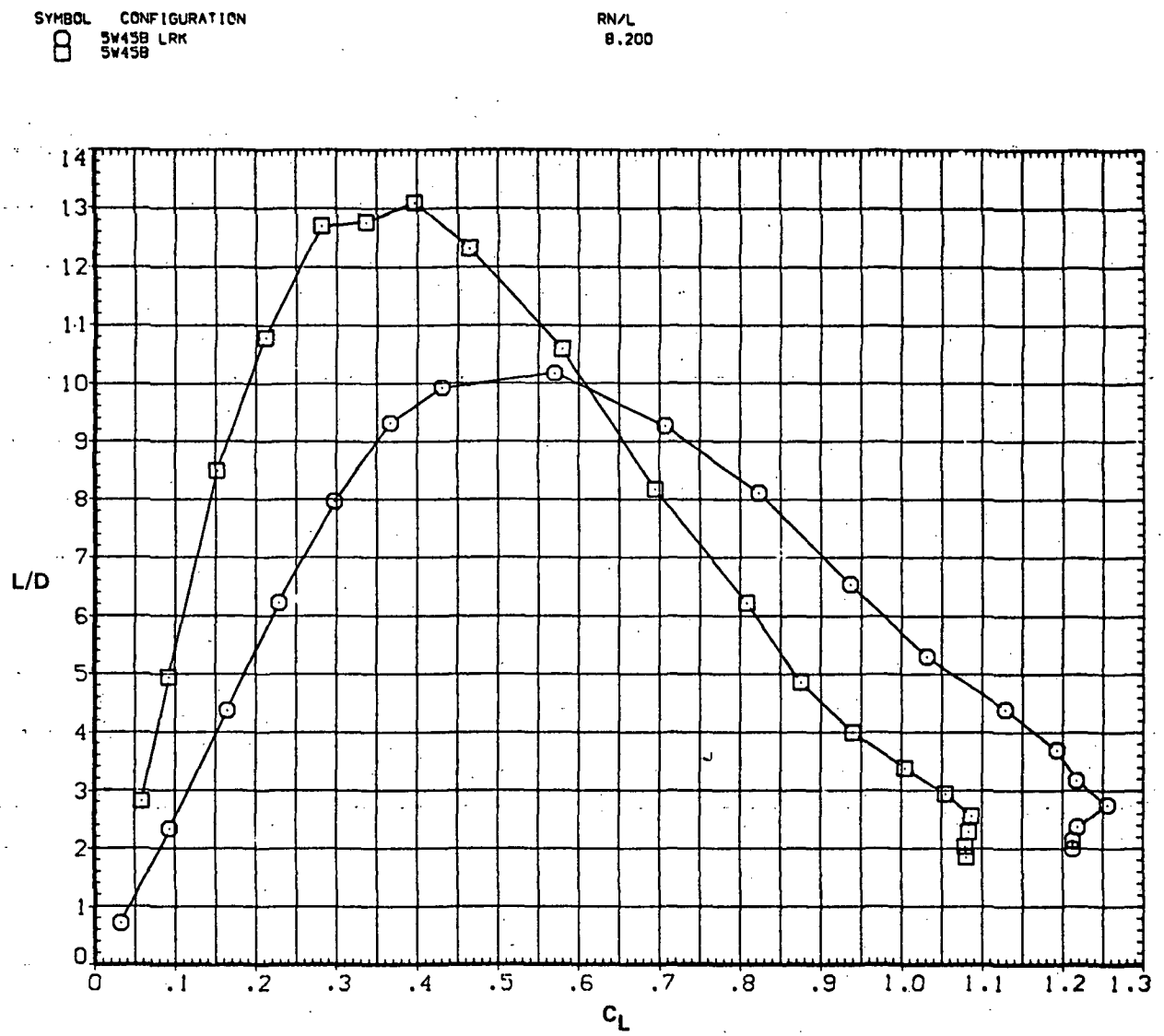

(d) L/D vs C_L

Figure 6.– Continued.

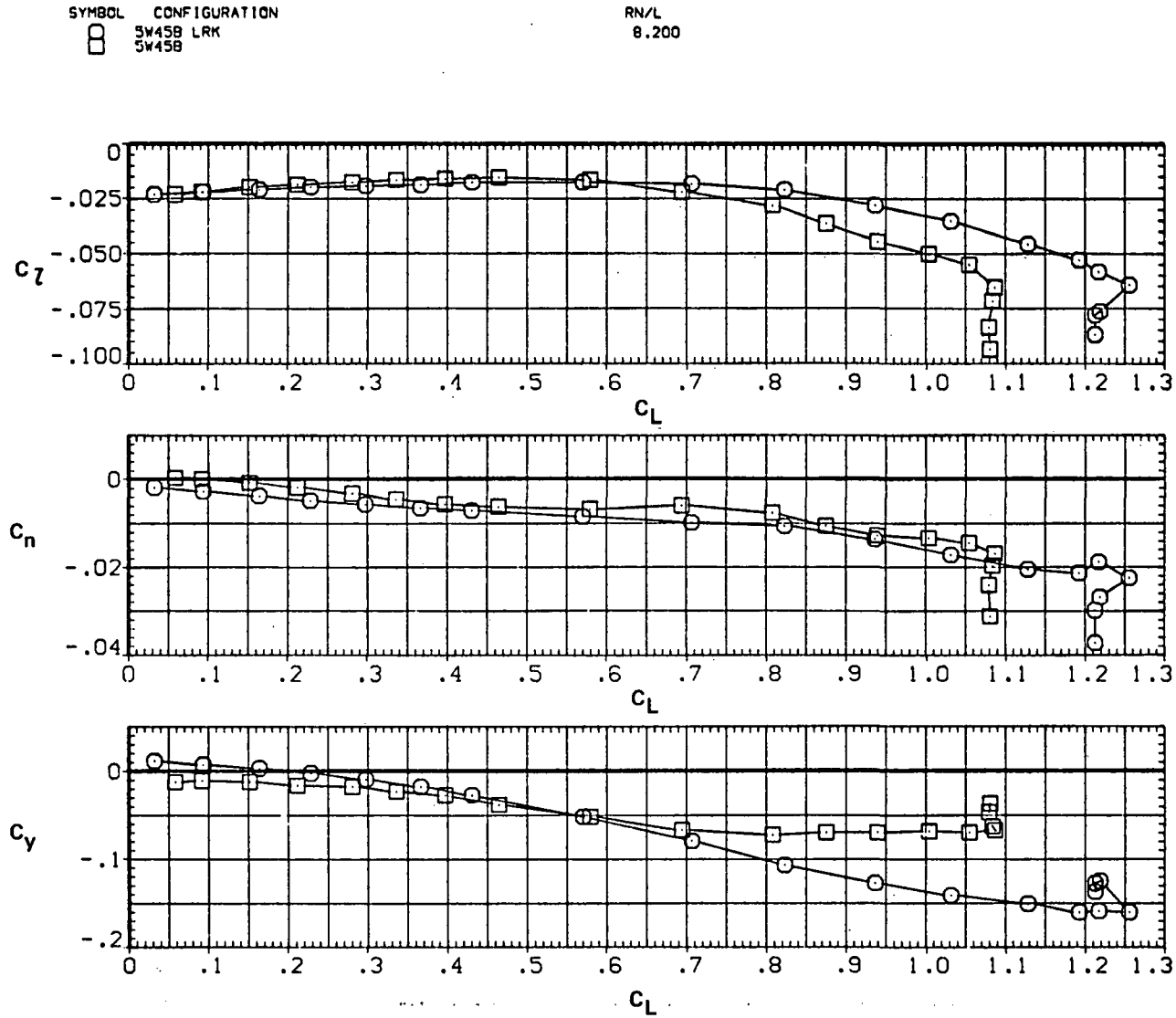

(e) C_l, C_n, and C_Y vs C_L

Figure 6.– Concluded.

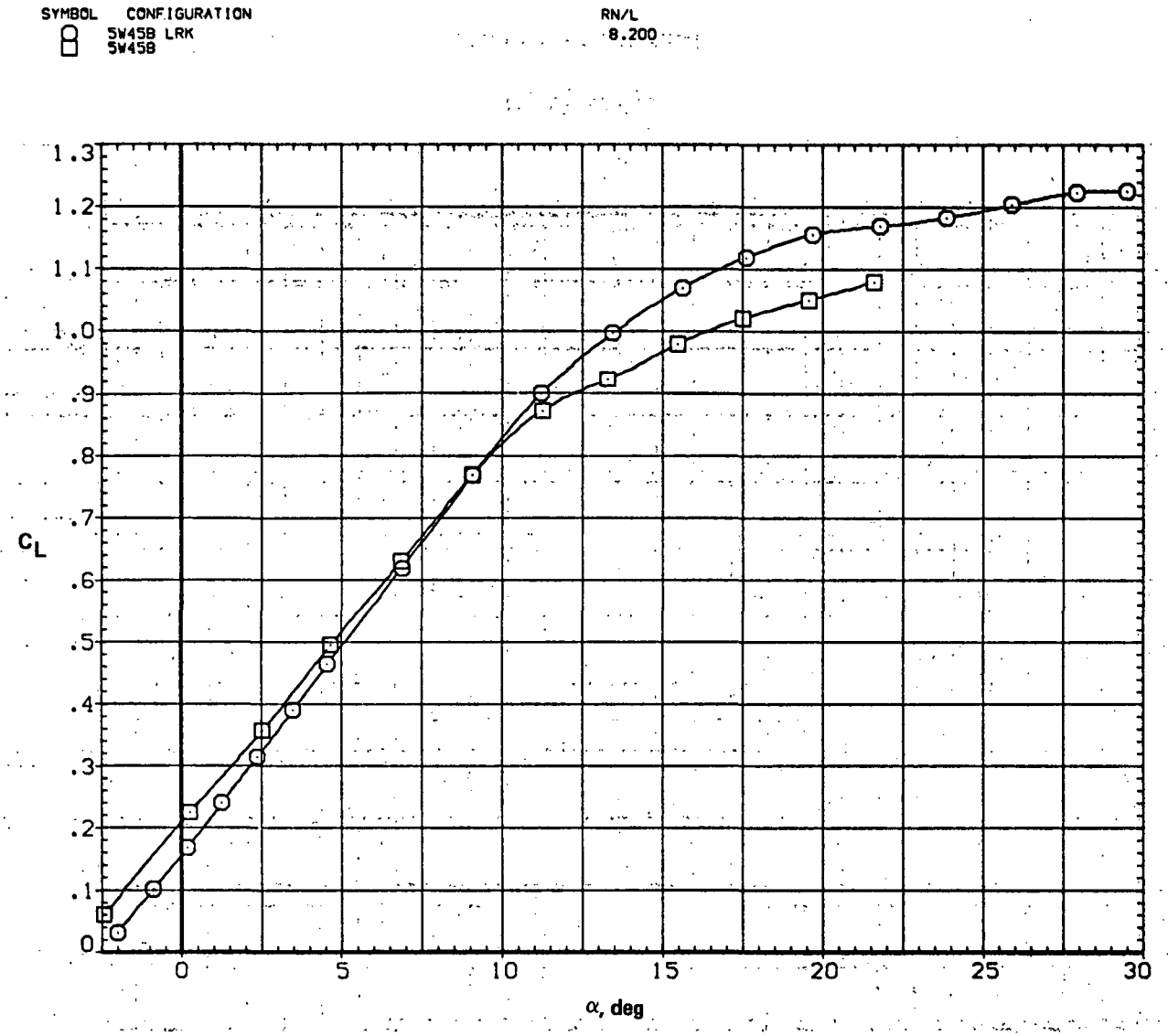

(a) C_L vs α

Figure 7.– Effect of having Krüger flaps on both wing panels on the static longitudinal characteristics of an oblique wing: $\Lambda = 45°$, $M = 0.80$.

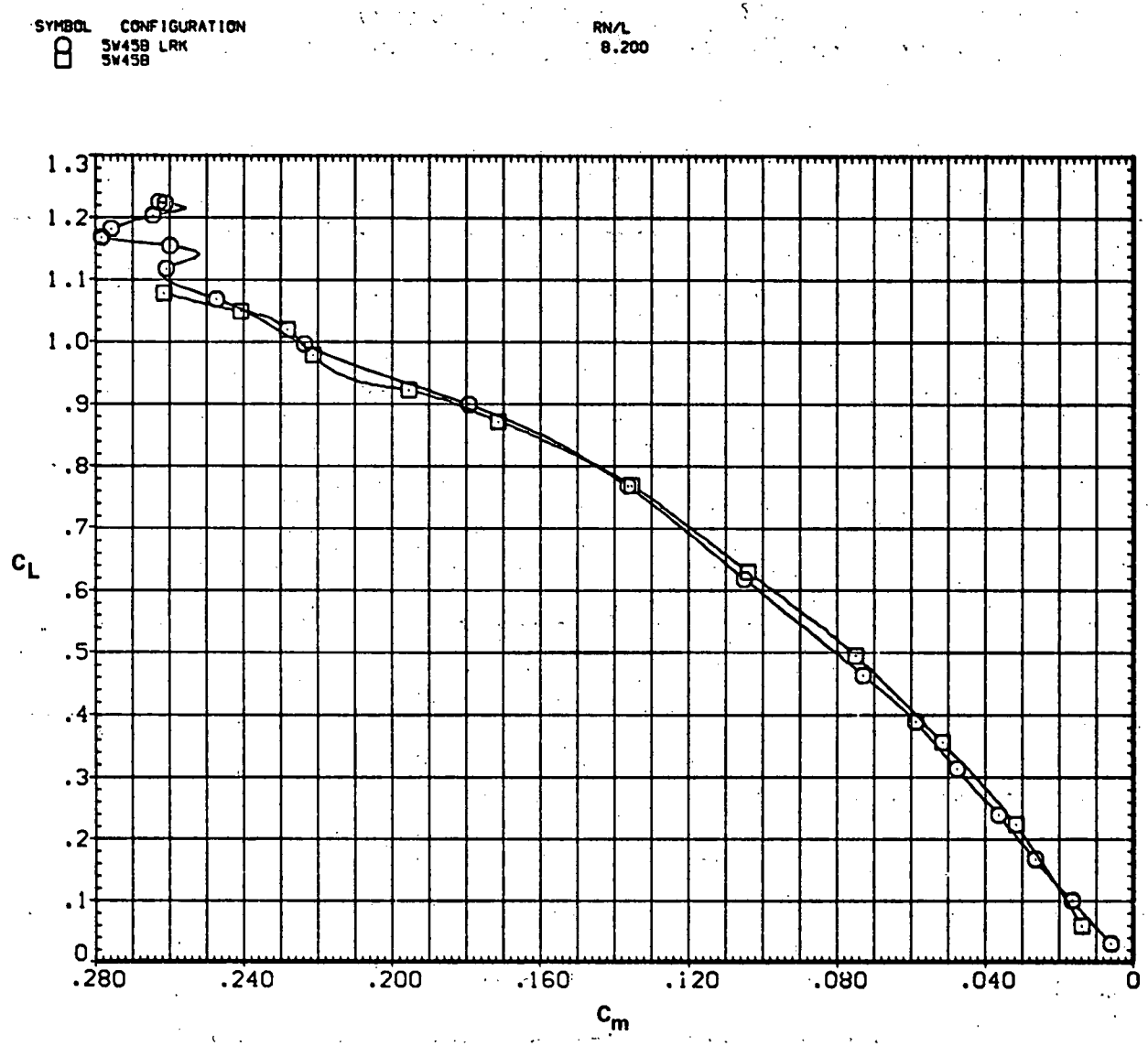

(b) C_L vs C_m

Figure 7.– Continued.

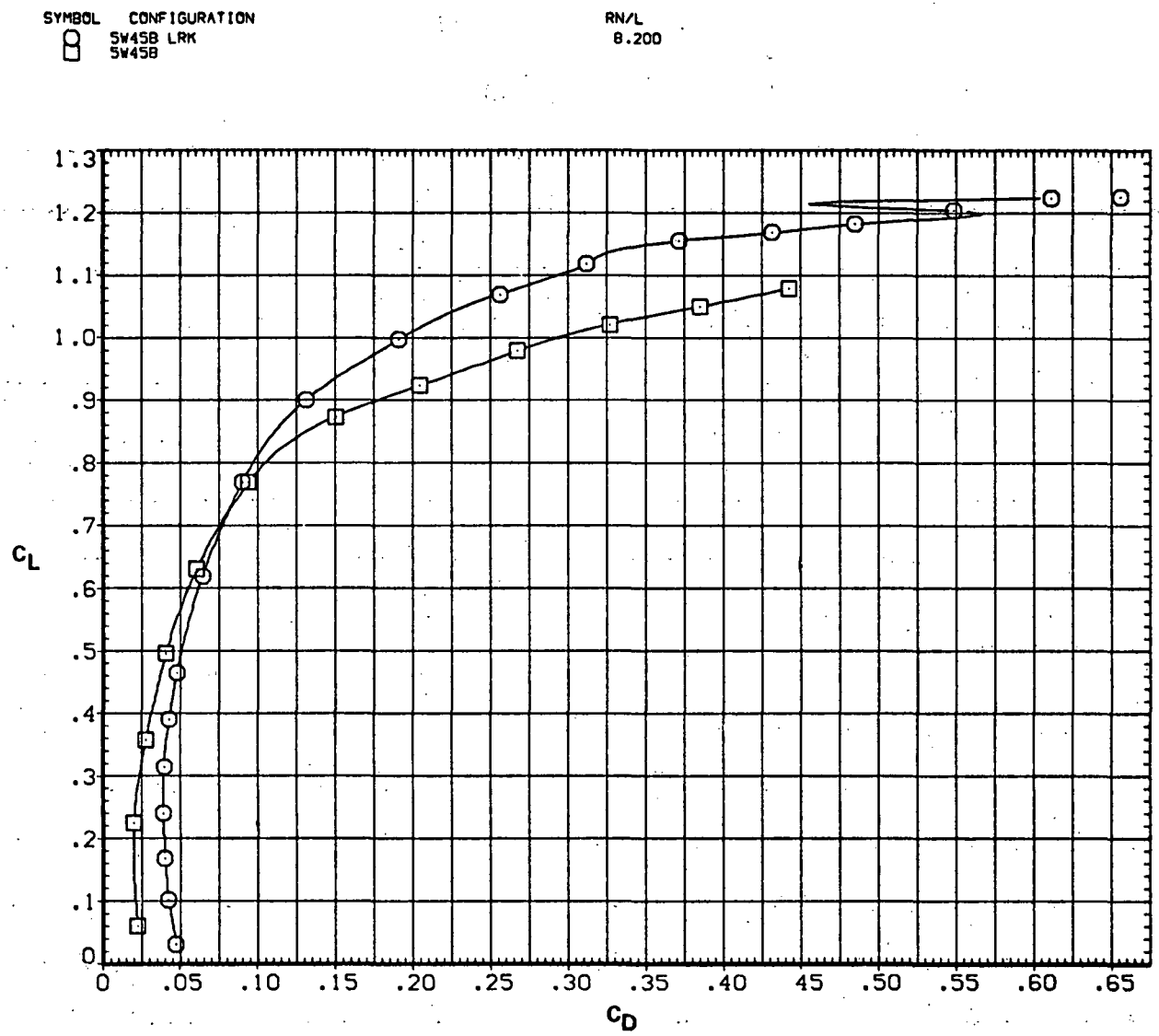

(c) C_L vs C_D

Figure 7.– Continued.

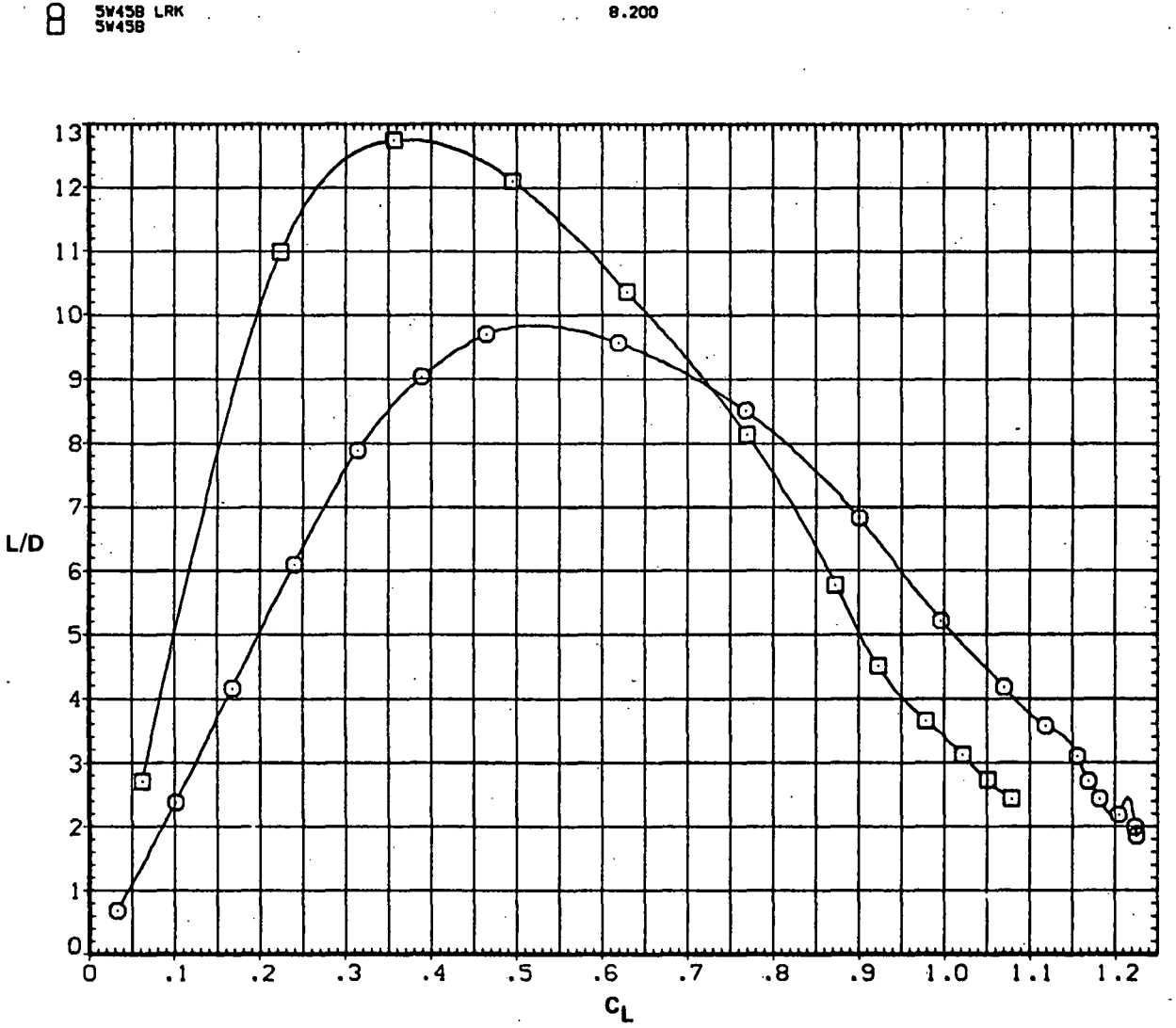

(d) L/D vs C_L

Figure 7.– Continued.

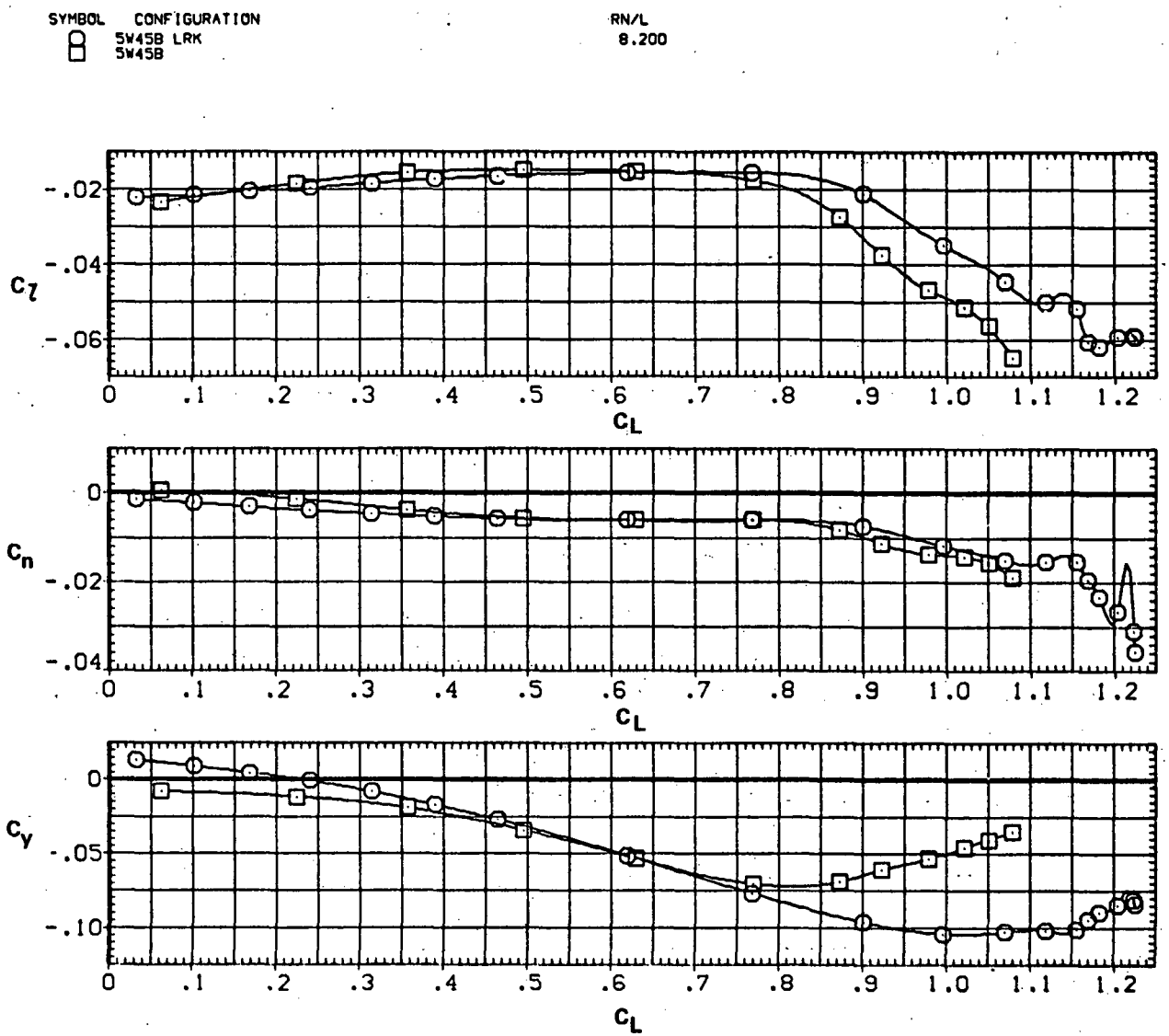

(e) C_l, C_n, and C_Y vs C_L

Figure 7.– Concluded.

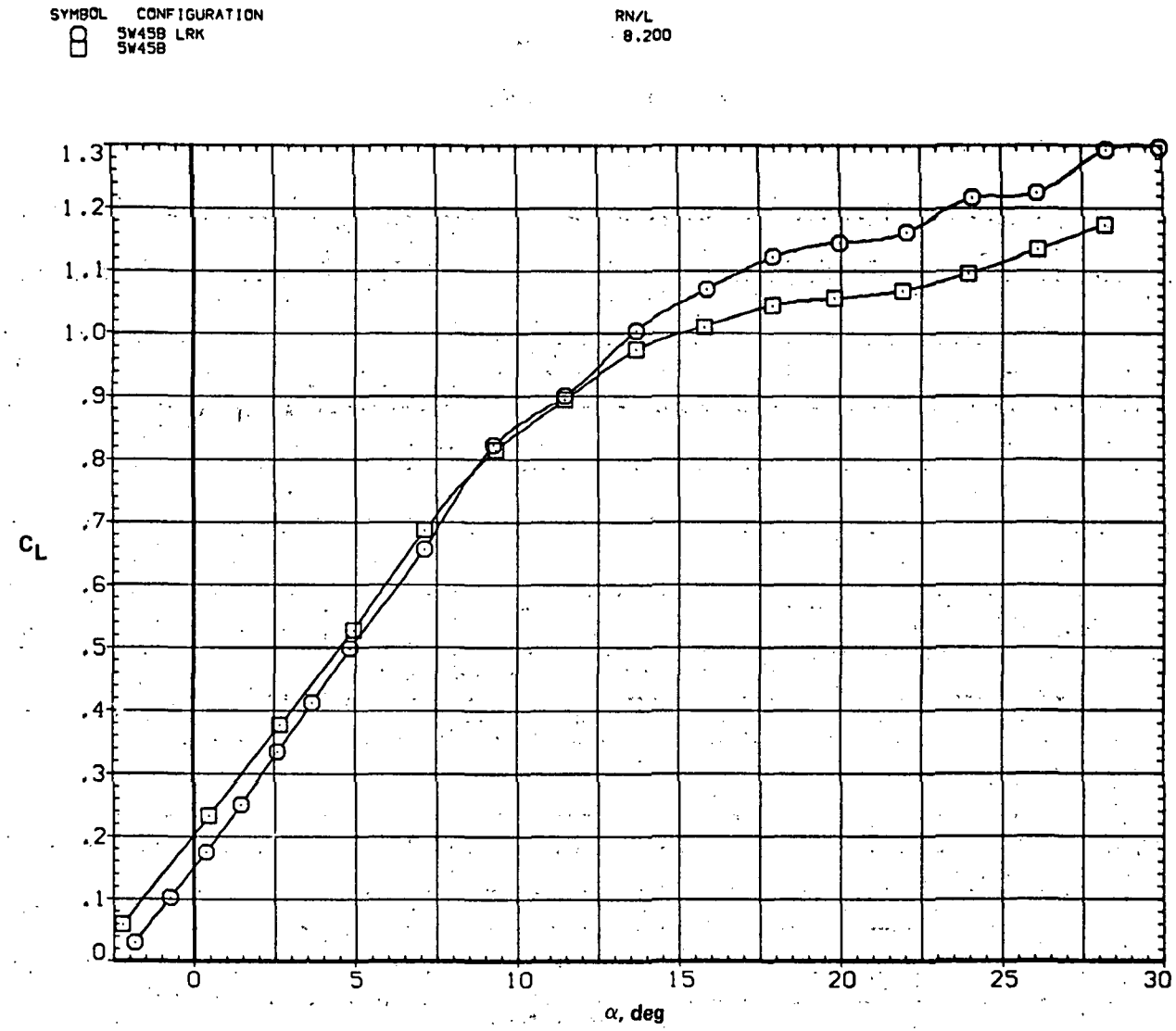

(a) C_L vs α

Figure 8.– Effect of having Krüger flaps on both wing panels on the static longitudinal characteristics of an oblique wing: $\Lambda = 45°$, $M = 0.90$.

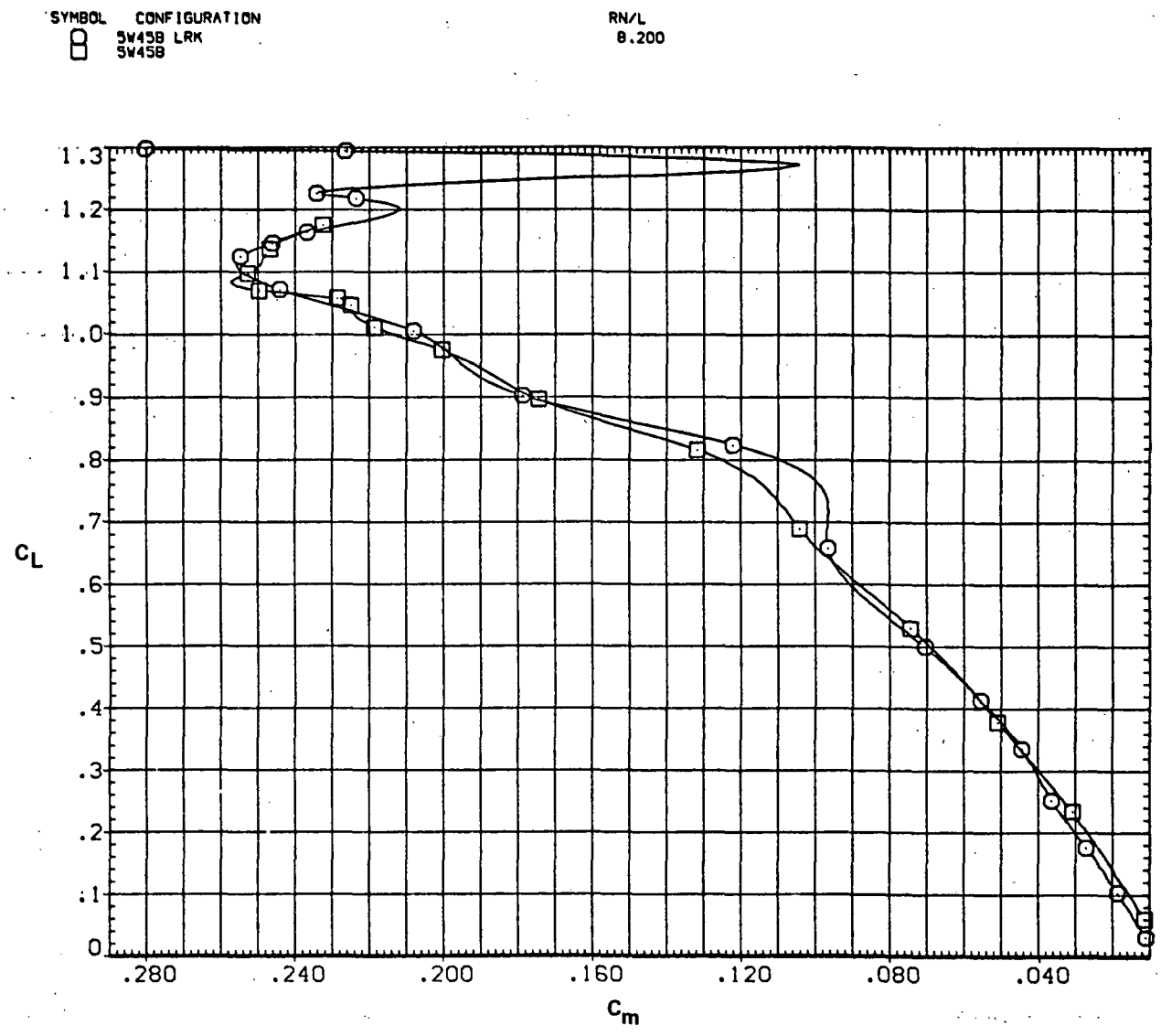

(b) C_L vs C_m

Figure 8.– Continued

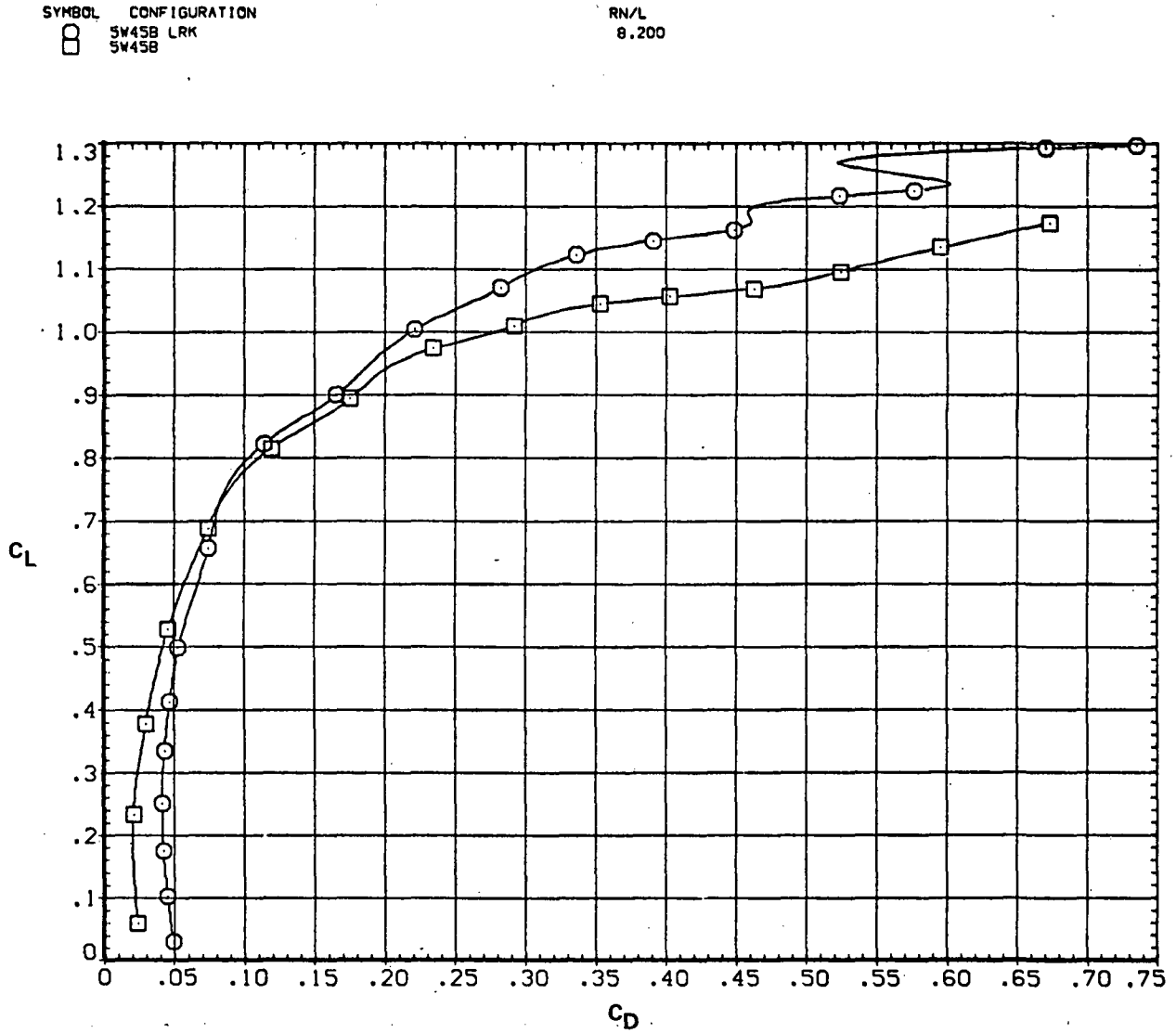

(c) C_L vs C_D

Figure 8.– Continued.

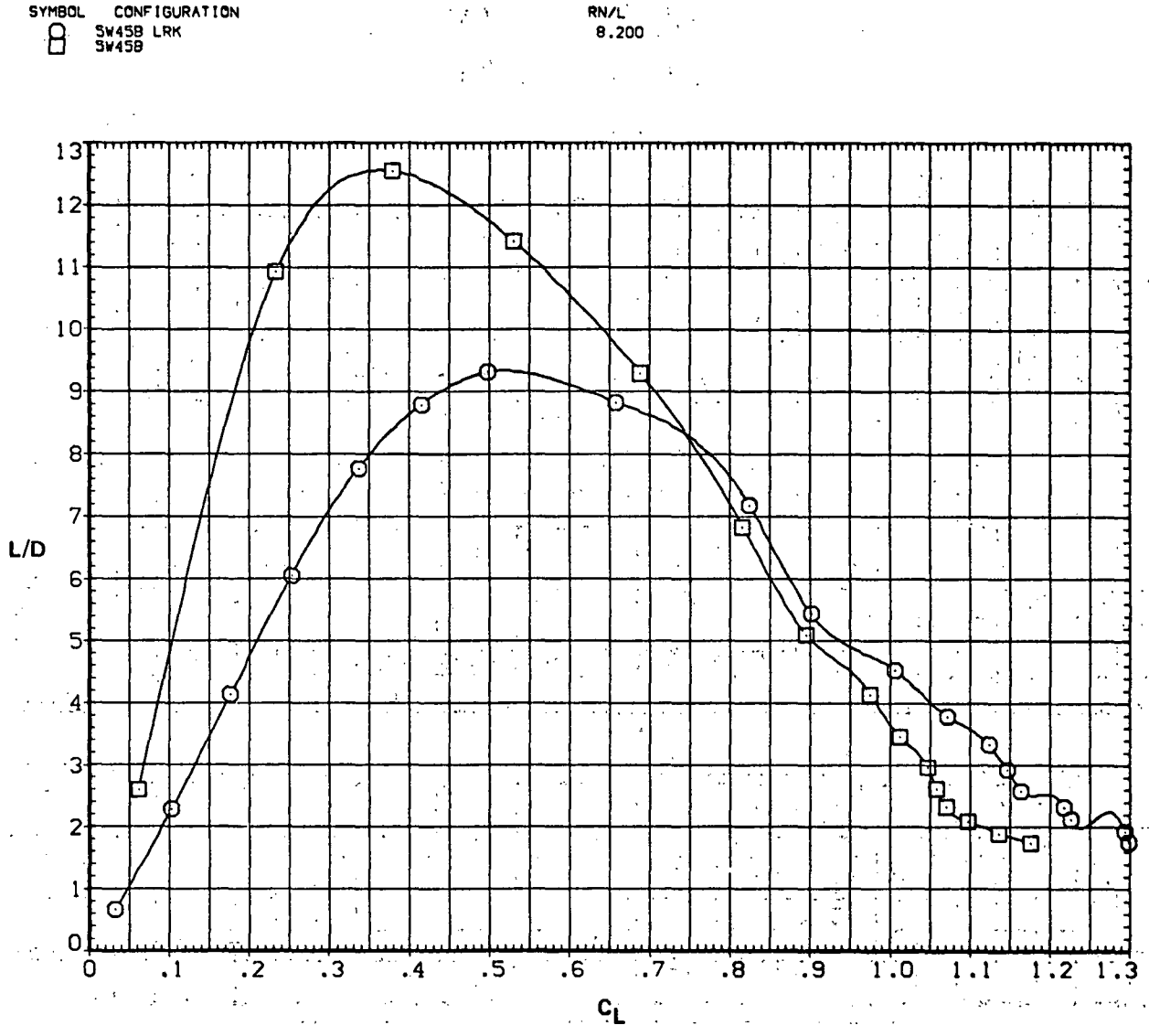

(d) L/D vs C_L

Figure 8.– Continued.

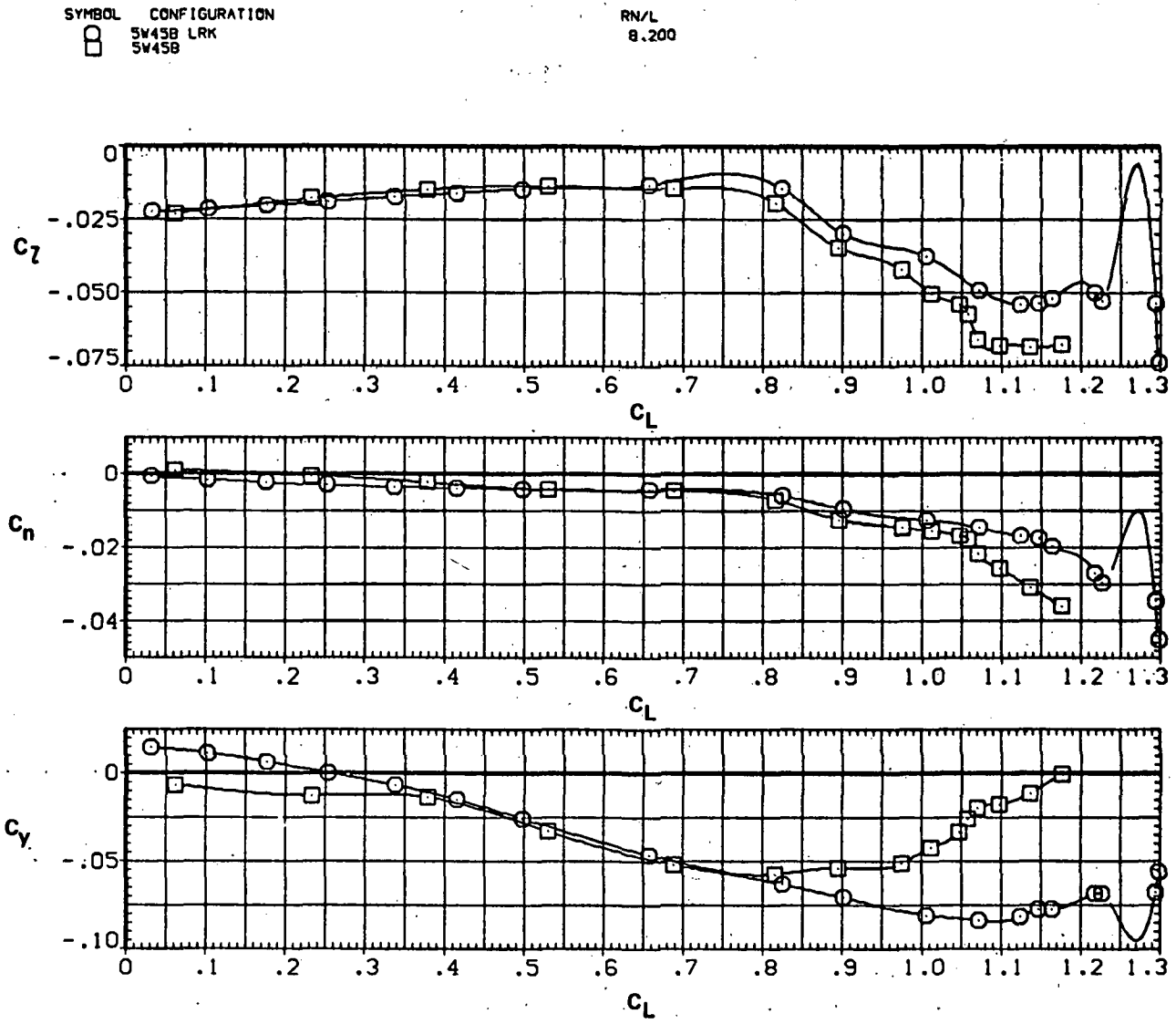

(e) C_l, C_n, and C_Y vs C_L

Figure 8.– Concluded.

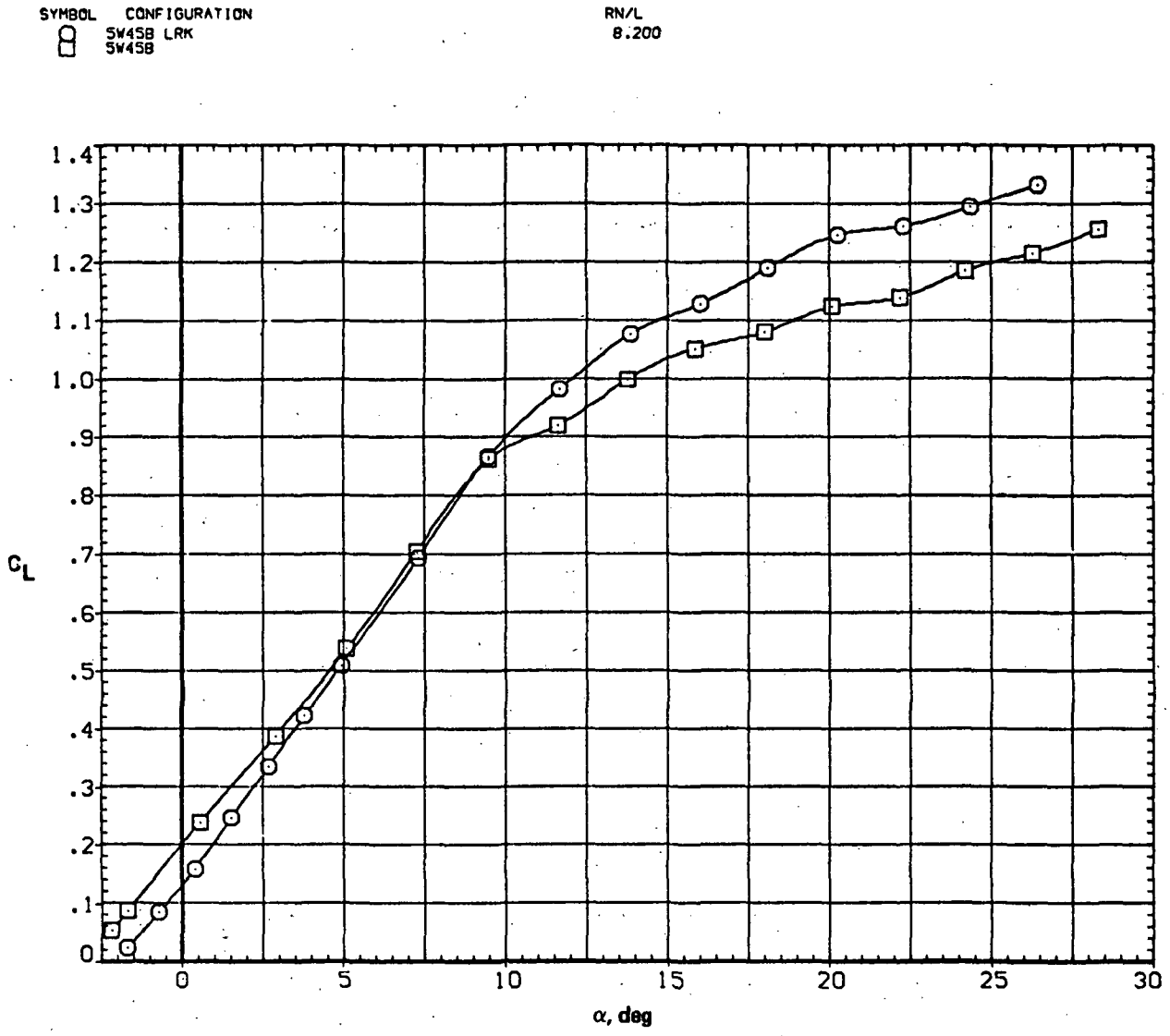

(a) C_L vs α

Figure 9.– Effect of having Krüger flaps on both wing panels on the static longitudinal characteristics of an oblique wing: $\Lambda = 45°$, $M = 0.95$.

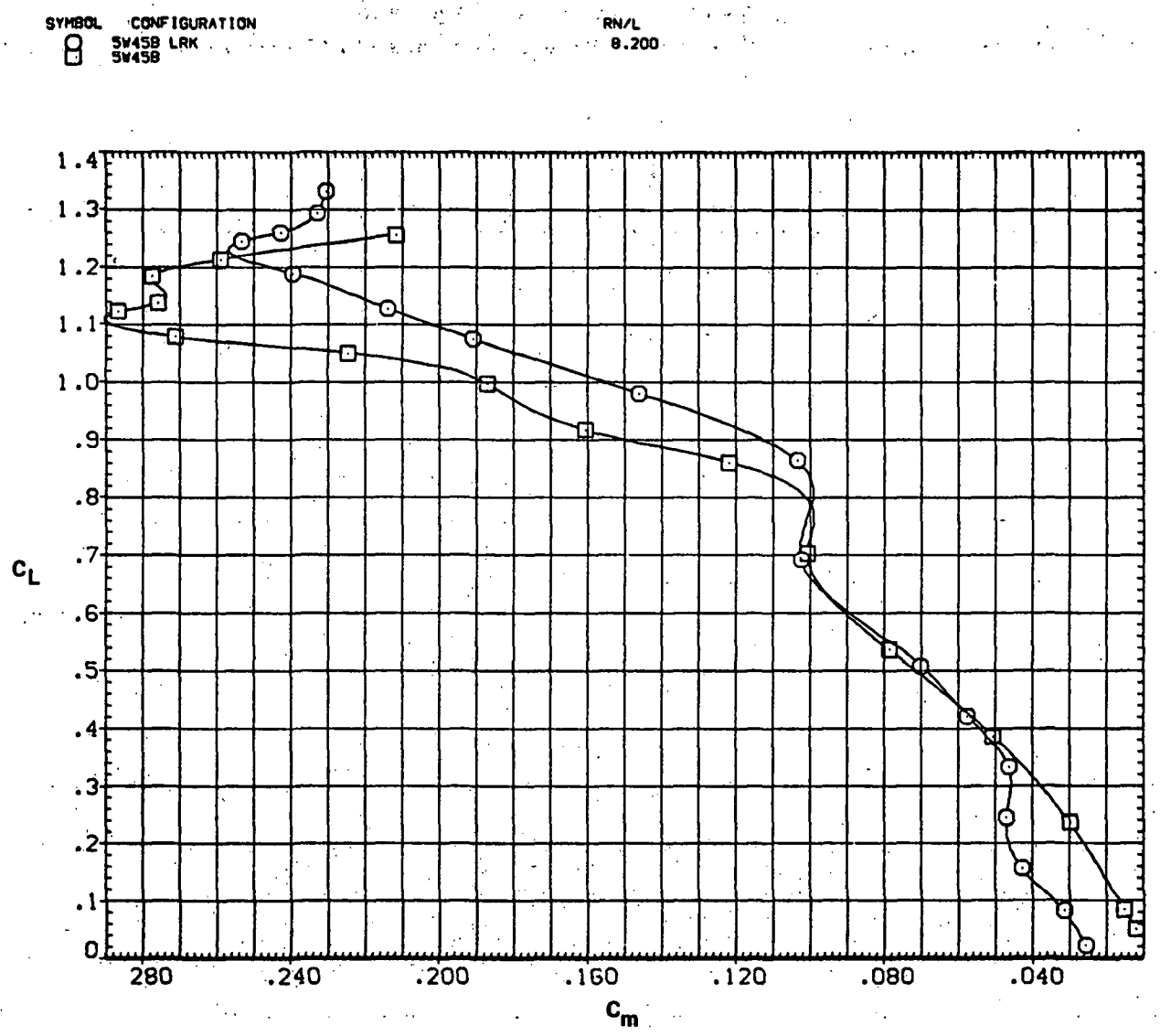

(b) C_L vs C_m

Figure 9.– Continued.

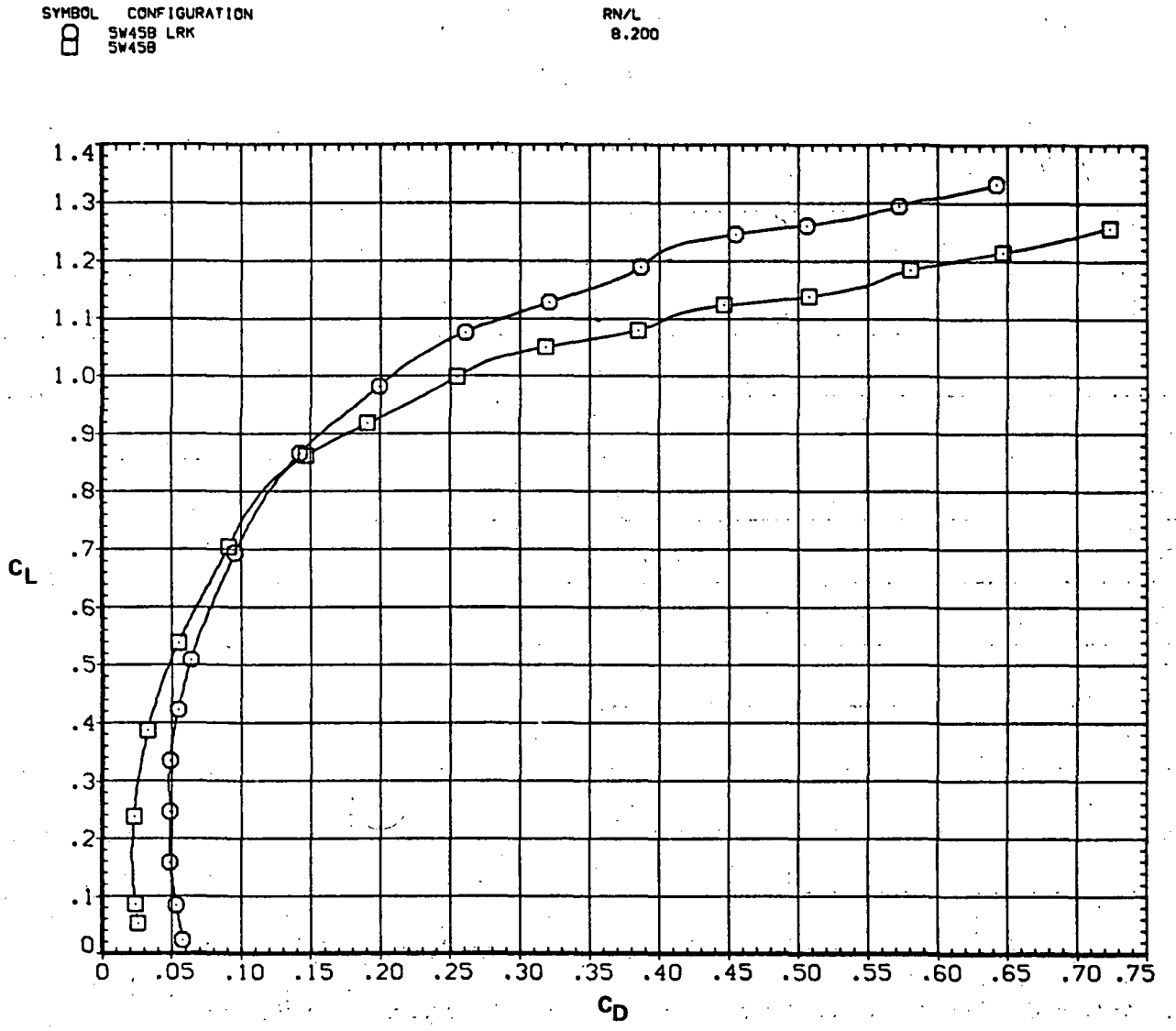

(c) C_L vs C_D

Figure 9.– Continued.

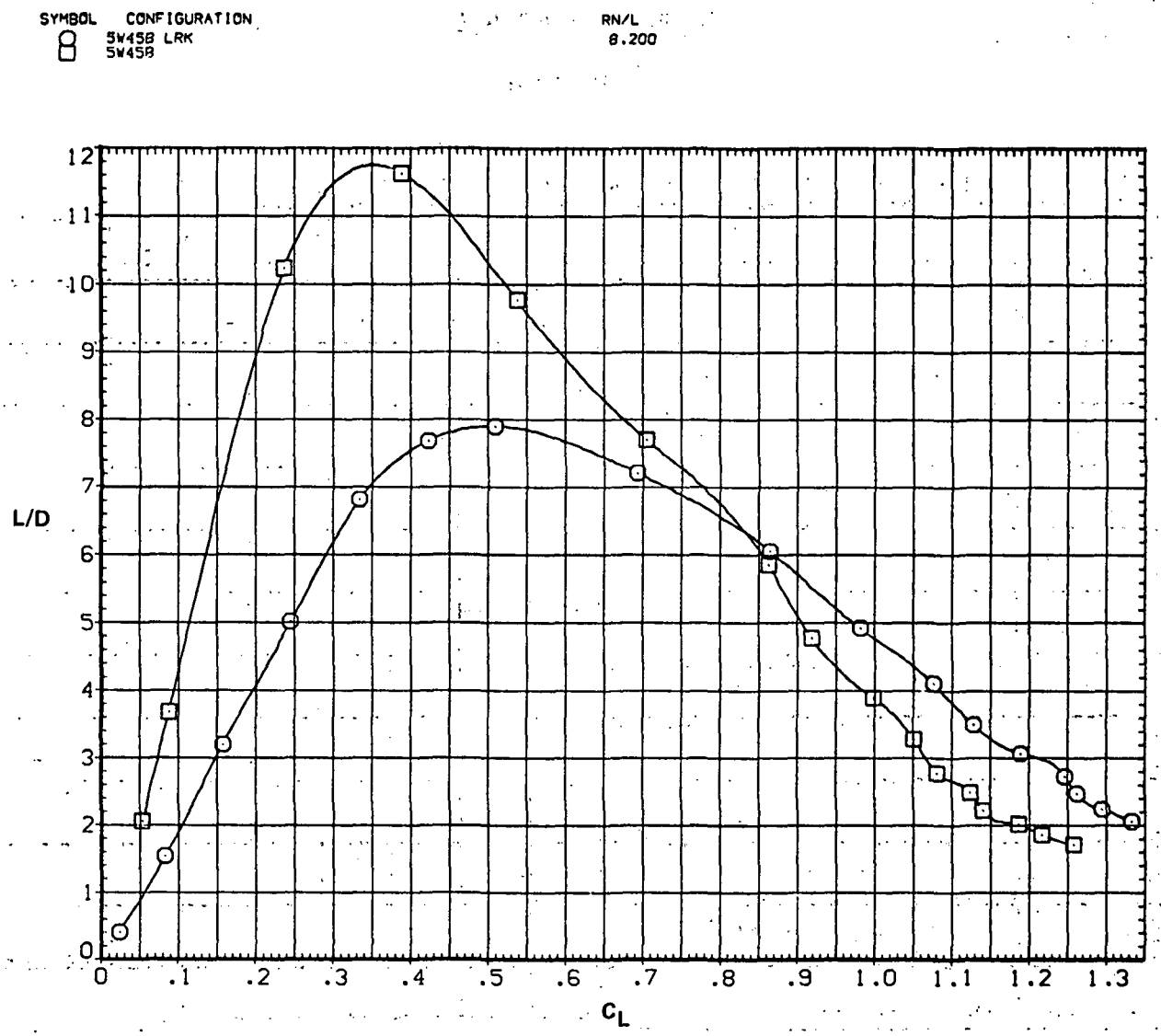

(d) L/D vs C_L

Figure 9.– Continued.

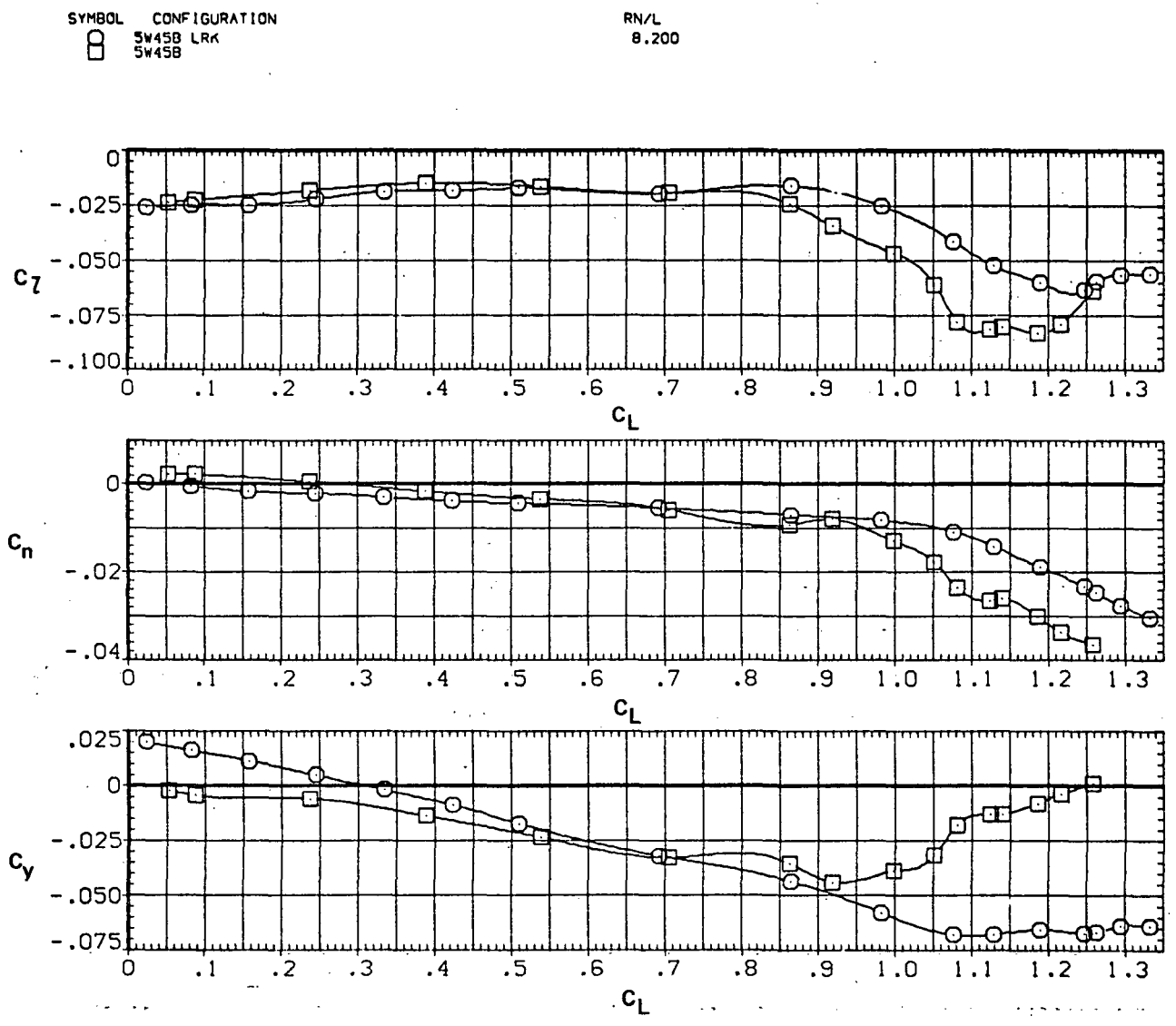

(e) C_l, C_n, and C_Y vs C_L

Figure 9.– Concluded.

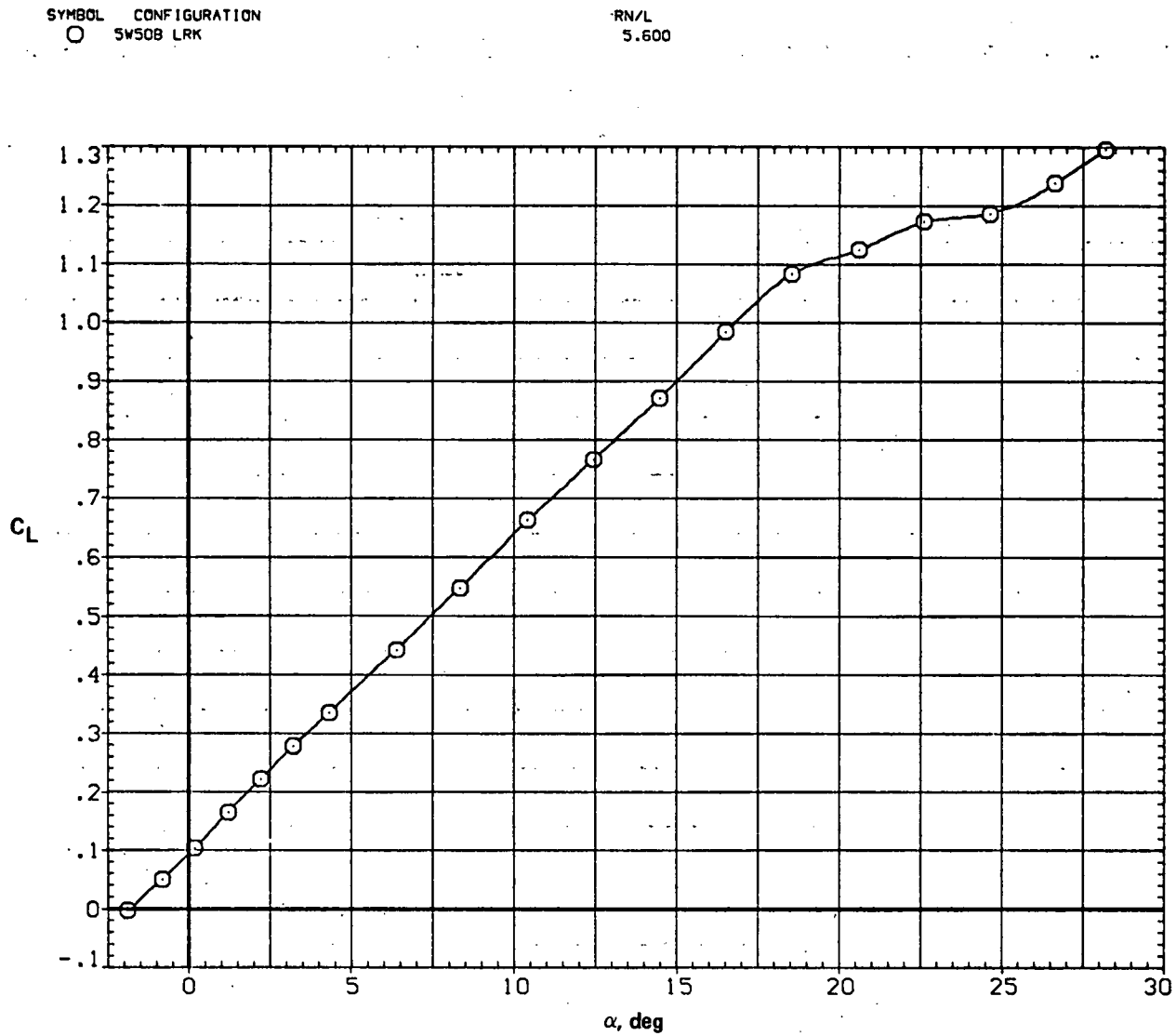

(a) C_L vs α

Figure 10.– Effect of having Krüger flaps on both wing panels on the static longitudinal characteristics of an oblique wing: $\Lambda = 50°$, $M = 0.25$.

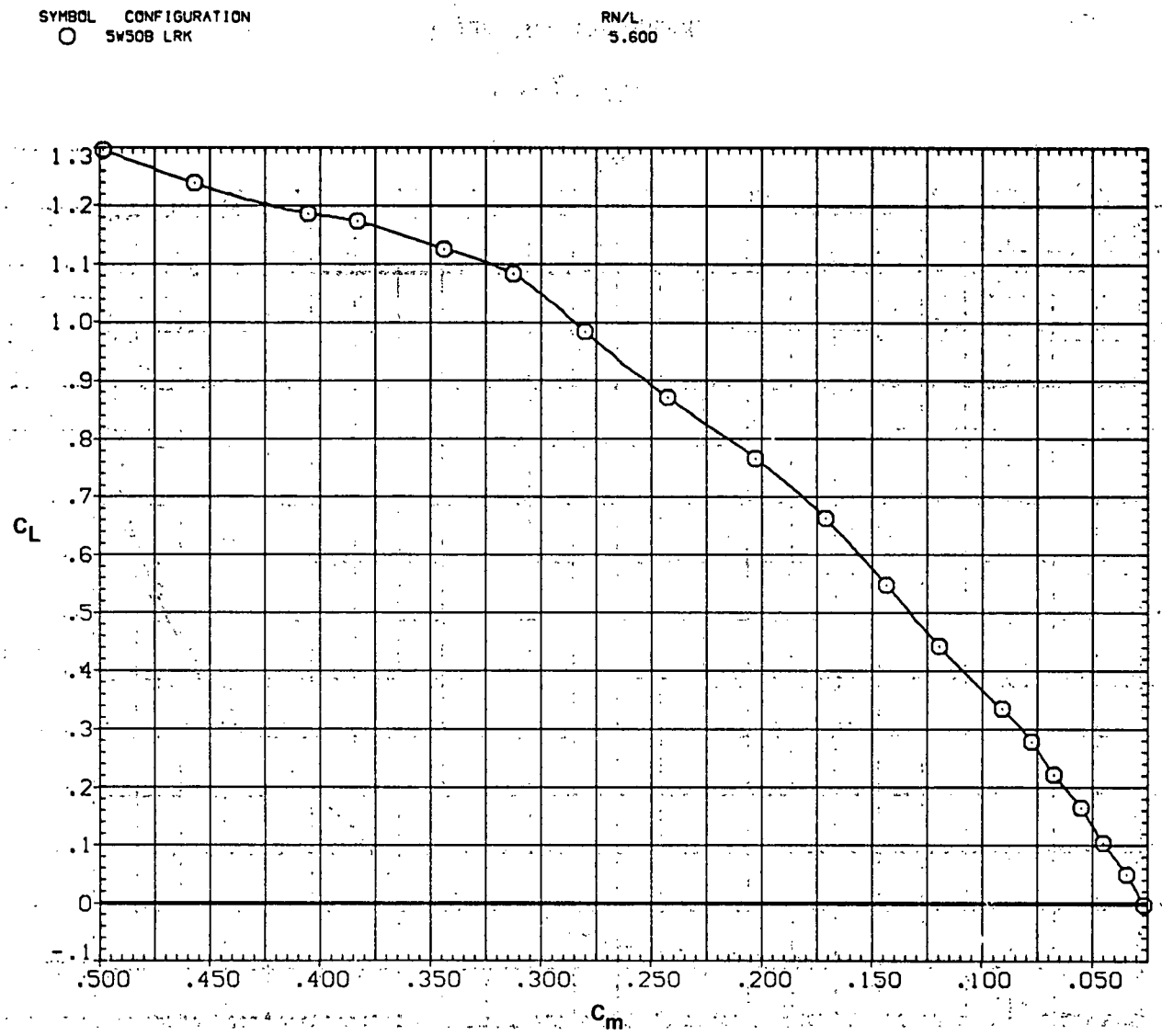

(b) C_L vs C_m

Figure 10.– Continued.

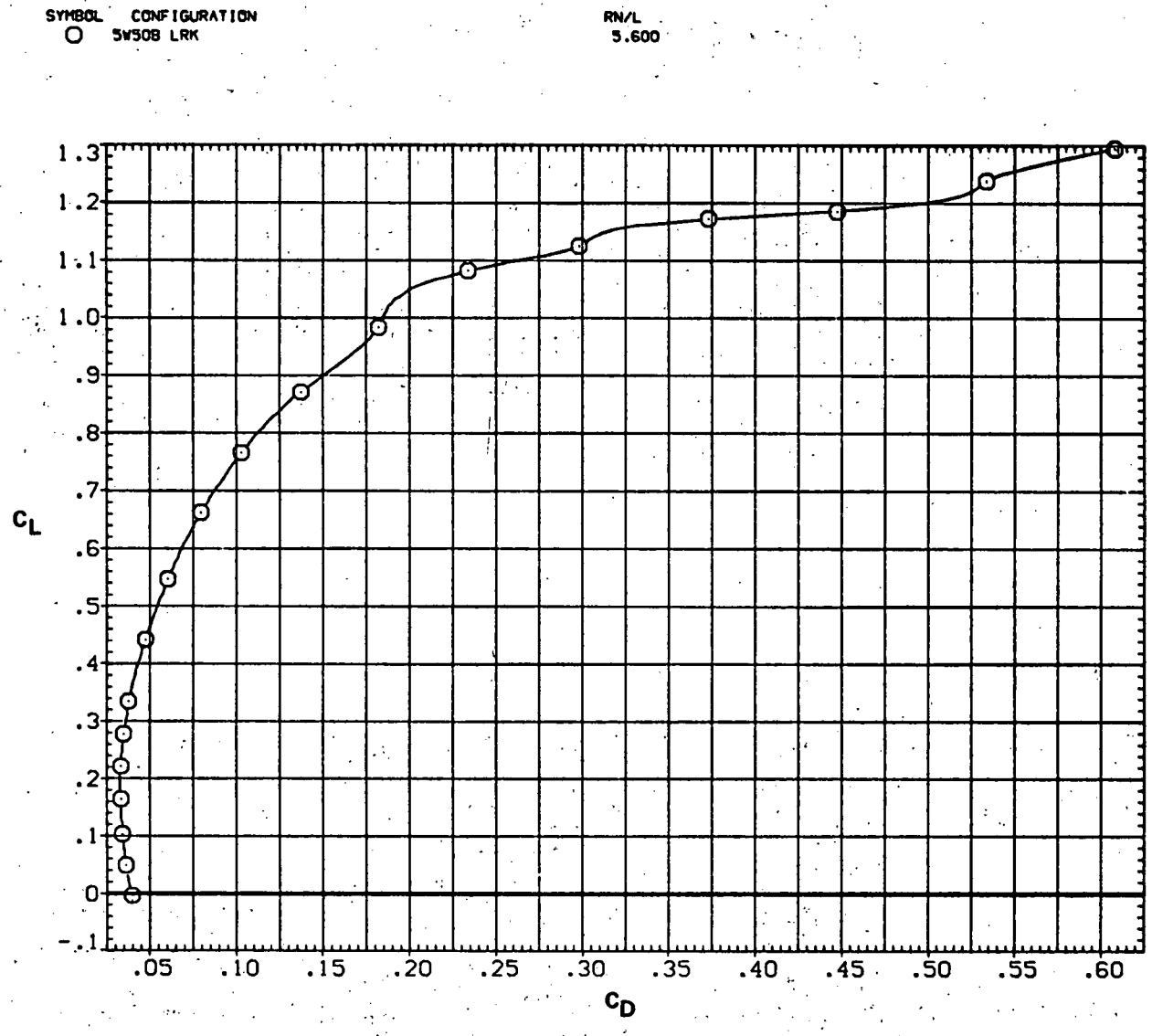

(c) C_L vs C_D

Figure 10.– Continued.

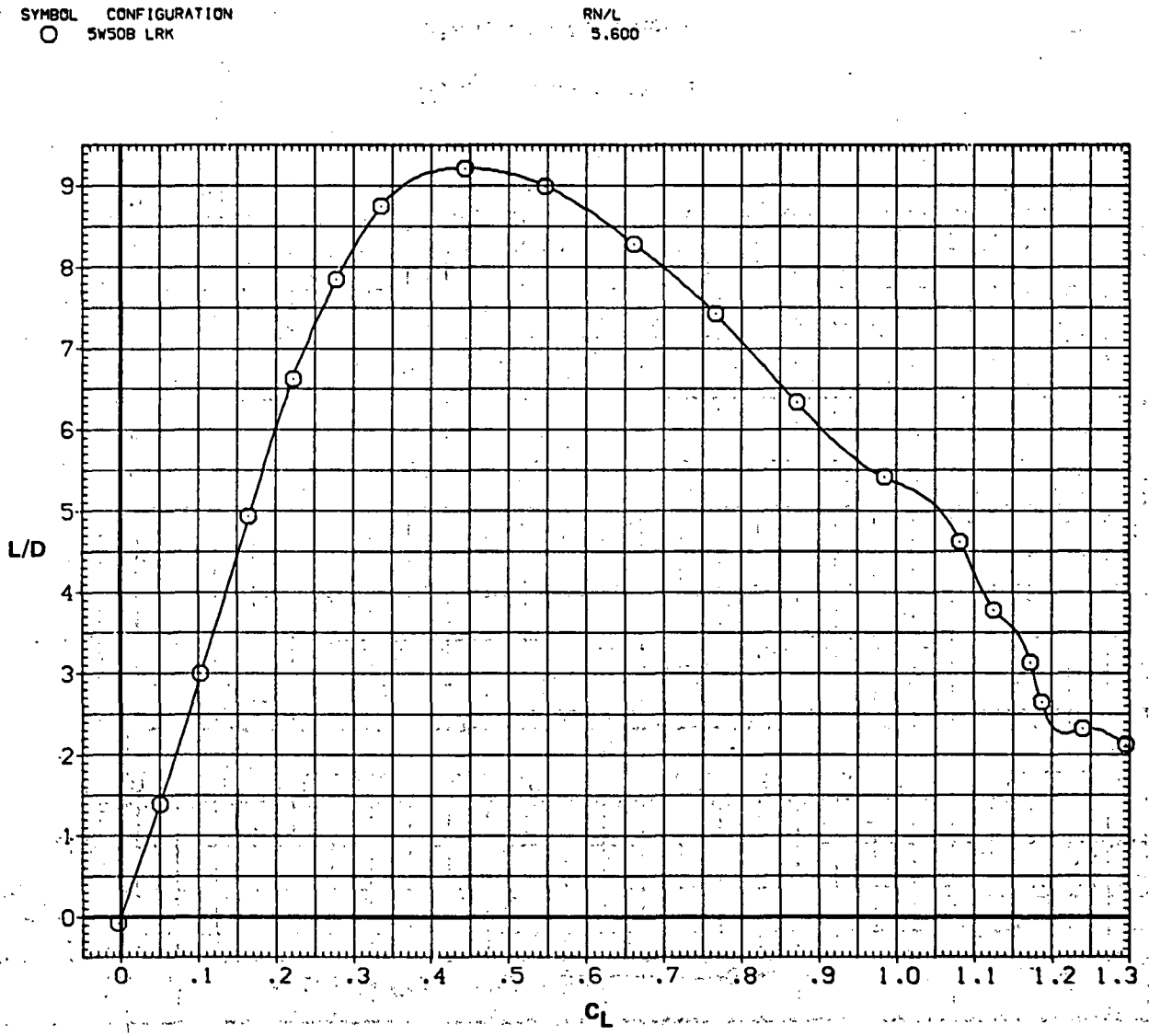

(d) L/D vs C_L

Figure 10.– Continued.

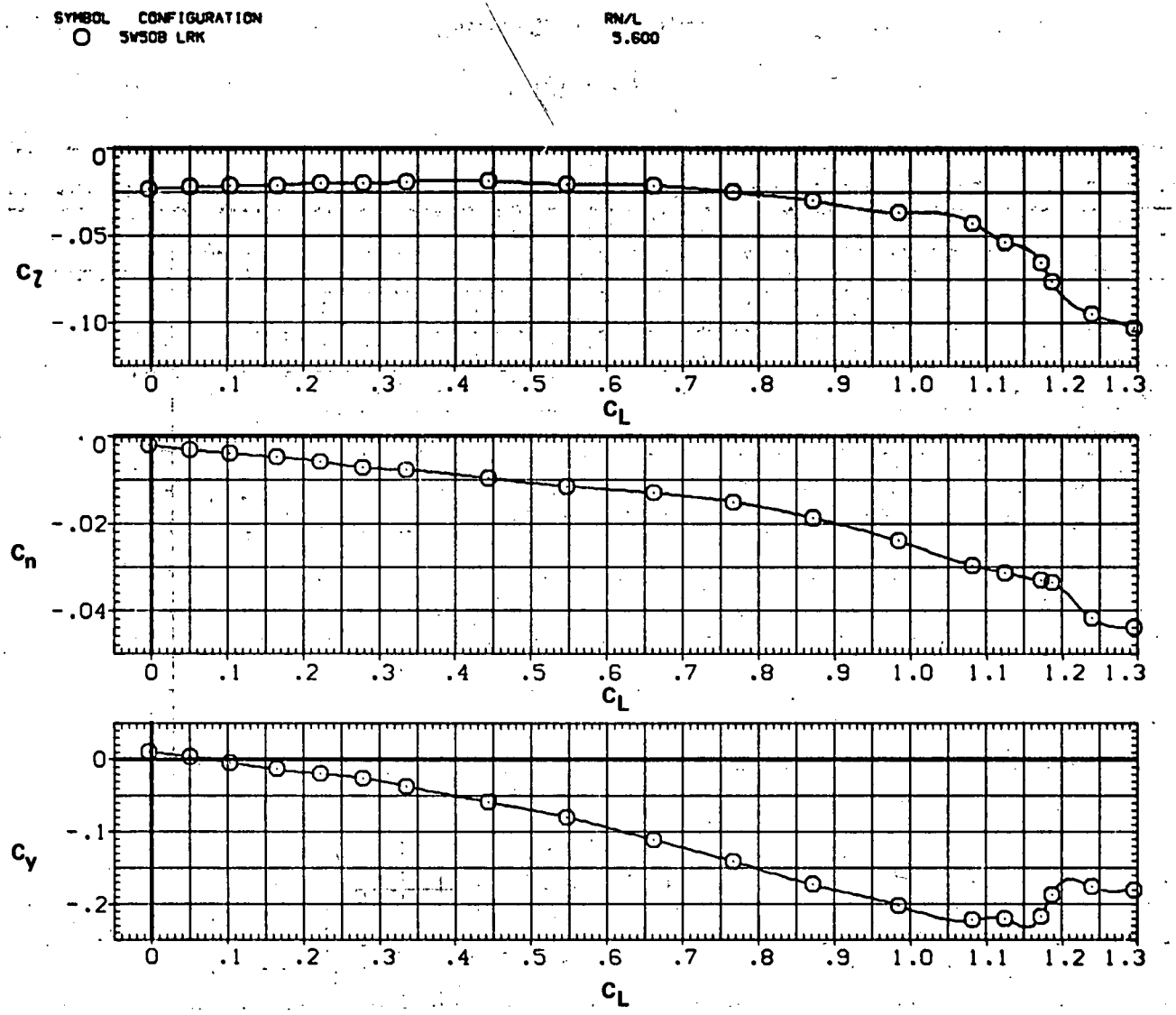

(e) C_l, C_n, and C_Y vs C_L

Figure 10.– Concluded.

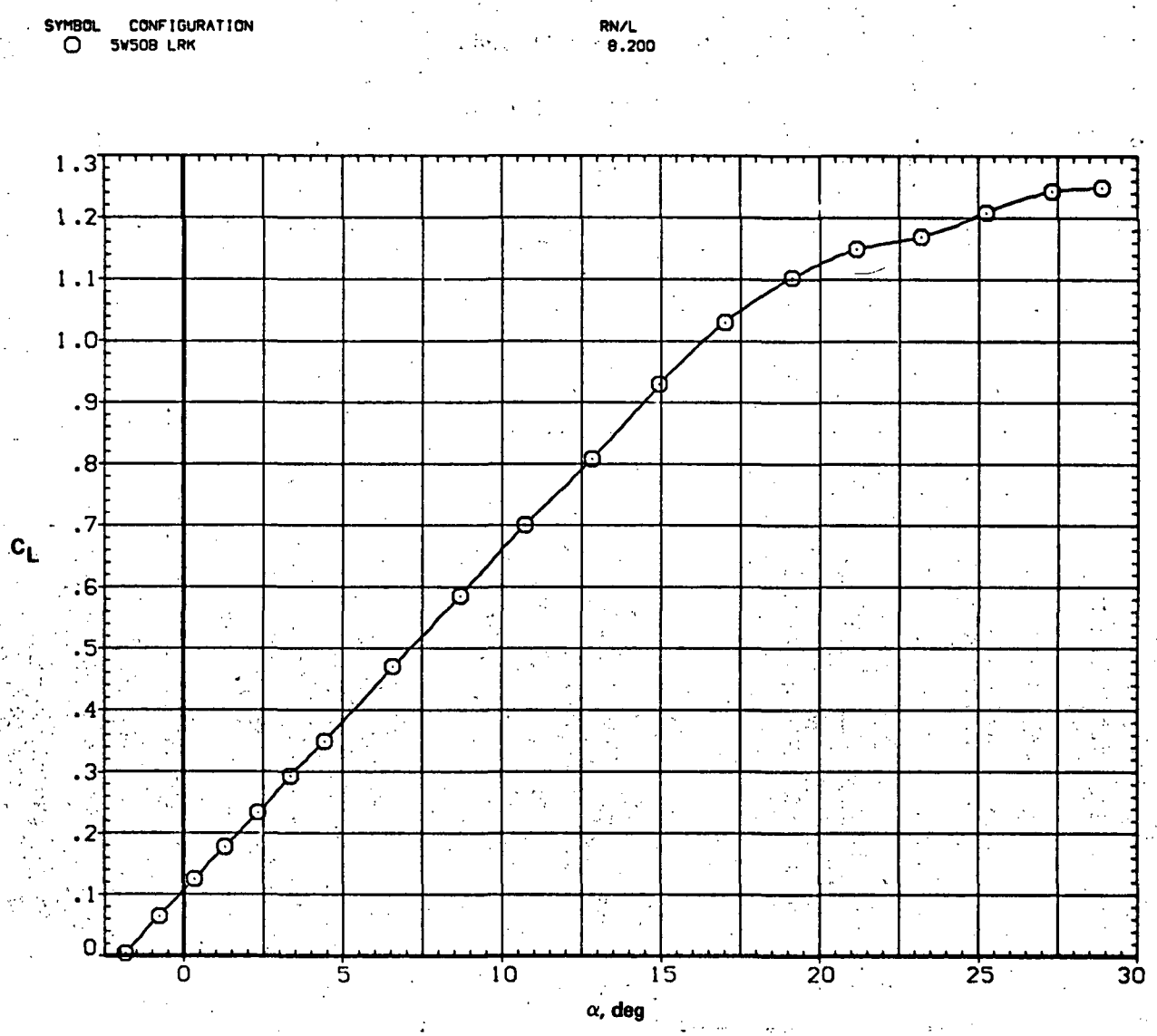

(a) C_L vs α

Figure 11.– Effect of having Krüger flaps on both wing panels on the static longitudinal characteristics of an oblique wing: $\Lambda = 50°$, $M = 0.40$.

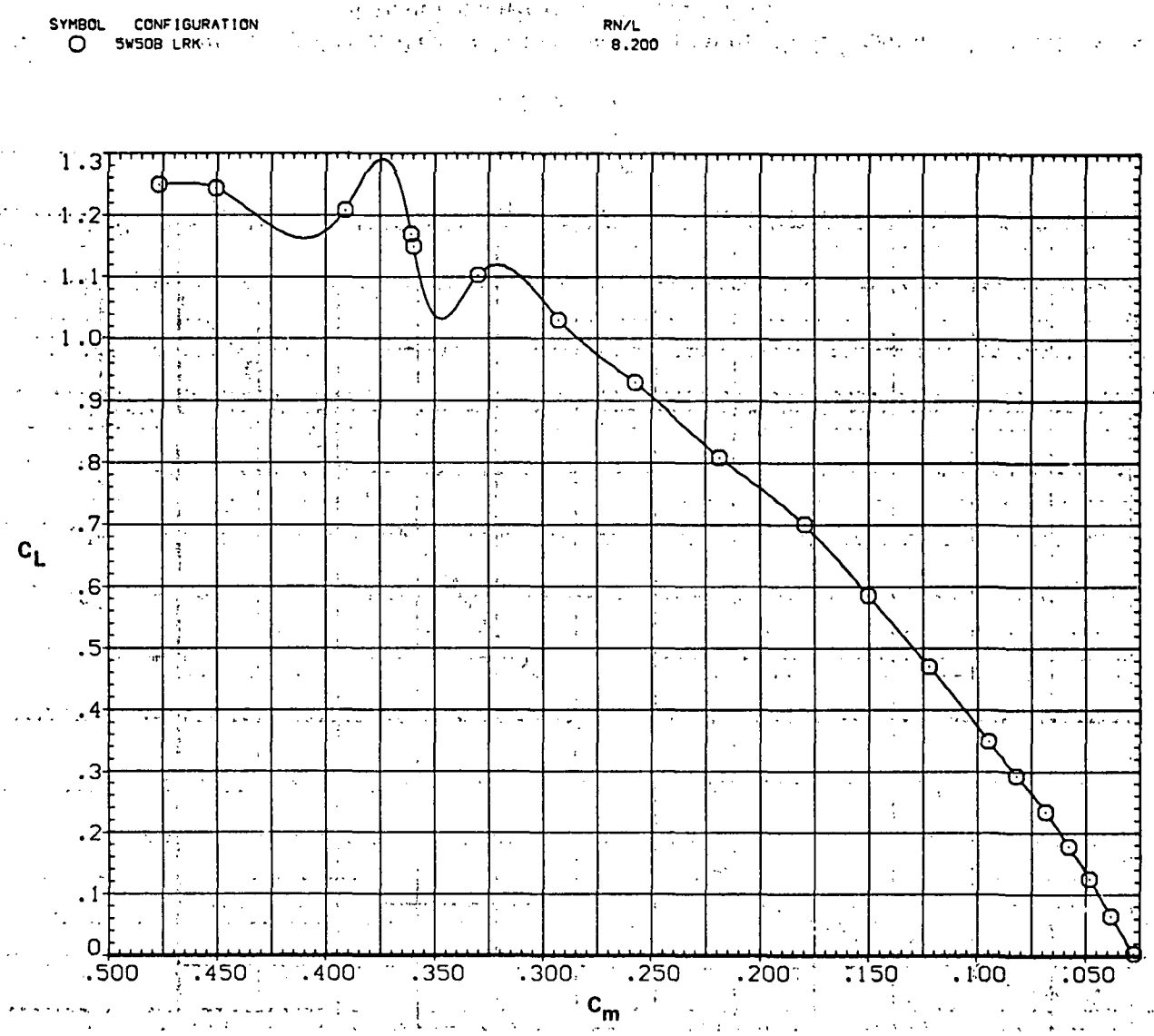

(b) C_L vs C_m

Figure 11.– Continued.

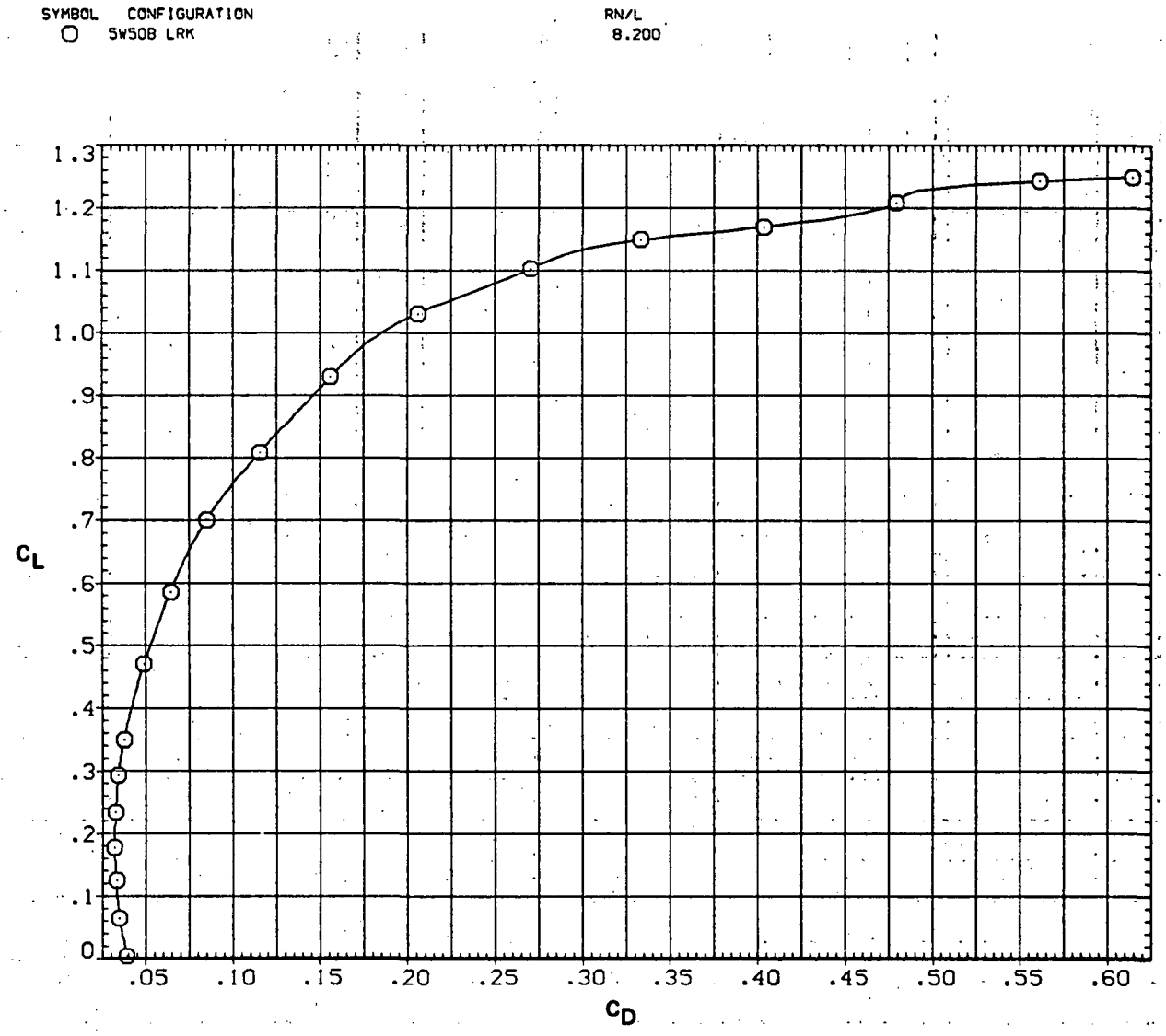

(c) C_L vs C_D

Figure 11.– Continued.

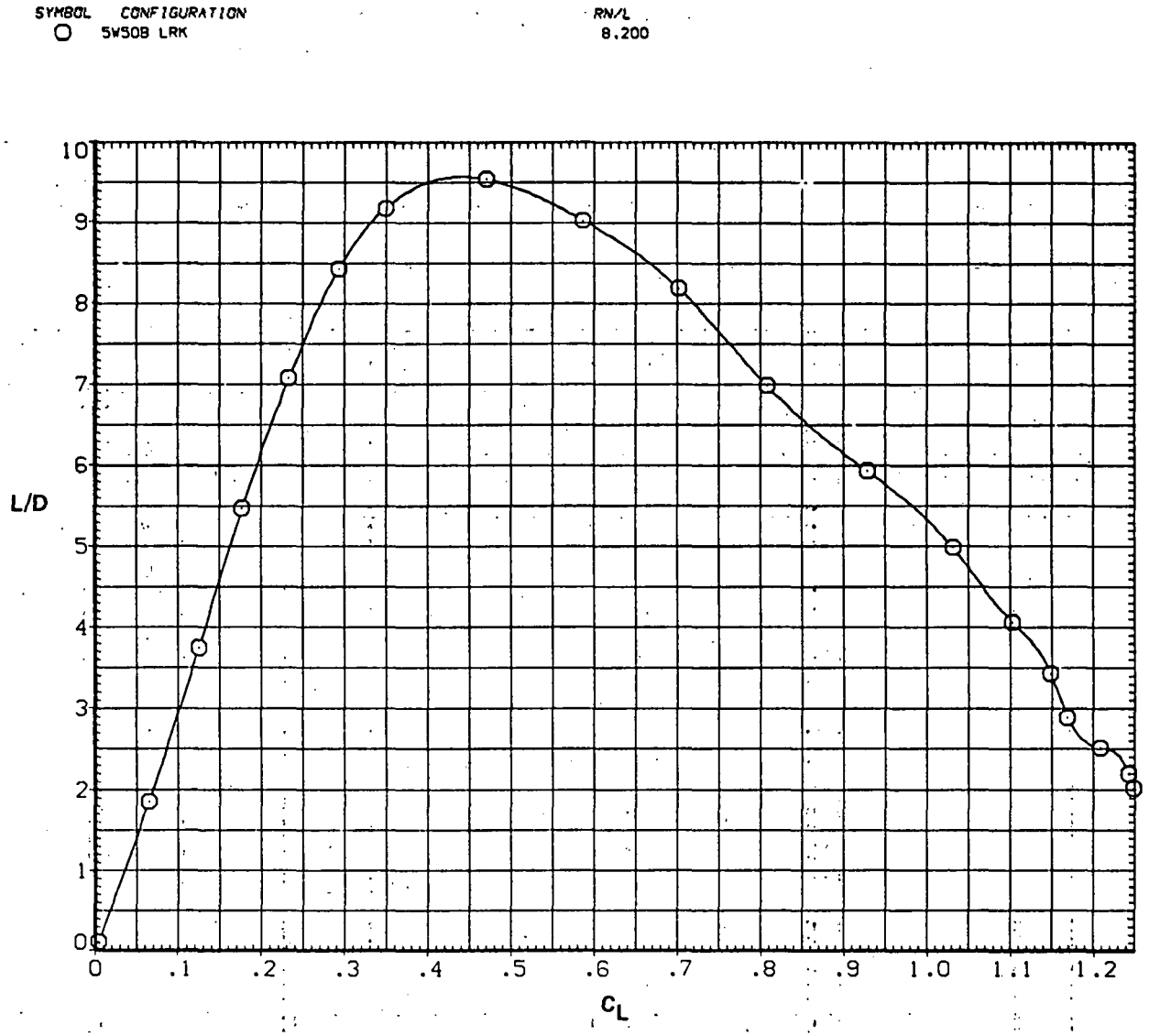

(d) L/D vs C_L

Figure 11.– Continued.

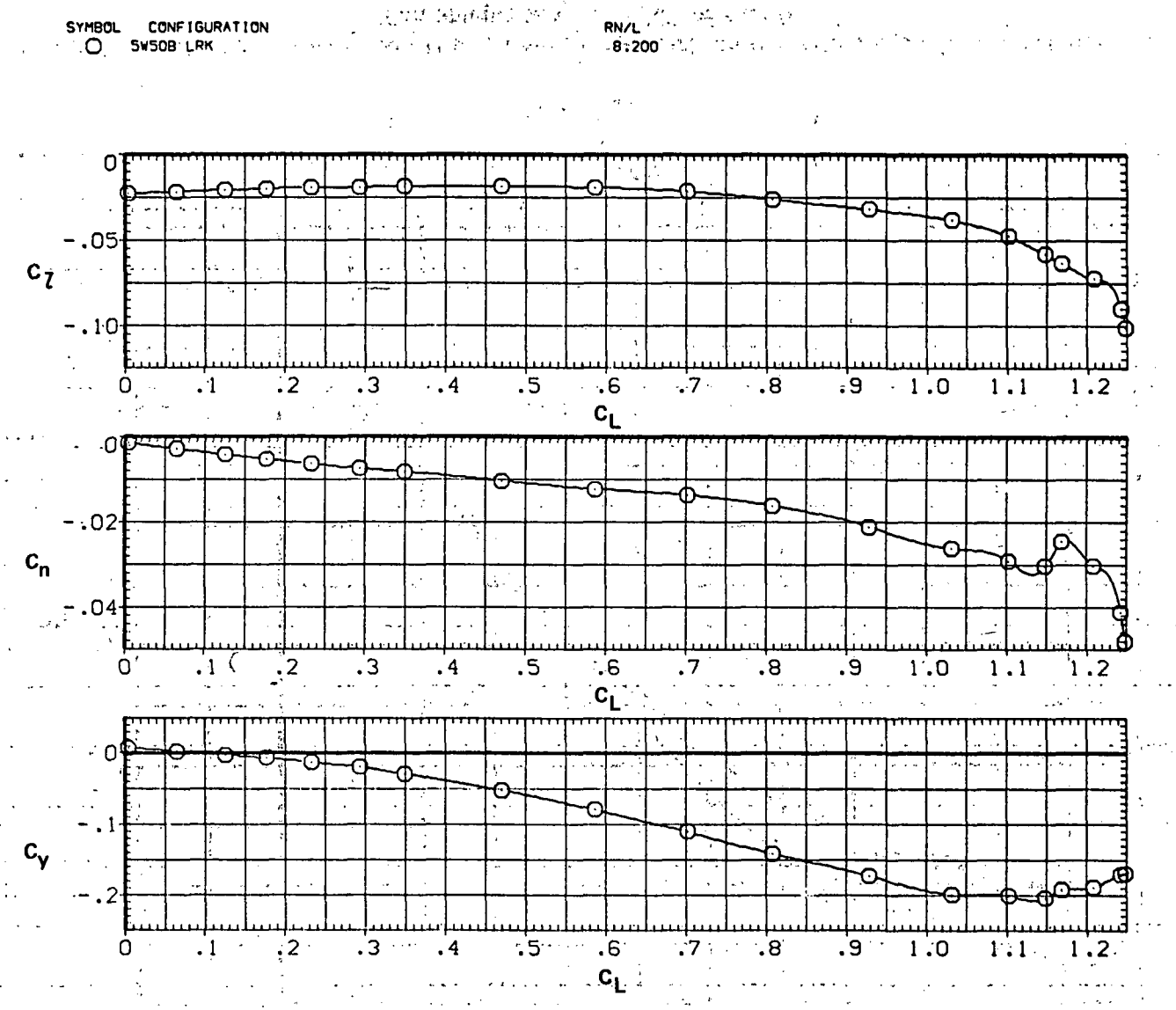

(e) C_l, C_n, and C_Y vs C_L

Figure 11.– Concluded.

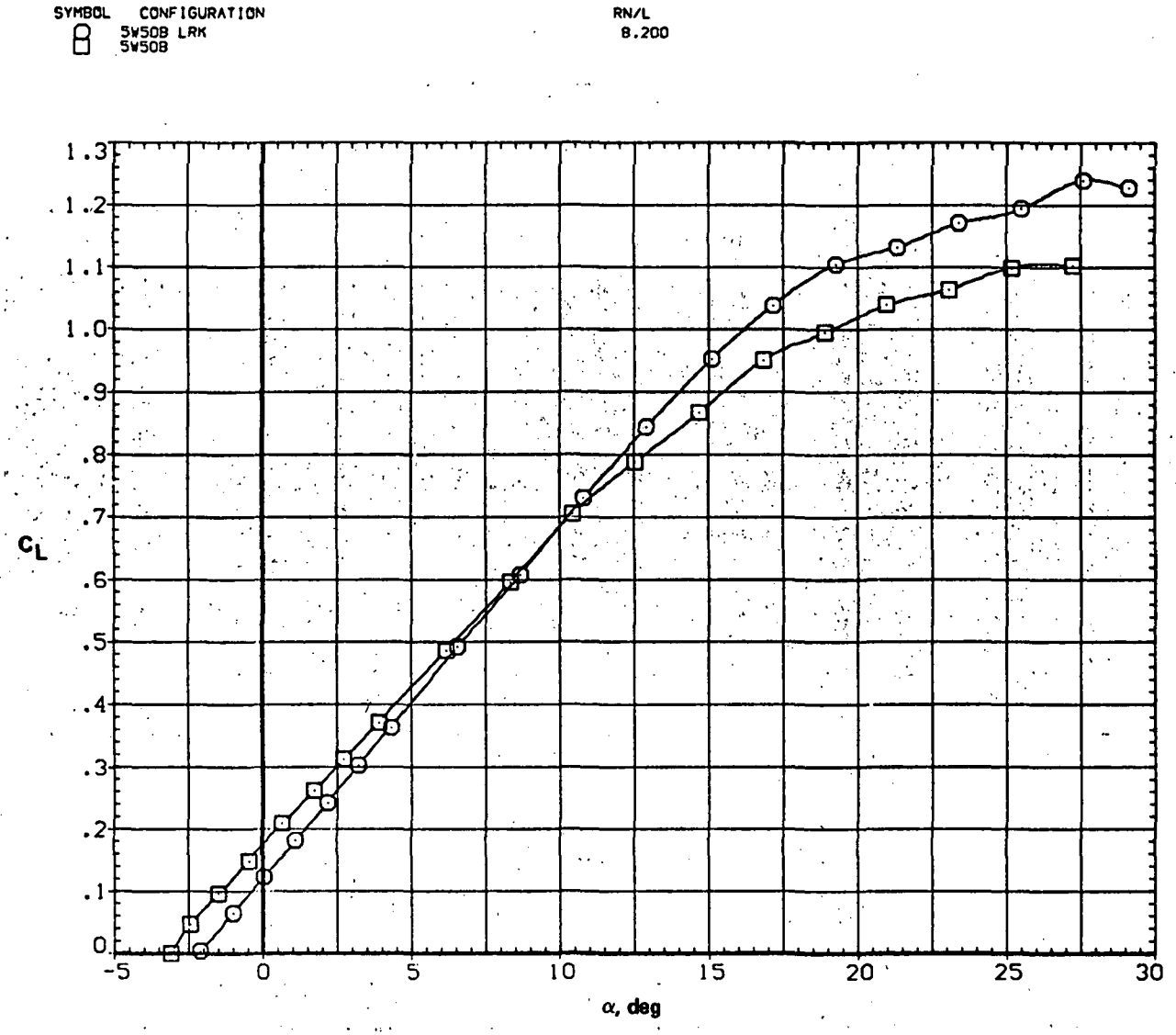

(a) C_L vs α

Figure 12.– Effect of having Krüger flaps on both wing panels on the static longitudinal characteristics of an oblique wing: $\Lambda = 50°$, $M = 0.60$.

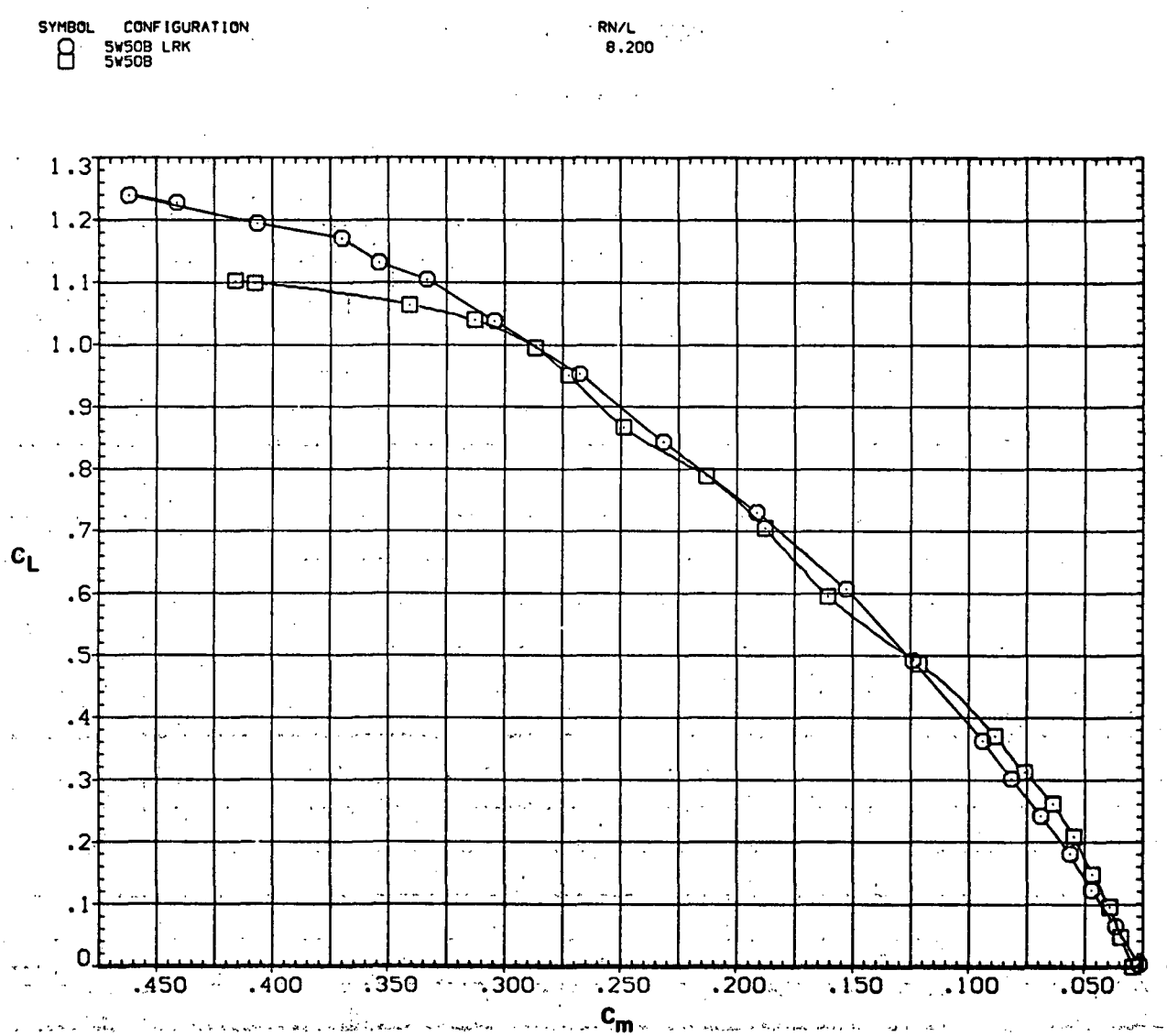

(b) C_L vs C_m

Figure 12.– Continued.

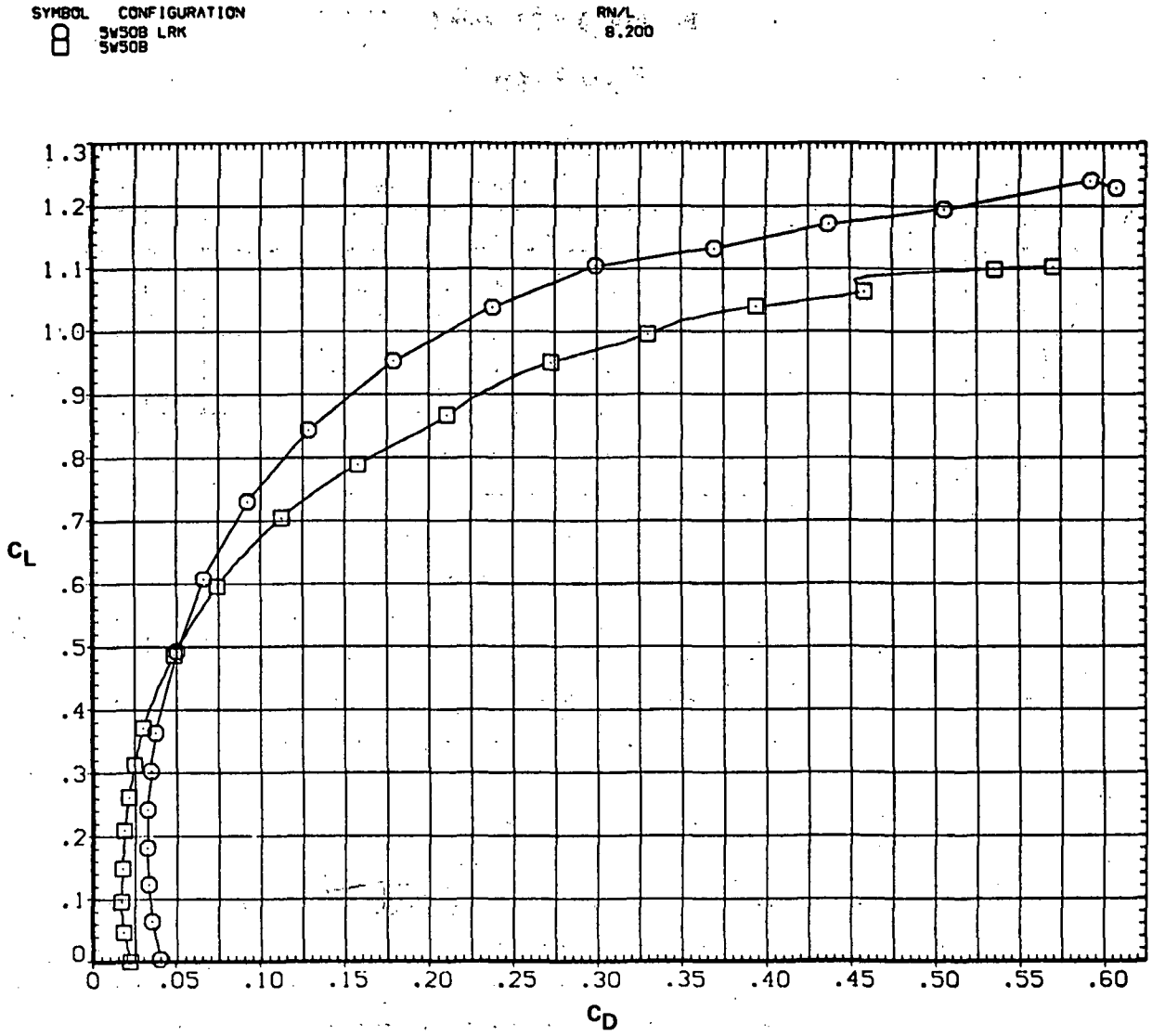

(c) C_L vs C_D

Figure 12.– Continued.

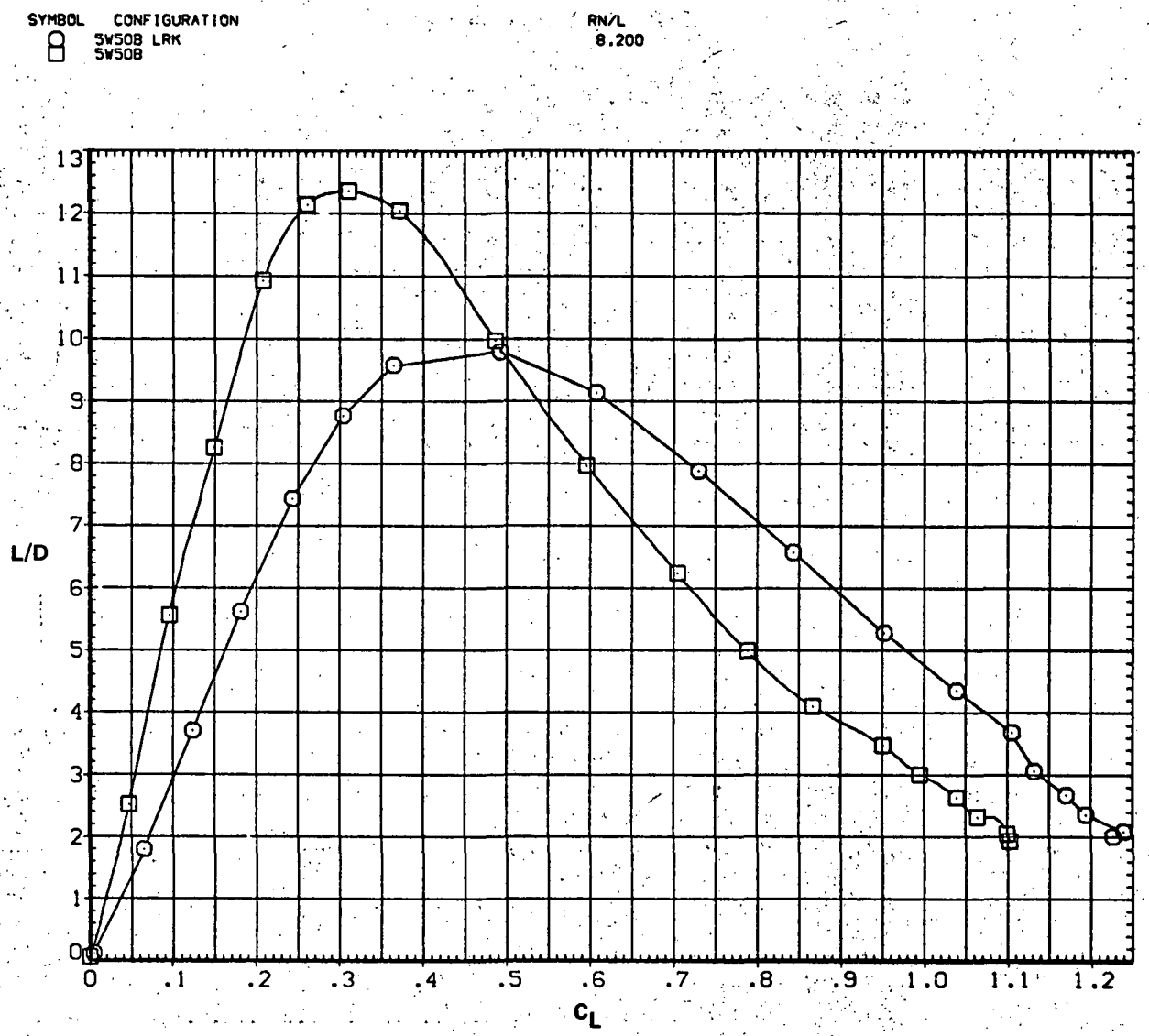

(d) L/D vs C_L

Figure 12.– Continued.

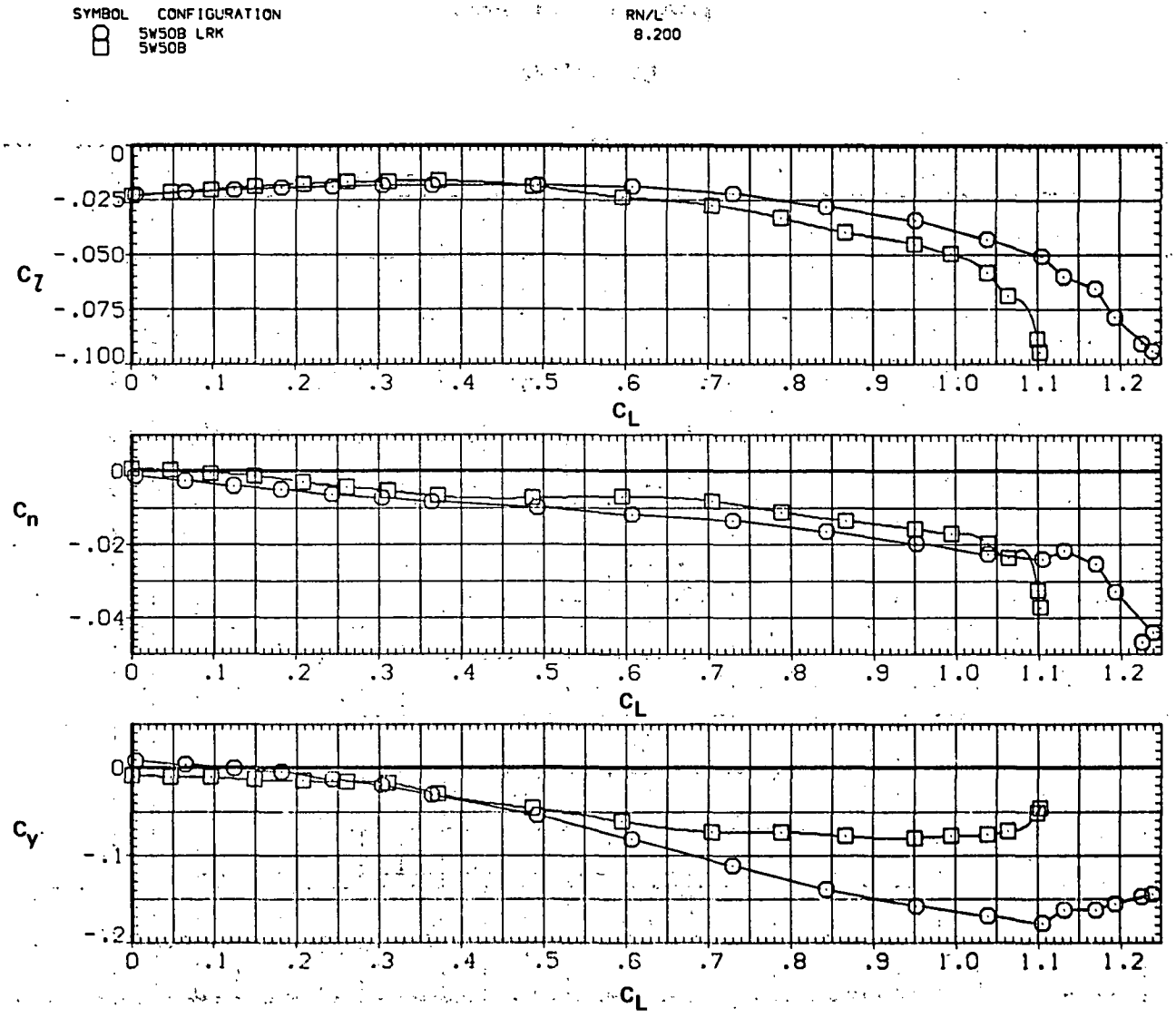

(e) C_l, C_n, and C_Y vs C

Figure 12.– Concluded.

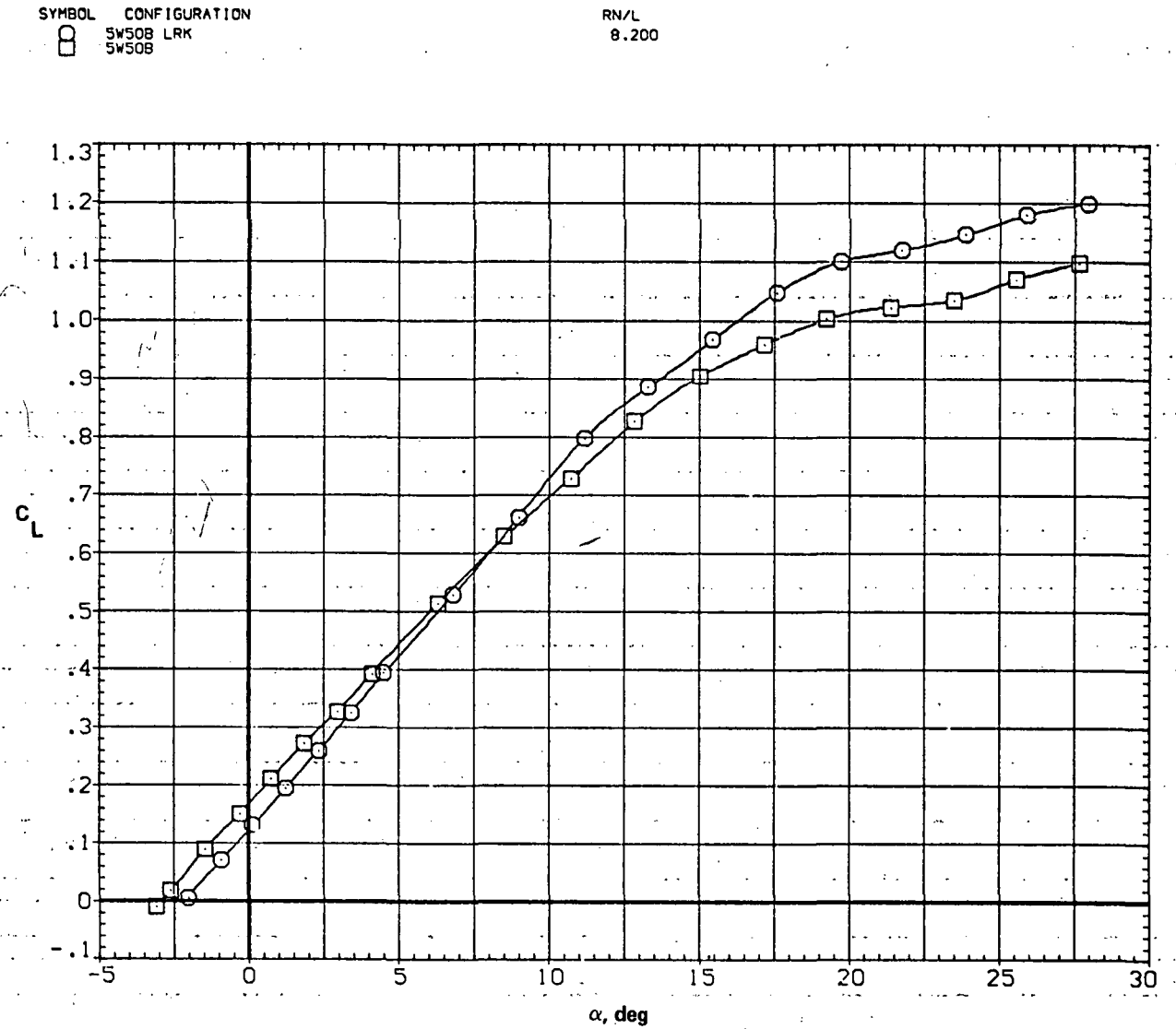

(a) C_L vs α

Figure 13.– Effect of having Krüger flaps on both wing panels on the static longitudinal characteristics of an oblique wing: $\Lambda = 50°$, $M = 0.80$.

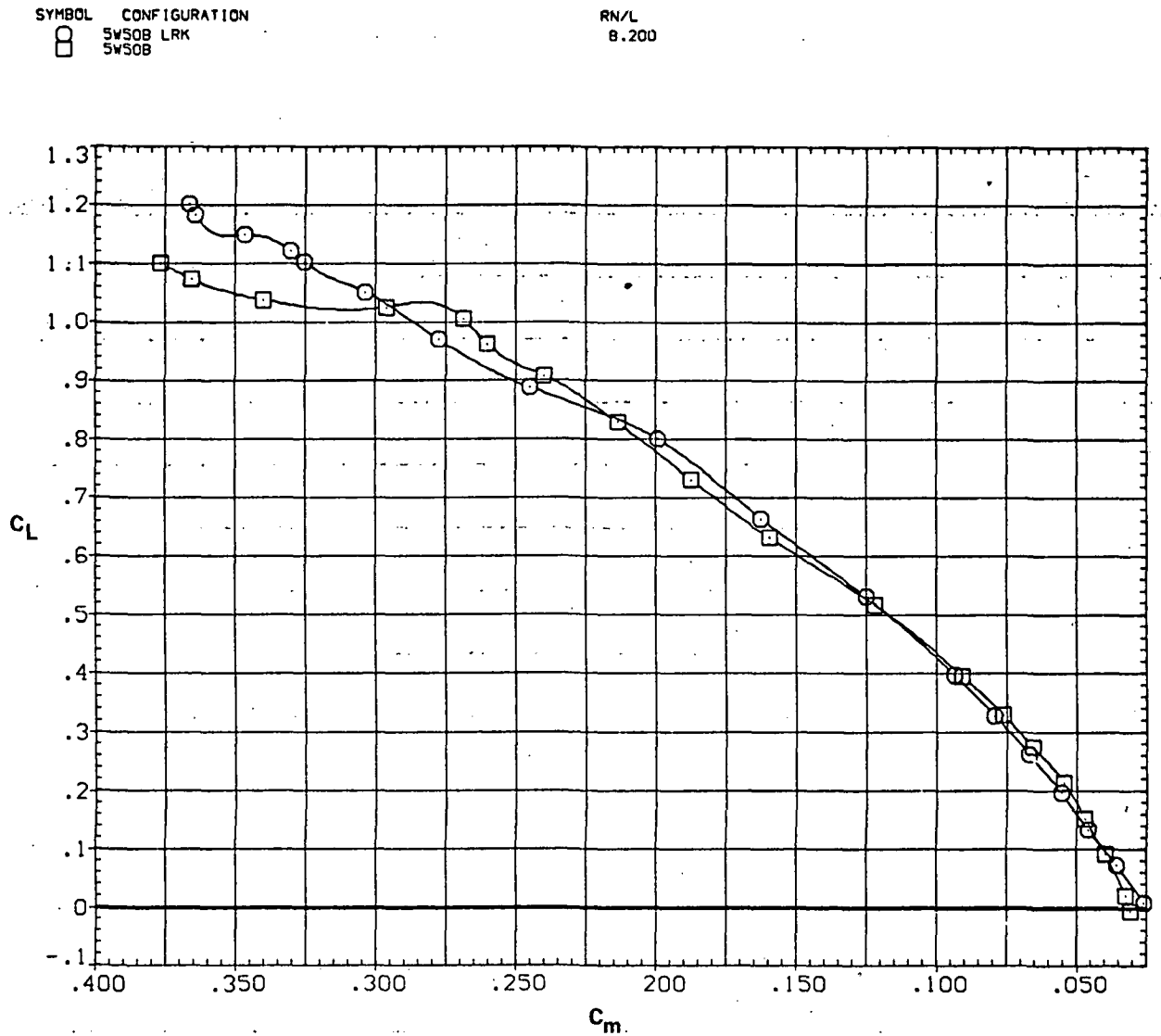

(b) C_L vs C_m

Figure 13.– Continued.

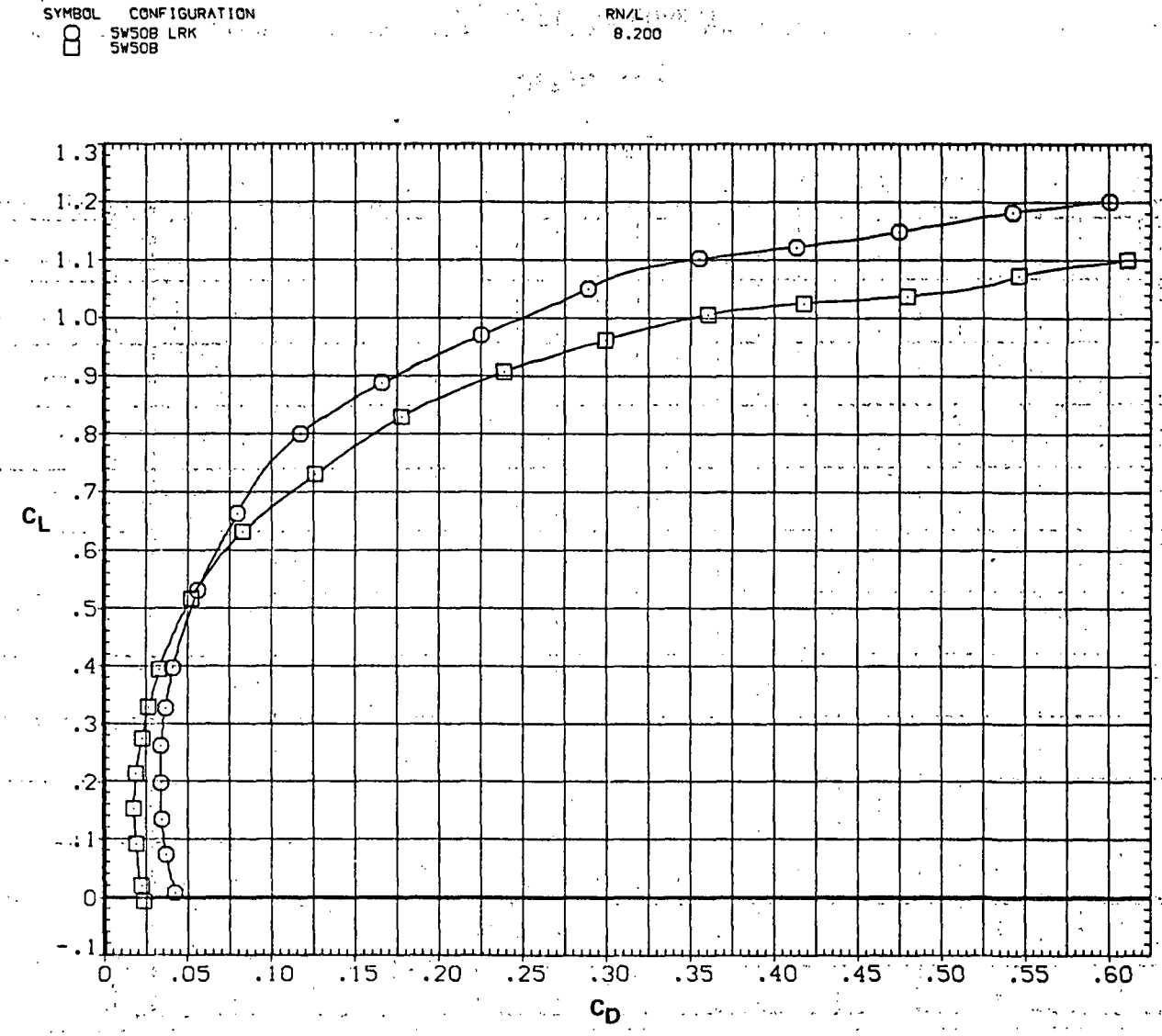

(c) C_L vs C_D

Figure 13.– Continued.

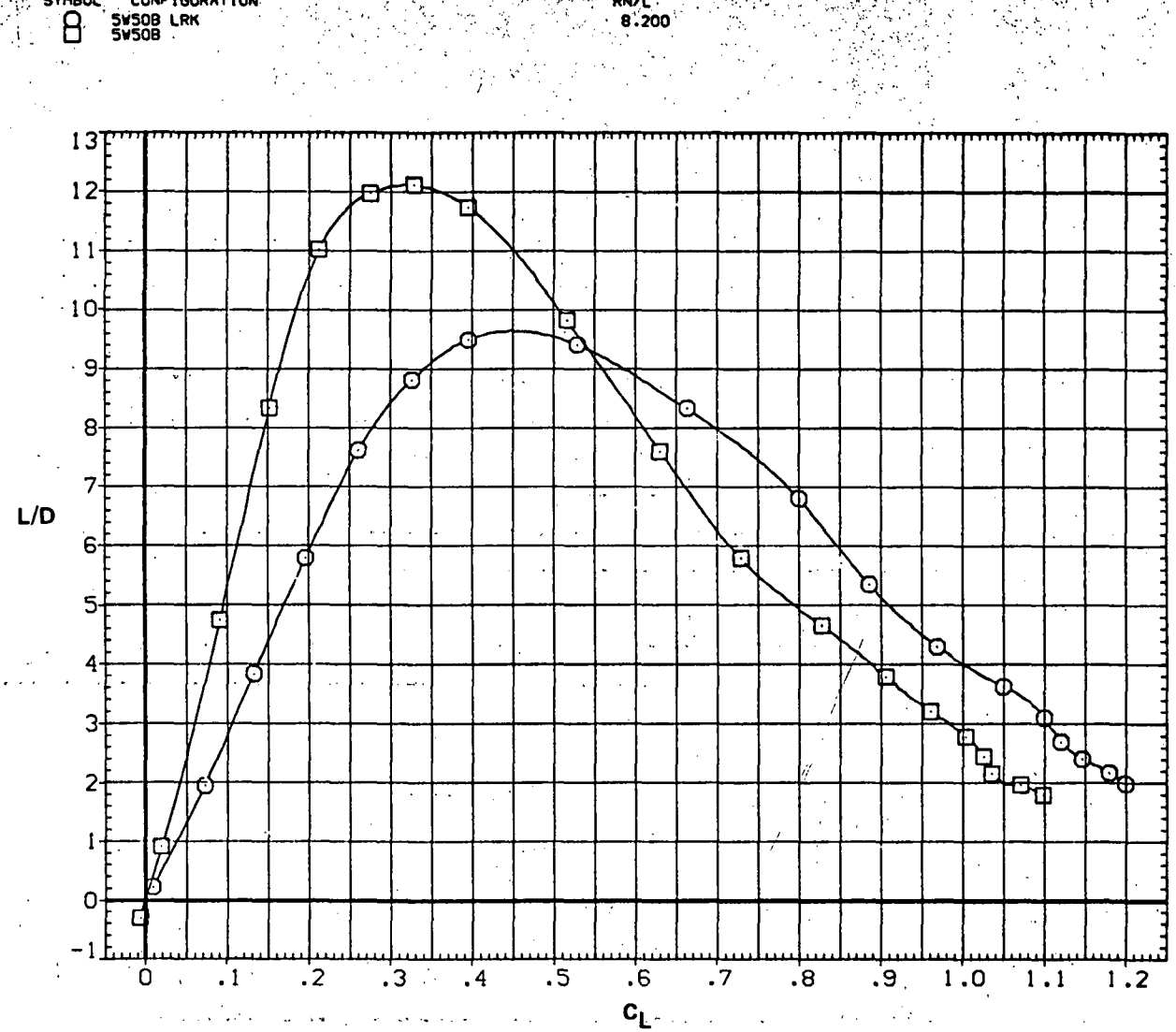

(d) L/D vs C_L

Figure 13.– Continued.

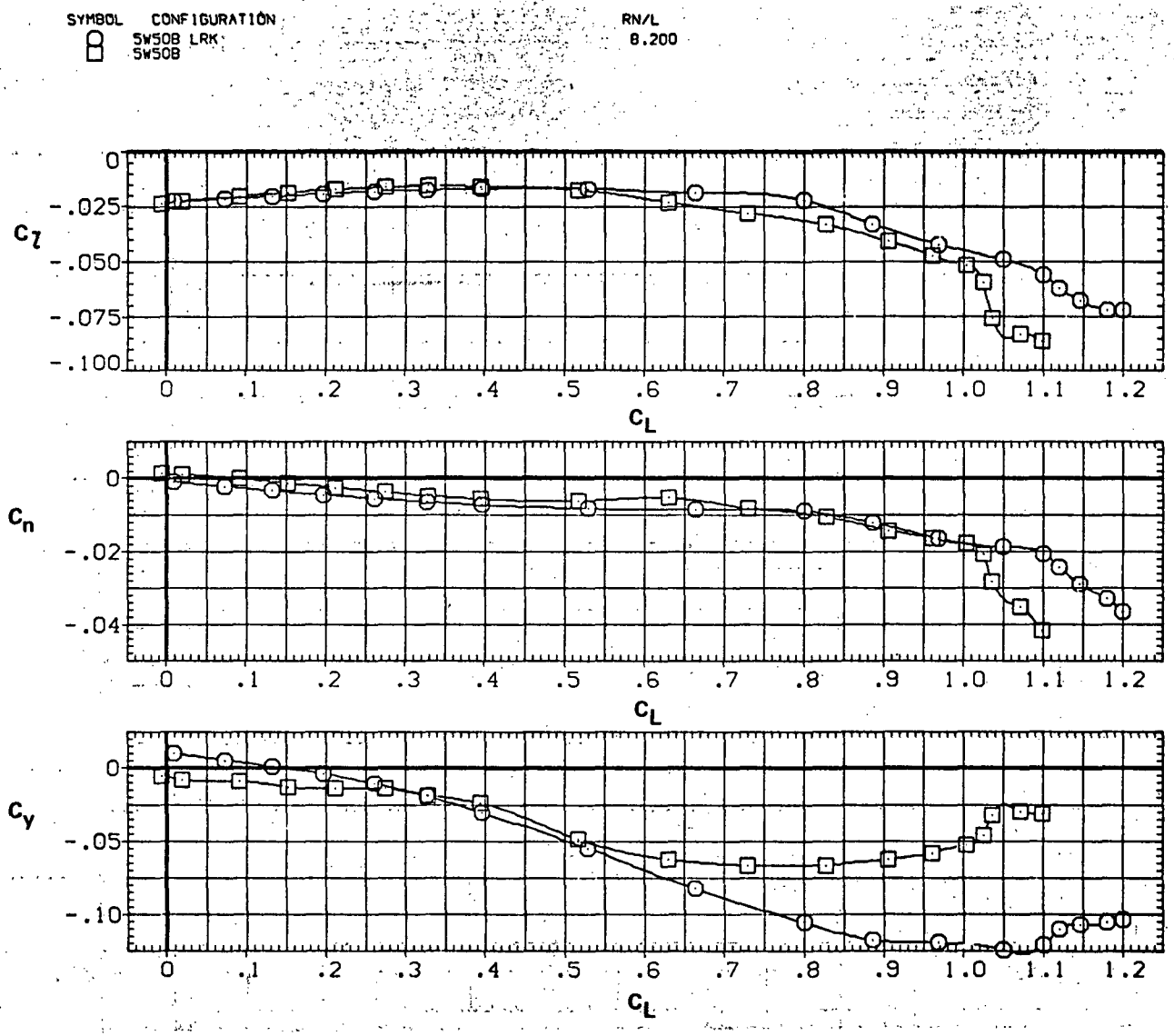

(e) C_l, C_n, and C_Y vs C_L

Figure 13.– Concluded.

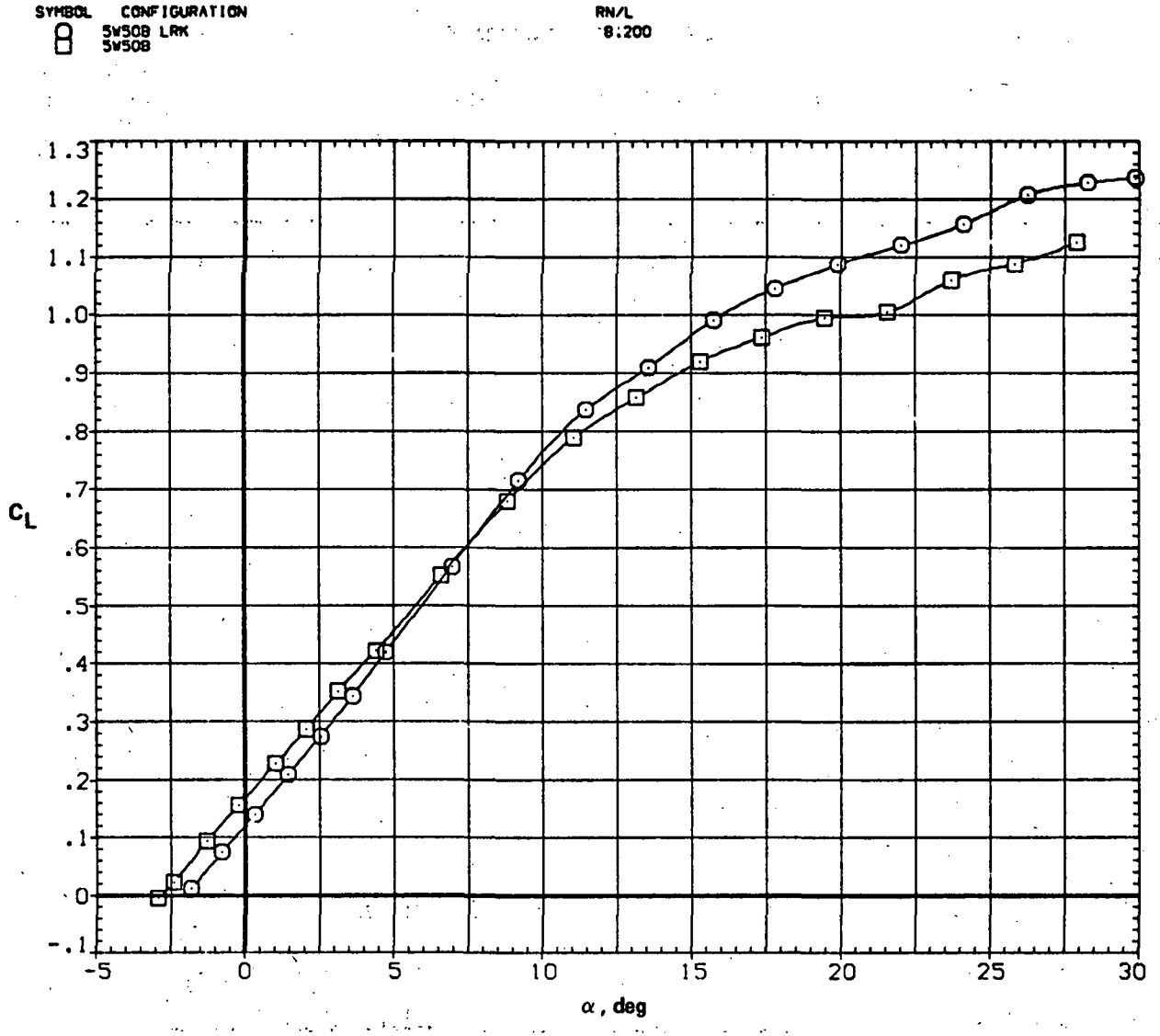

(a) C_L vs α

Figure 14.– Effect of having Krüger flaps on both wing panels on the static longitudinal characteristics of an oblique wing: $\Lambda = 50°$, $M = 0.90$.

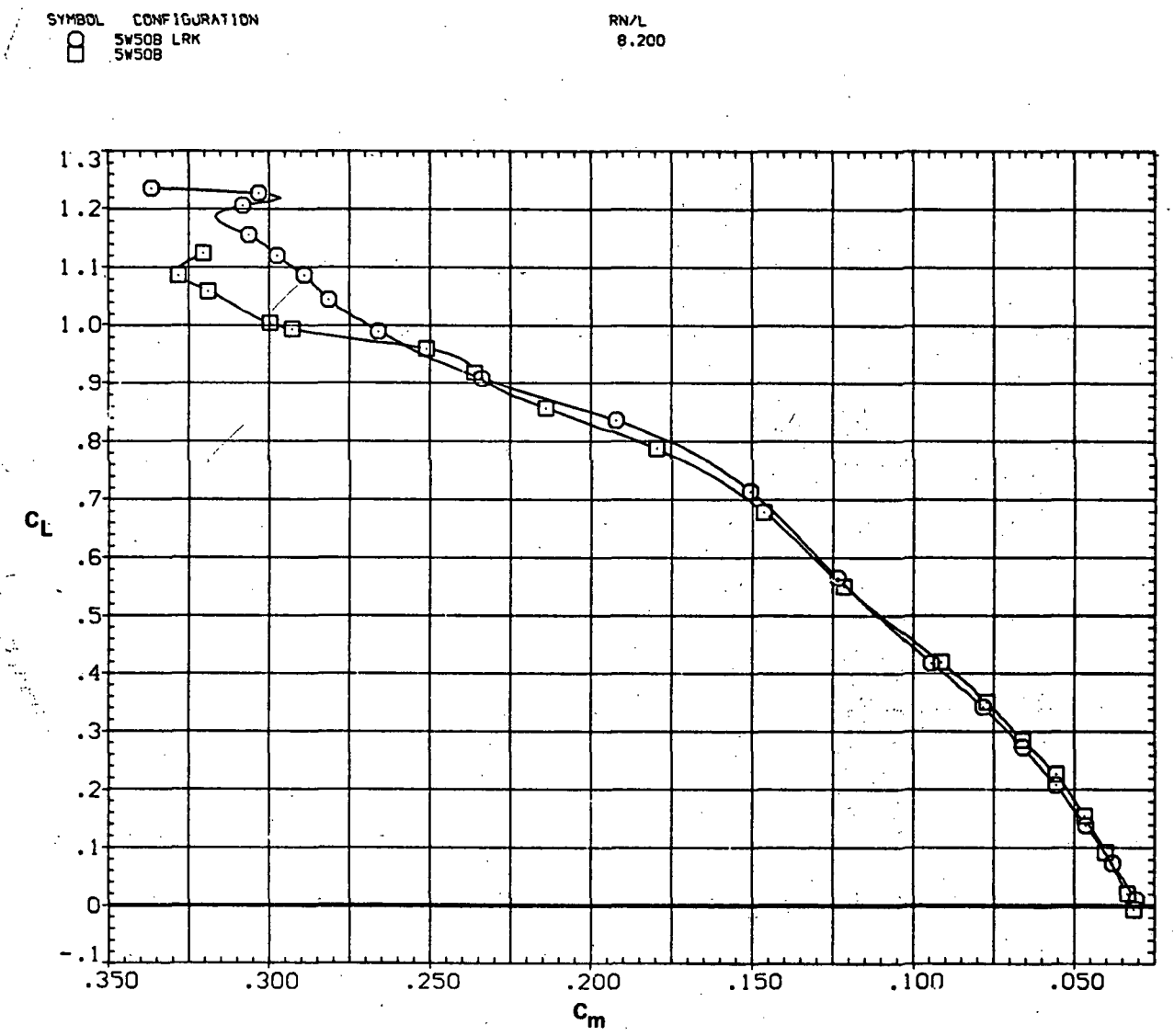

(b) C_L vs C_m

Figure 14.– Continued.

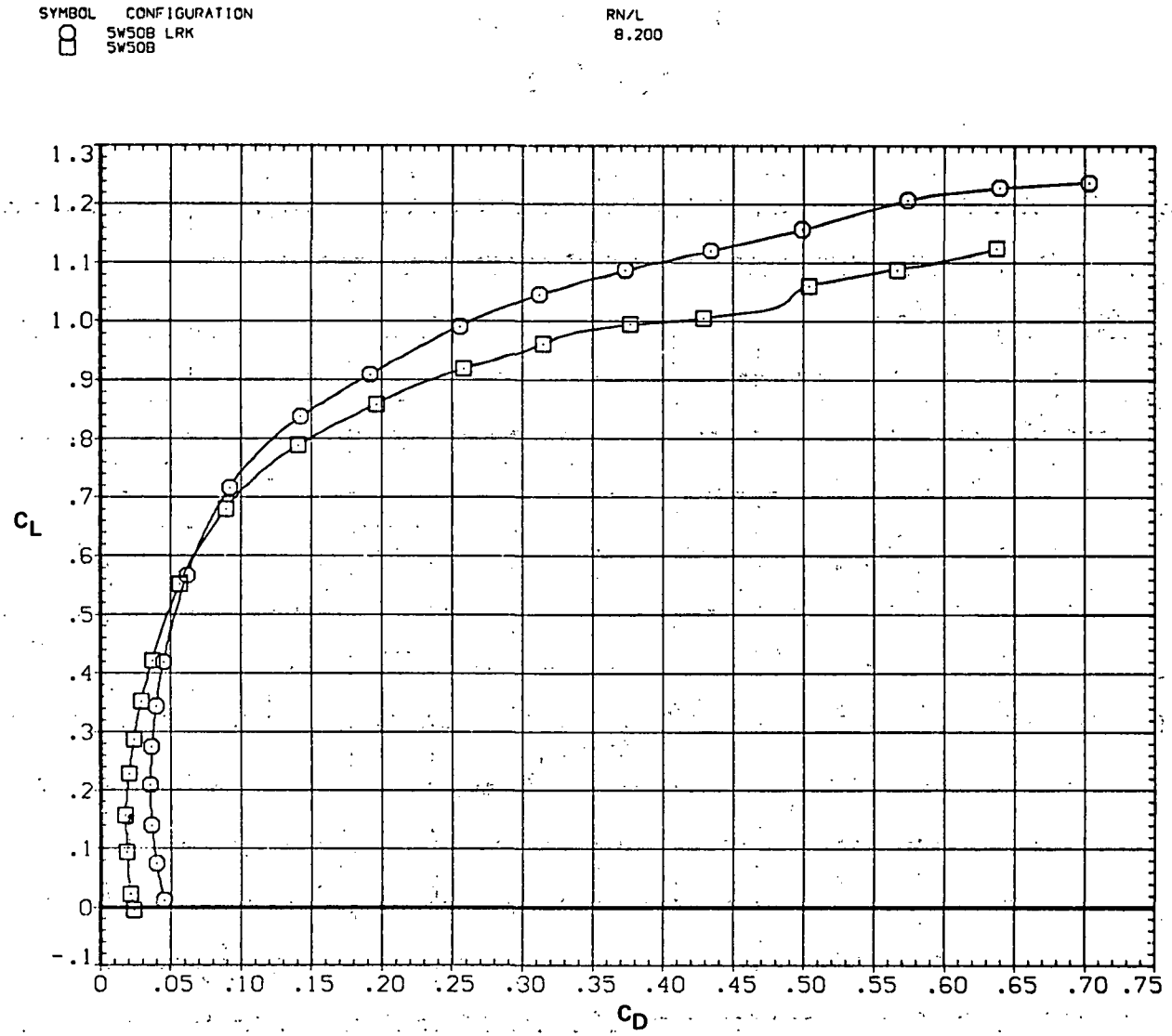

(c) C_L vs C_D

Figure 14.– Continued.

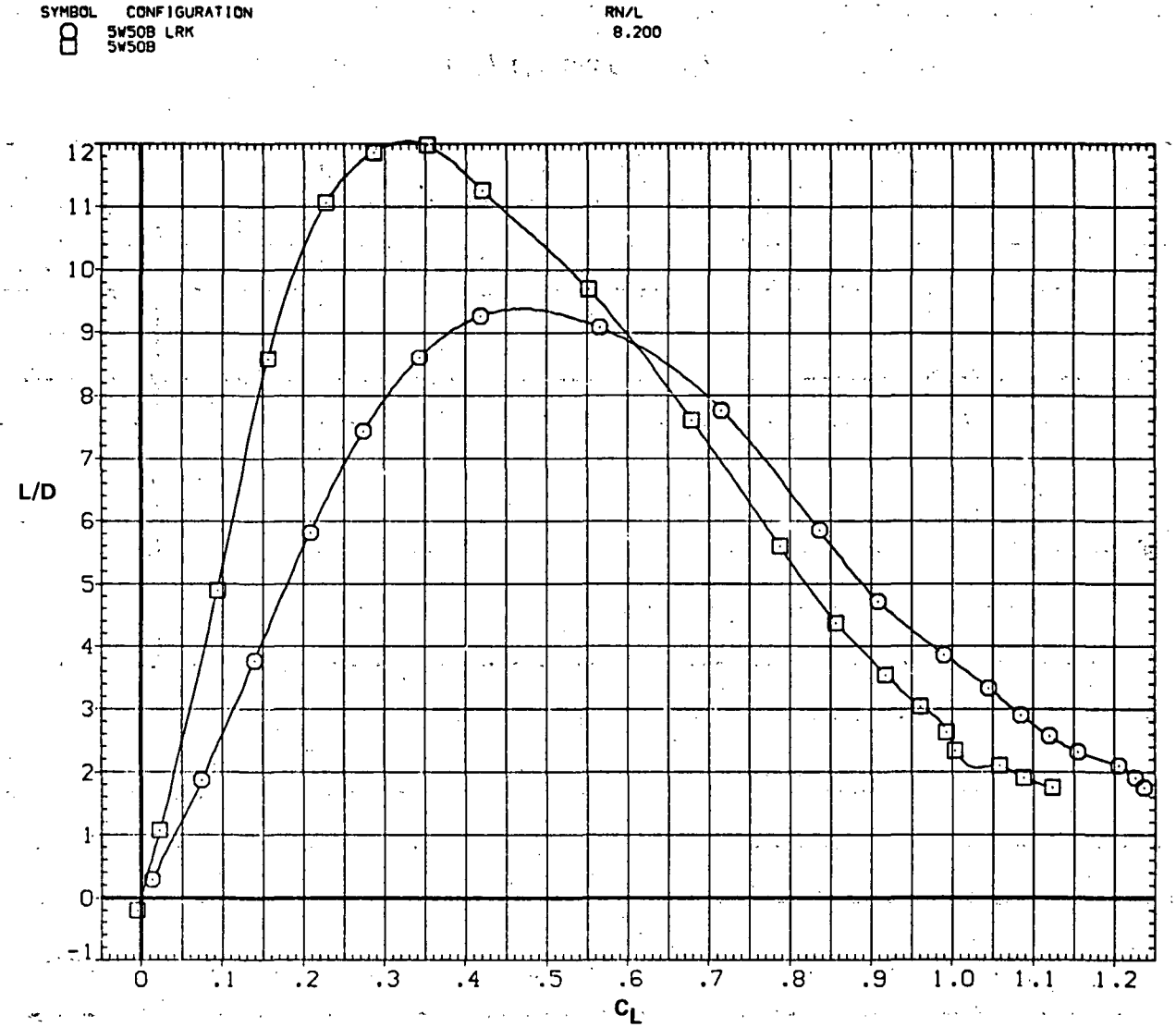

(d) L/D vs C_L

Figure 14.– Continued.

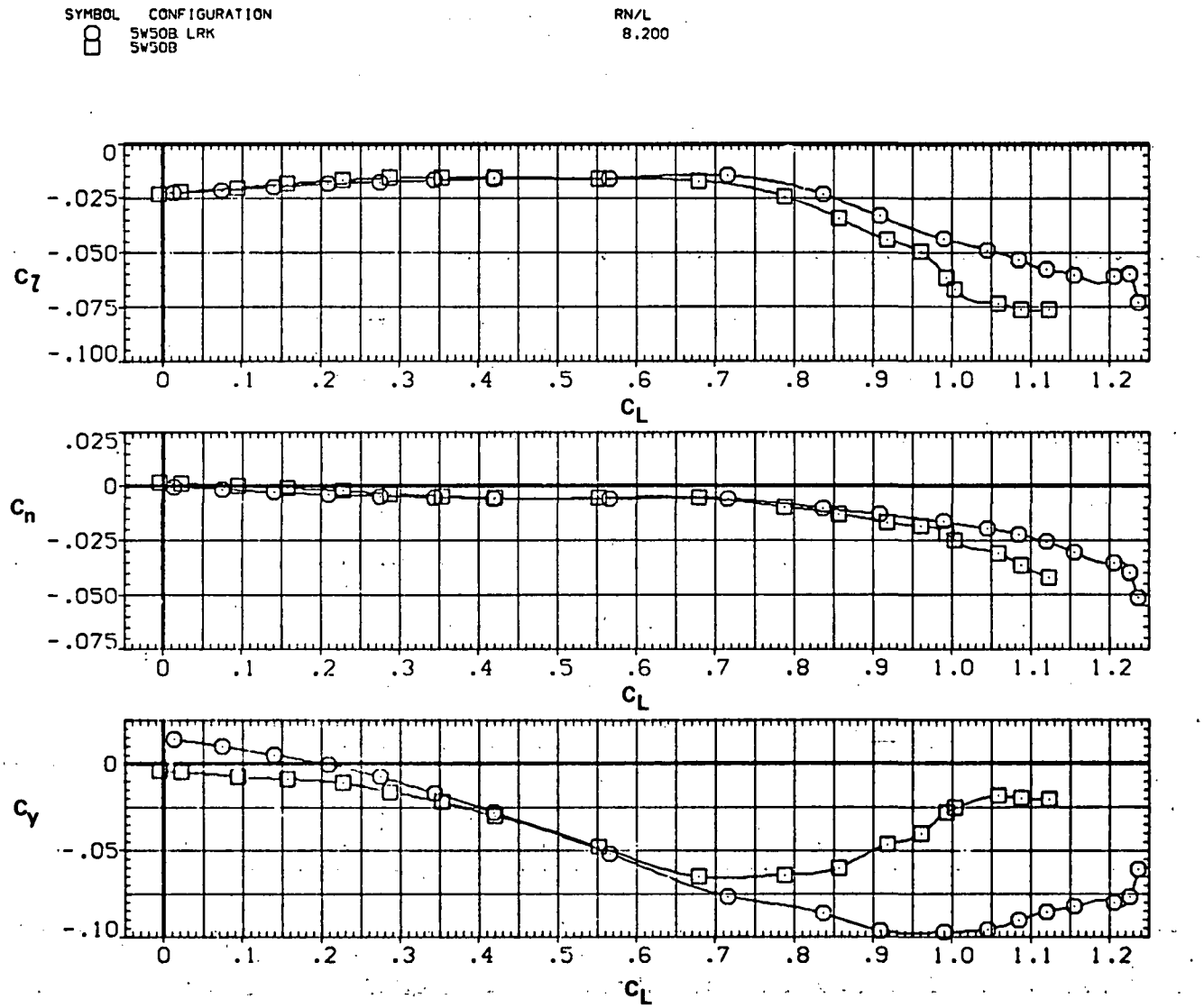

(e) C_l, C_n, and C_Y vs C_L

Figure 14.– Concluded.

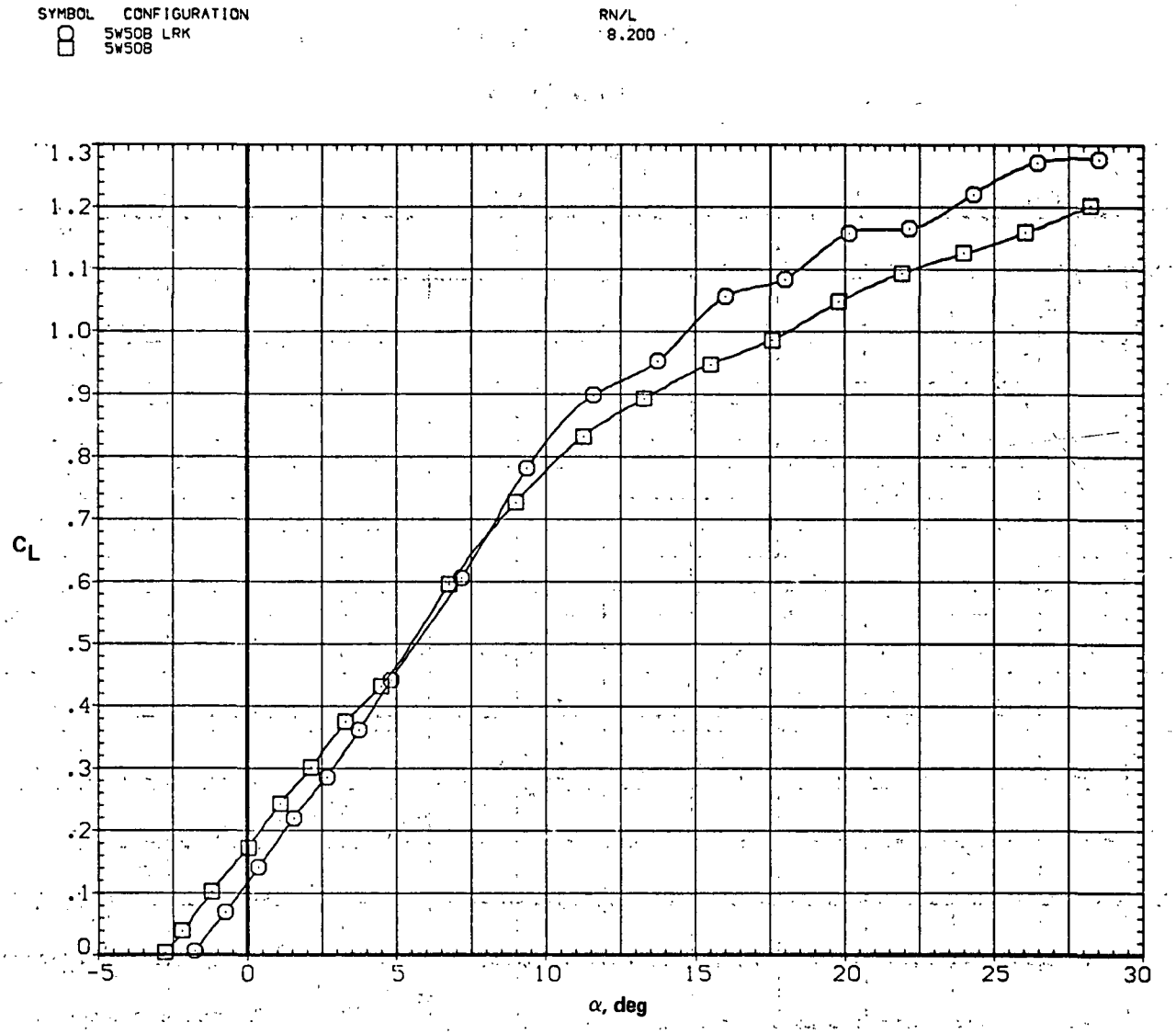

(a) C_L vs α

Figure 15.– Effect of having Krüger flaps on both wing panels on the static longitudinal characteristics of an oblique wing: $\Lambda = 50°$, $M = 0.95$.

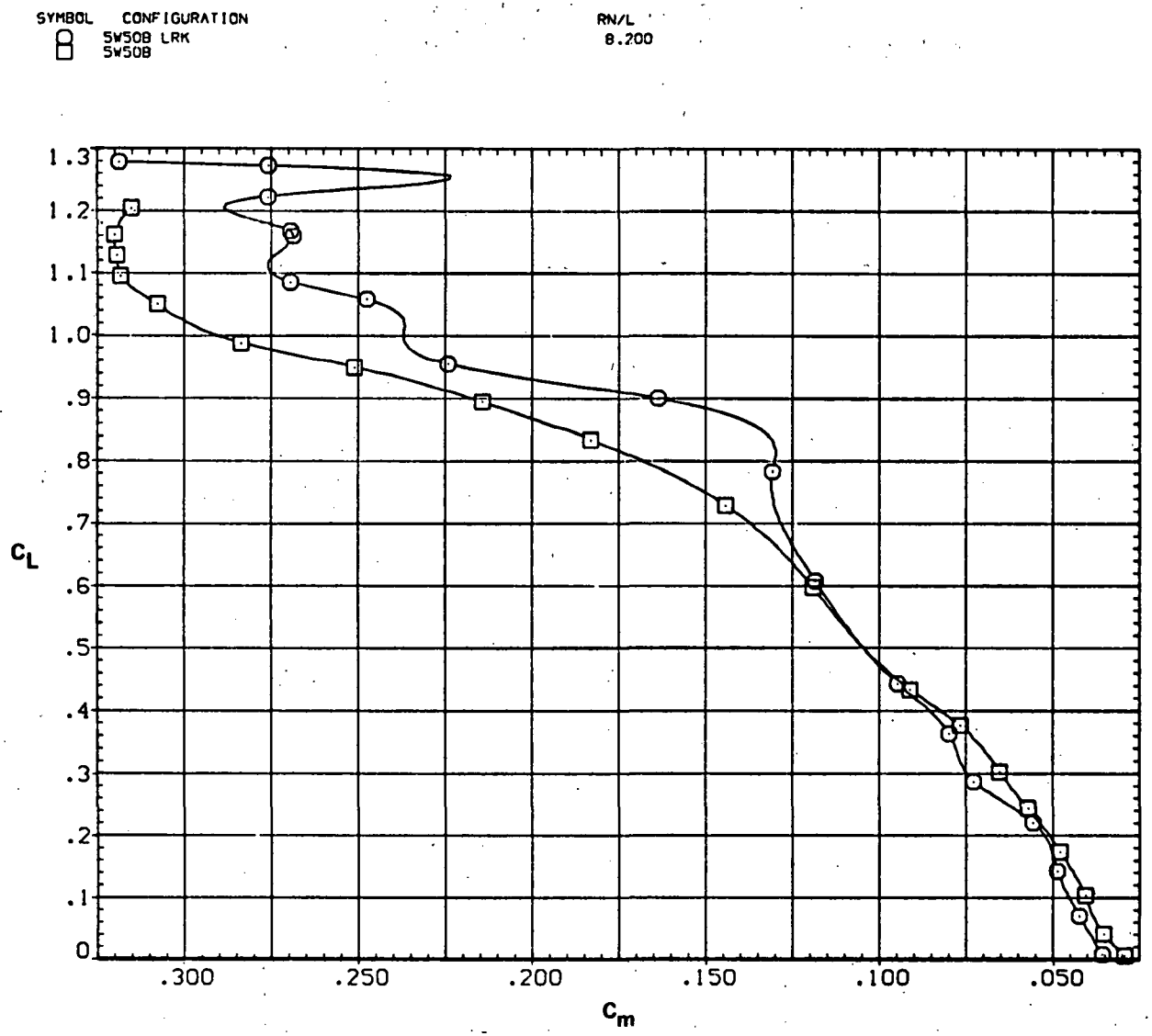

(b) C_L vs C_m

Figure 15.– Continued.

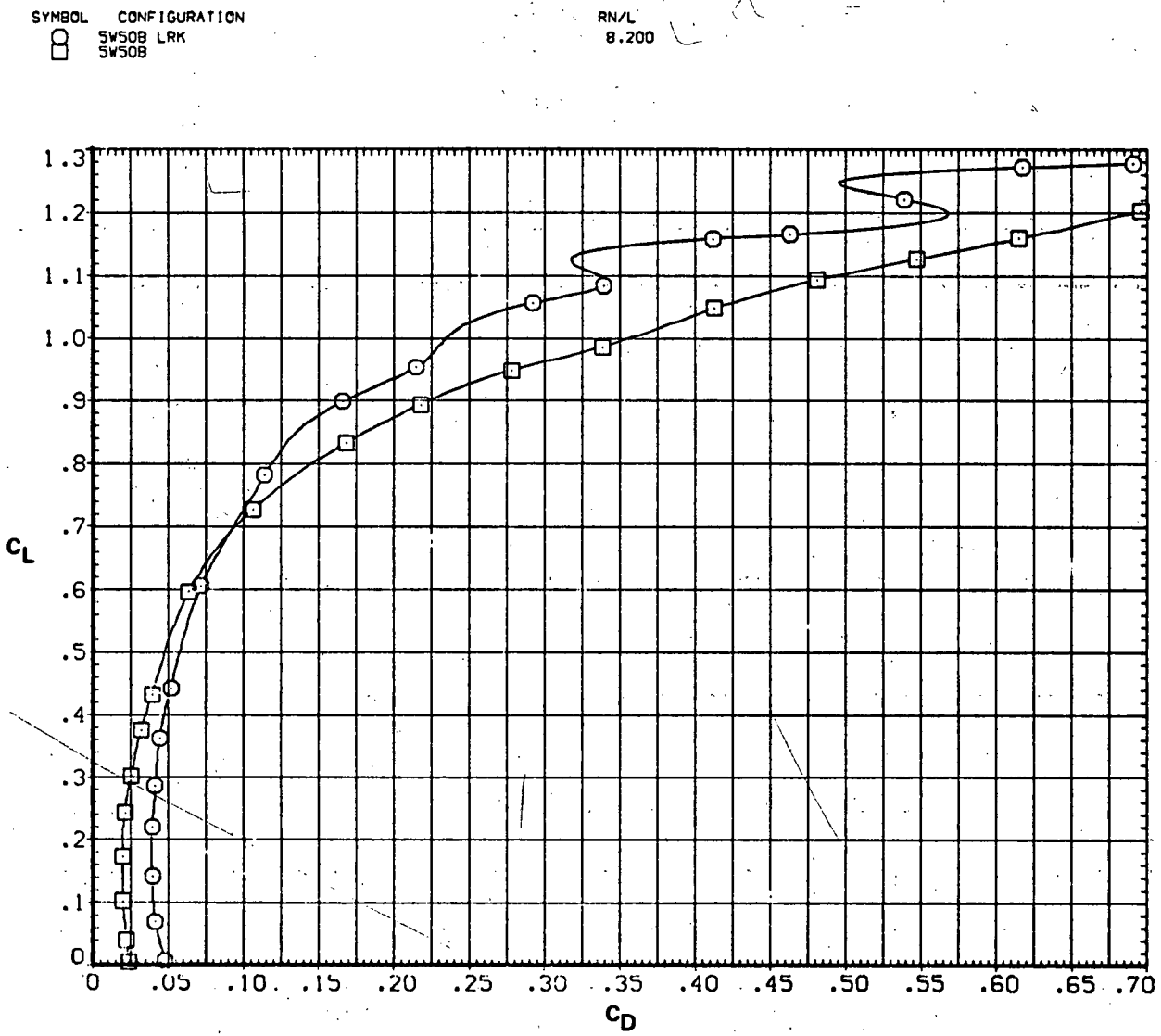

(c) C_L vs C_D

Figure 15.– Continued.

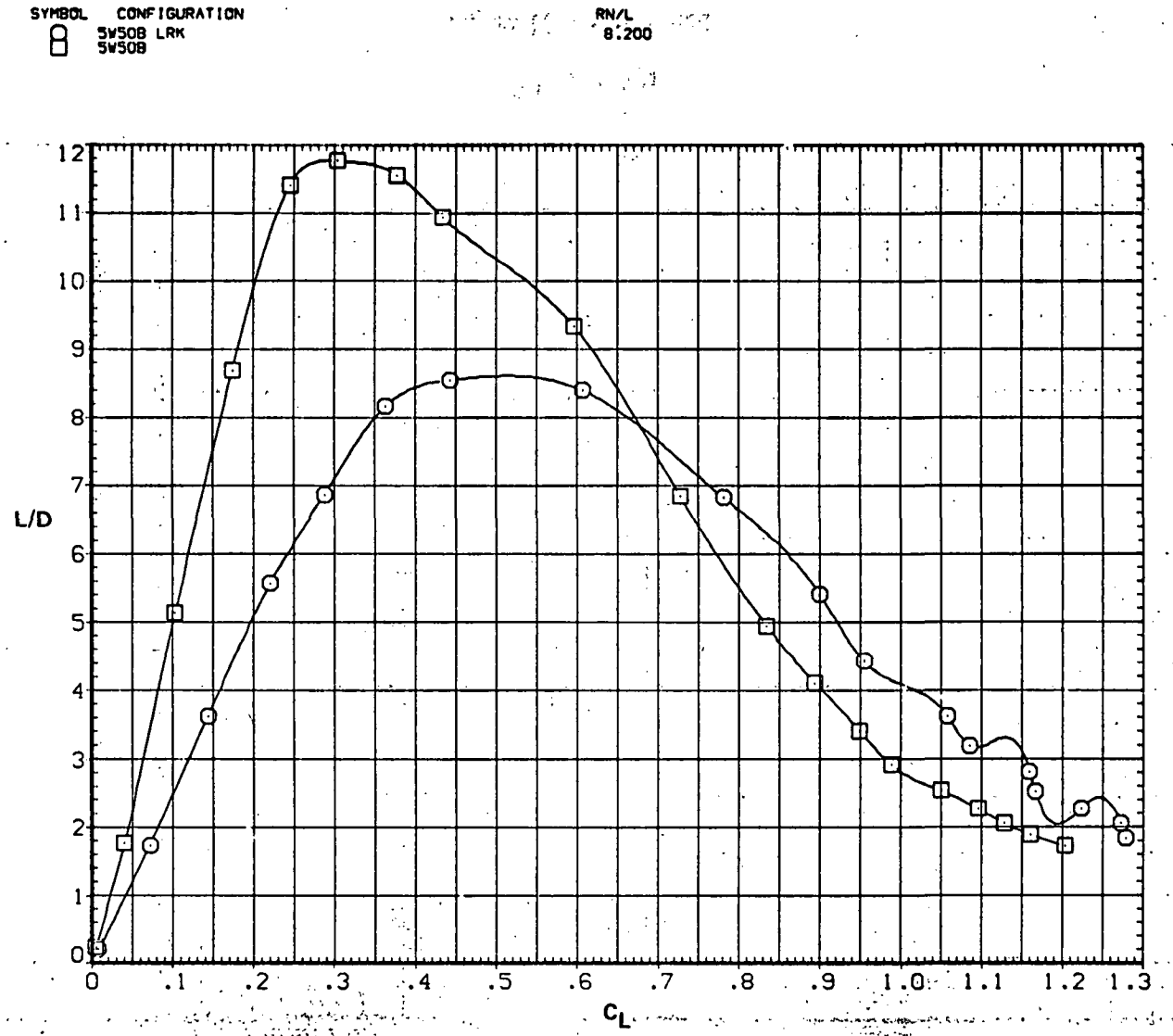

(d) L/D vs C_L

Figure 15.– Continued.

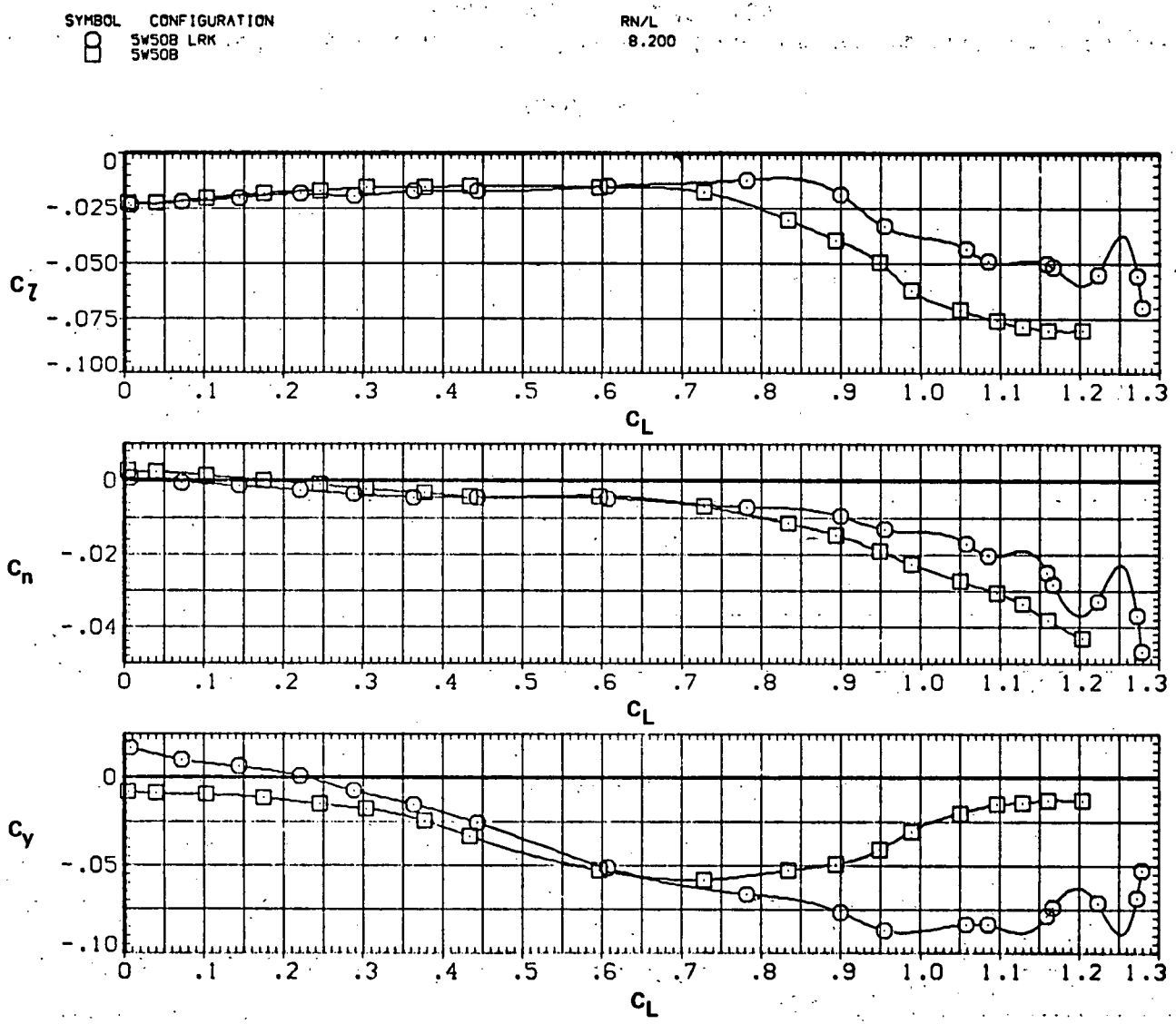

(e) C_l, C_n, and C_Y vs C_L

Figure 15.– Concluded.

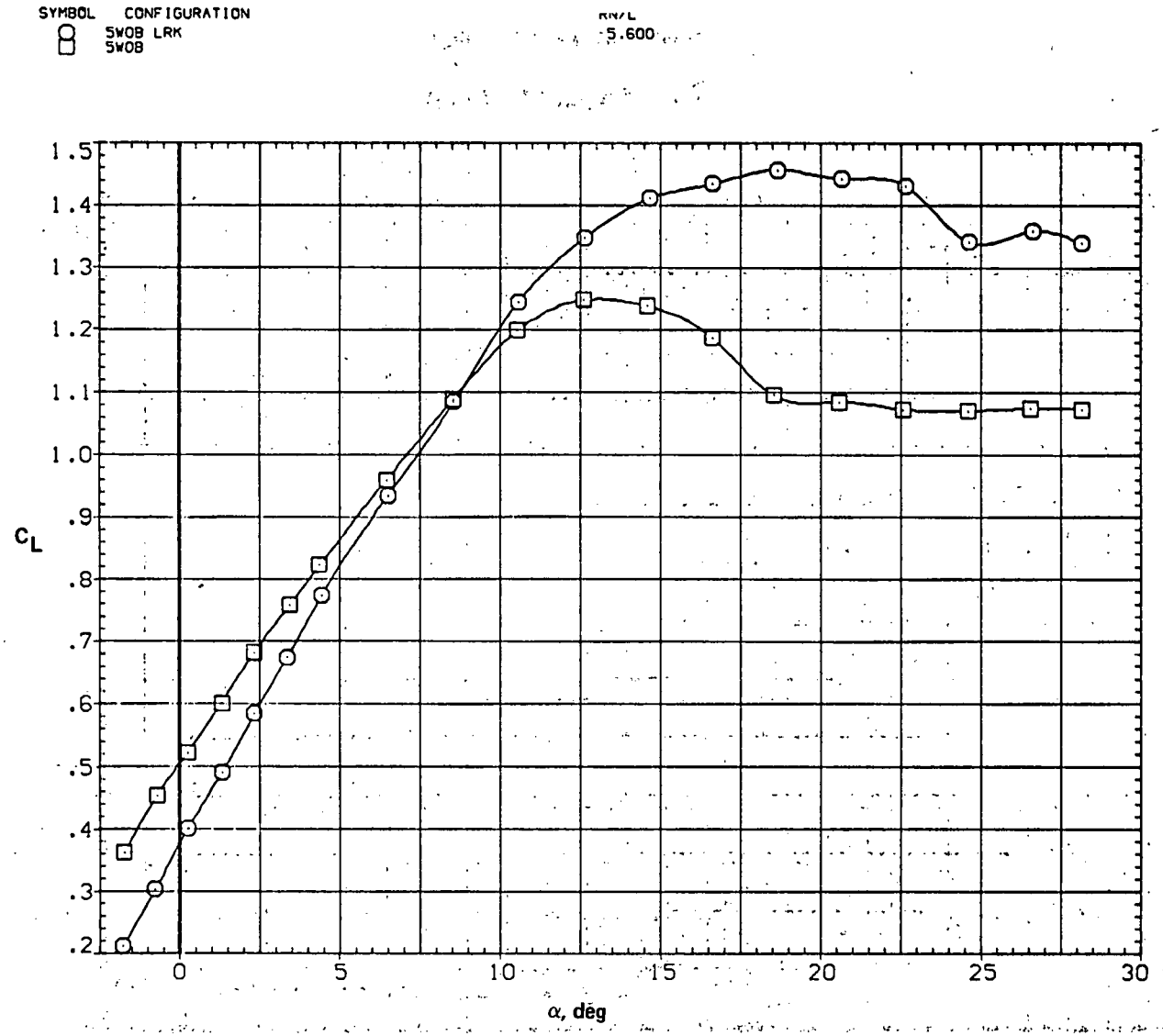

(a) C_L vs α

Figure 16.– Effect of having Krüger flaps on both wing panels on the static longitudinal characteristics of an oblique wing: $\Lambda = 0$, $M = 0.25$.

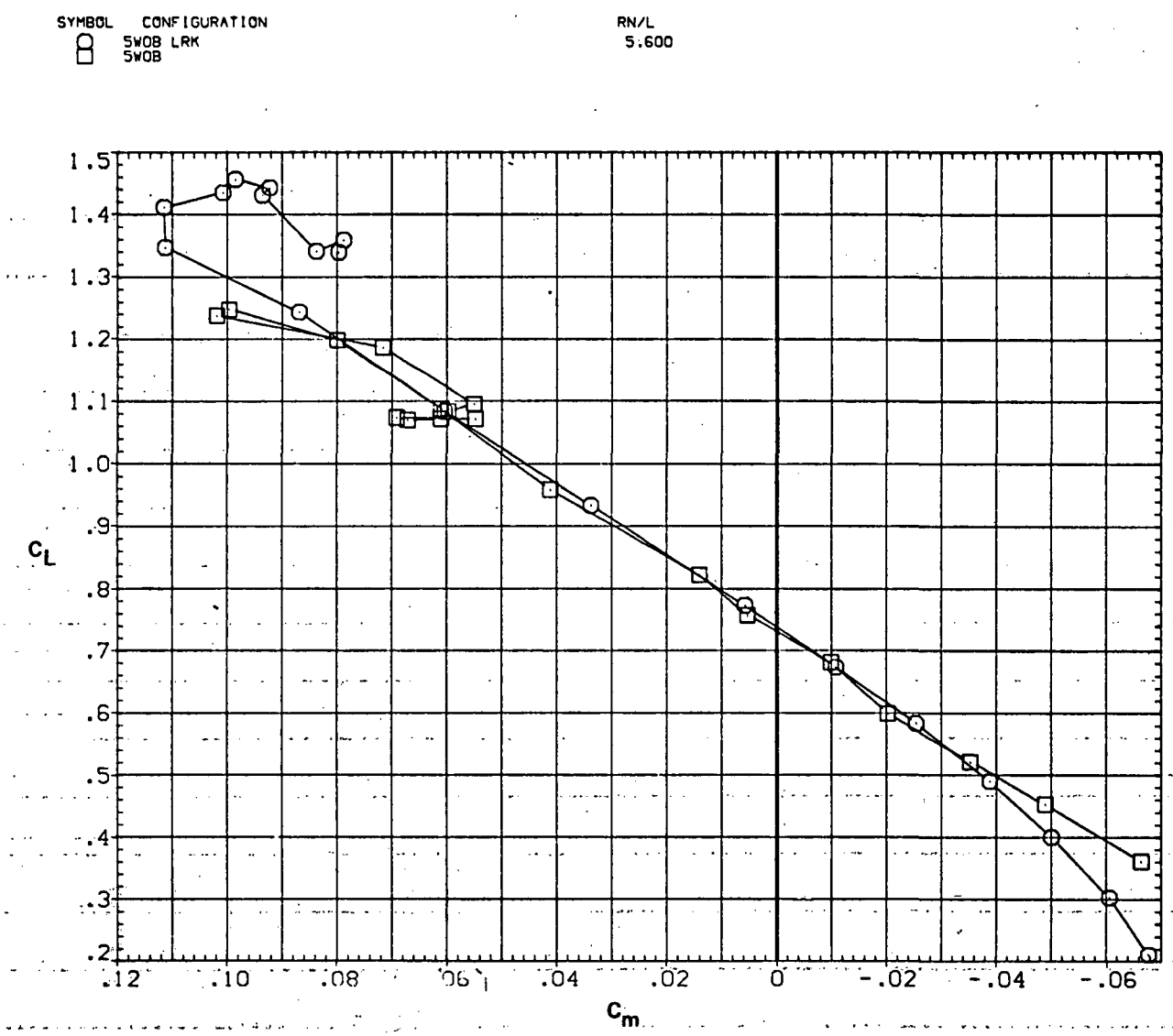

(b) C_L vs C_m

Figure 16.– Continued.

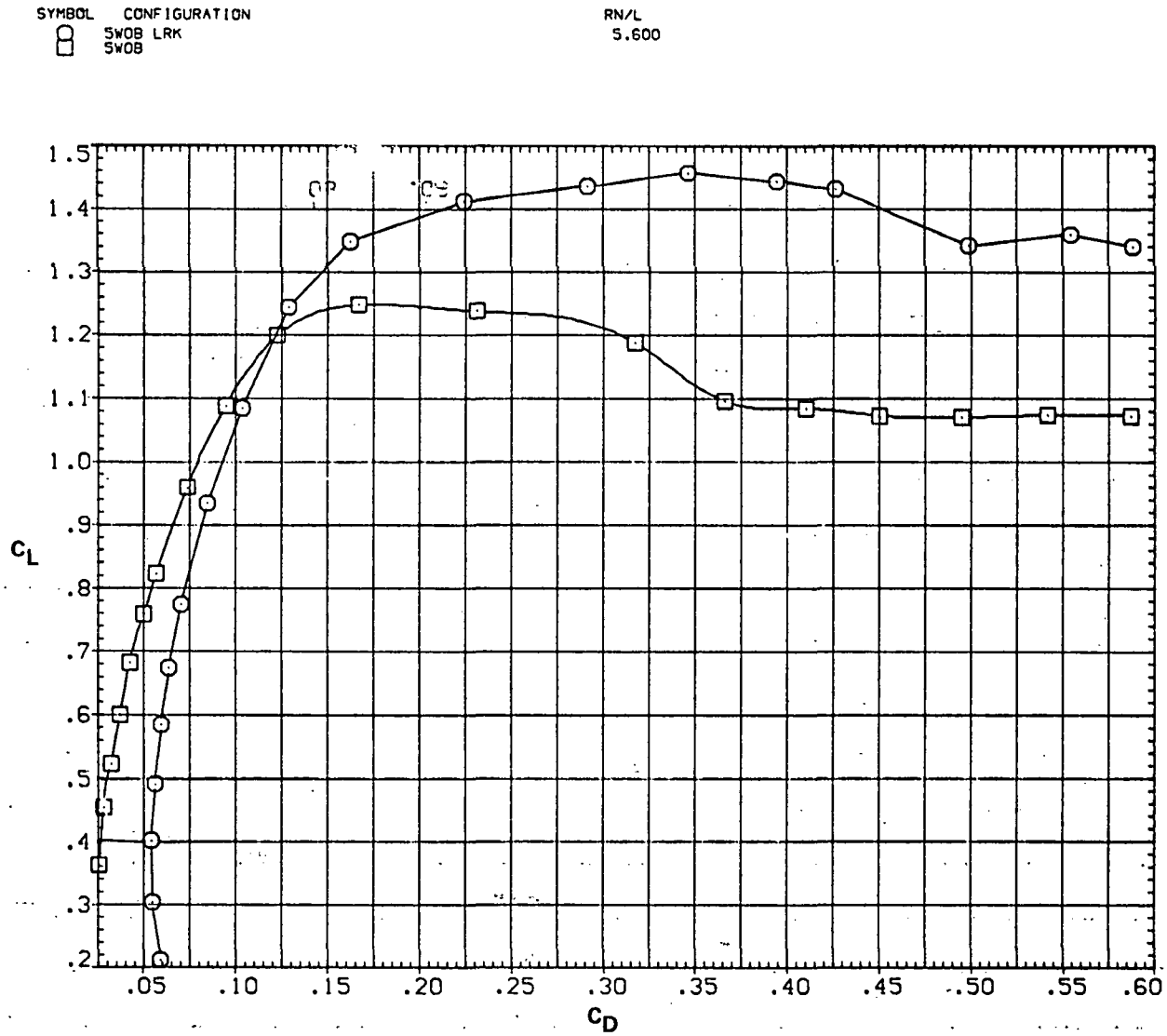

(c) C_L vs C_D

Figure 16.– Continued.

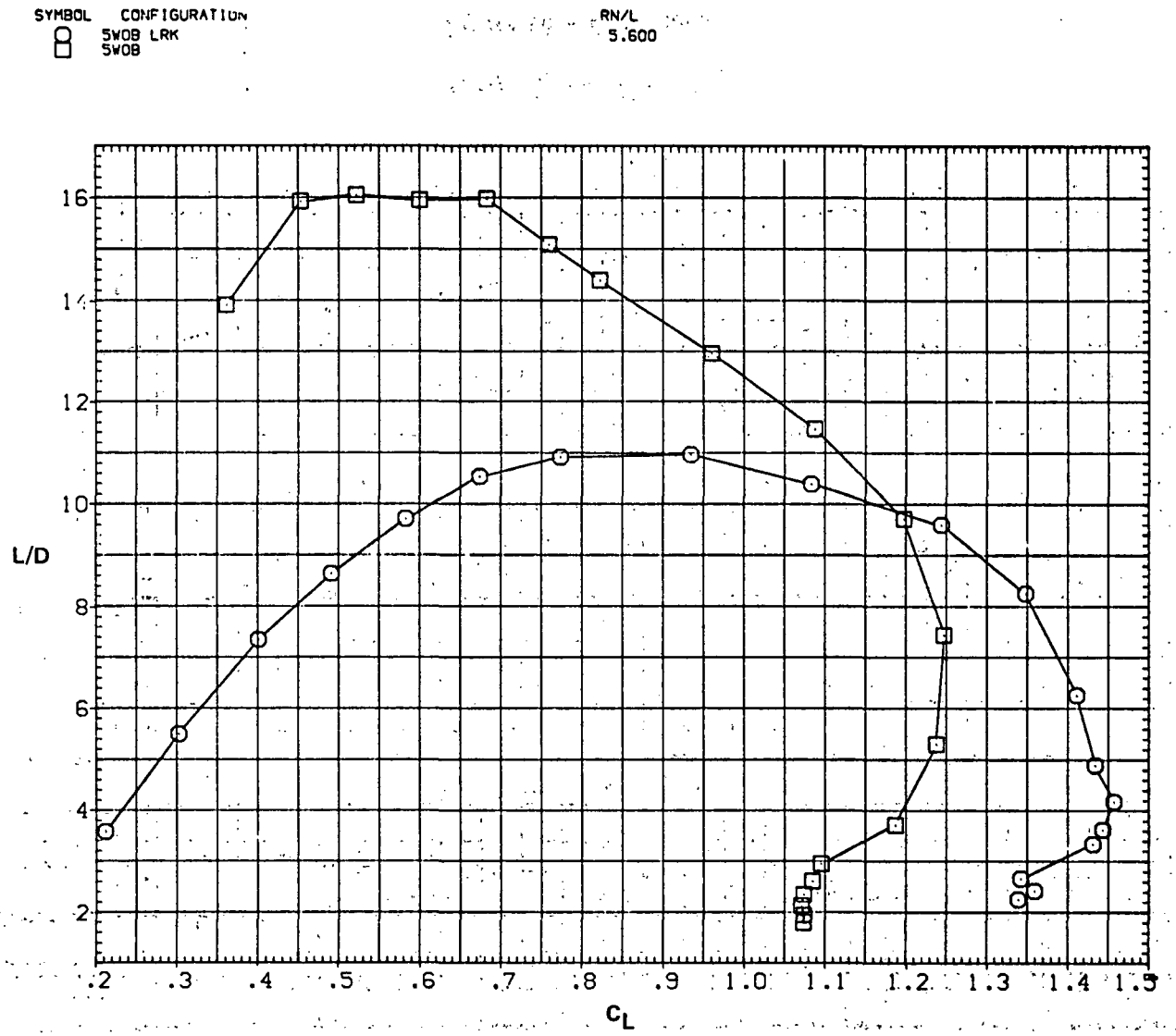

(d) L/D vs C_L

Figure 16.– Continued.

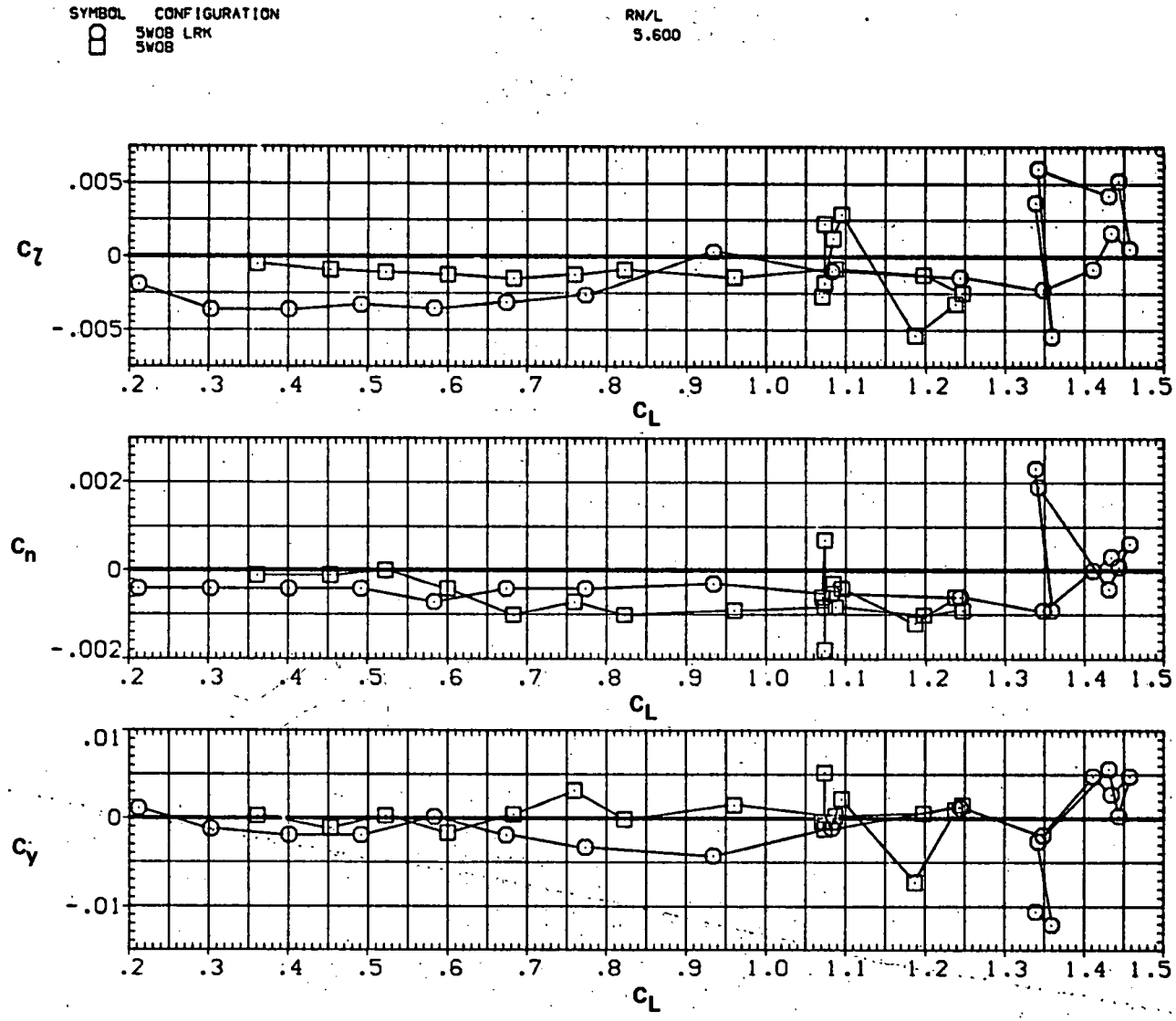

(e) C_l, C_n, and C_Y vs C_L

Figure 16.– Concluded.

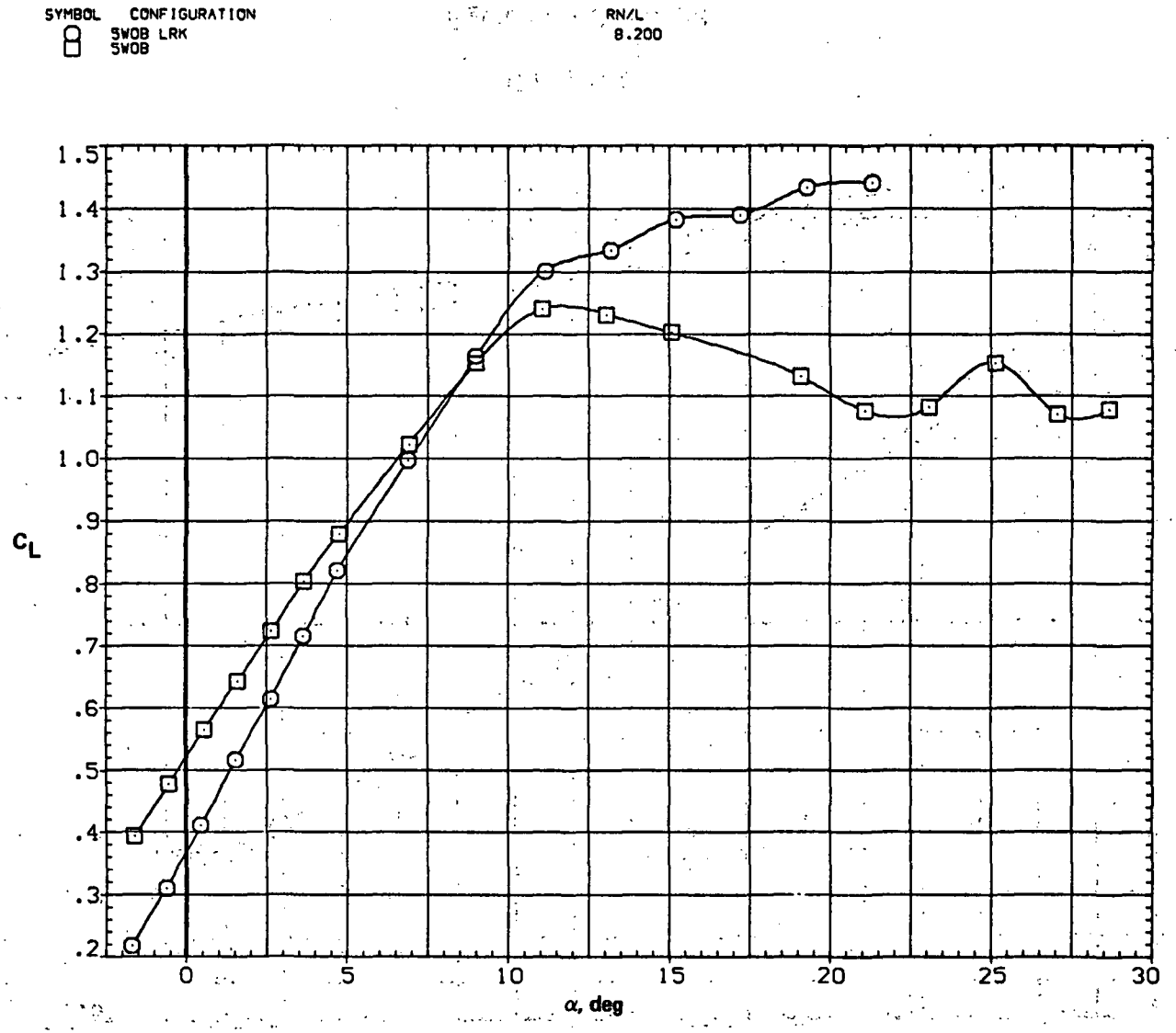

(a) C_L vs α

Figure 17.— Effect of having Krüger flaps on both wing panels on the static longitudinal characteristics of an oblique wing: $\Lambda = 0$, $M = 0.40$.

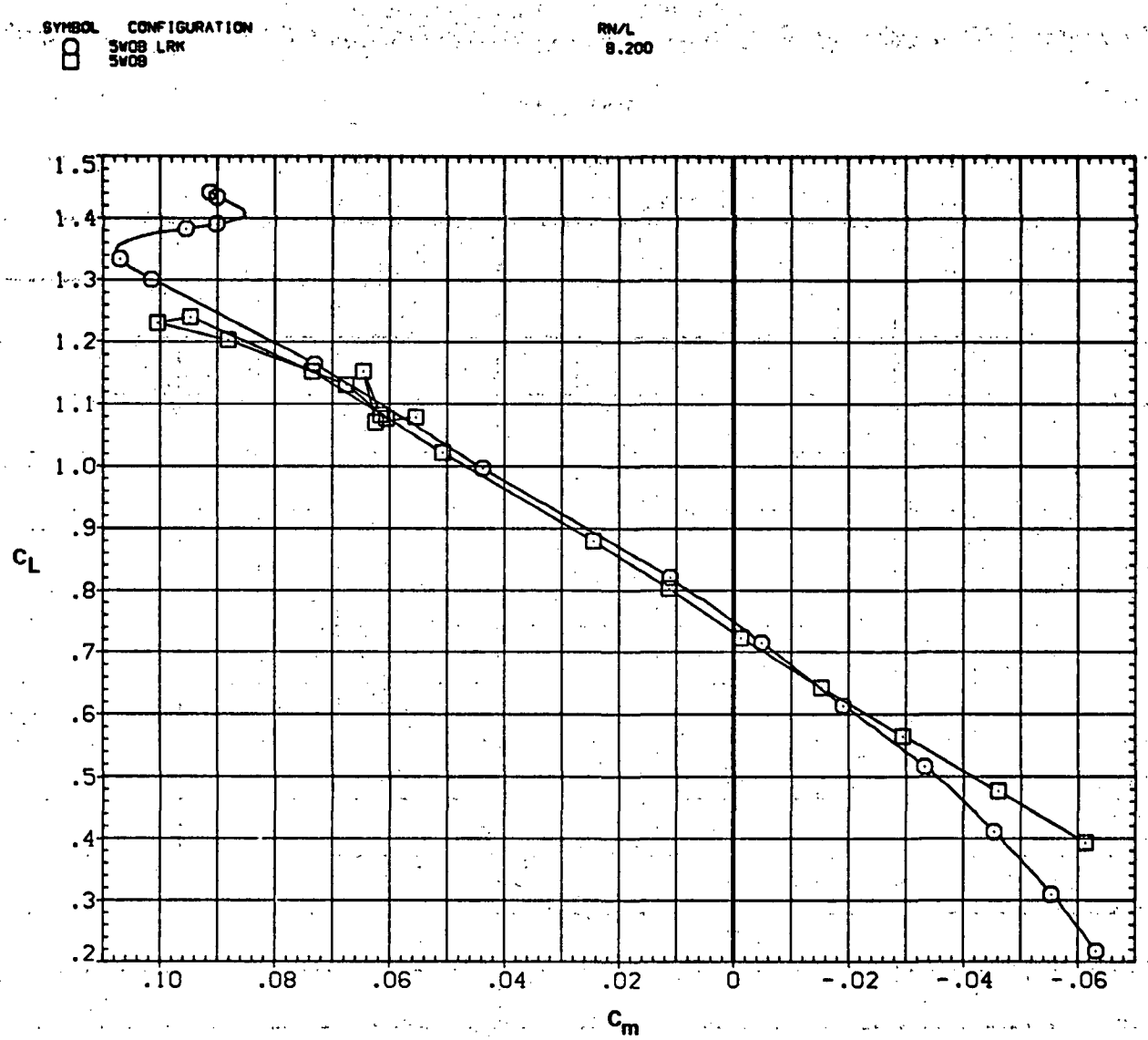

(b) C_L vs C_m

Figure 17.– Continued.

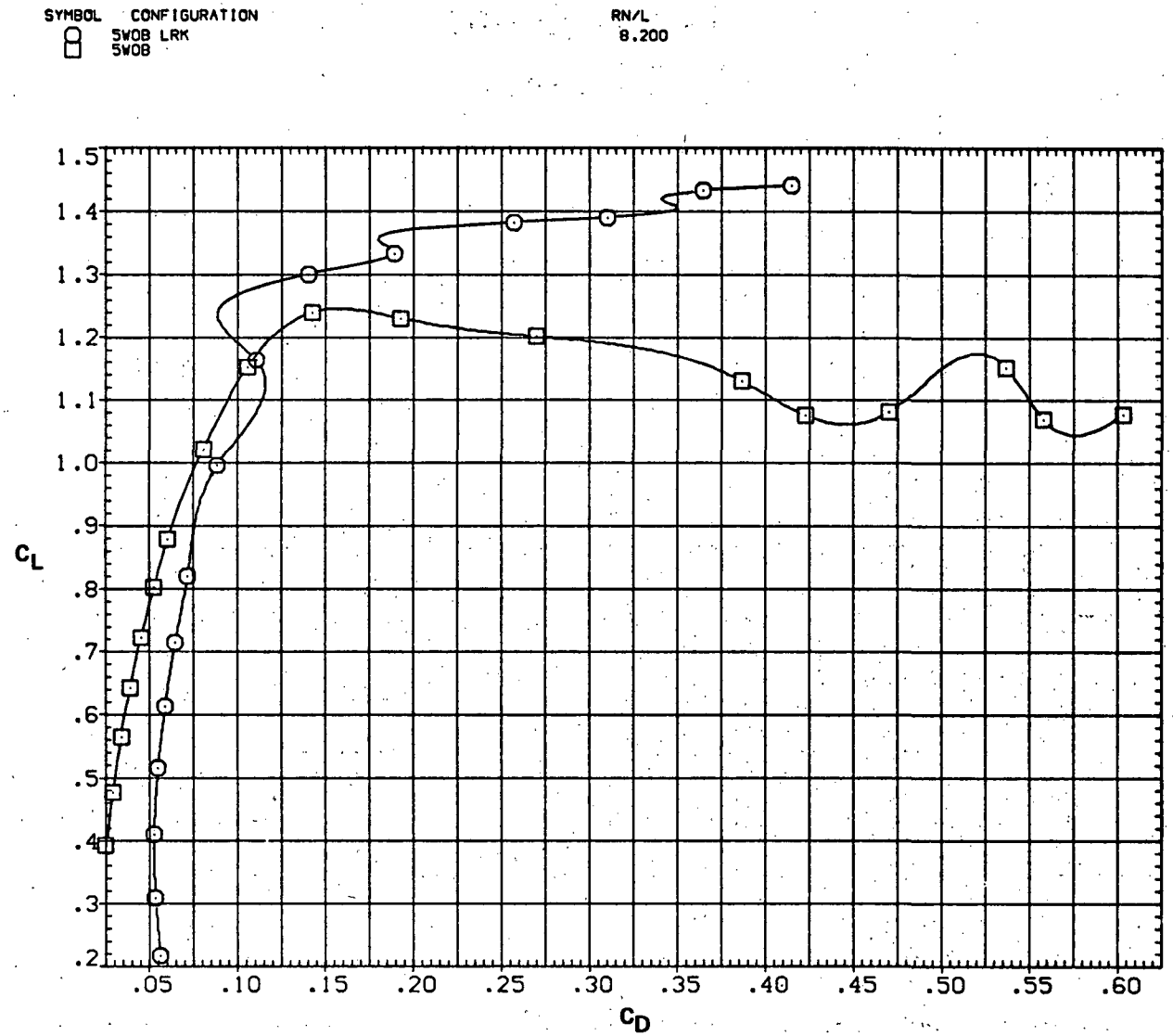

(c) C_L vs C_D

Figure 17.– Continued.

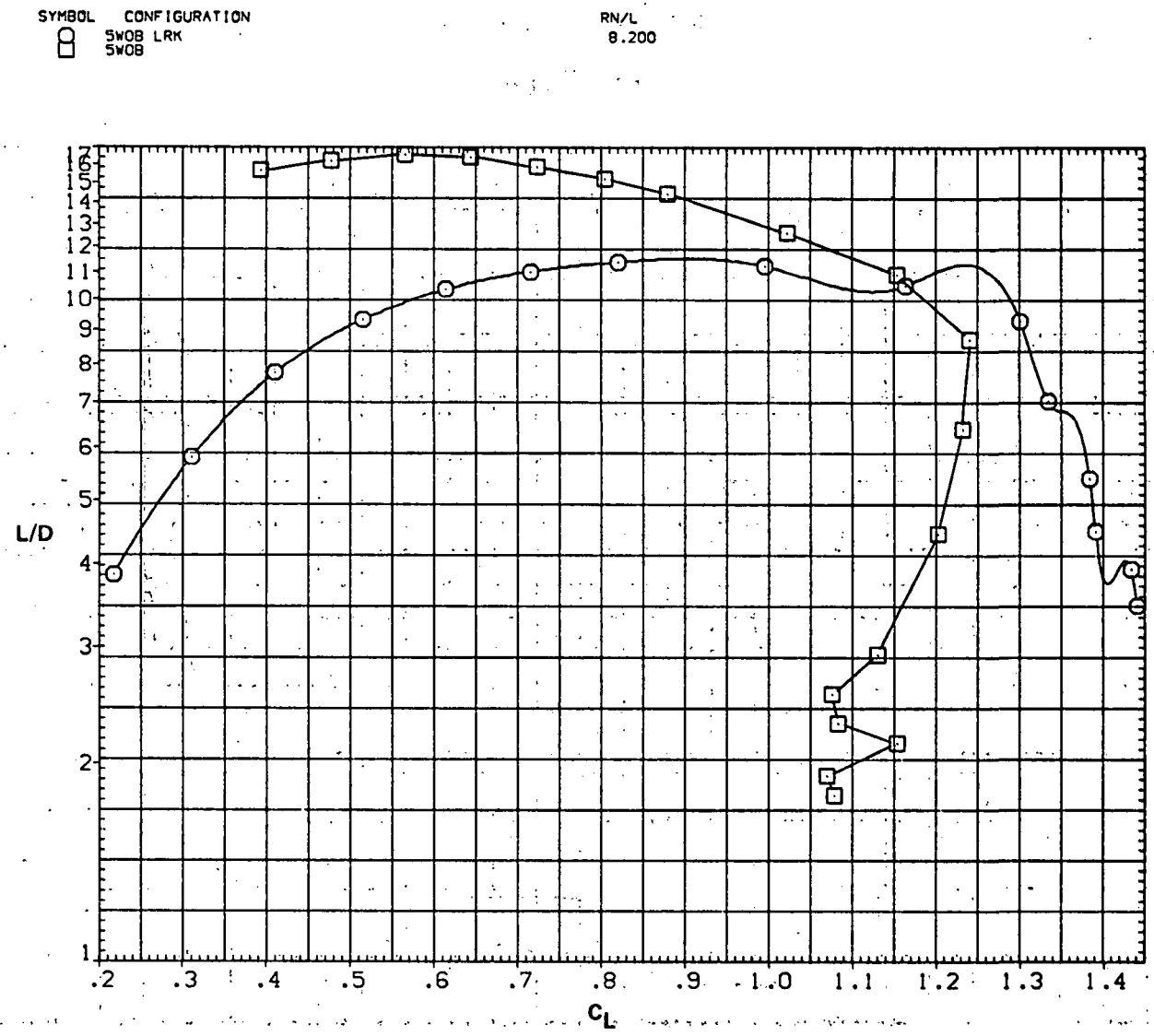

(d) L/D vs C_L

Figure 17.– Continued.

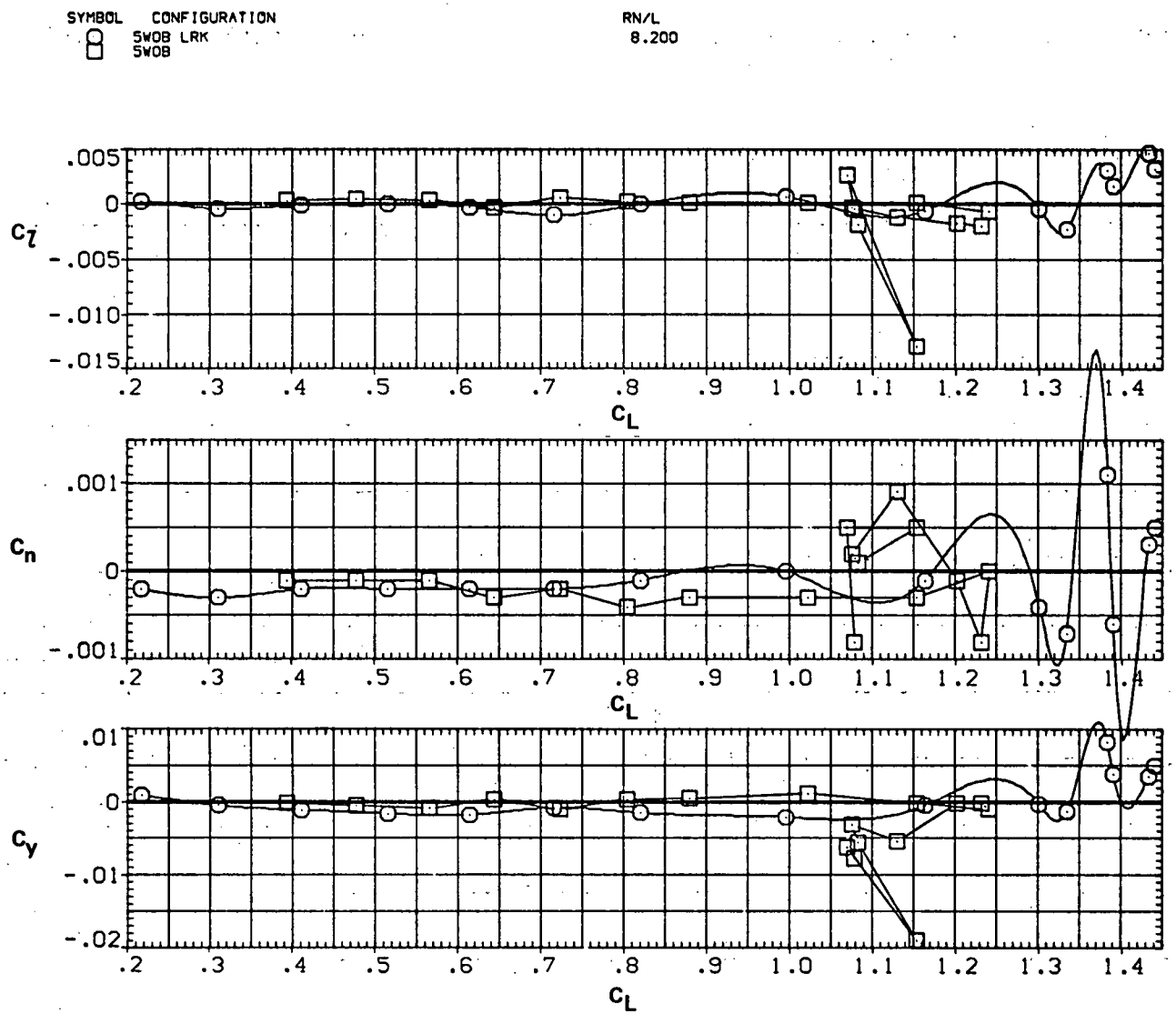

(e) C_l, C_n, and C_Y vs C_L

Figure 17.– Concluded.

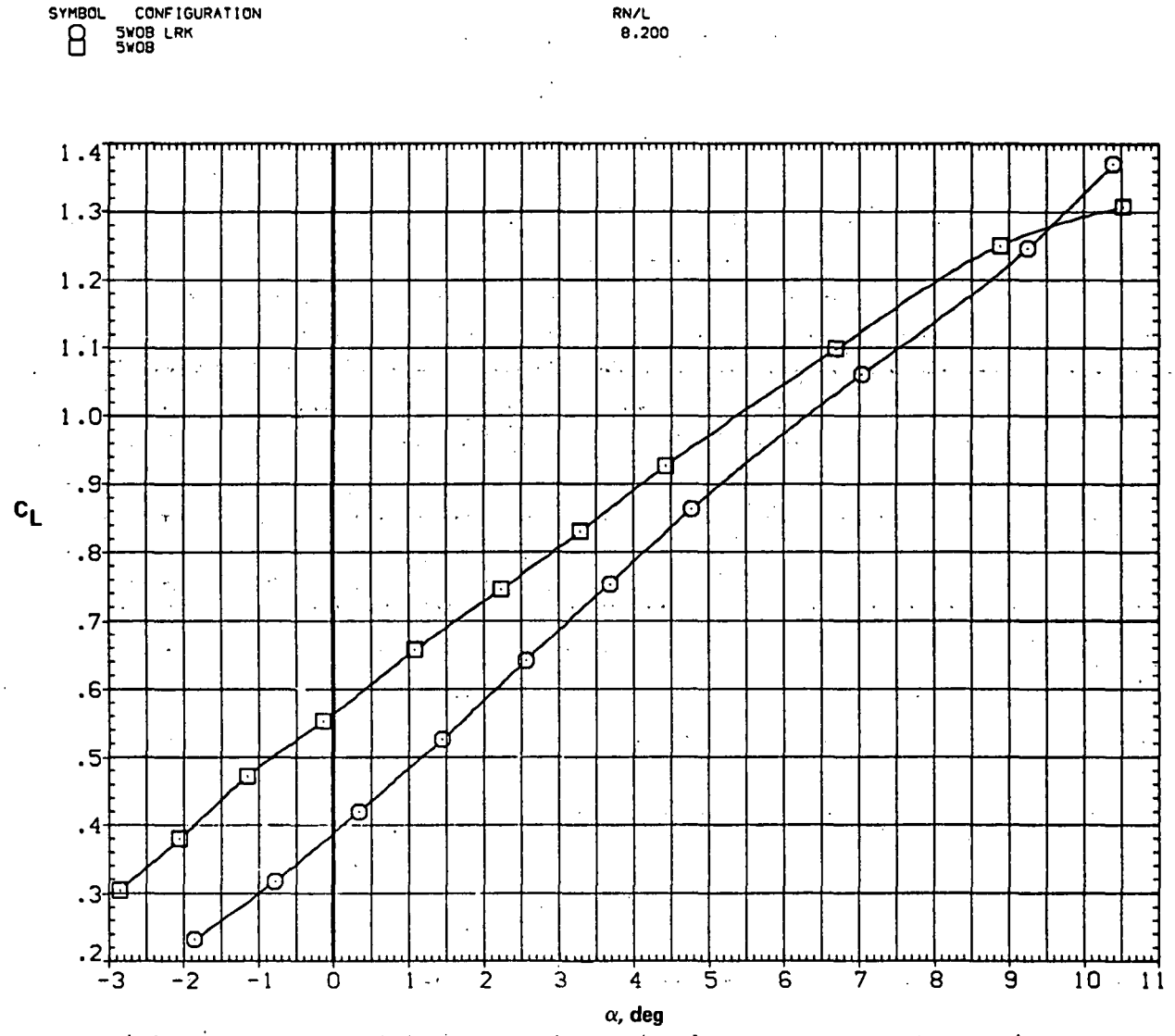

(a) C_L vs α

Figure 18.– Effect of having Krüger flaps on both wing panels on the static longitudinal characteristics of an oblique wing: $\Lambda = 0$, $M = 0.60$.

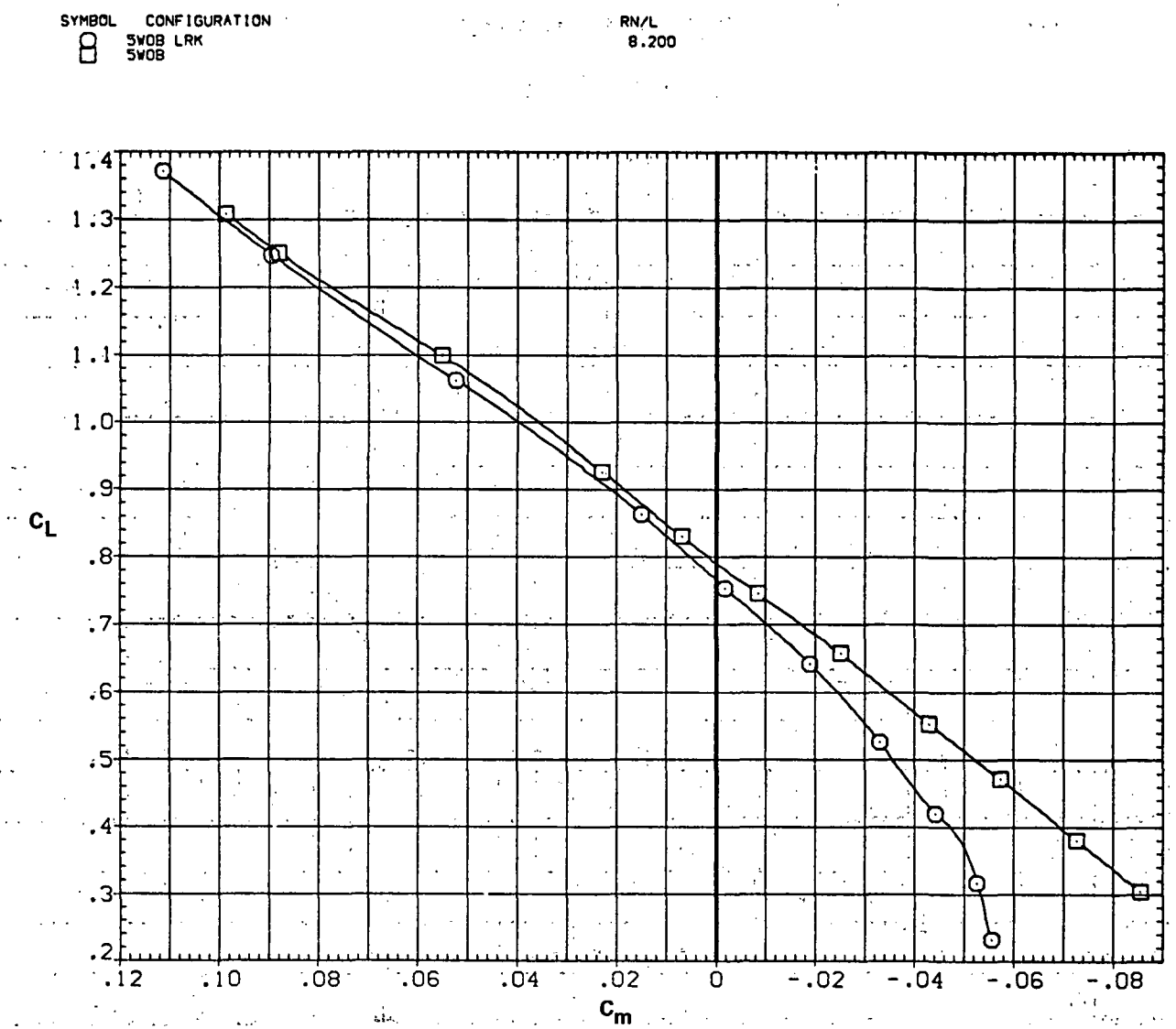

(b) C_L vs C_m

Figure 18.– Continued.

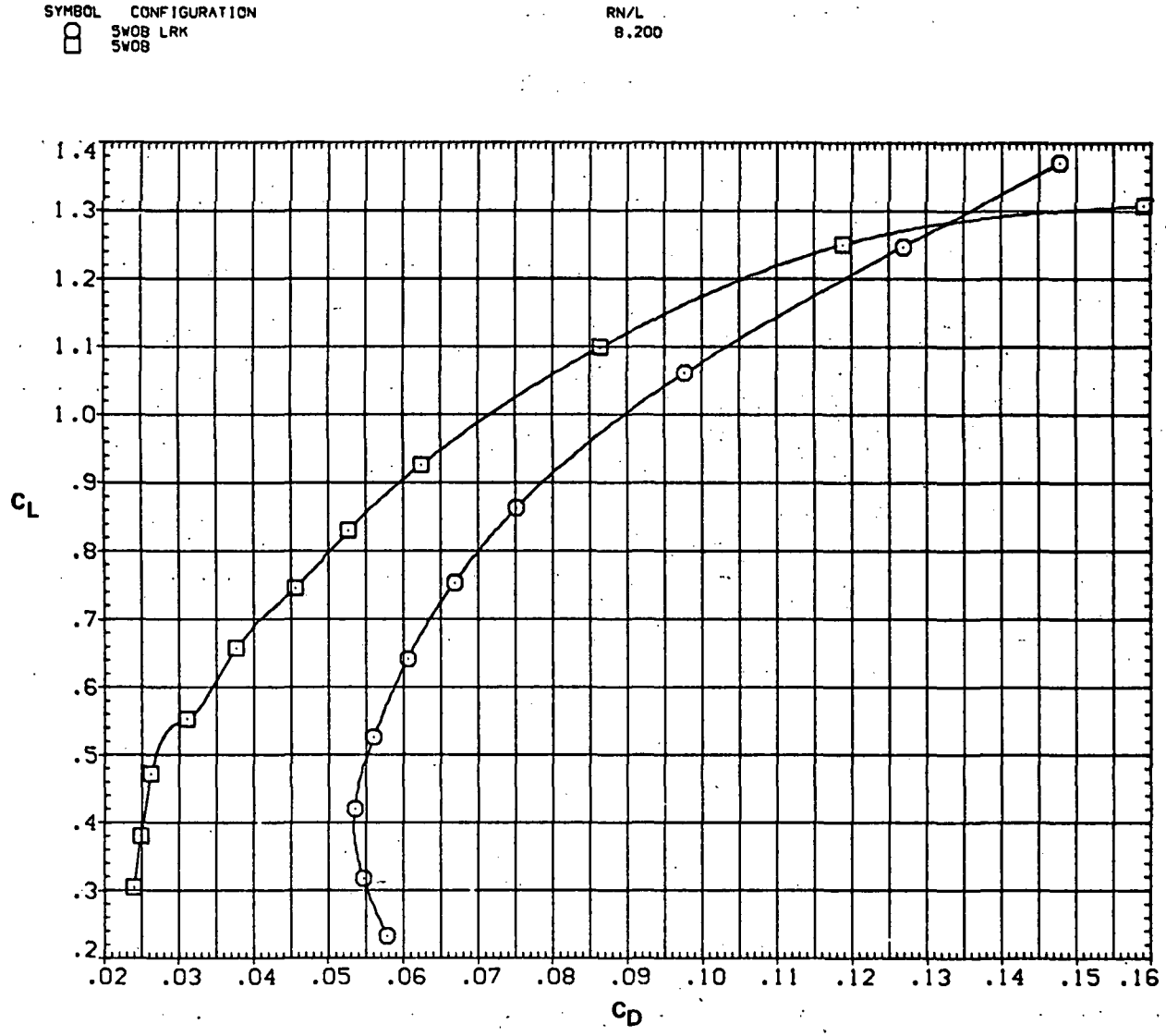

(c) C_L vs C_D

Figure 18.– Continued.

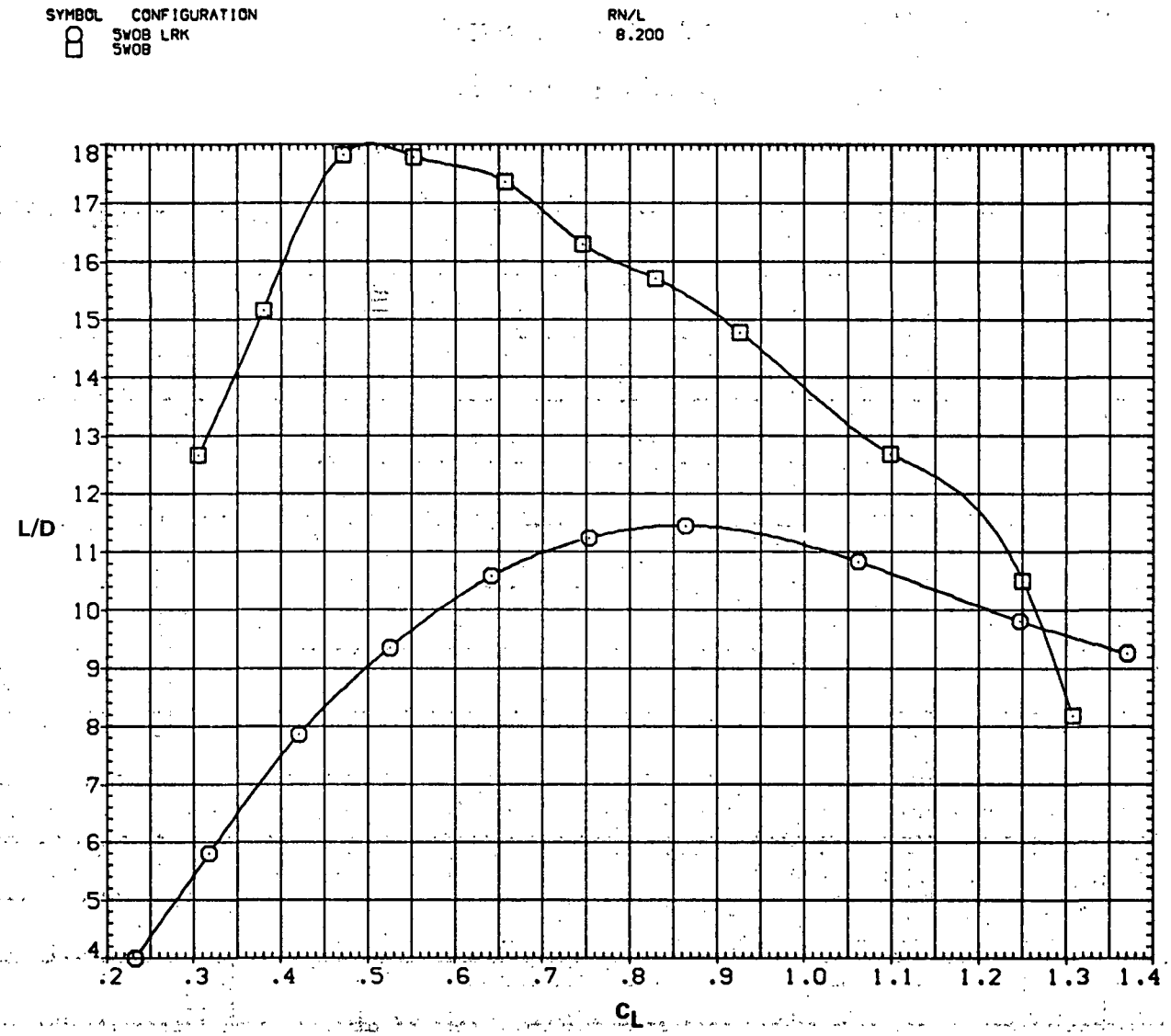

(d) L/D vs C_L

Figure 18.– Continued.

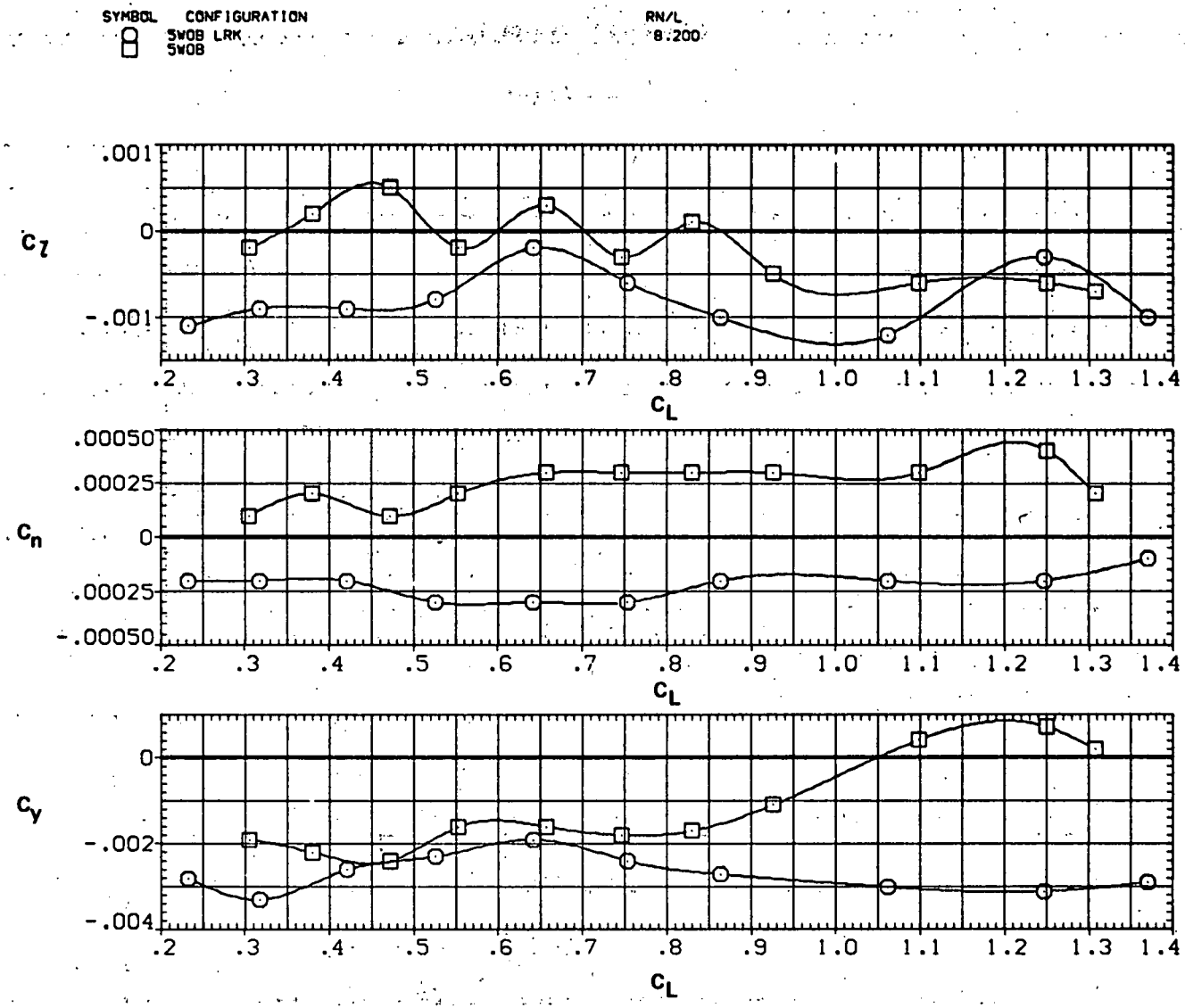

(e) C_l, C_n, and C_Y vs C_L

Figure 18.– Concluded.

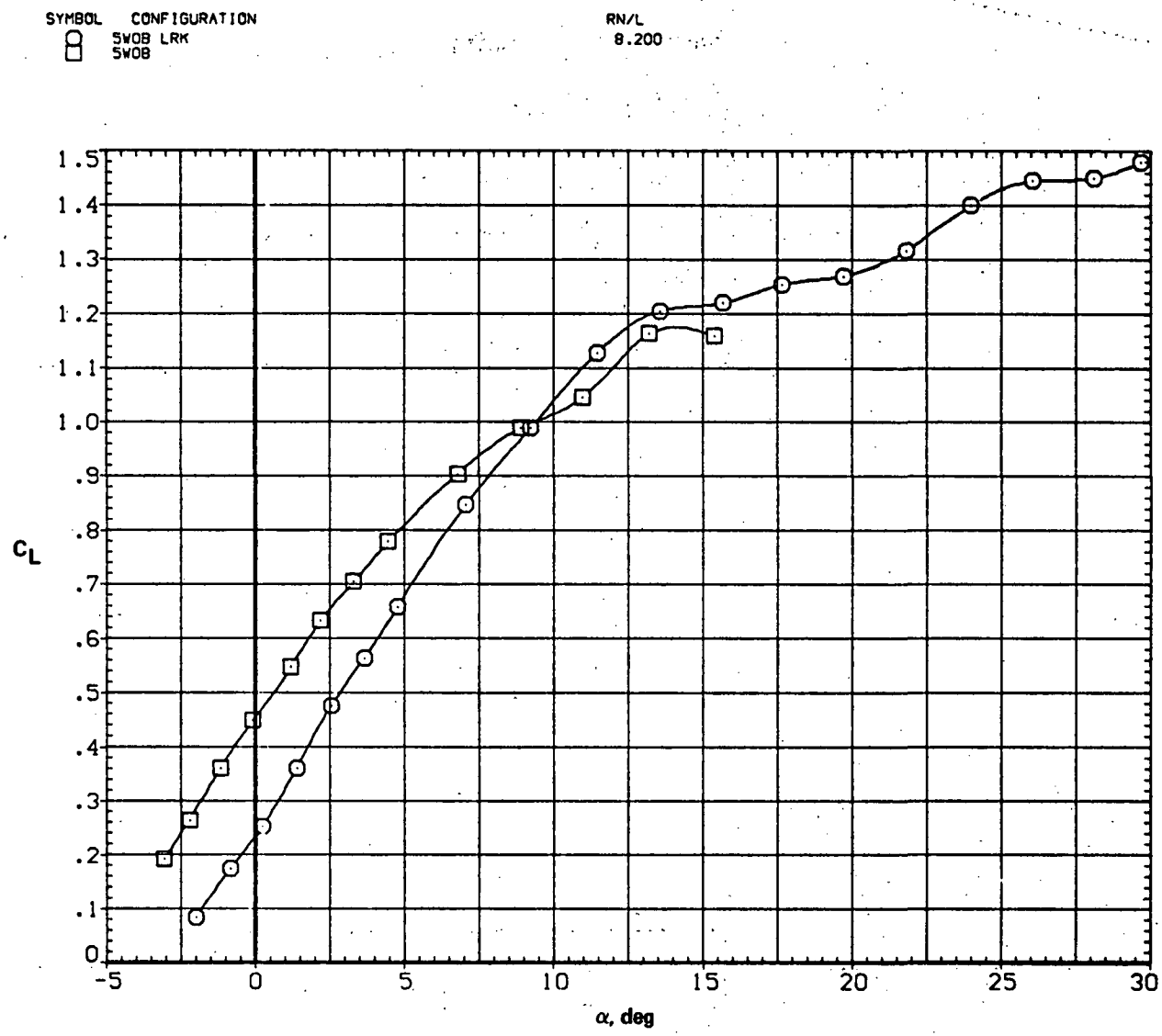

(a) C_L vs α

Figure 19.– Effect of having Krüger flaps on both wing panels on the static longitudinal characteristics of an oblique wing: $\Lambda = 0$, $M = 0.80$.

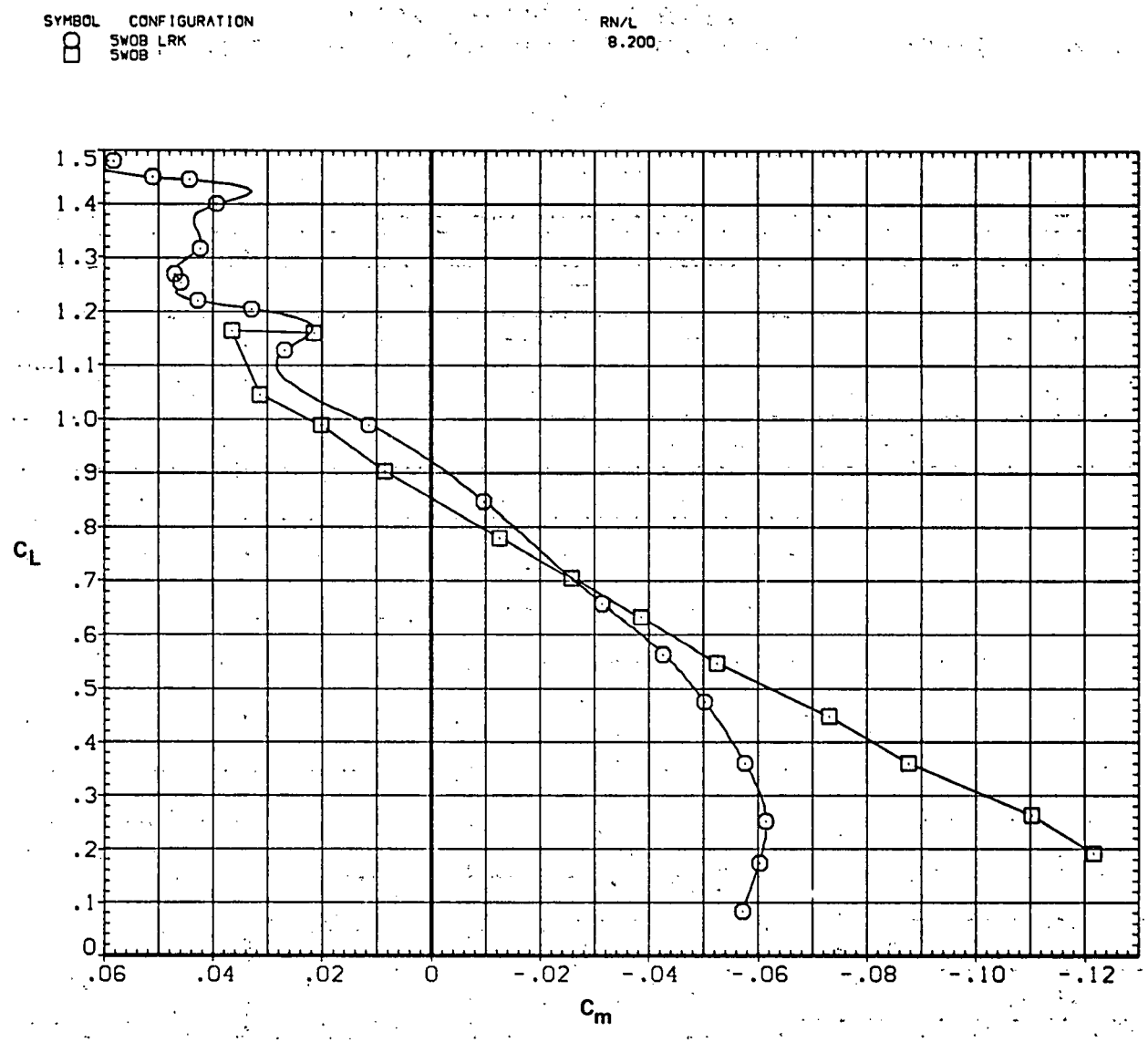

(b) C_L vs C_m

Figure 19.– Continued.

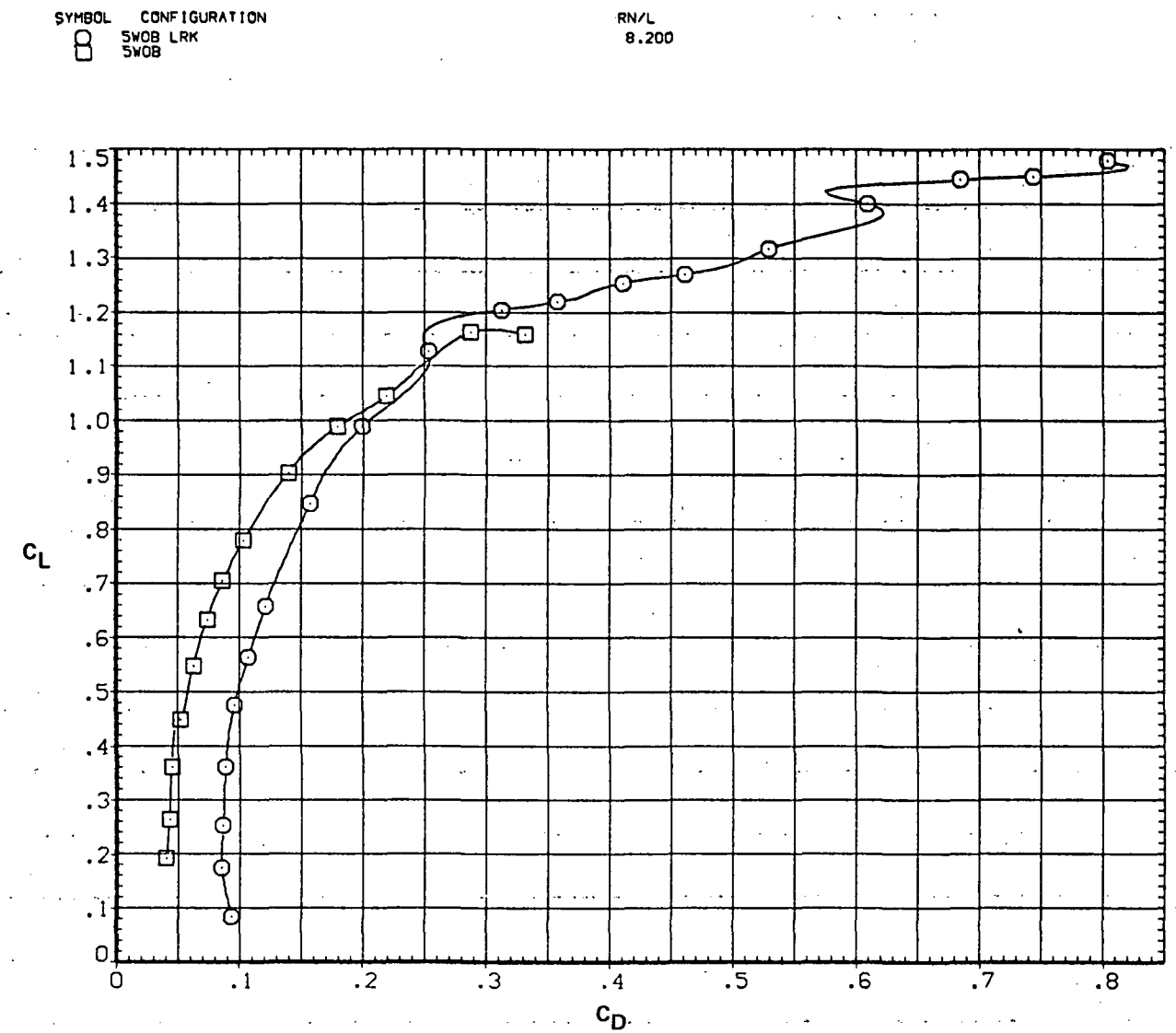

(c) C_L vs C_D

Figure 19.– Continued.

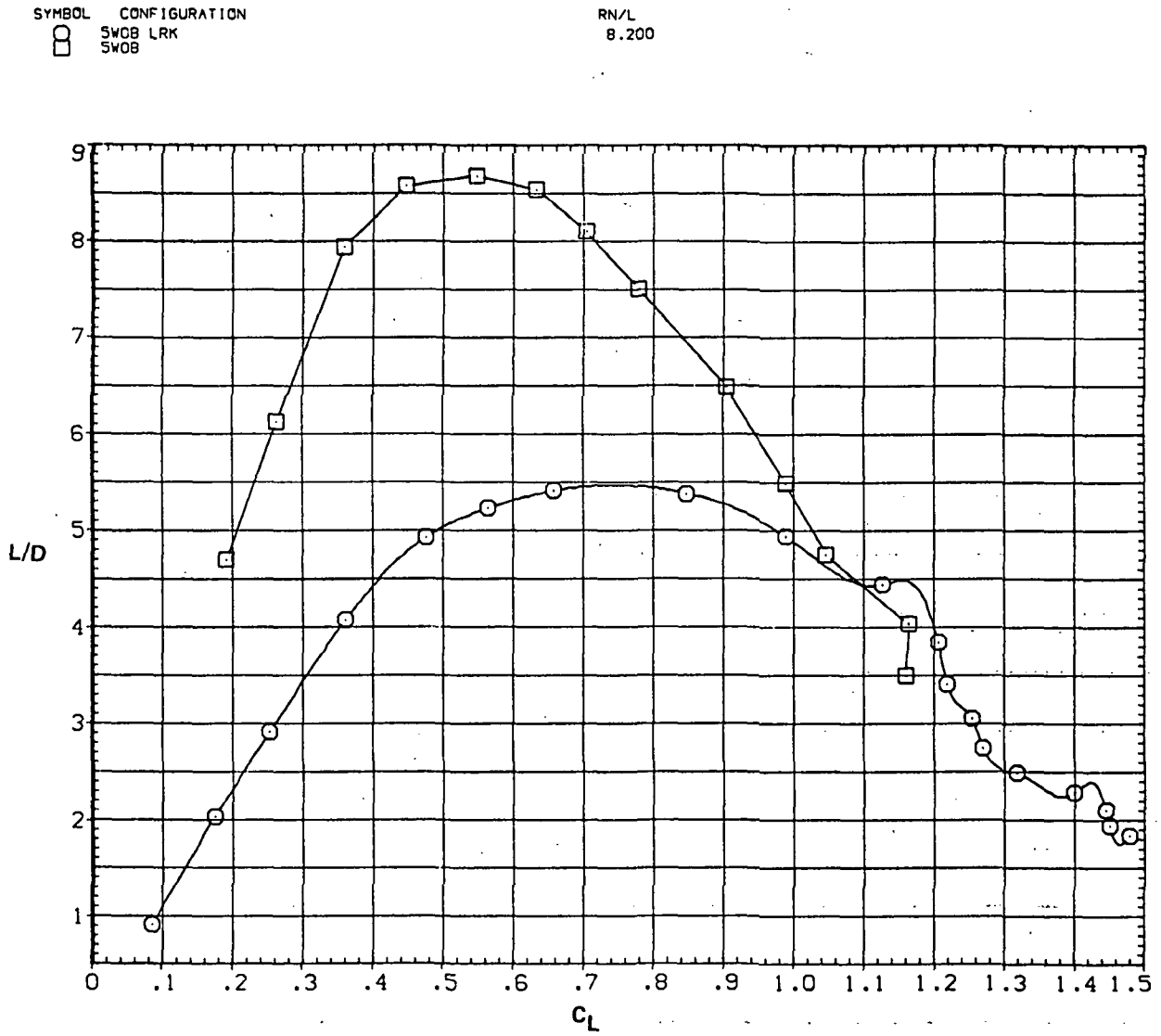

(d) L/D vs C_L

Figure 19.– Continued.

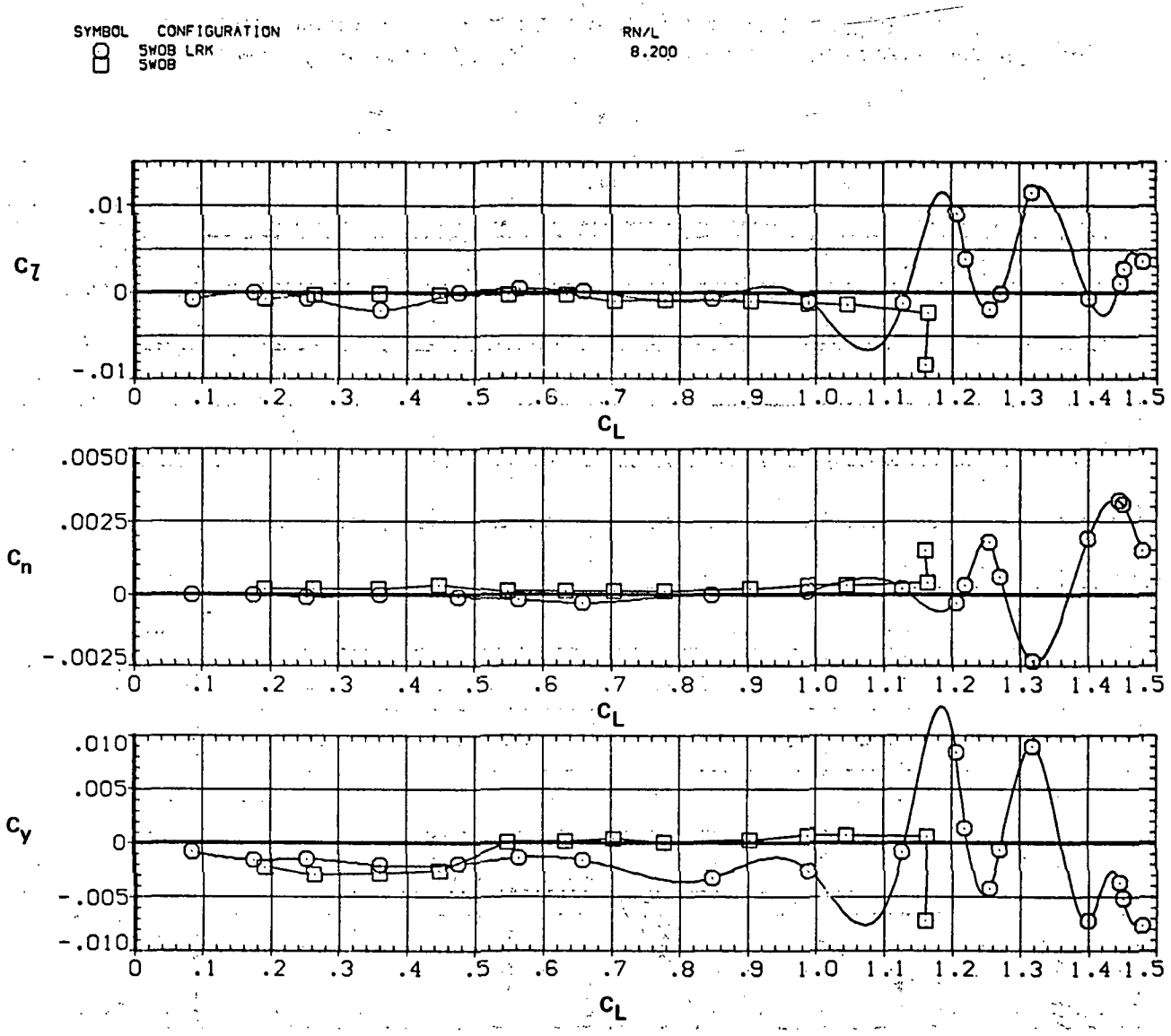

(e) C_l, C_n, and C_Y vs C_L

Figure 19.– Concluded.

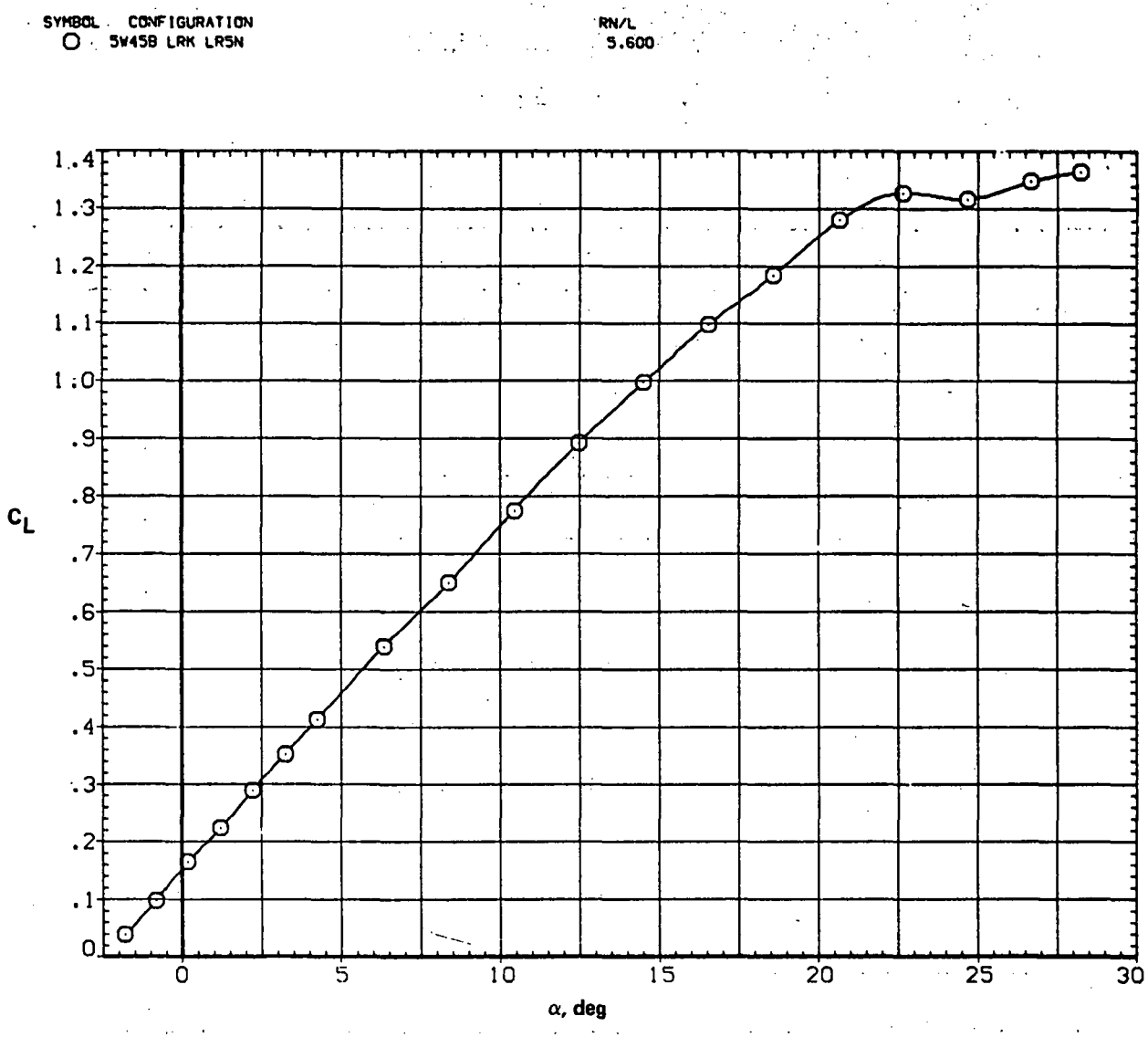

(a) C_L vs α

Figure 20.– Effect of having Krüger flaps on both wing panels with a nose droop of 5° on the static longitudinal characteristics of oblique wing: $\Lambda = 45°, M = 0.25$.

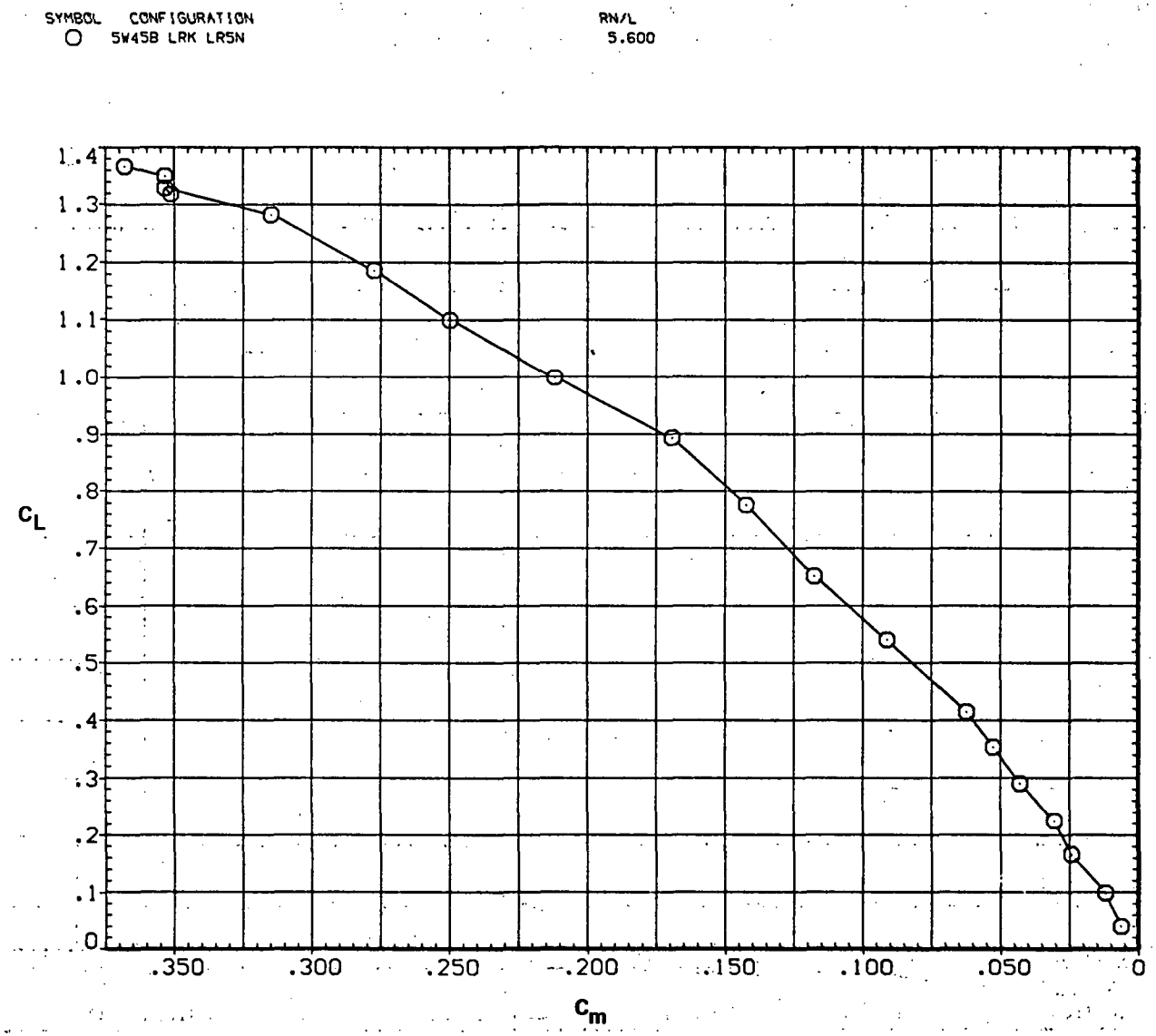

(b) C_L vs C_m

Figure 20.– Continued.

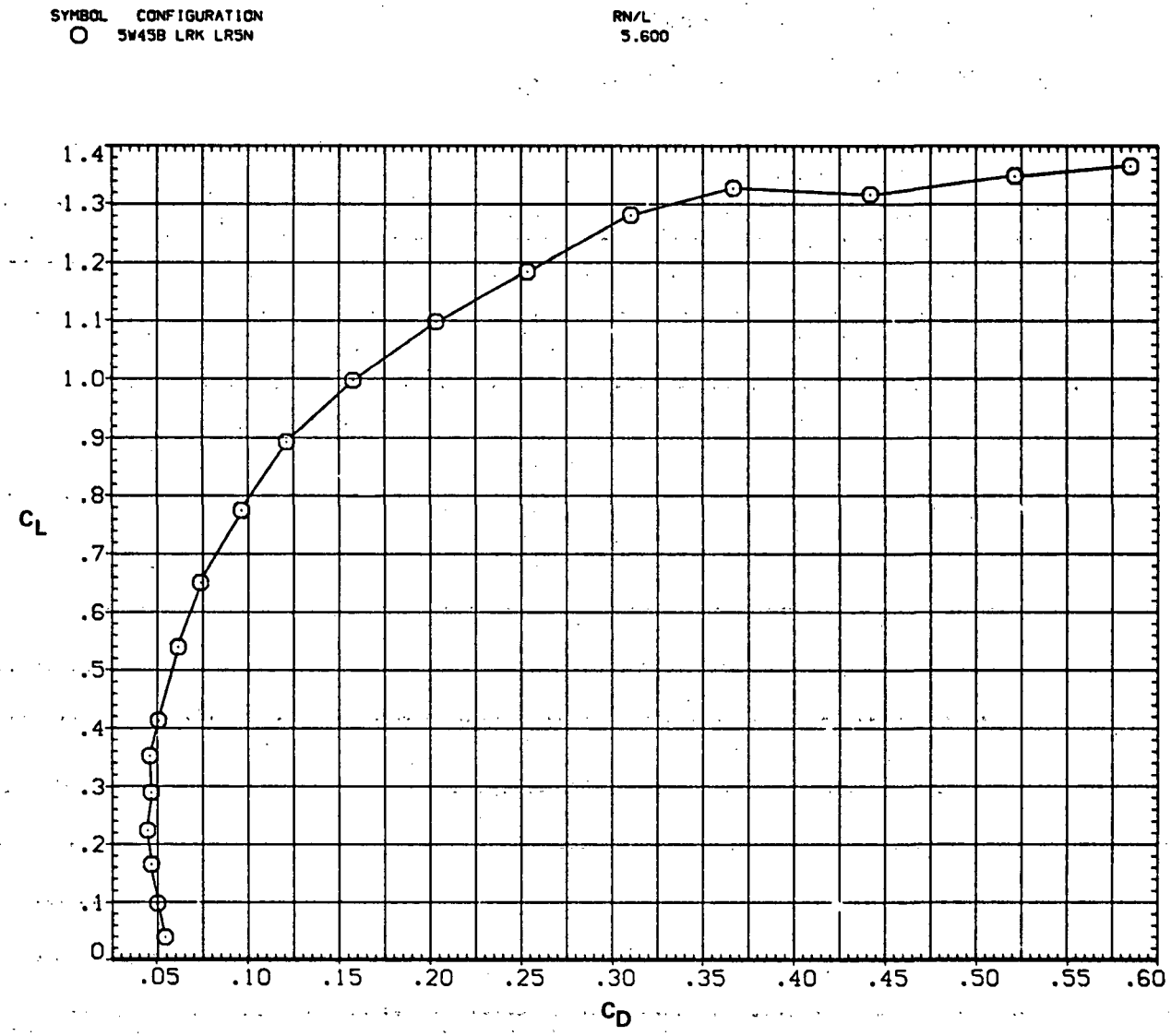

(c) C_L vs C_D

Figure 20.– Continued.

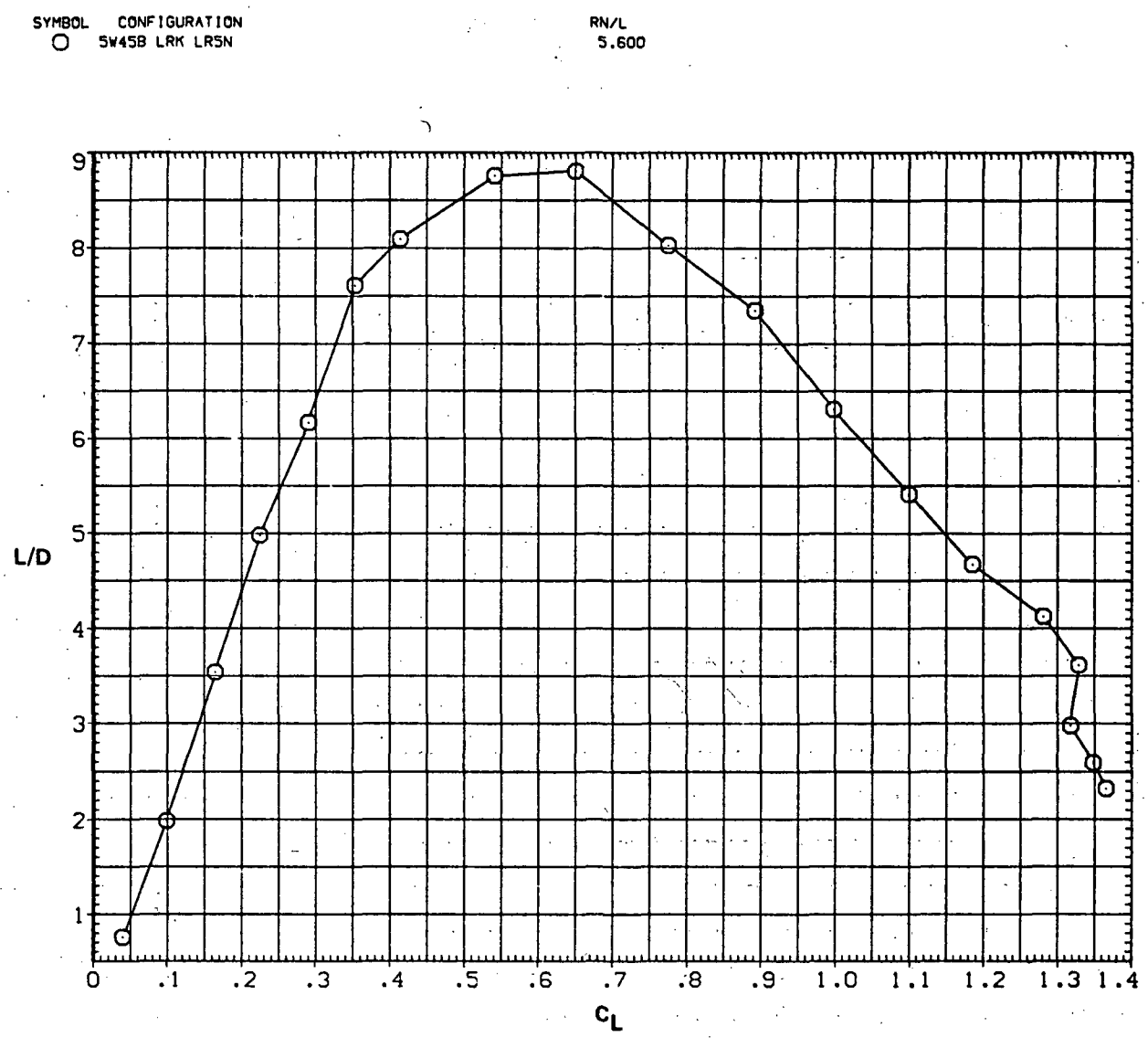

(d) L/D vs C_L

Figure 20.– Continued.

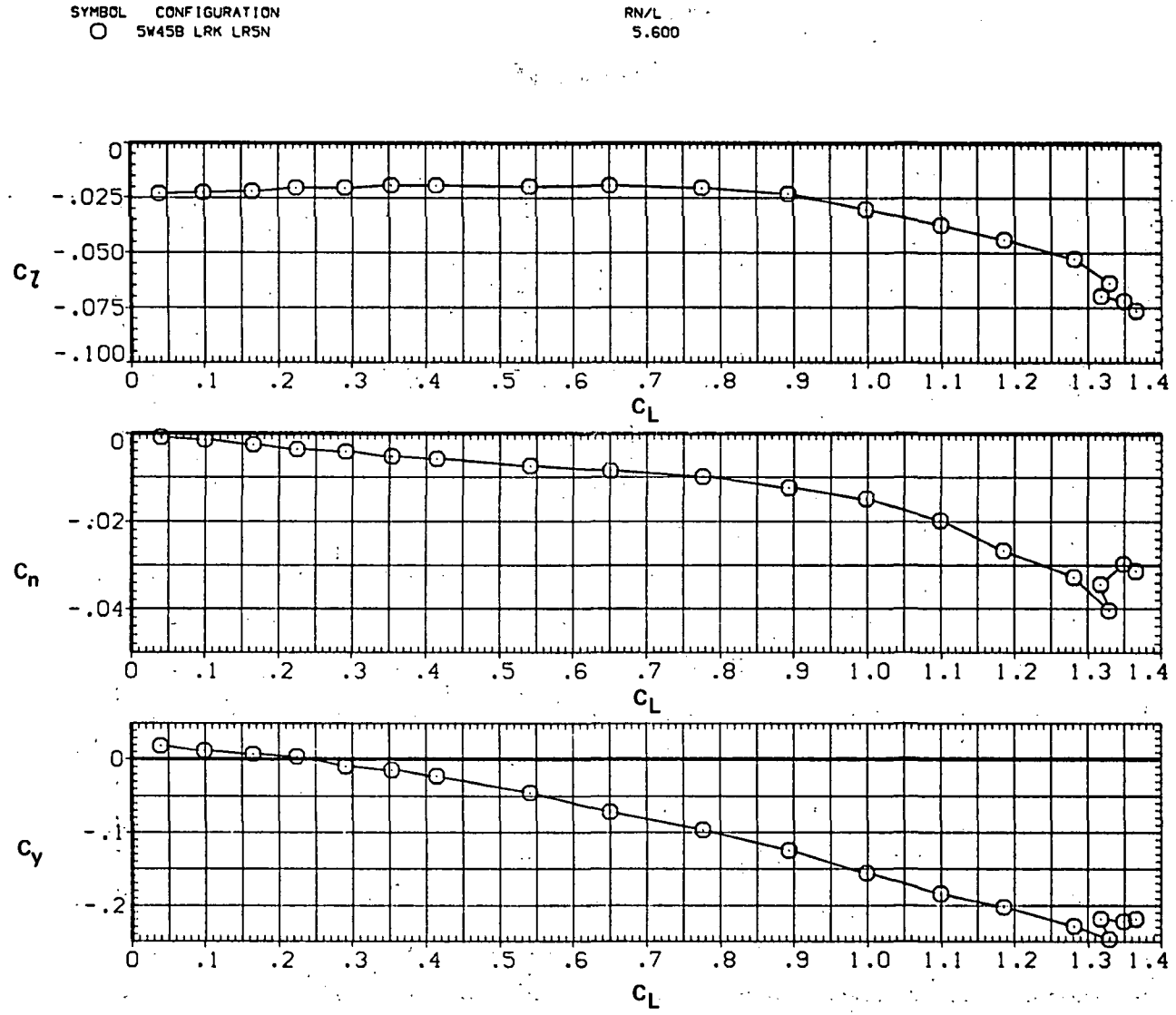

(e) C_l, C_n, and C_Y vs C_L

Figure 20.– Concluded.

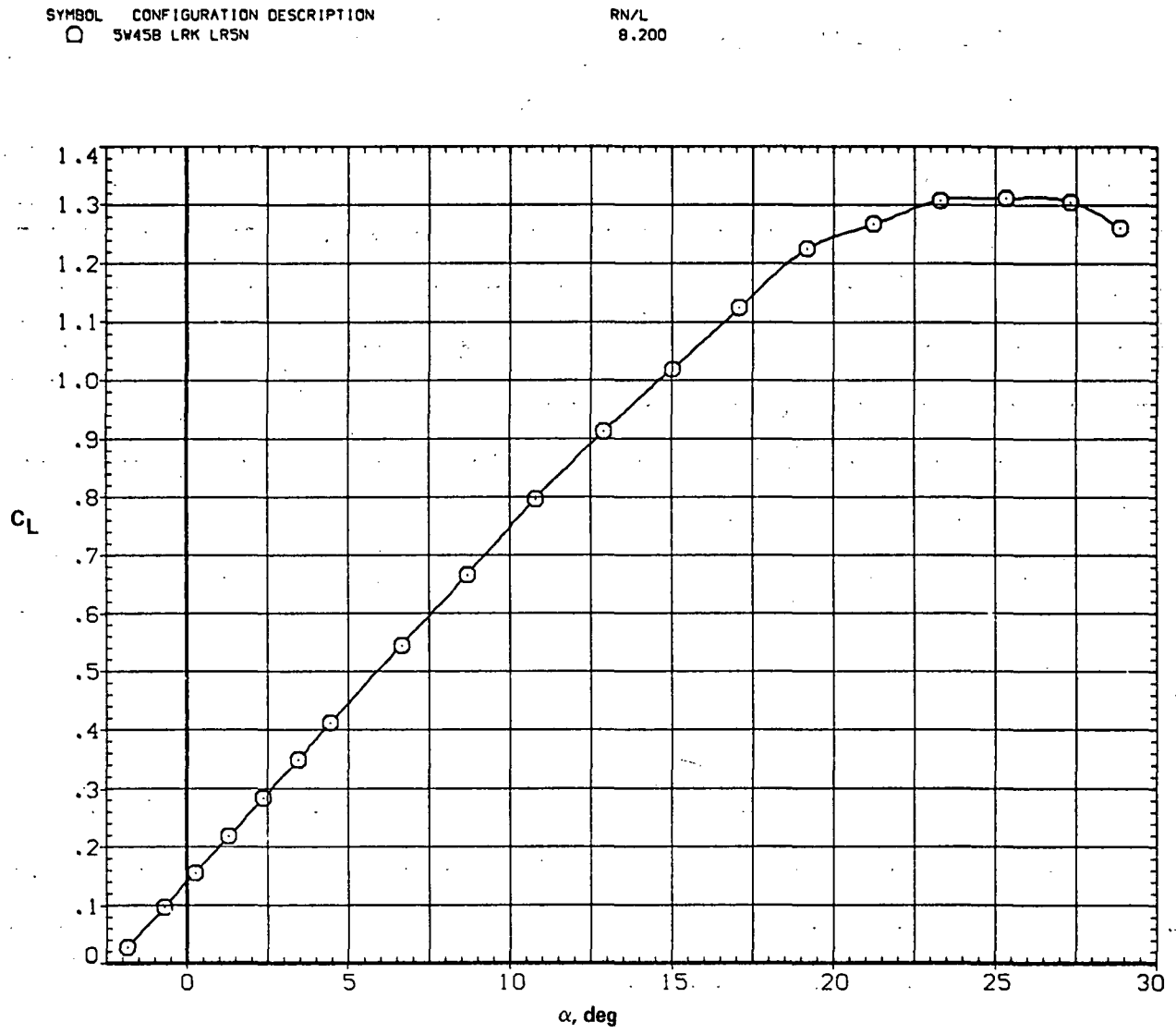

(a) C_L vs α

Figure 21.– Effect of having Krüger flaps on both wing panels with a nose droop of 5° on the static longitudinal characteristics of an oblique wing: $\Lambda = 45°$, $M = 0.40$.

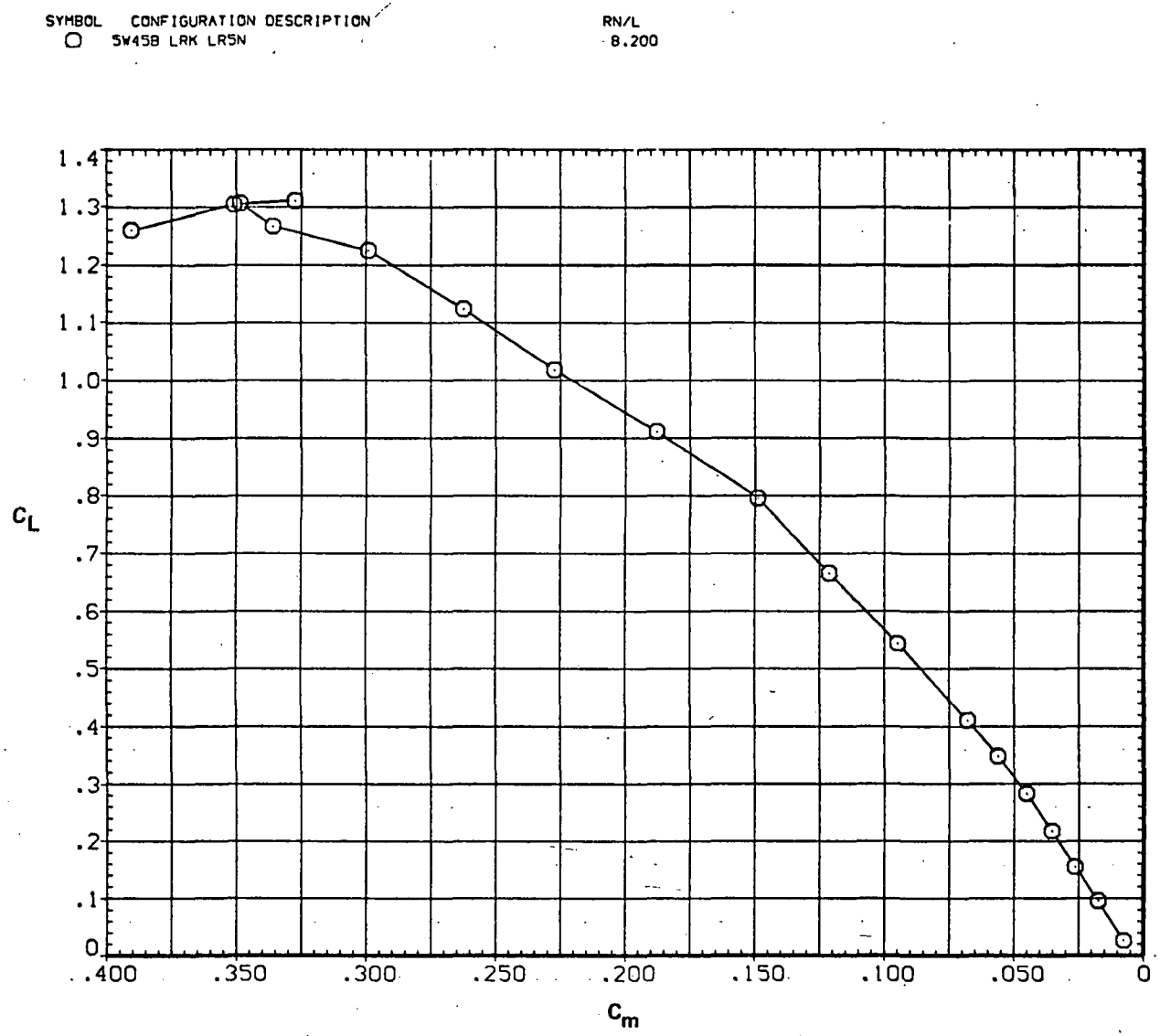

(b) C_L vs C_m

Figure 21.– Continued.

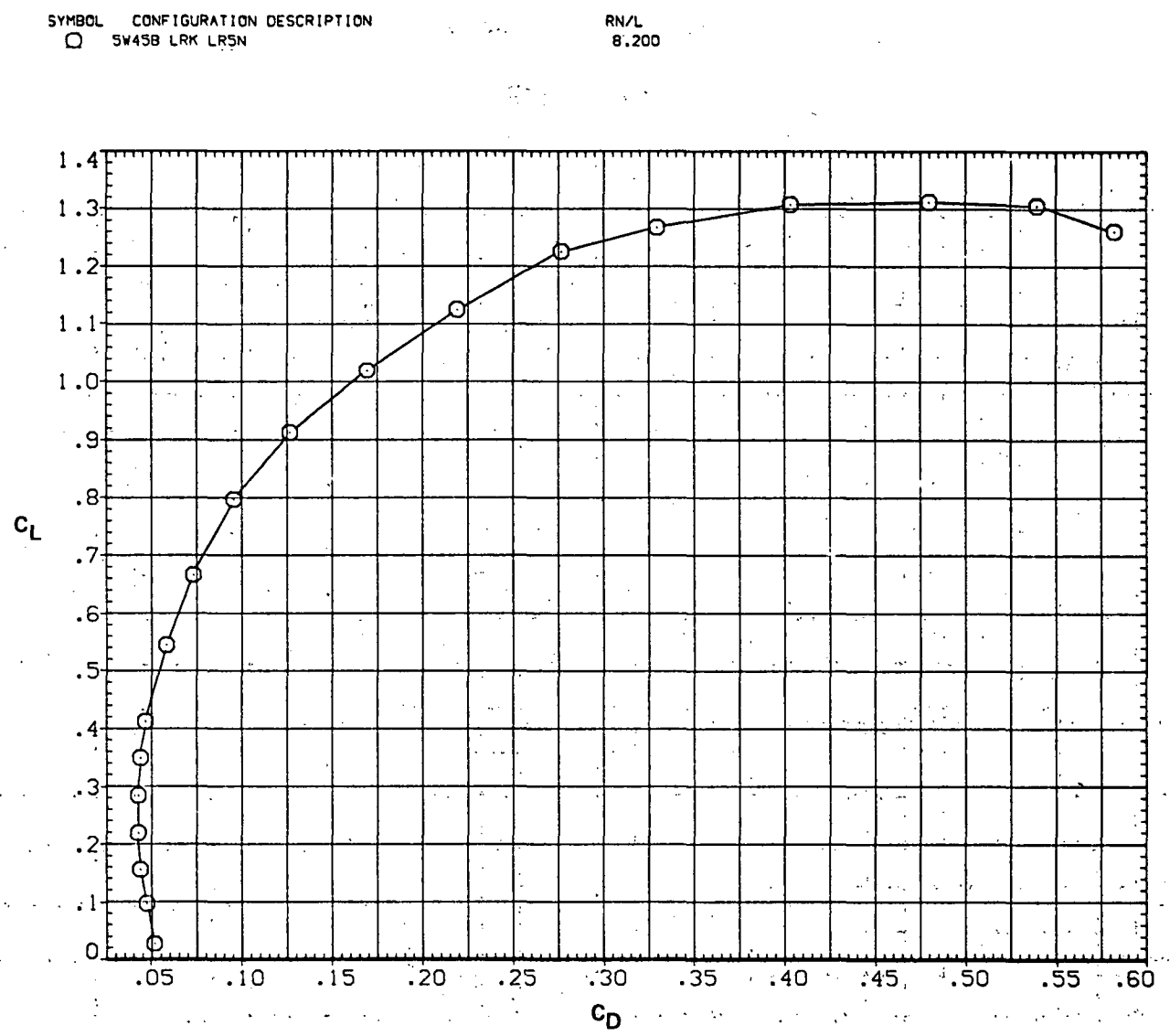

(c) C_L vs C_D

Figure 21.– Continued.

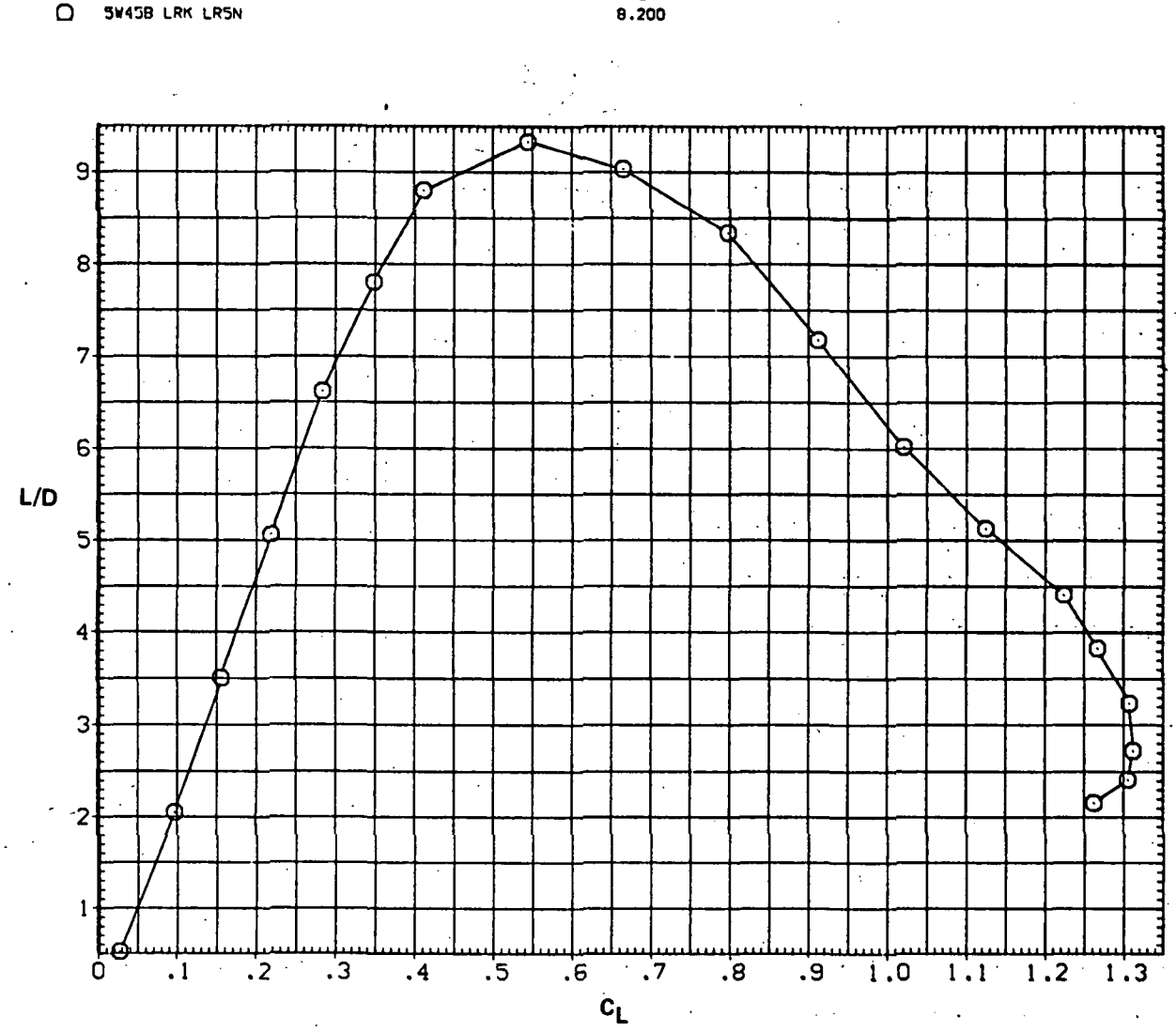

(d) L/D vs C_L

Figure 21.– Continued.

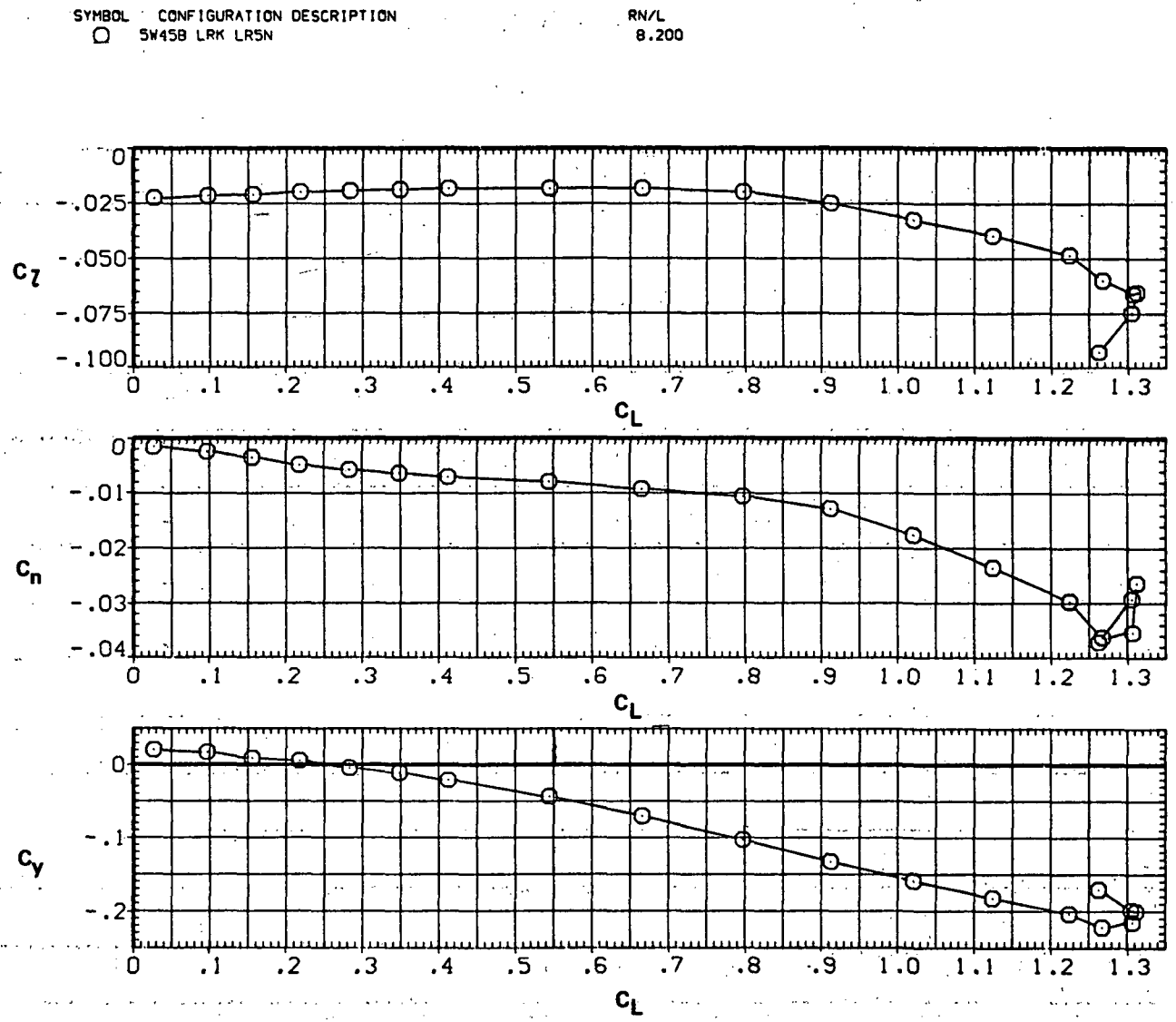

(e) C_l, C_n, and C_Y vs C_L

Figure 21.– Concluded.

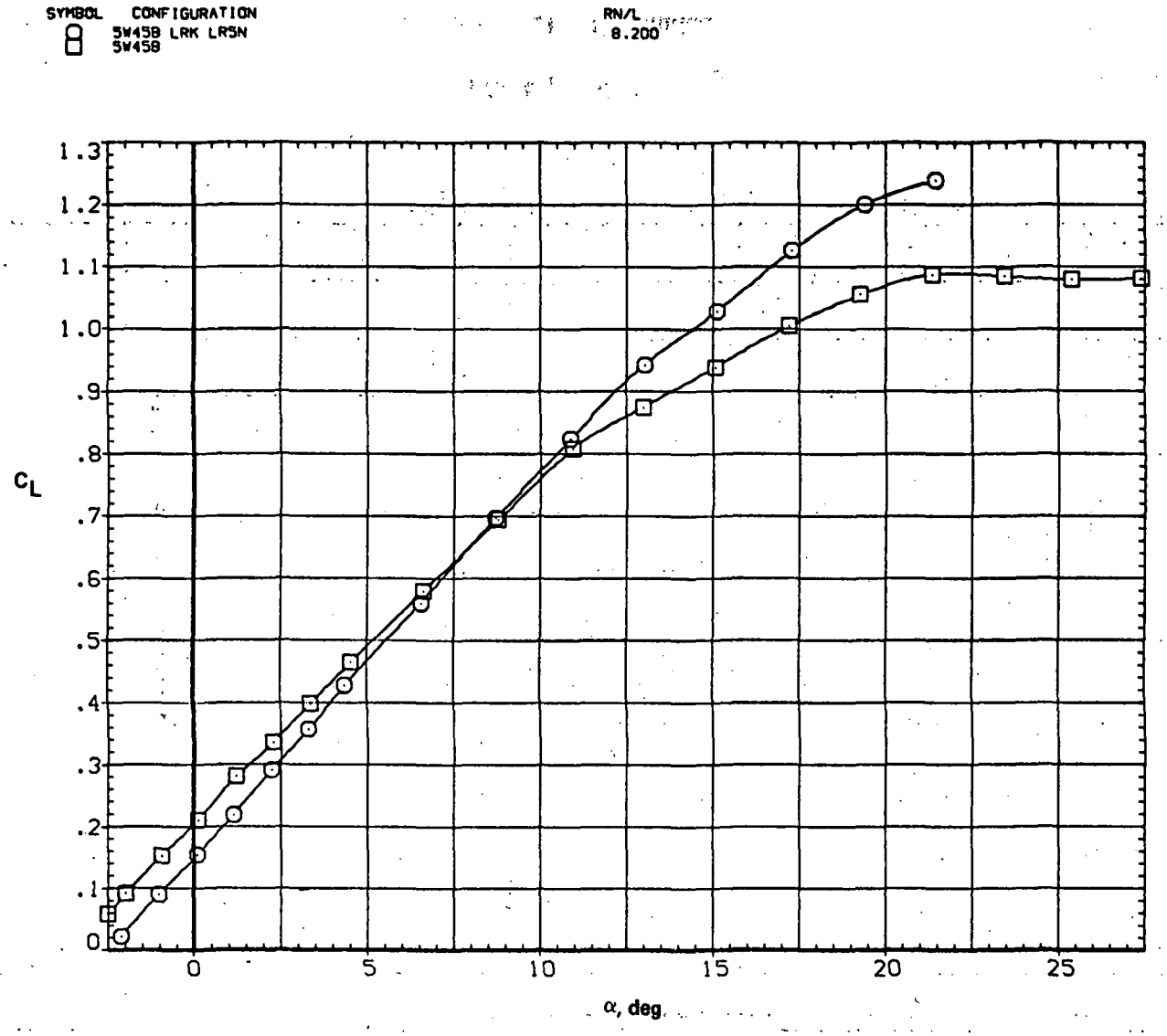

(a) C_L vs α

Figure 22.– Effect of having Krüger flaps on both wing panels with a nose droop of 5° on the static longitudinal characteristics of an oblique wing: $\Lambda = 45°$, $M = 0.60$.

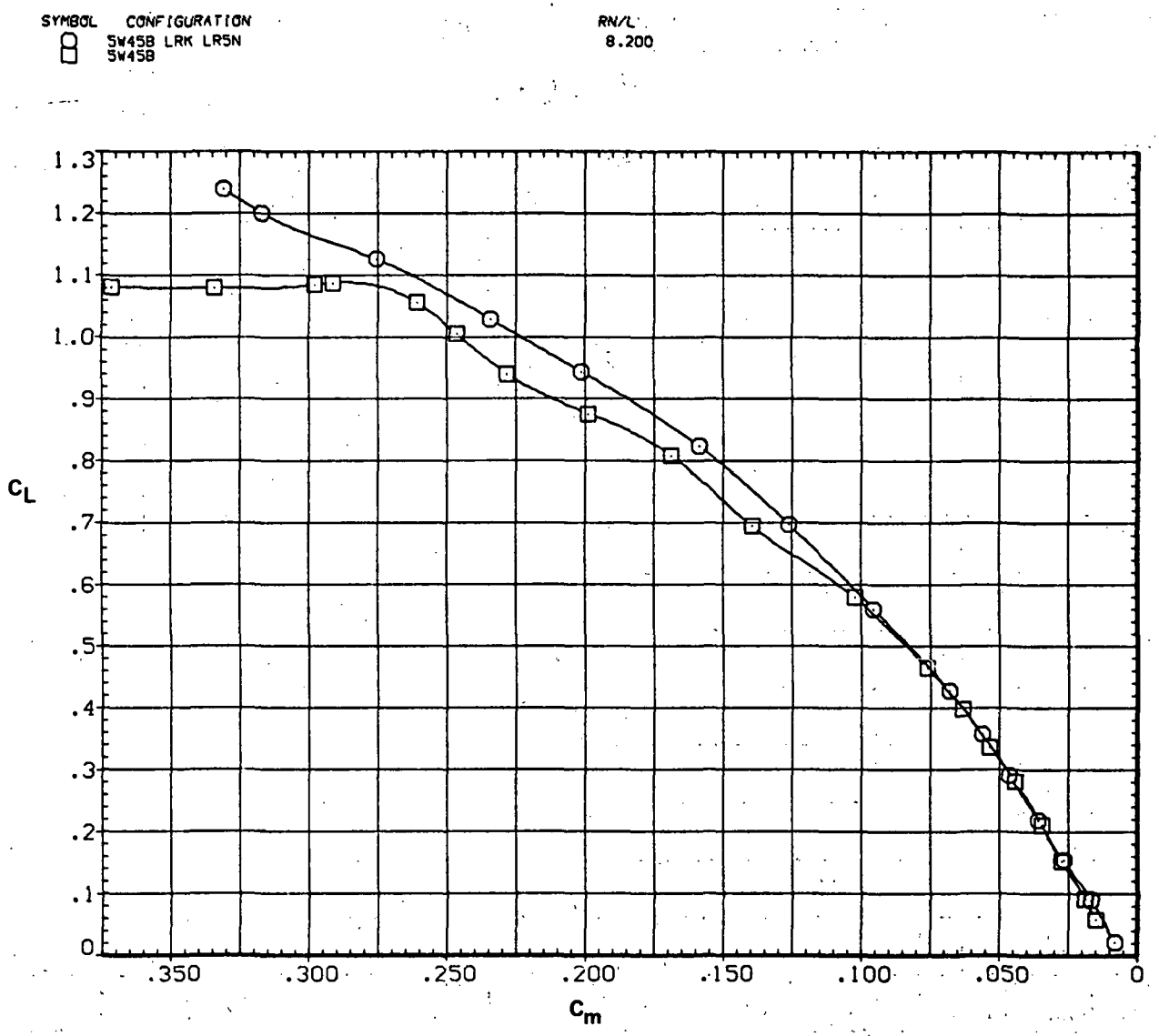

(b) C_L vs C_m

Figure 22.– Continued.

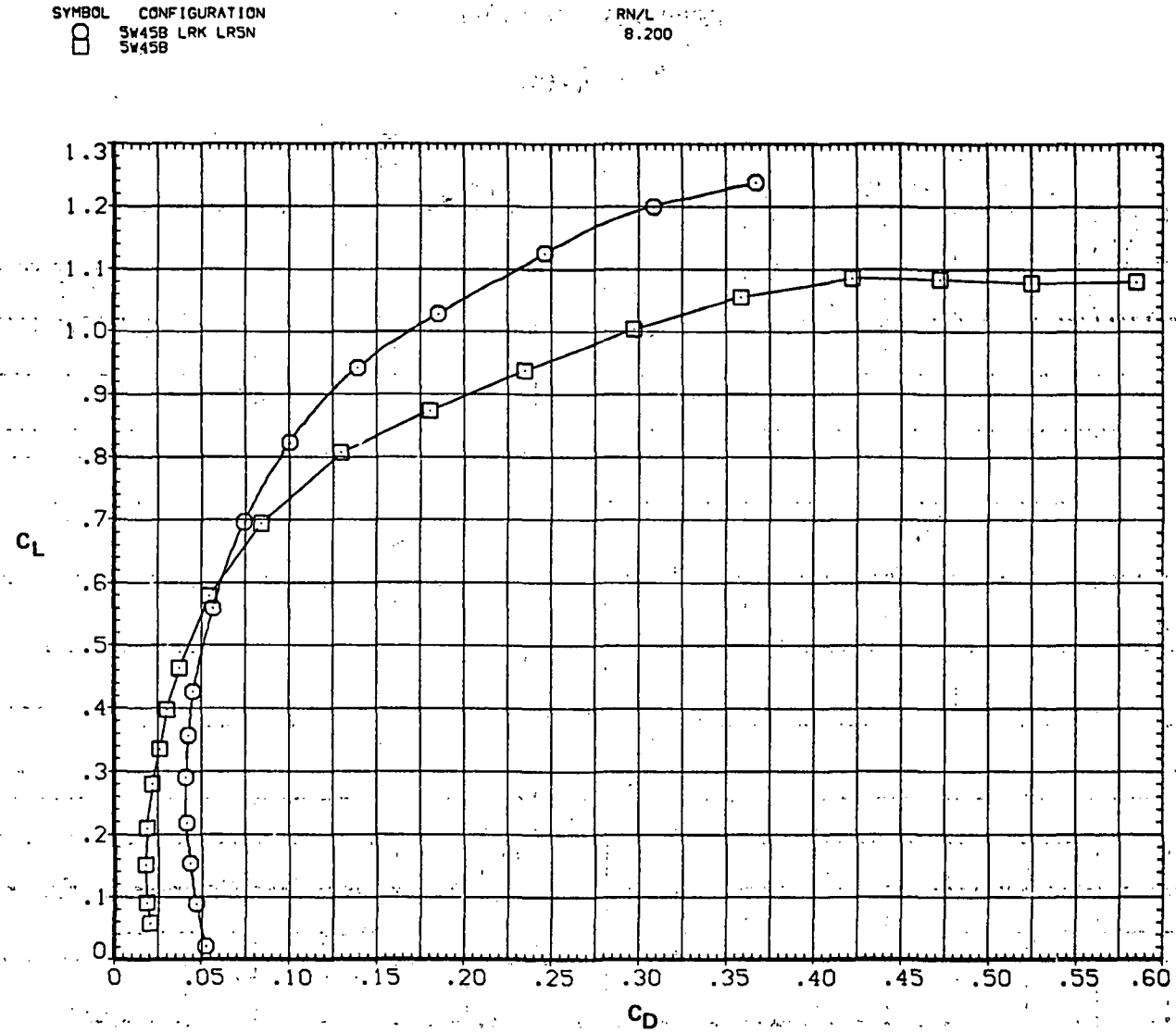

(c) C_L vs C_D

Figure 22.– Continued.

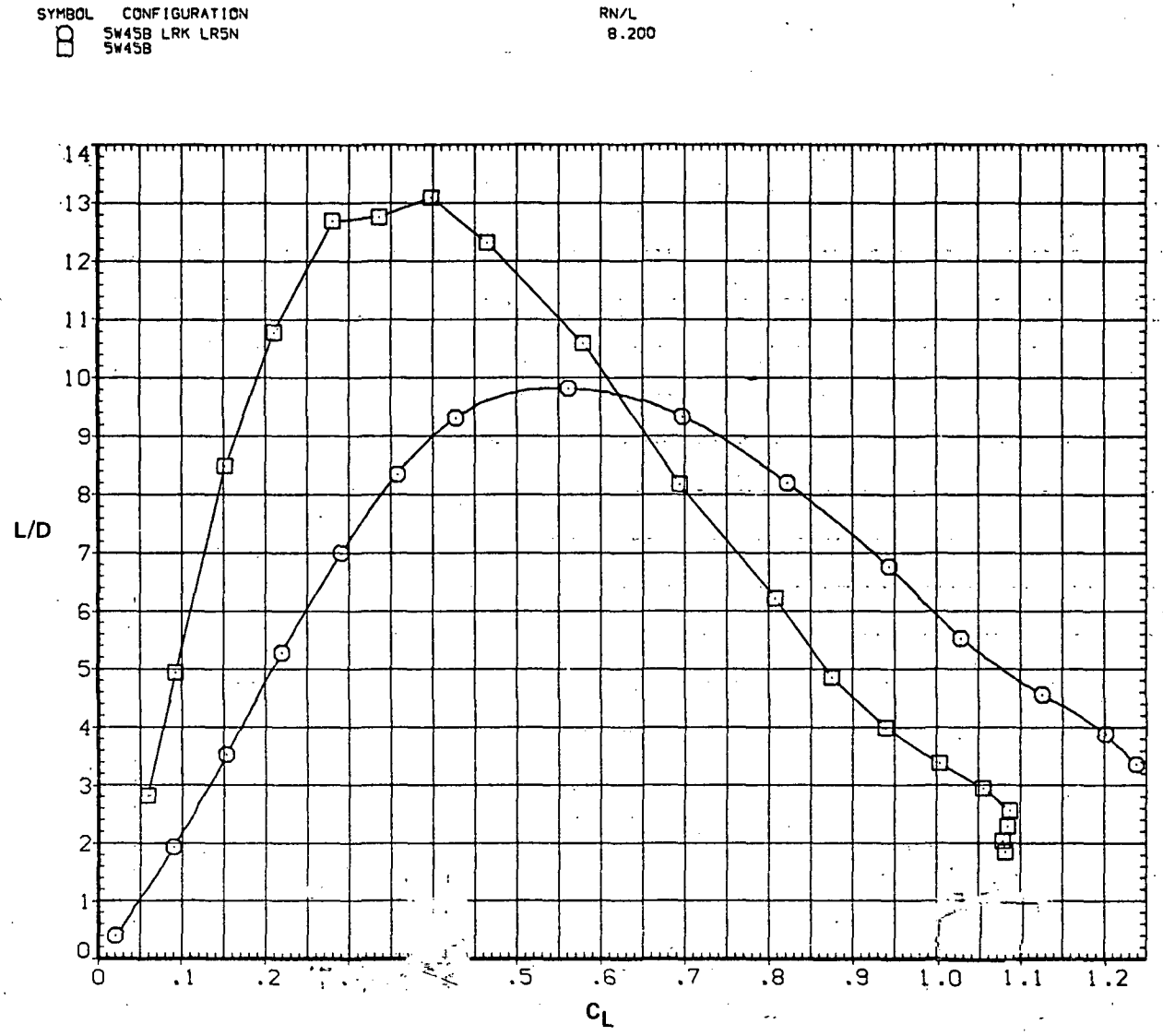

(d) L/D vs C_L

Figure 22.– Continued.

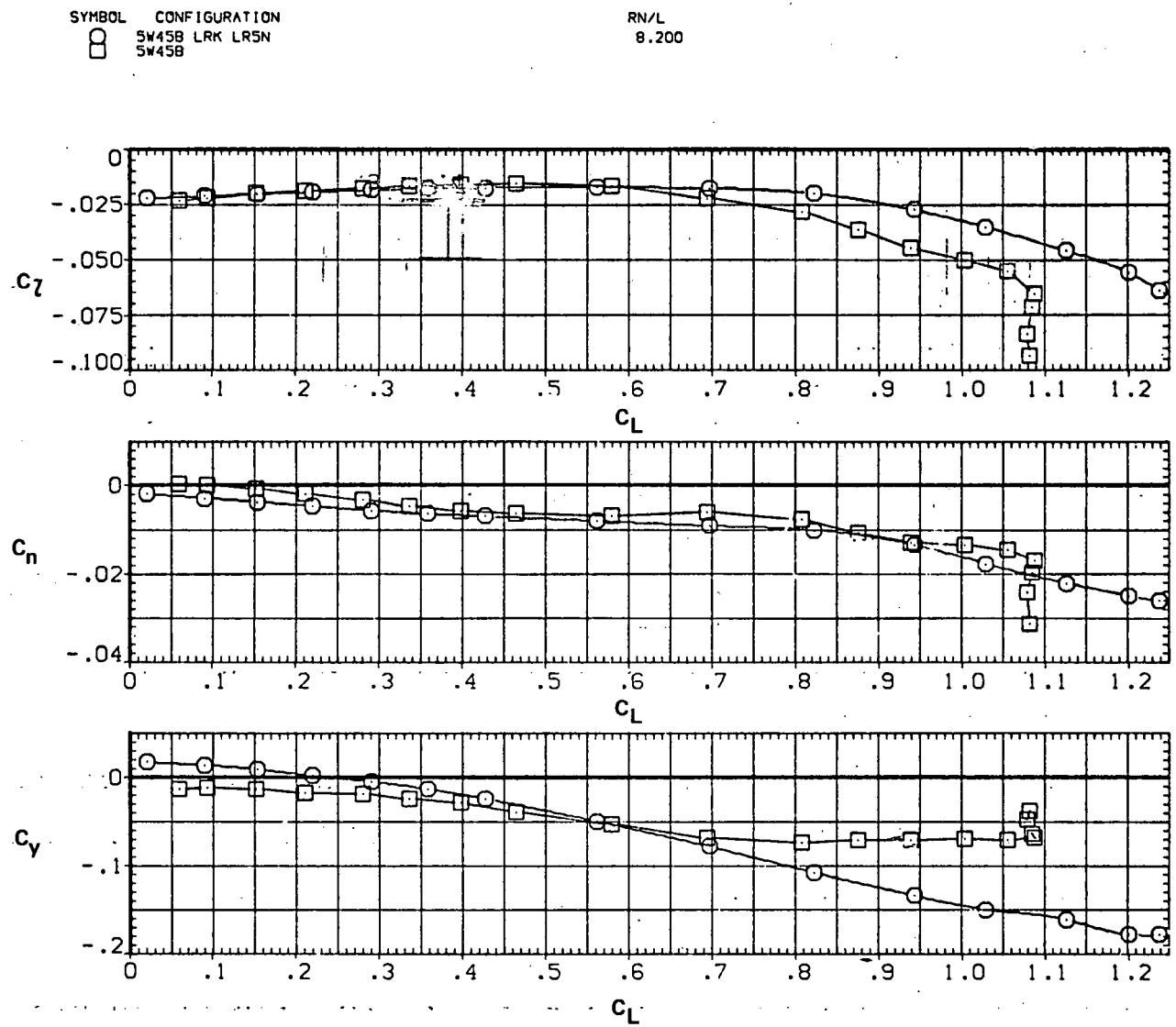

(e) C_l, C_n, and C_Y vs C_L

Figure 22.– Concluded.

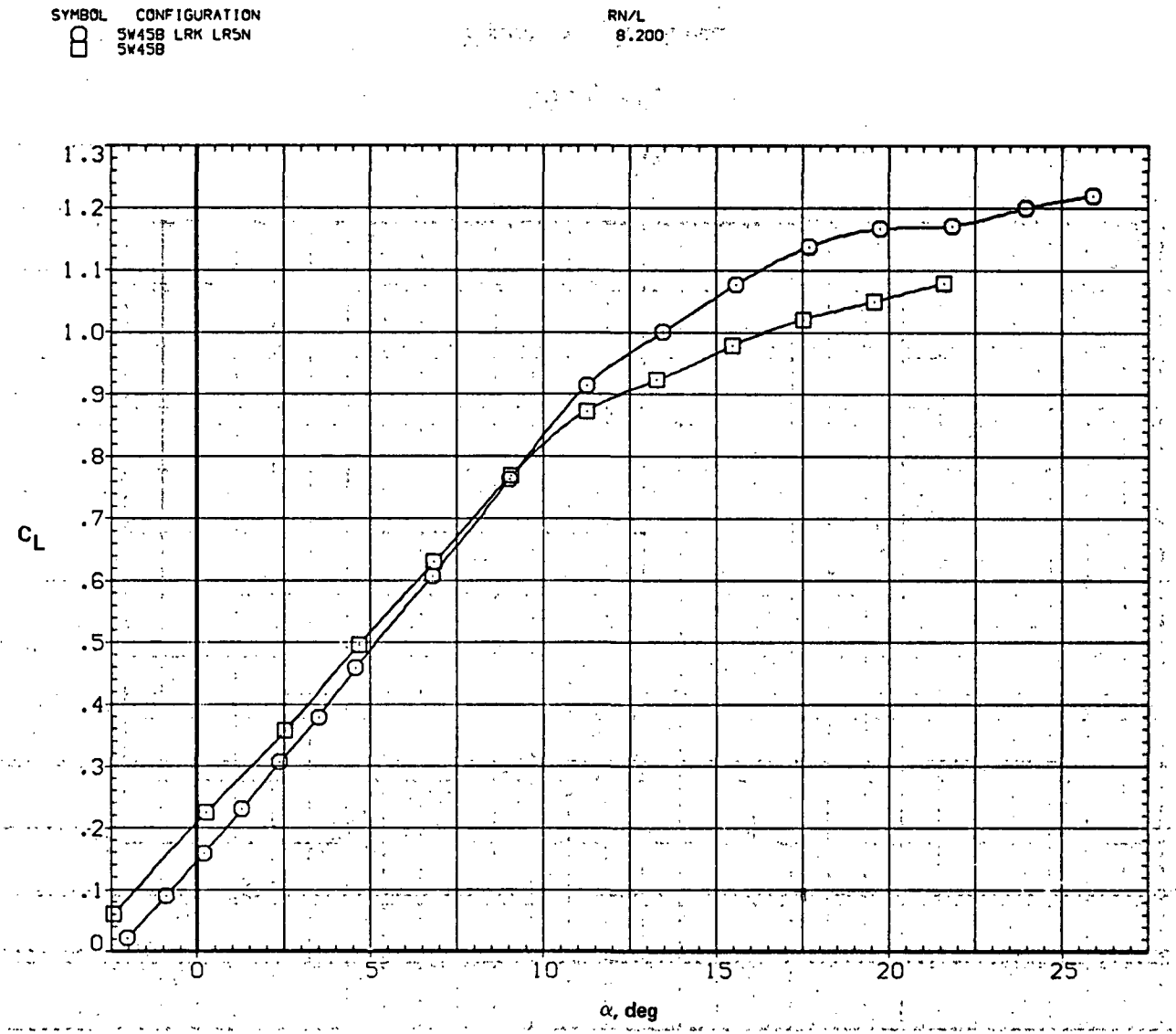

(a) C_L vs α

Figure 23.– Effect of having Krüger flaps on both wing panels with a nose droop of 5° on the static longitudinal characteristics of an oblique wing: $\Lambda = 45°$, $M = 0.80$.

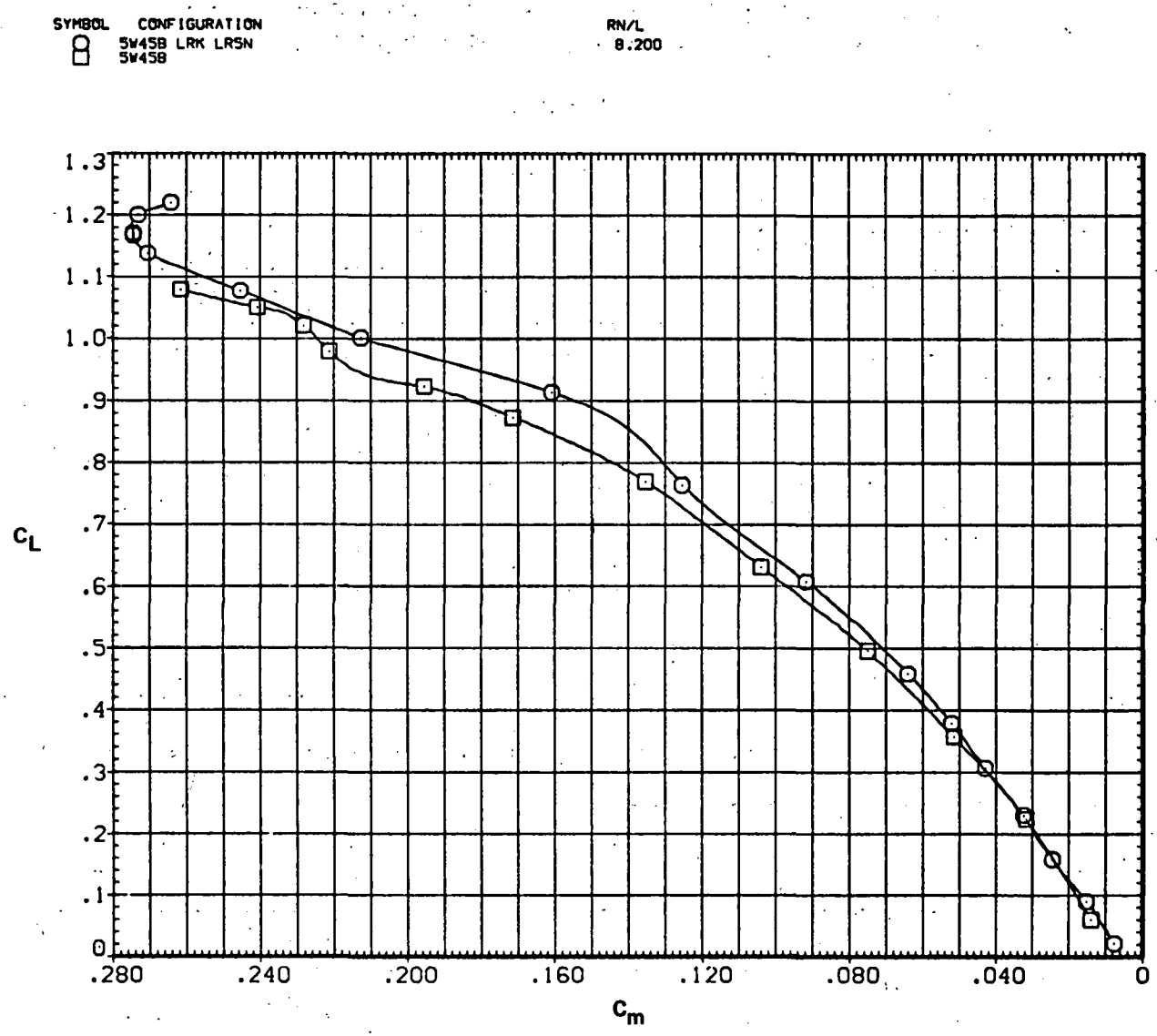

(b) C_L vs C_m

Figure 23.– Continued.

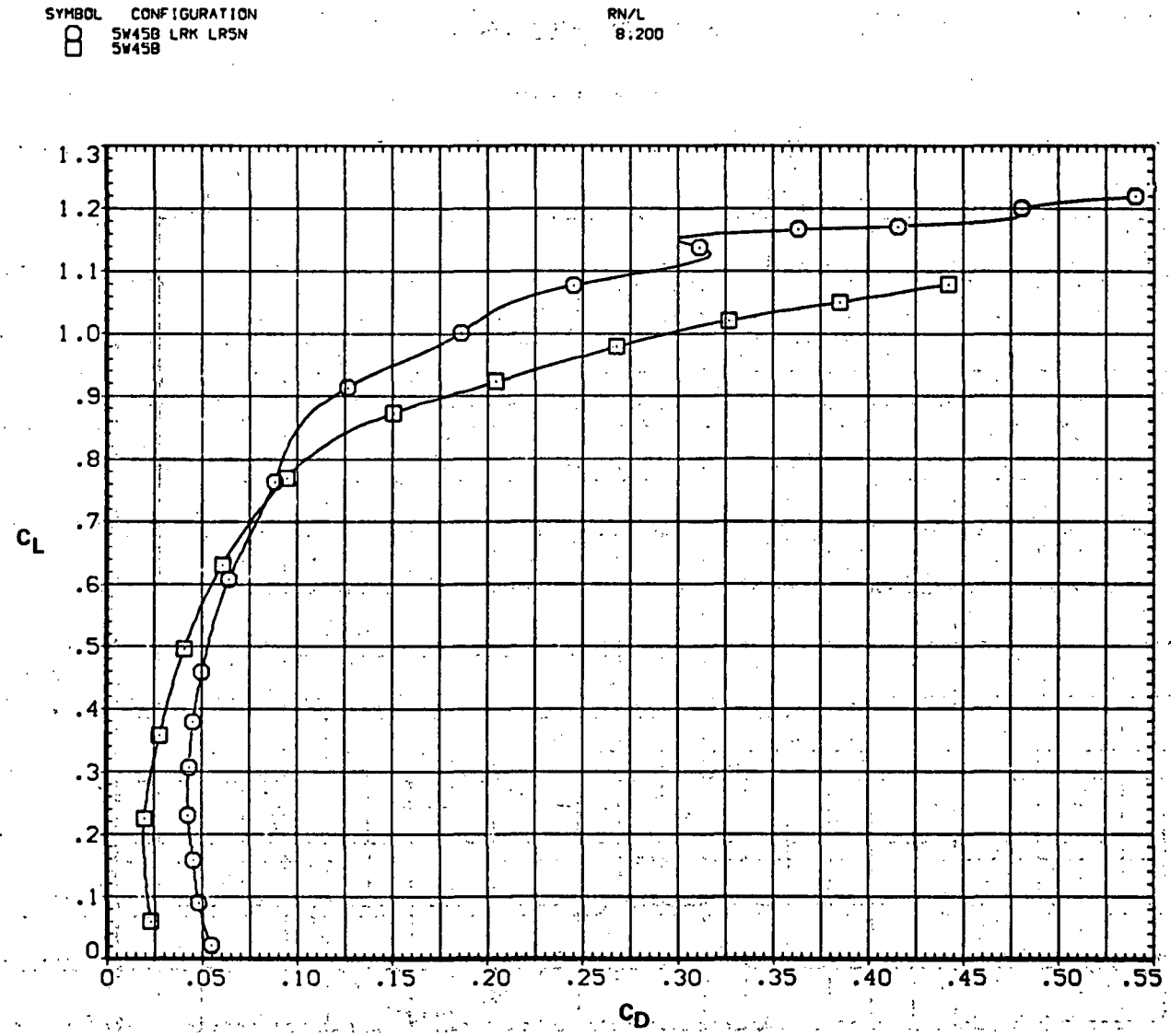

(c) C_L vs C_D

Figure 23.– Continued.

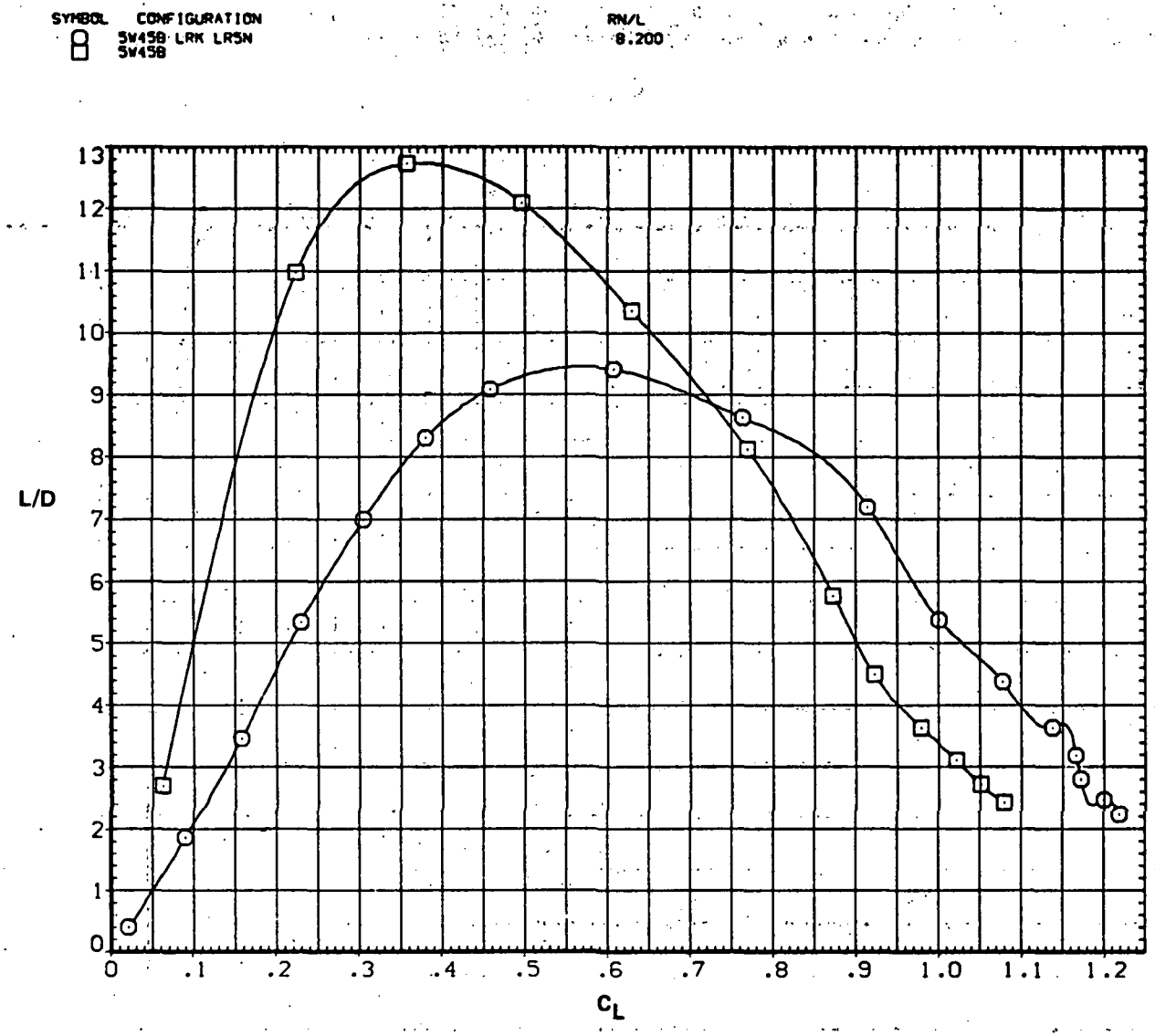

(d) L/D vs C_L

Figure 23.– Continued.

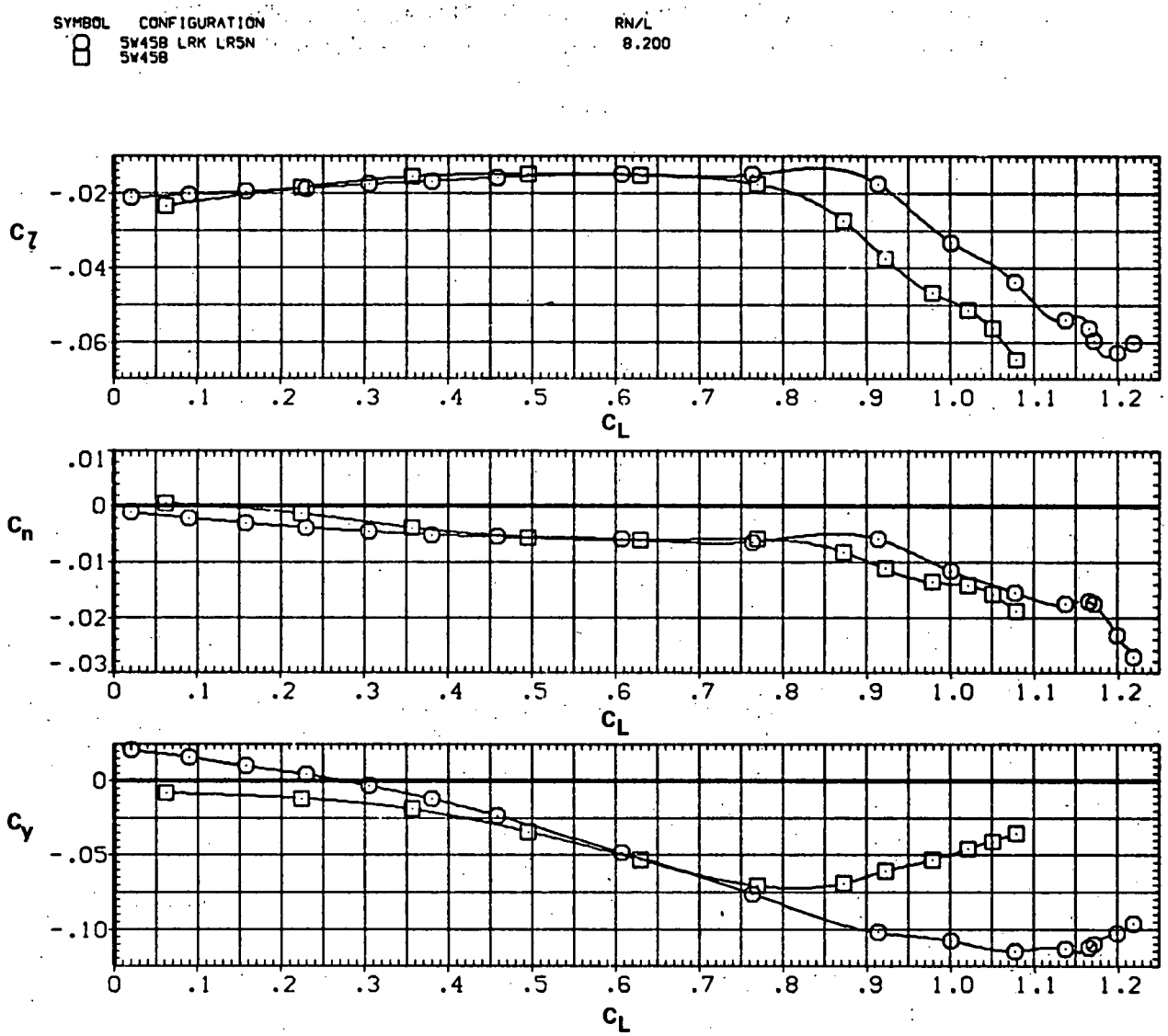

(e) C_l, C_n, and C_Y vs C_L

Figure 23.– Concluded.

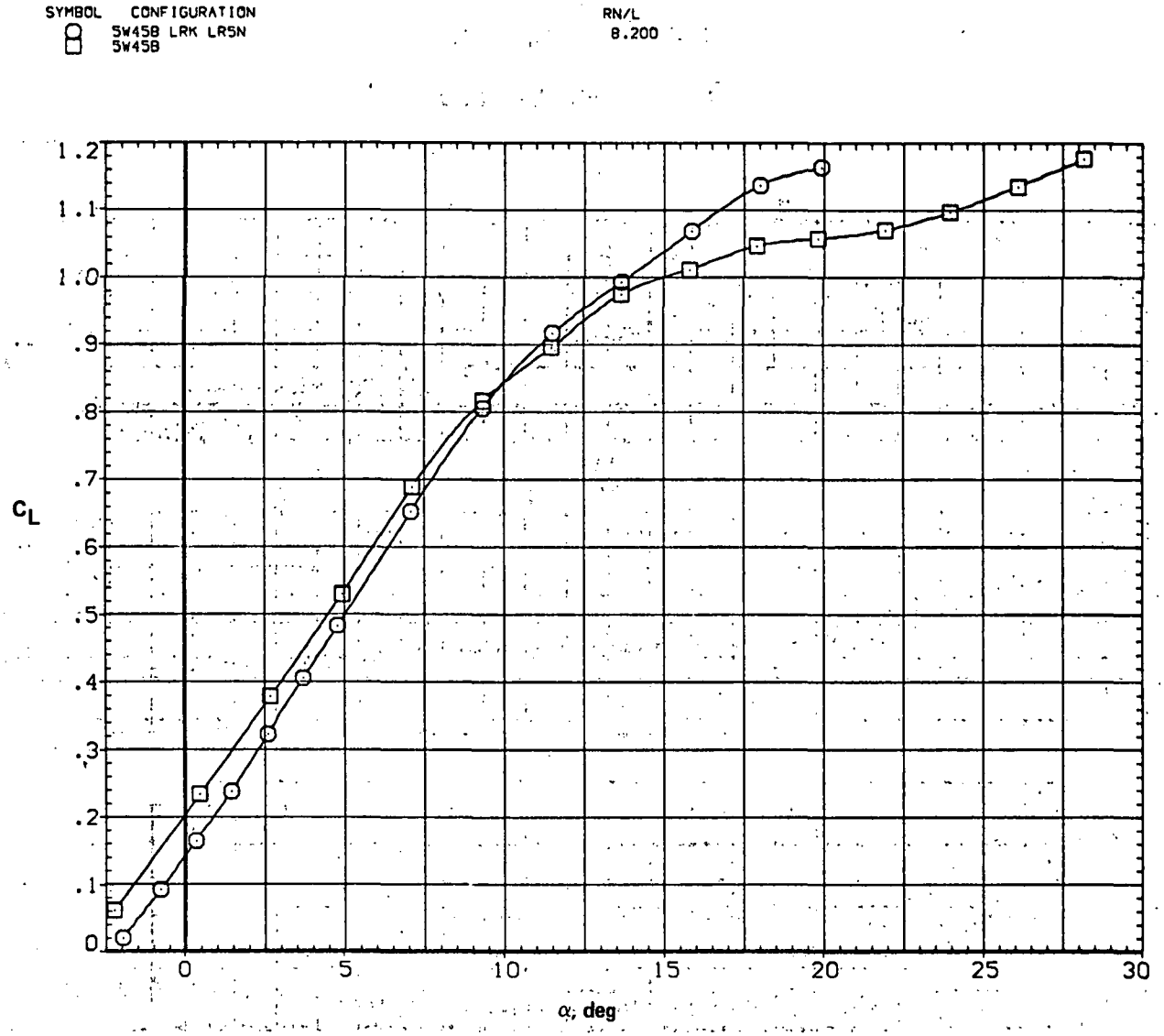

(a) C_L vs α

Figure 24.– Effect of having Krüger flaps on both wing panels with a nose droop of 5° on the static longitudinal characteristics of an oblique wing: $\Lambda = 45°$, $M = 0.90$.

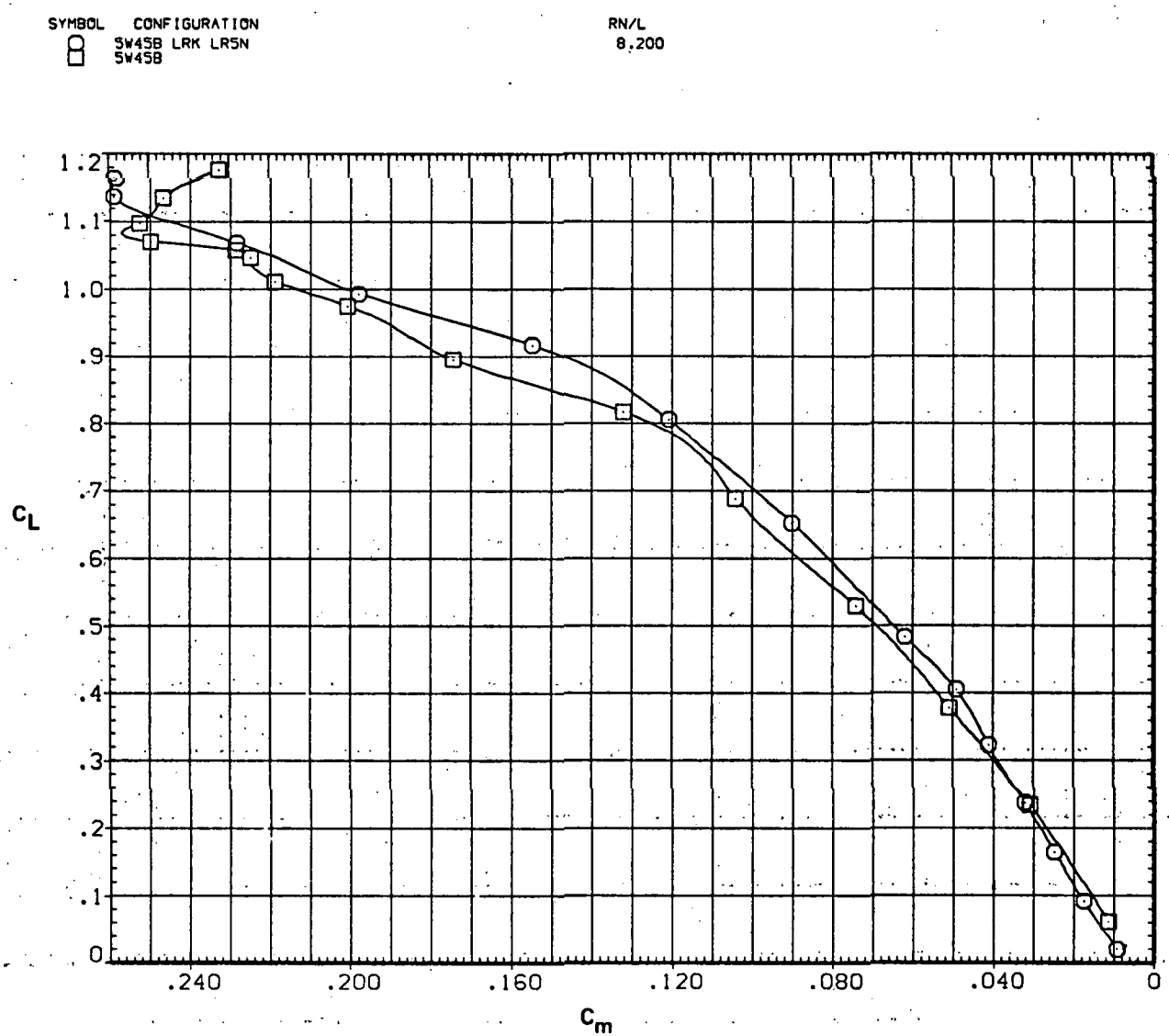

(b) C_L vs C_m

Figure 24.– Continued.

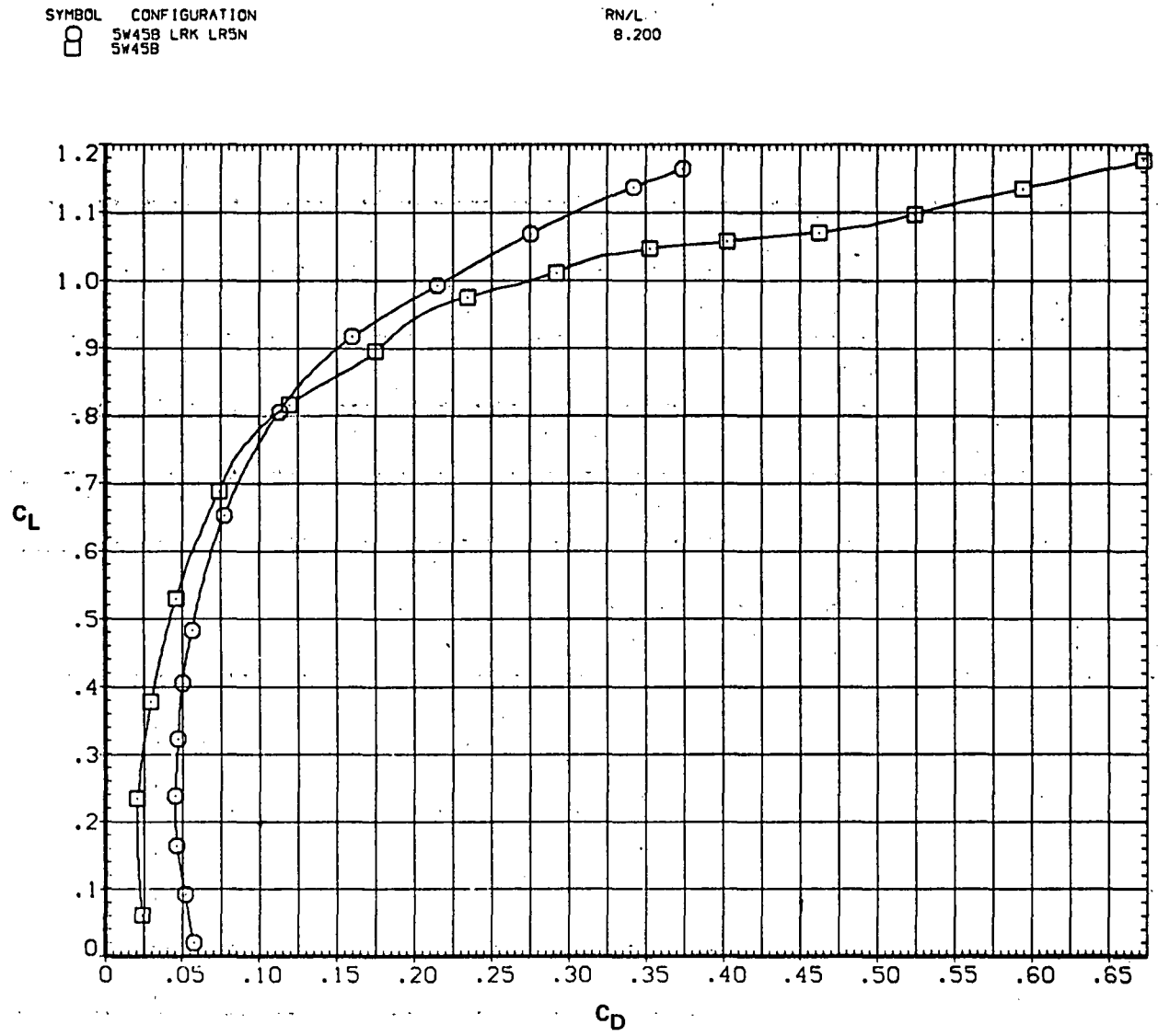

(c) C_L vs C_D

Figure 24.– Continued.

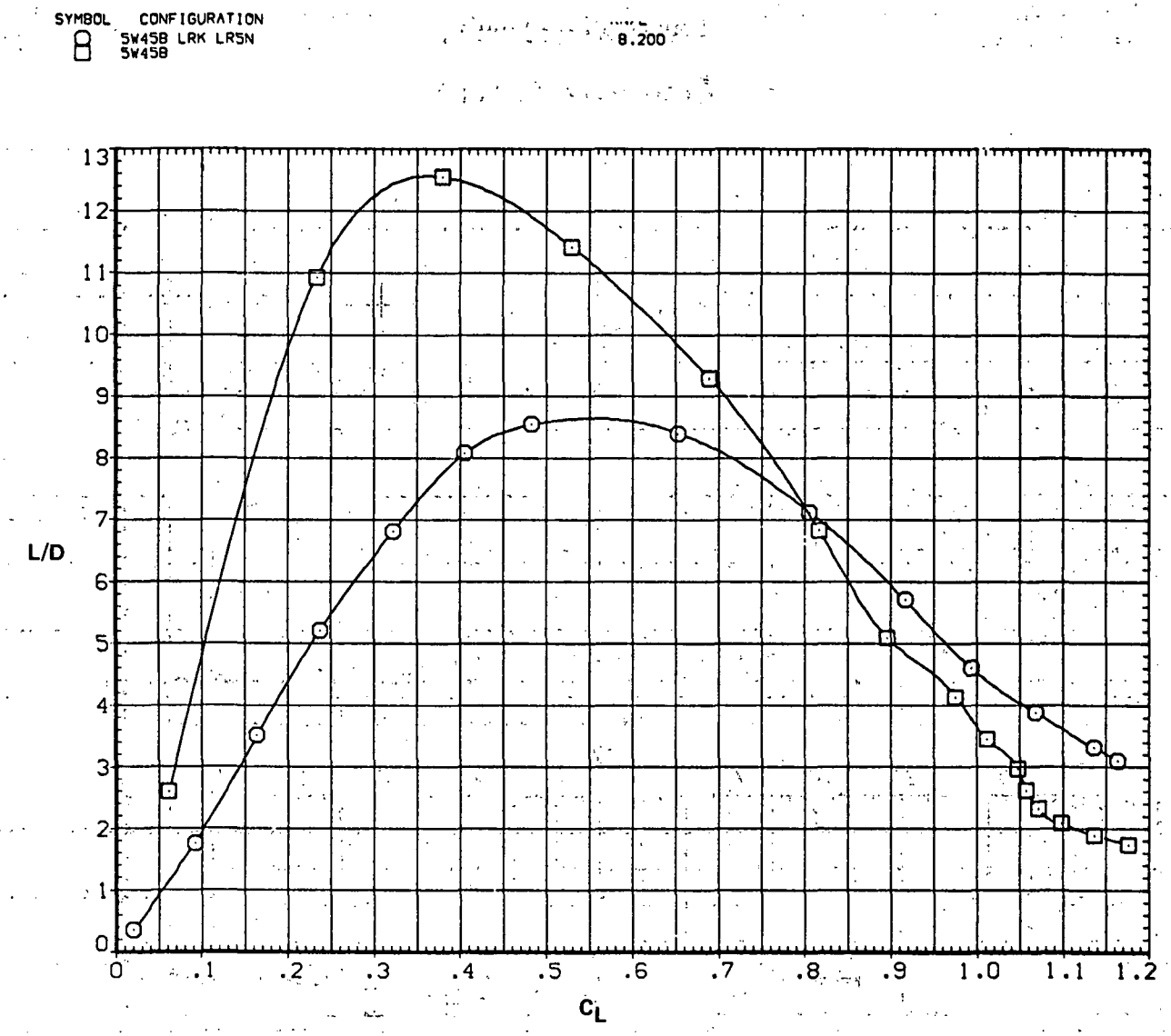

(d) L/D vs C_L

Figure 24.– Continued.

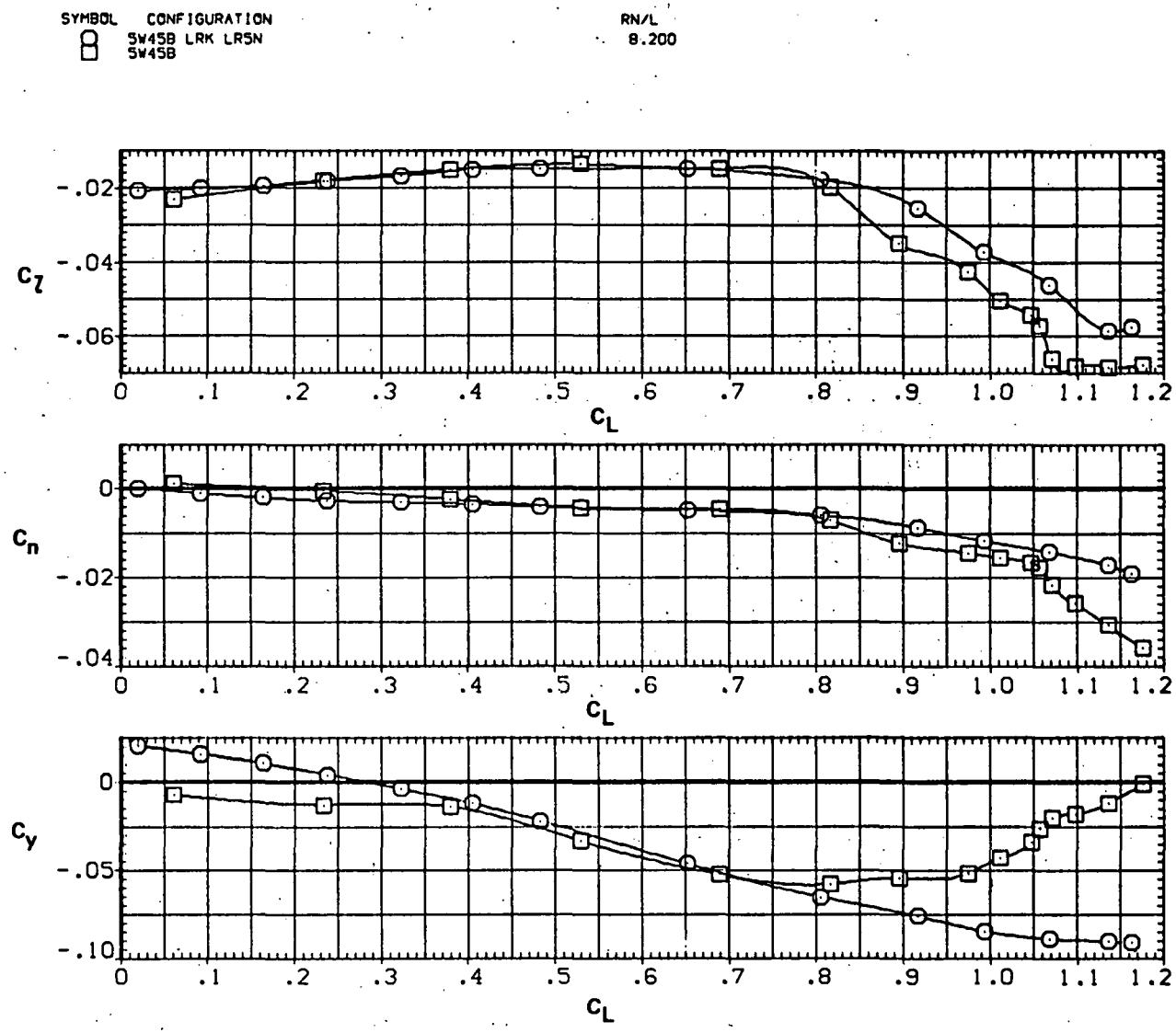

(e) C_l, C_n, and C_Y vs C_L

Figure 24.– Concluded.

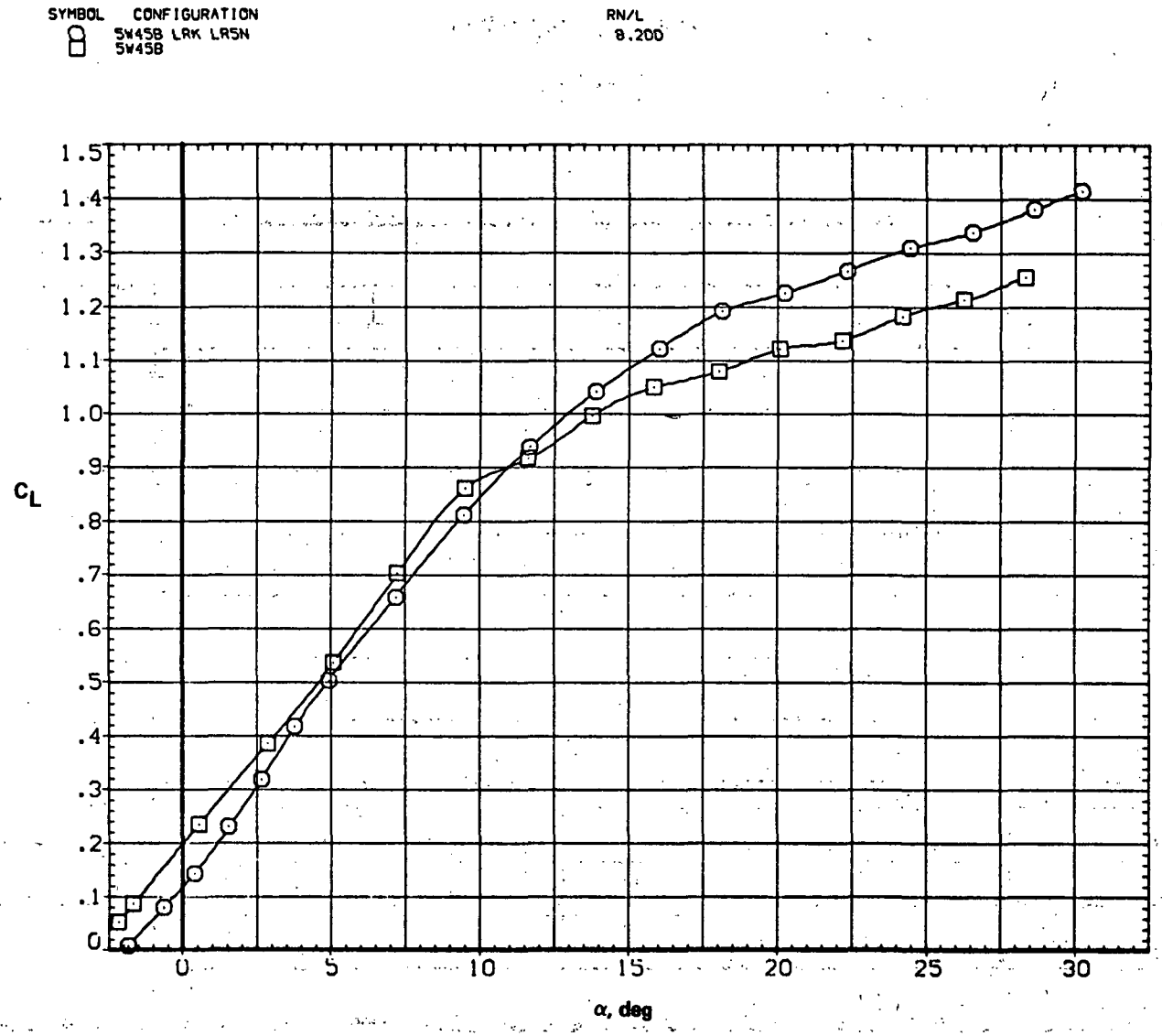

(a) C_L vs α

Figure 25.– Effect of having Krüger flaps on both wing panels with a nose droop of 5° on the static longitudinal characteristics of an oblique wing: $\Lambda = 45°$, $M = 0.95$.

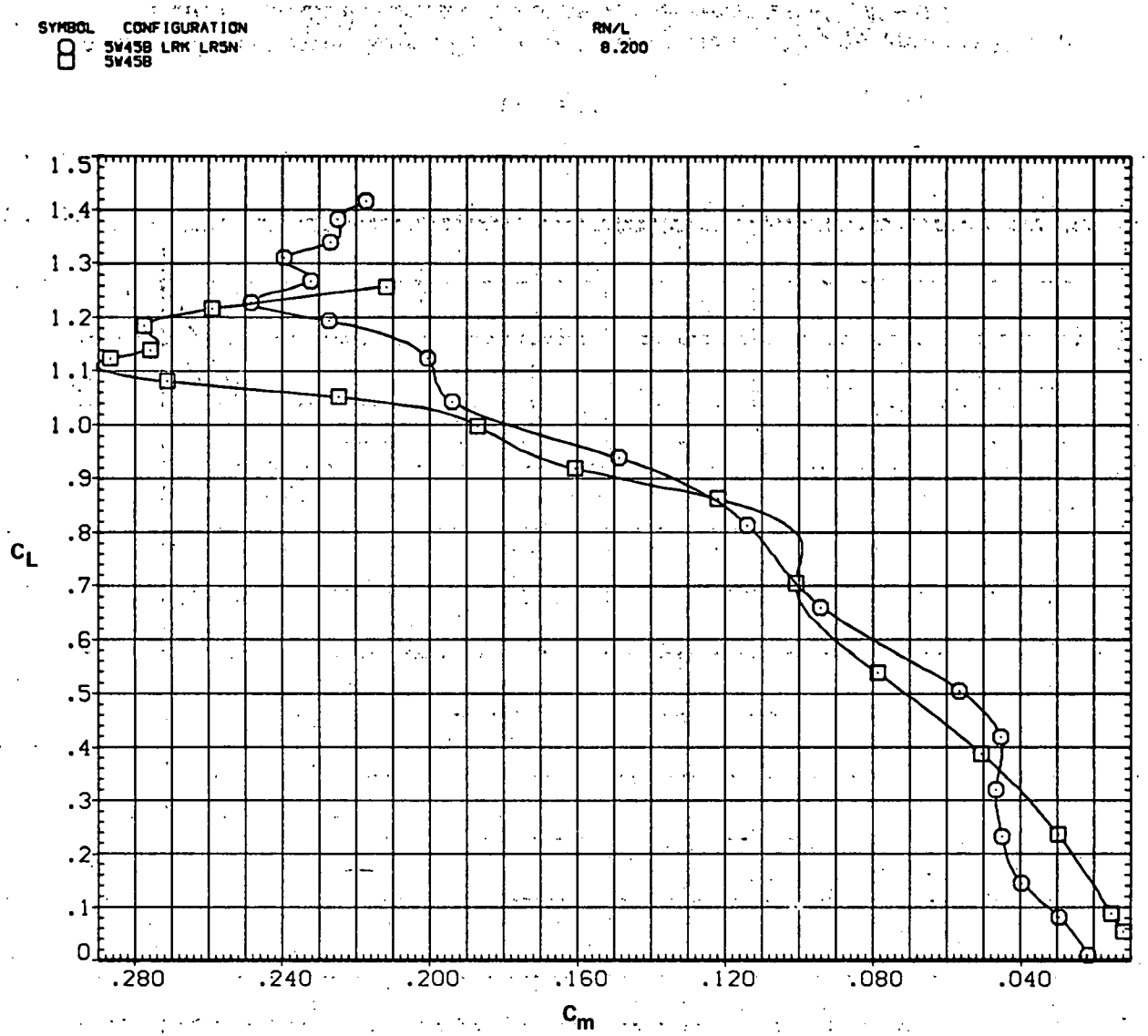

(b) C_L vs C_m

Figure 25.– Continued.

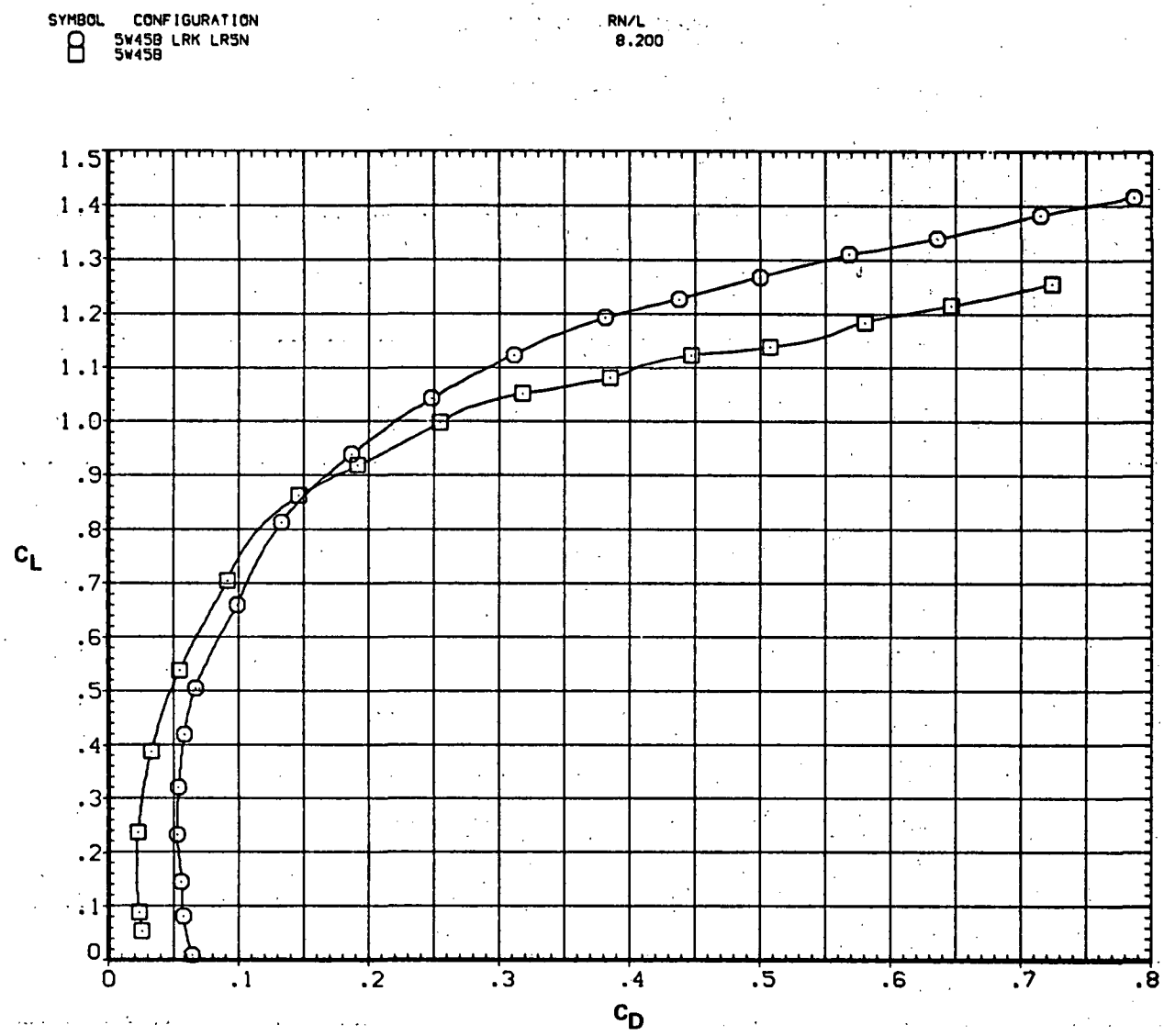

(c) C_L vs C_D

Figure 25.– Continued.

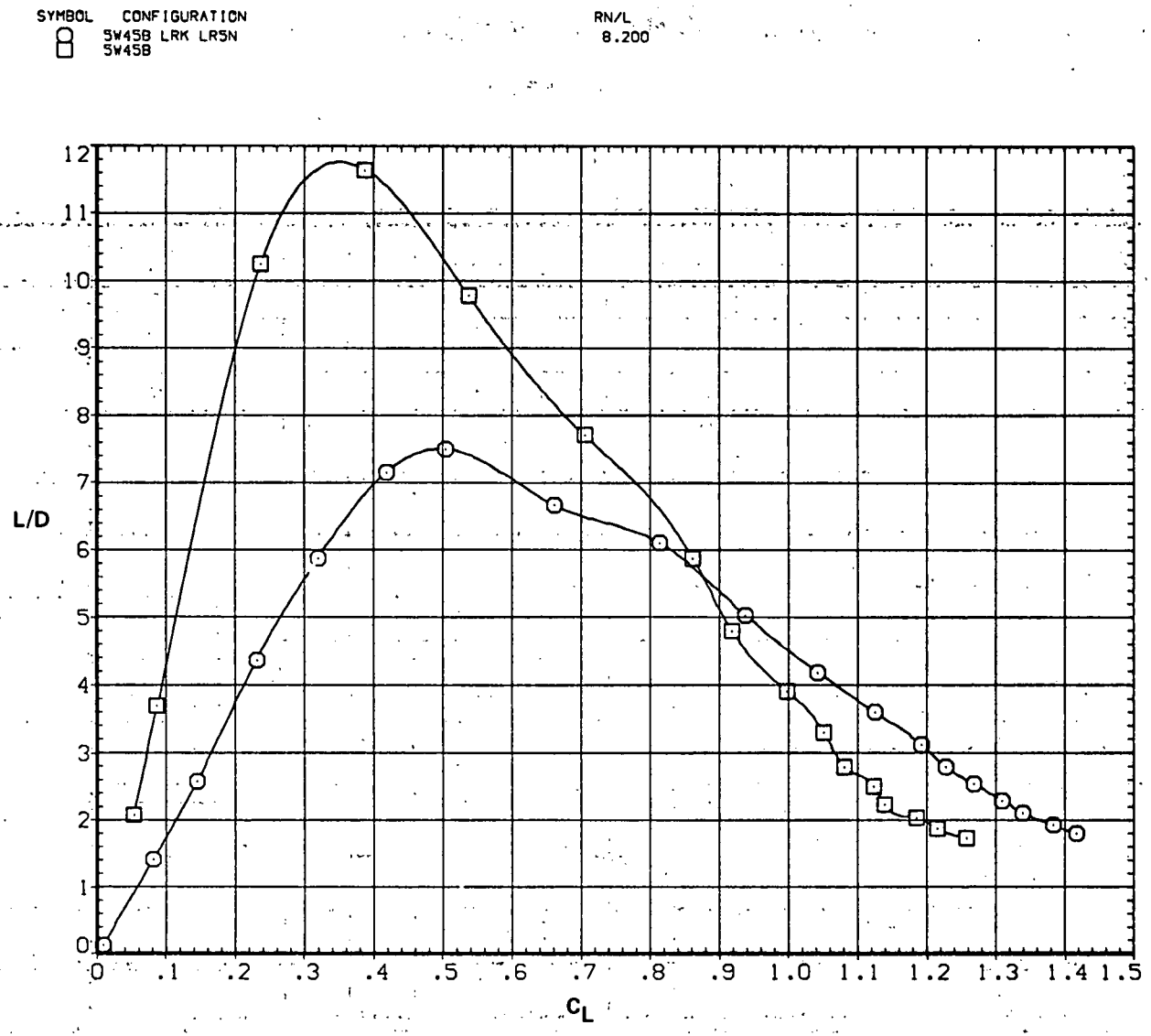

(d) L/D vs C_L

Figure 25.– Continued.

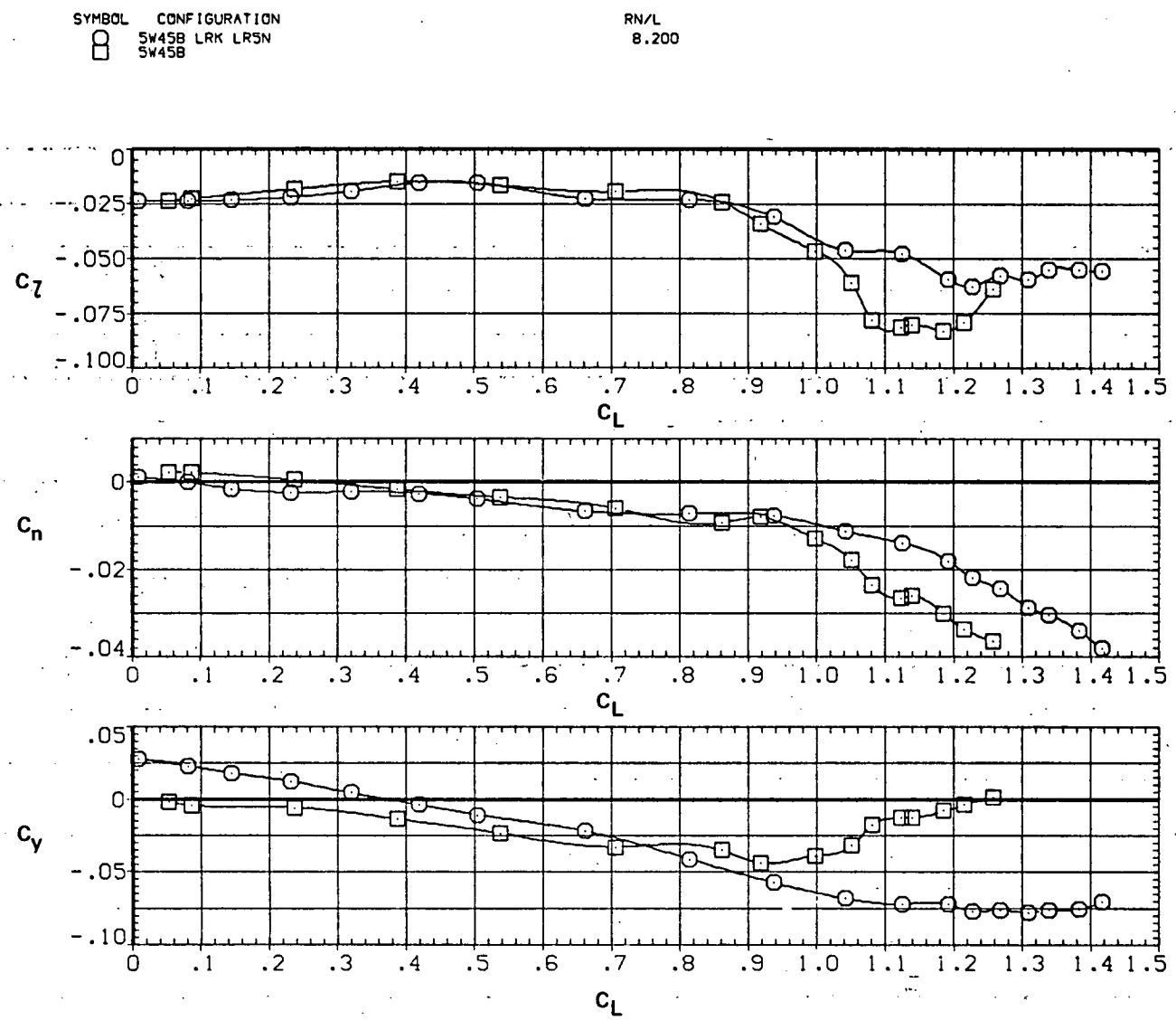

(e) C_l, C_n, and C_Y vs C_L

Figure 25.– Concluded.

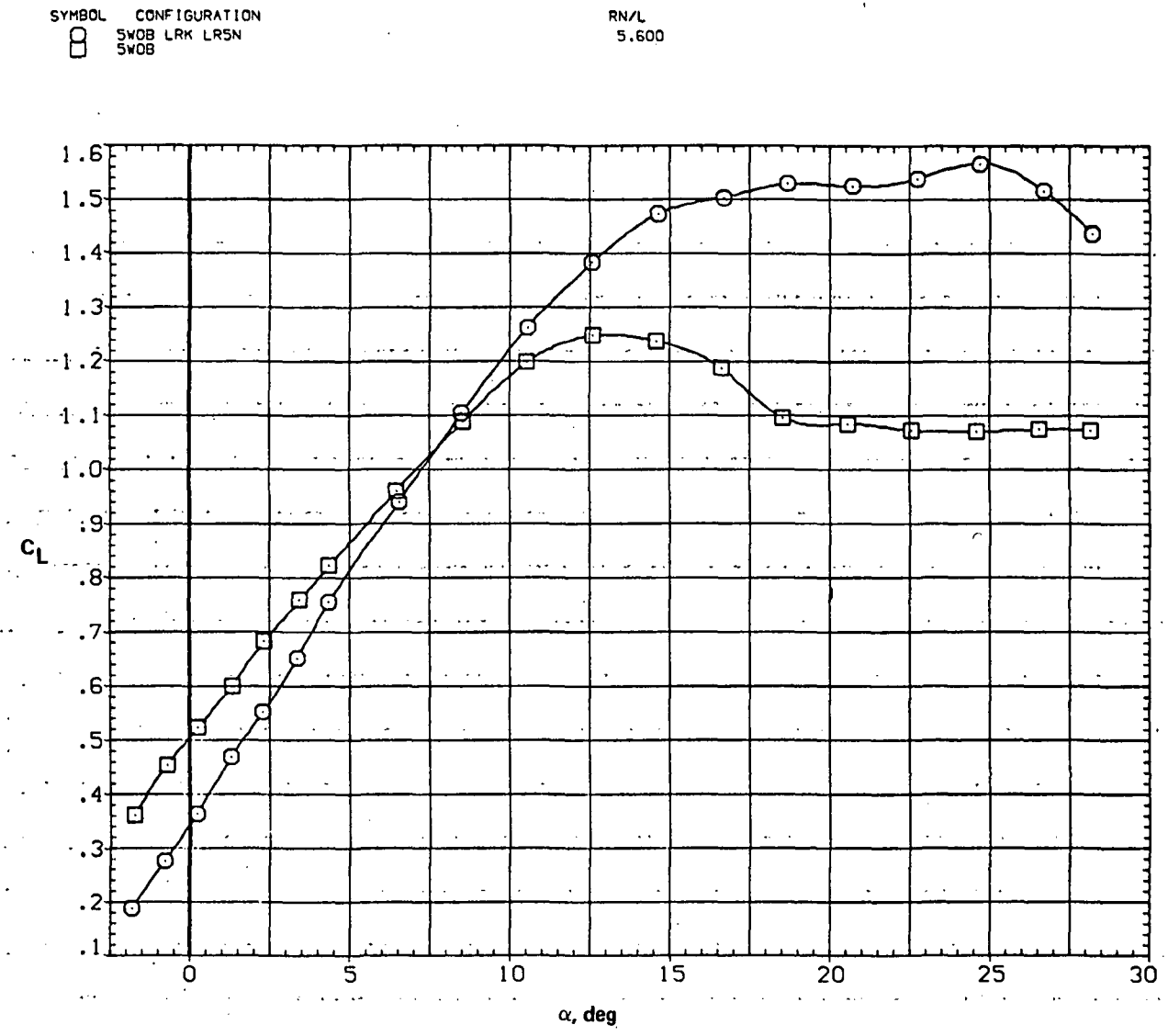

(a) C_L vs α

Figure 26.– Effect of having Krüger flaps on both wing panels with a nose droop of 5° on the static longitudinal characteristics of an oblique wing: $\Lambda = 0$, $M = 0.25$.

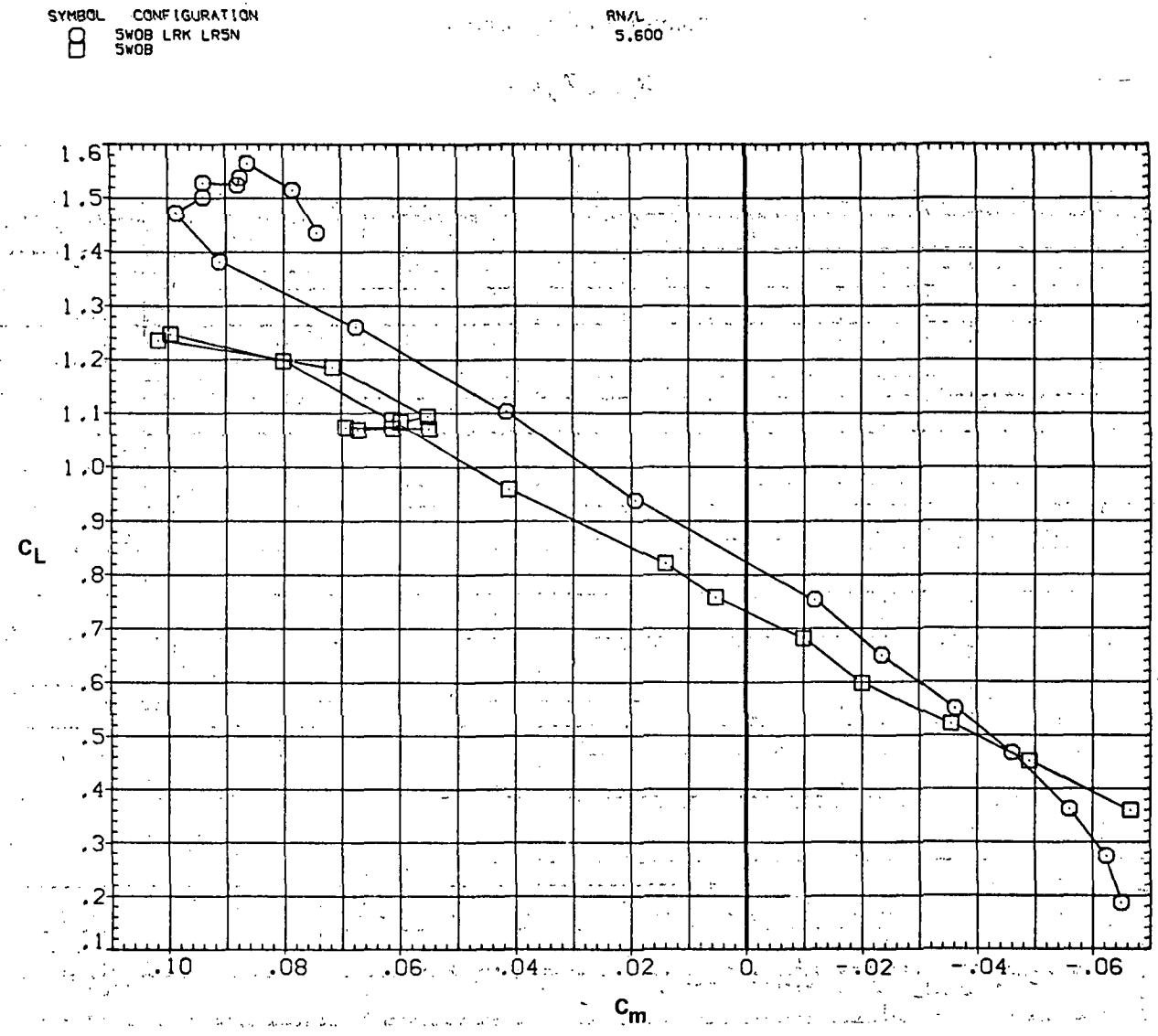

(b) C_L vs C_m

Figure 26.– Continued.

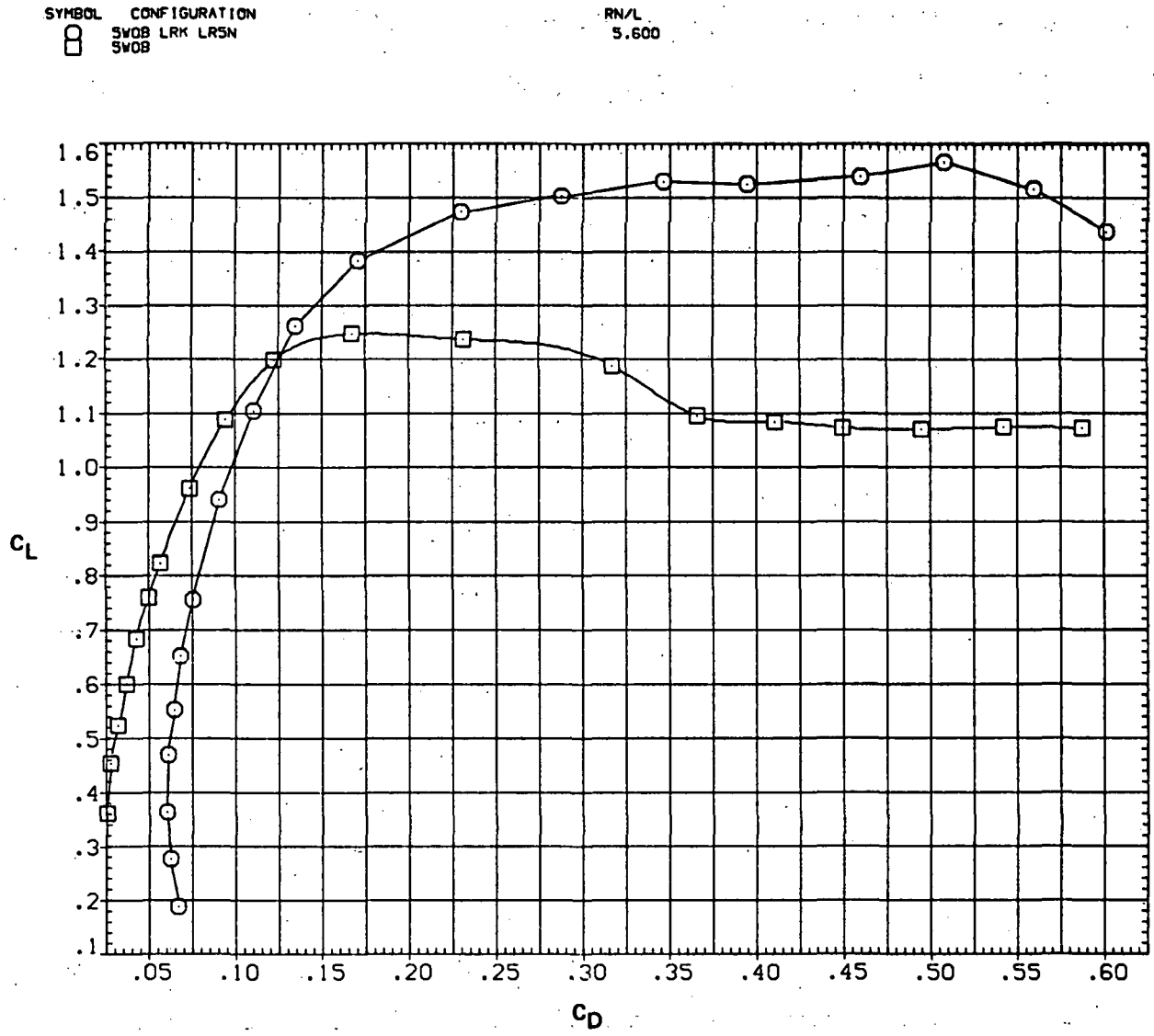

(c) C_L vs C_D

Figure 26.– Continued.

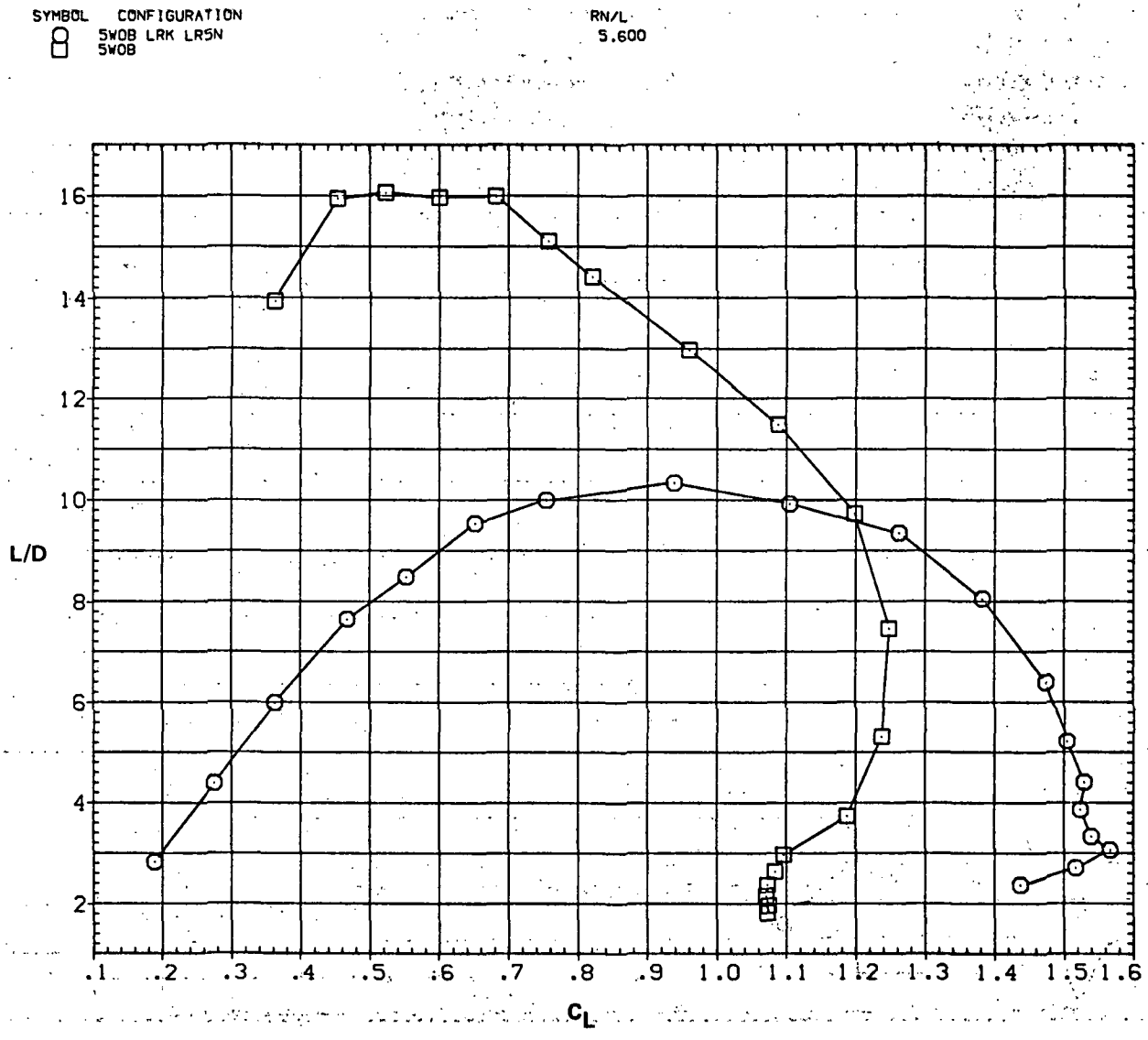

(d) L/D vs C_L

Figure 26.– Continued.

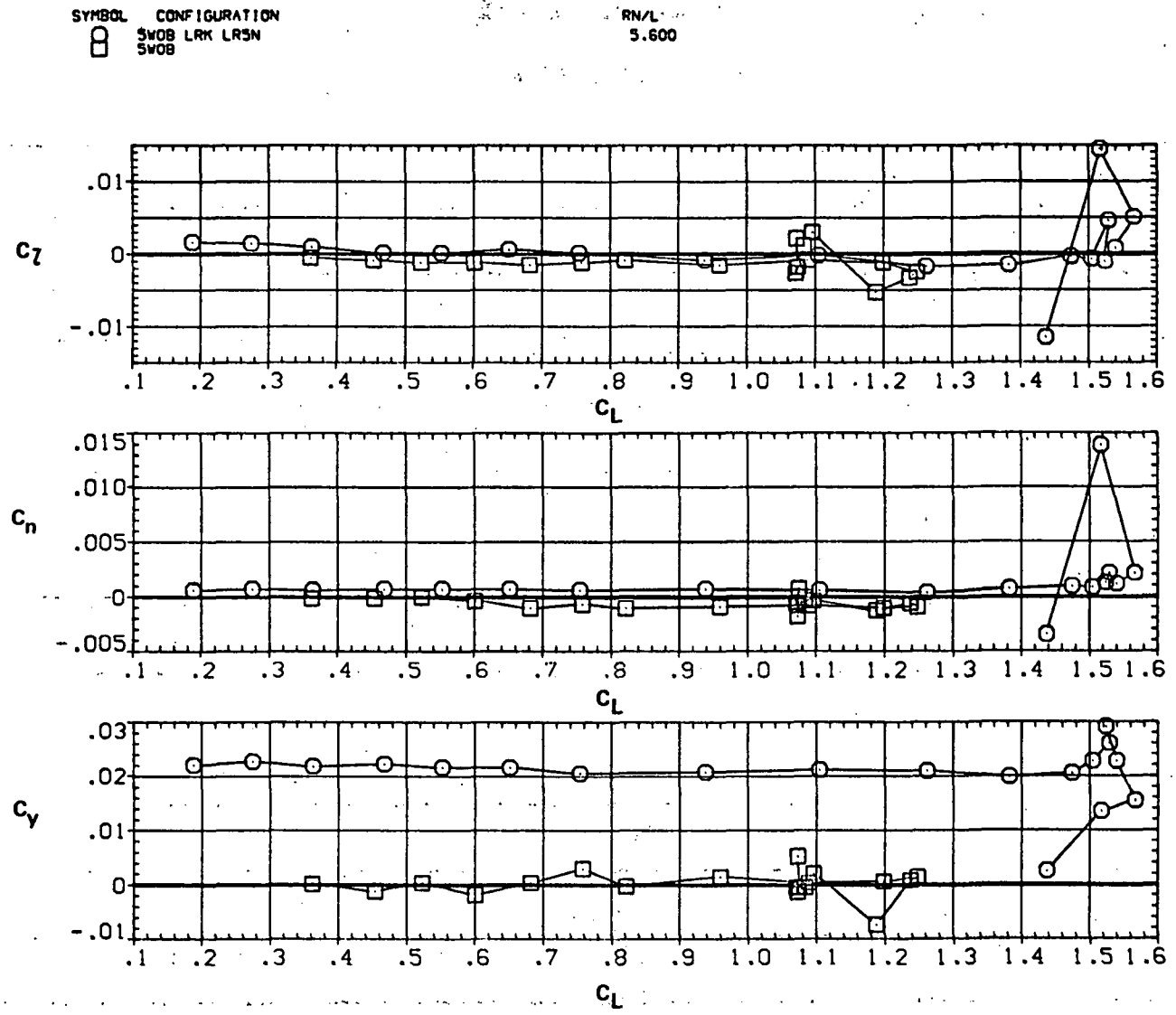

(e) C_l, C_n, and C_Y vs C_L

Figure 26.– Concluded.

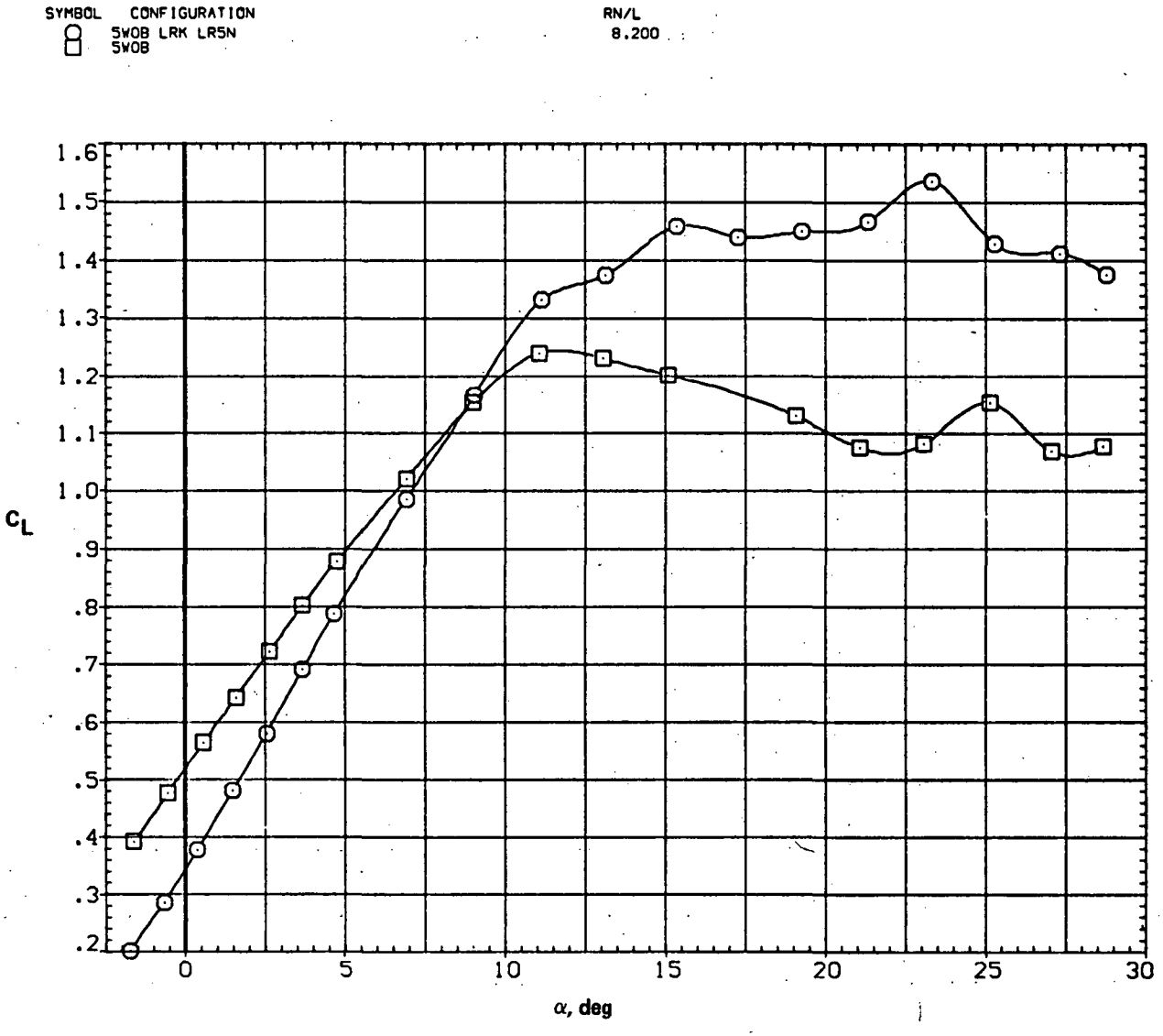

(a) C_L vs α

Figure 27.– Effect of having Krüger flaps on both wing panels with a nose droop of 5° on the static longitudinal characteristics of an oblique wing: $\Lambda = 0$, $M = 0.40$.

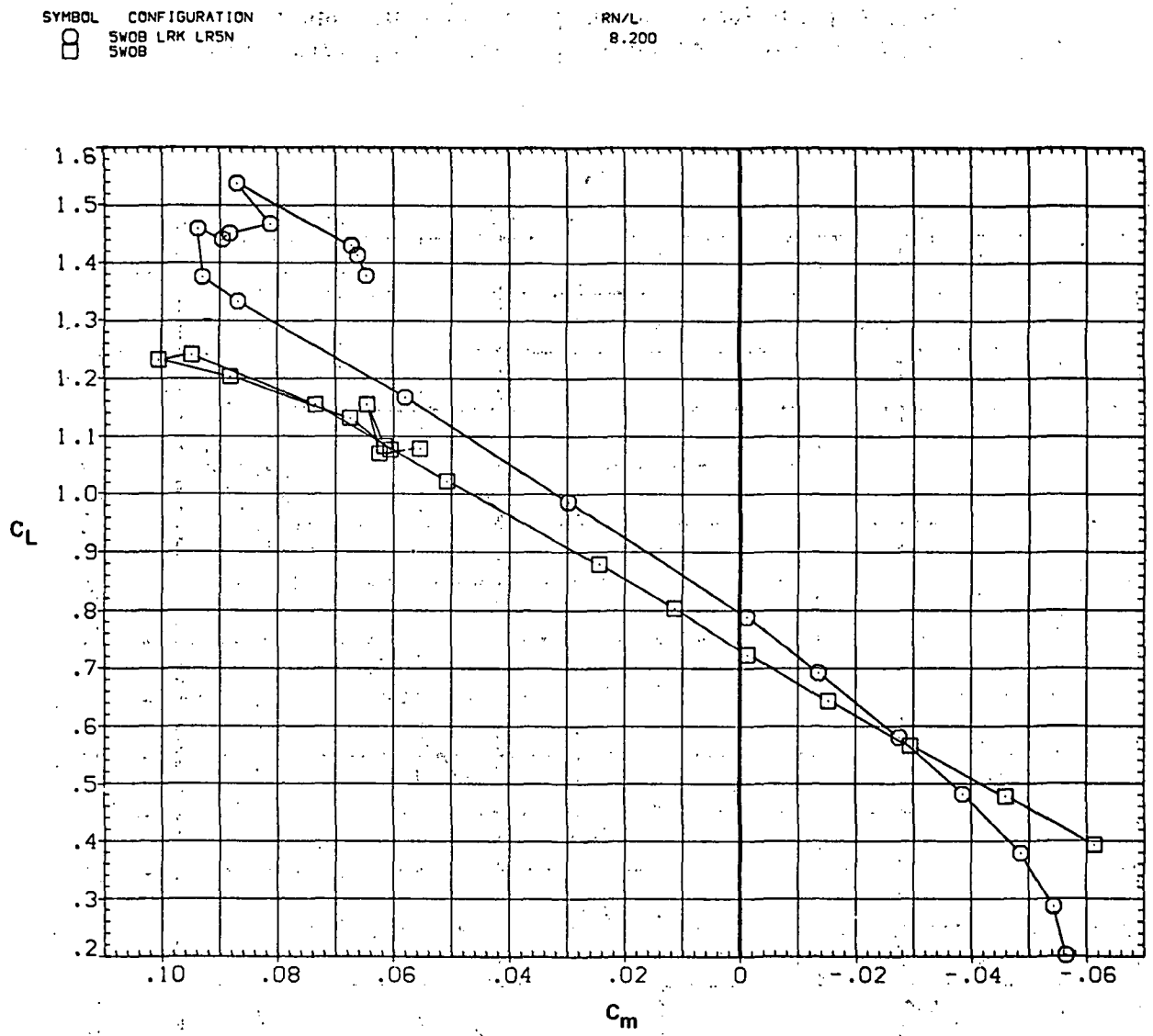

(b) C_L vs C_m

Figure 27.– Continued.

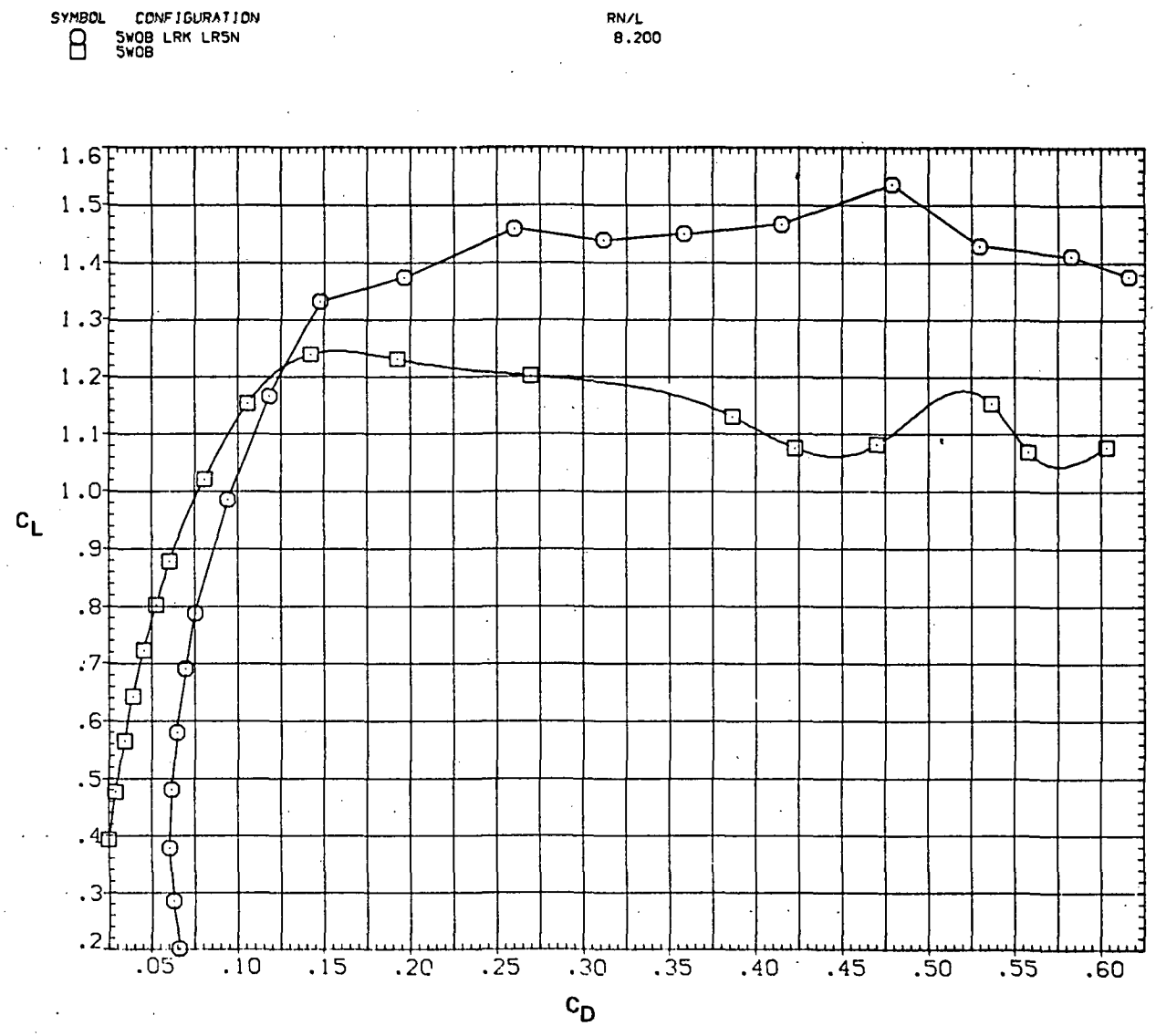

(c) C_L vs C_D

Figure 27.– Continued.

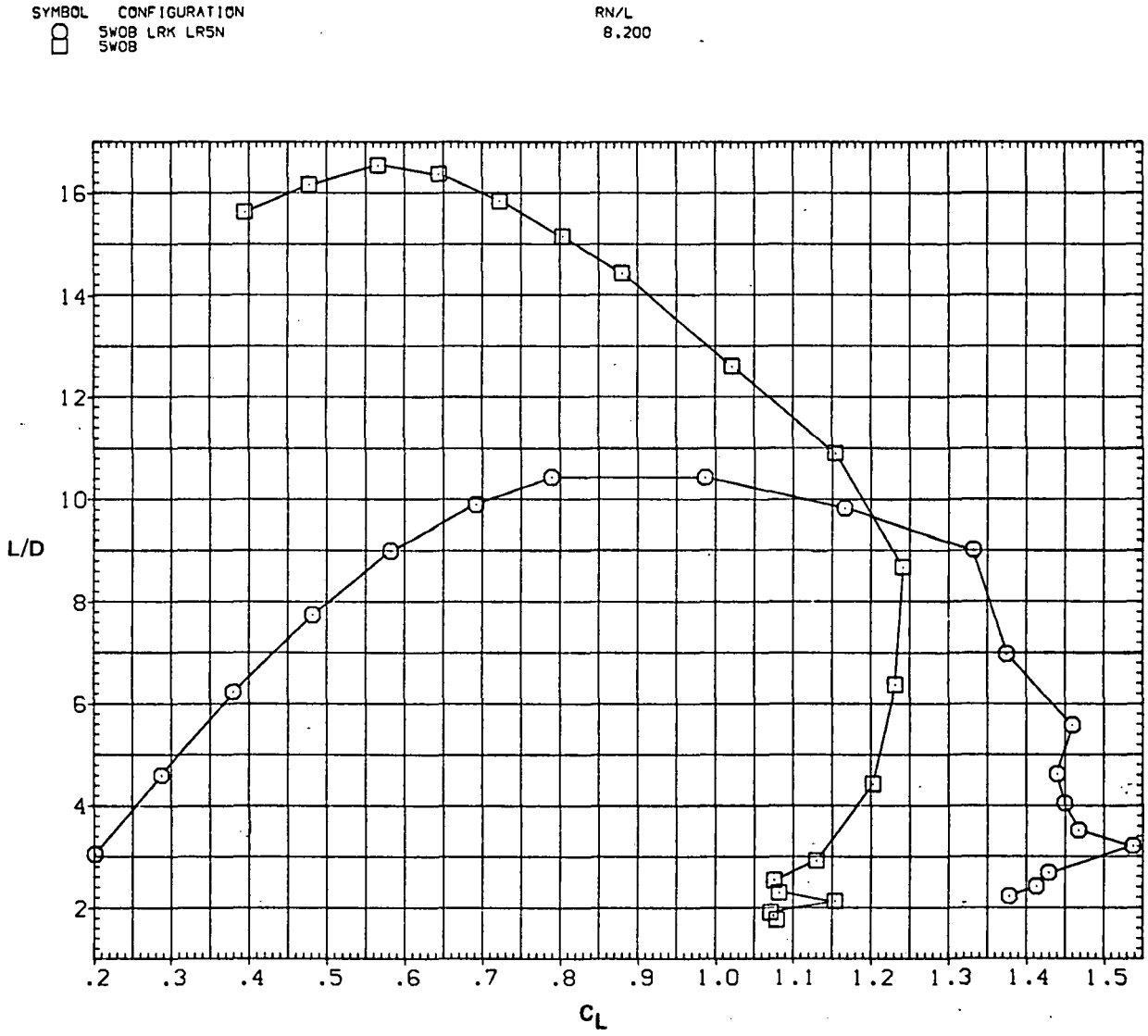

(d) L/D vs C_L

Figure 27.– Continued.

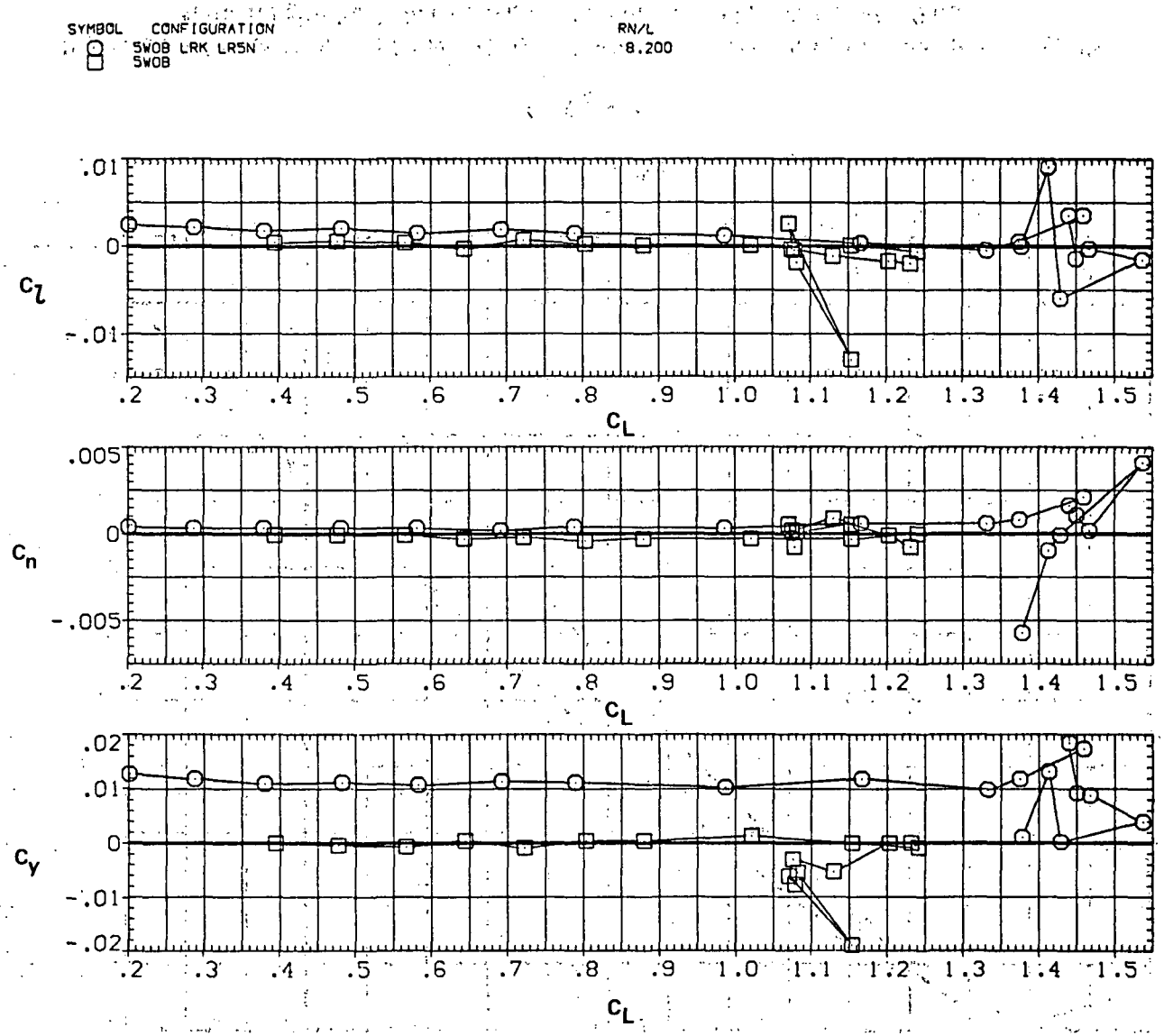

(e) C_l, C_n, and C_Y vs C_L

Figure 27.– Concluded.

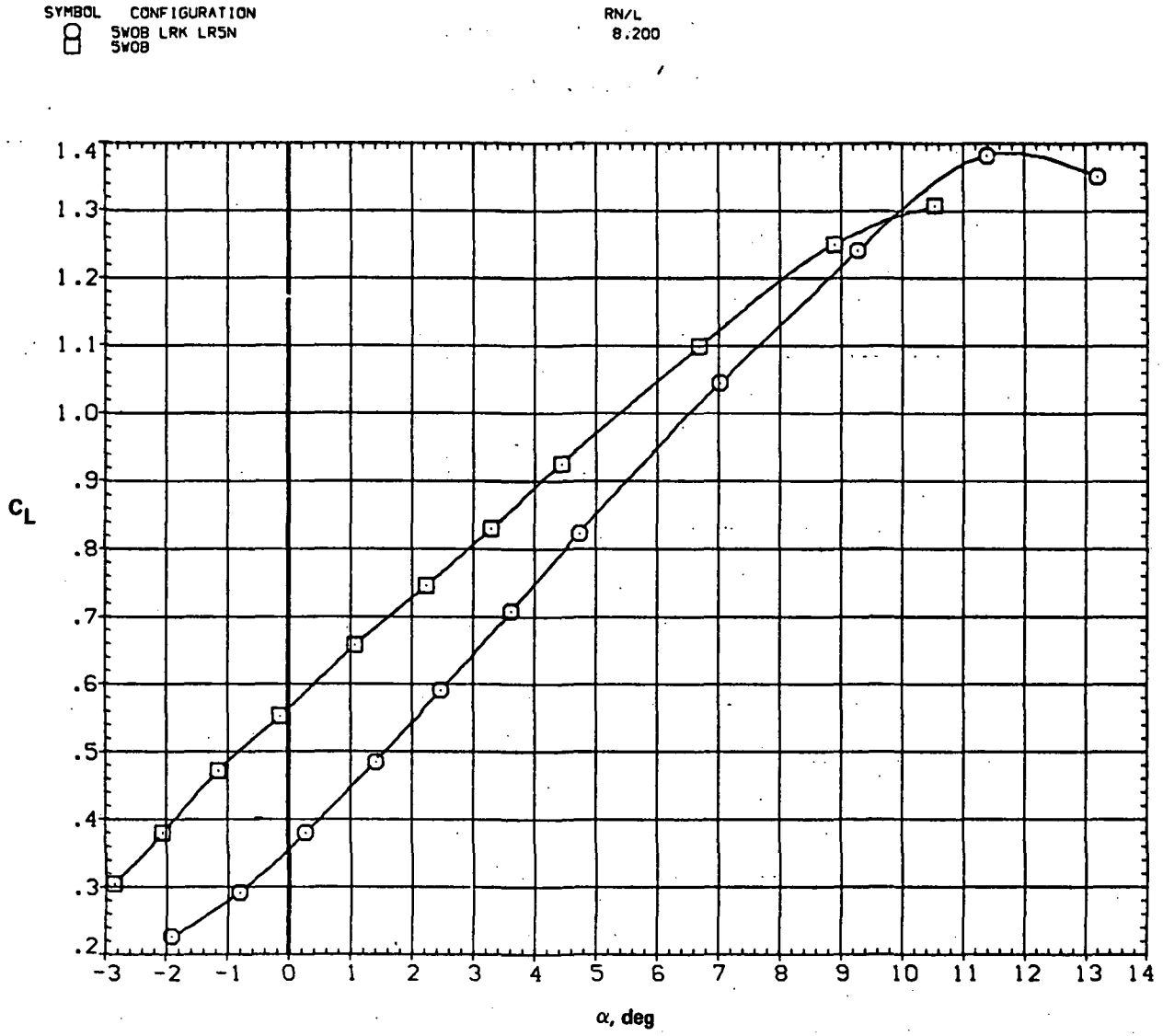

(a) C_L vs α

Figure 28.– Effect of having Krüger flaps on both wing panels with a nose droop of 5° on the static longitudinal characteristics of an oblique wing: $\Lambda = 0$, $M = 0.60$.

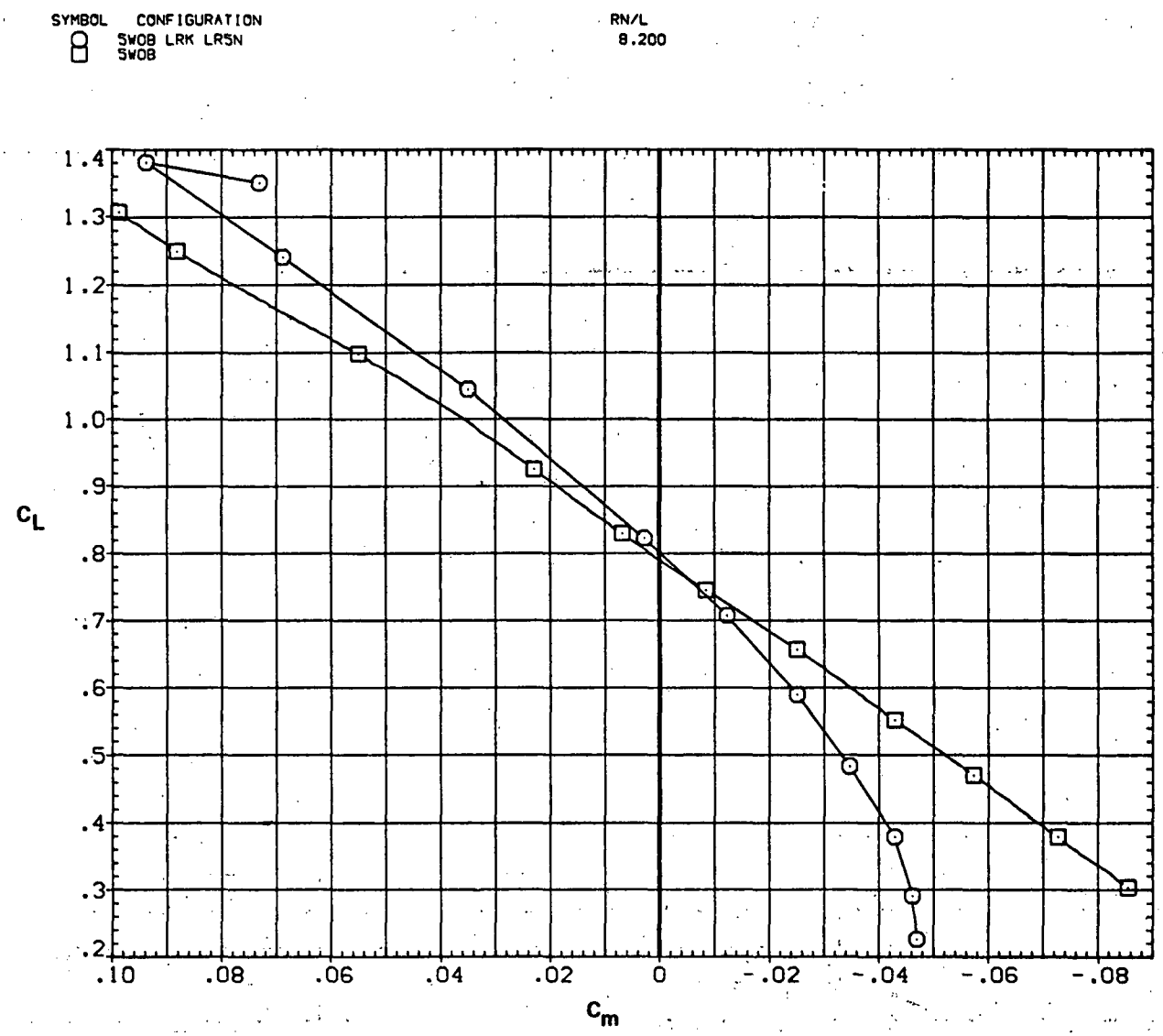

(b) C_L vs C_m

Figure 28.– Continued.

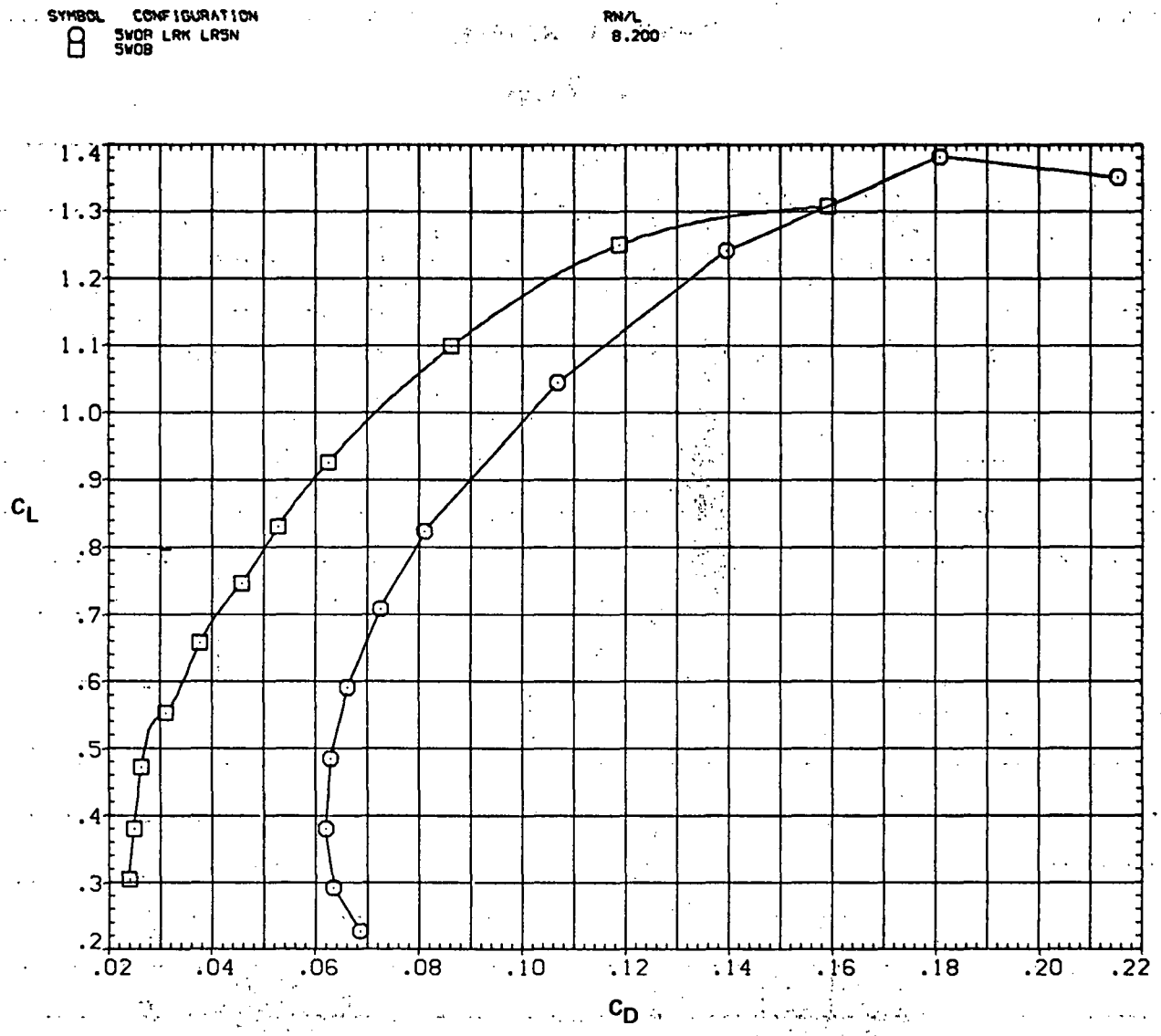

(c) C_L vs C_D

Figure 28.– Continued.

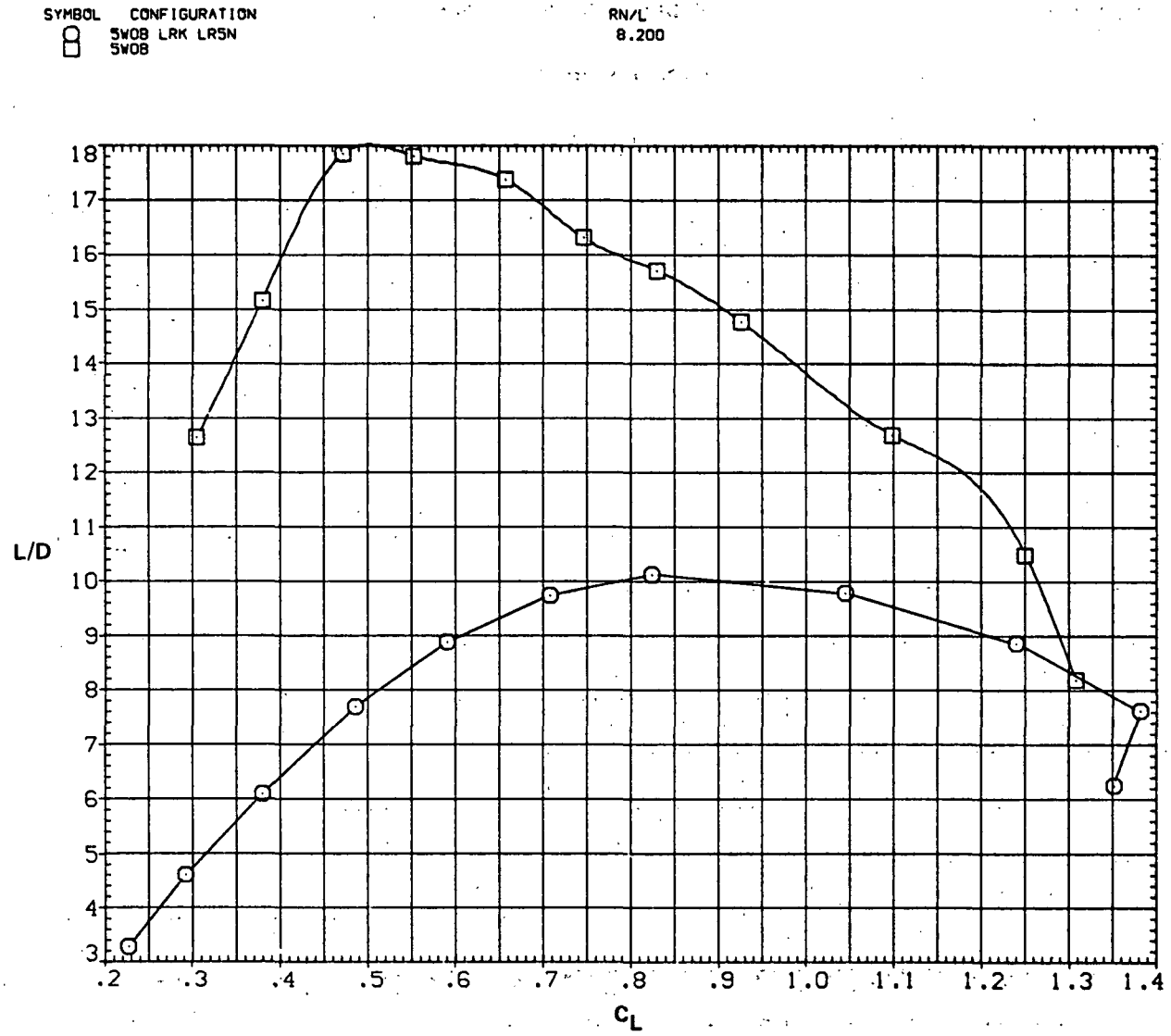

(d) L/D vs C_L

Figure 28.– Continued.

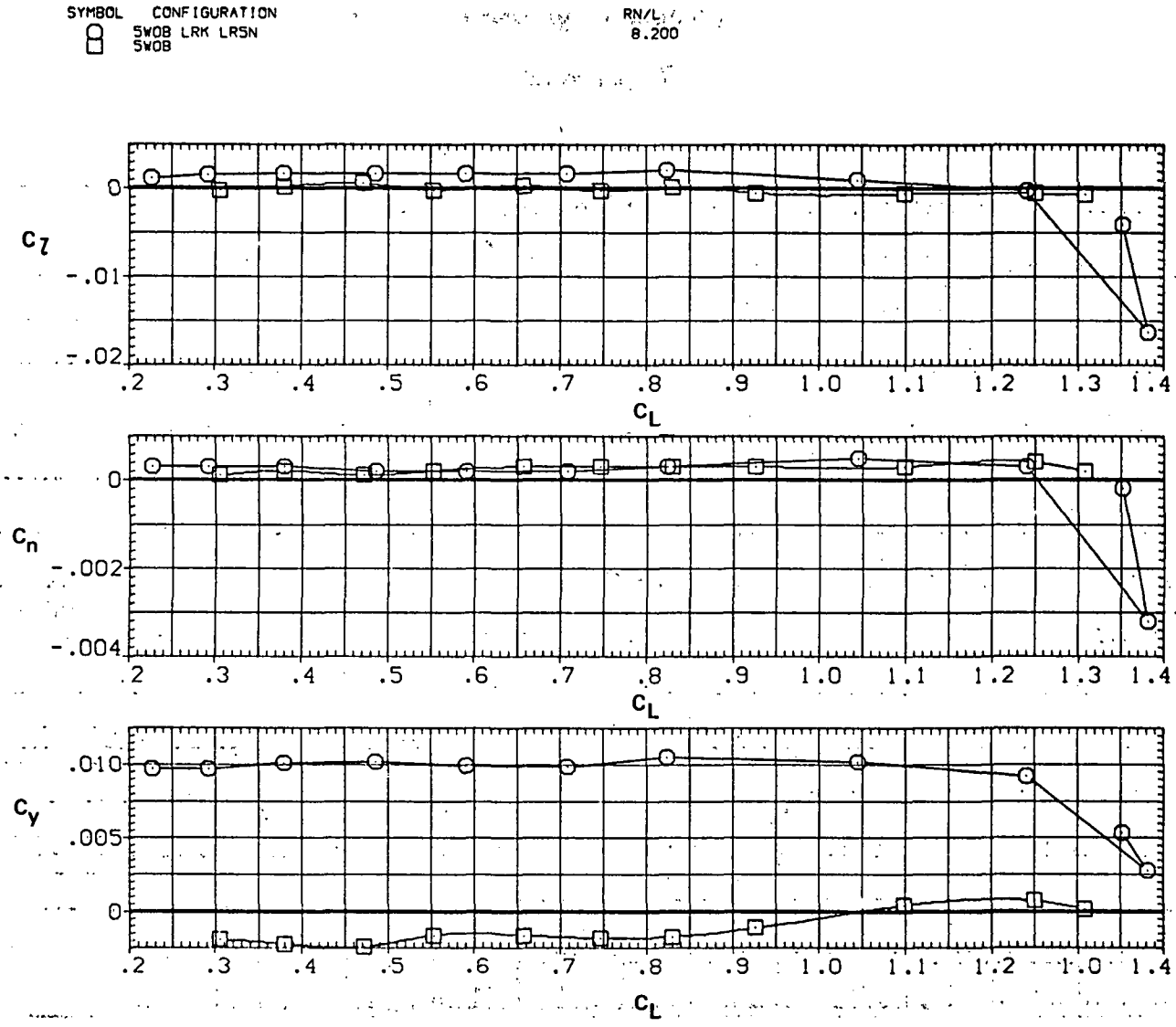

(e) C_l, C_n, and C_Y vs C_L

Figure 28.– Concluded.

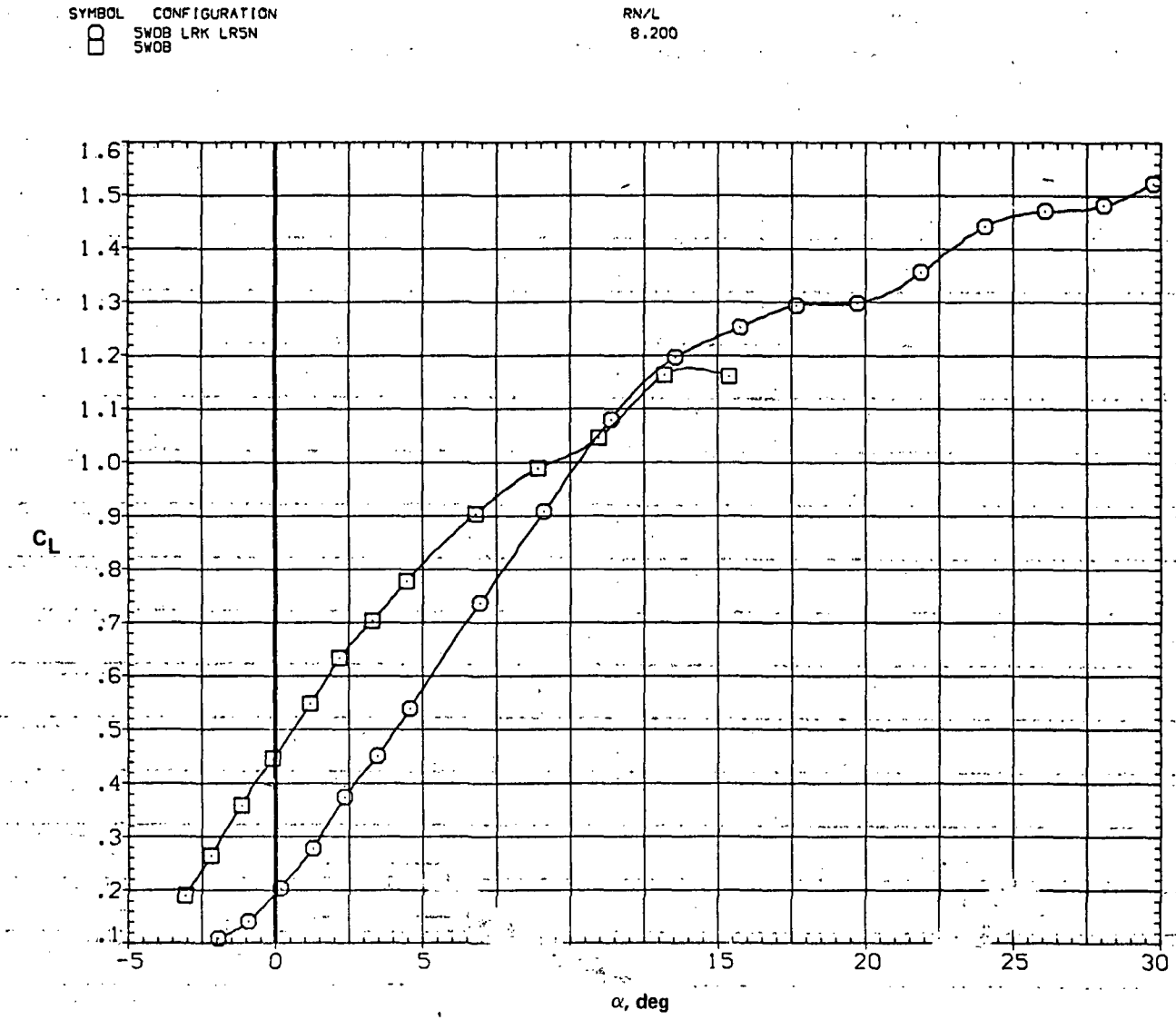

(a) C_L vs α

Figure 29.– Effect of having Krüger flaps on both wing panels with a nose droop of 5° on the static longitudinal characteristics of an oblique wing: $\Lambda = 0$, $M = 0.80$.

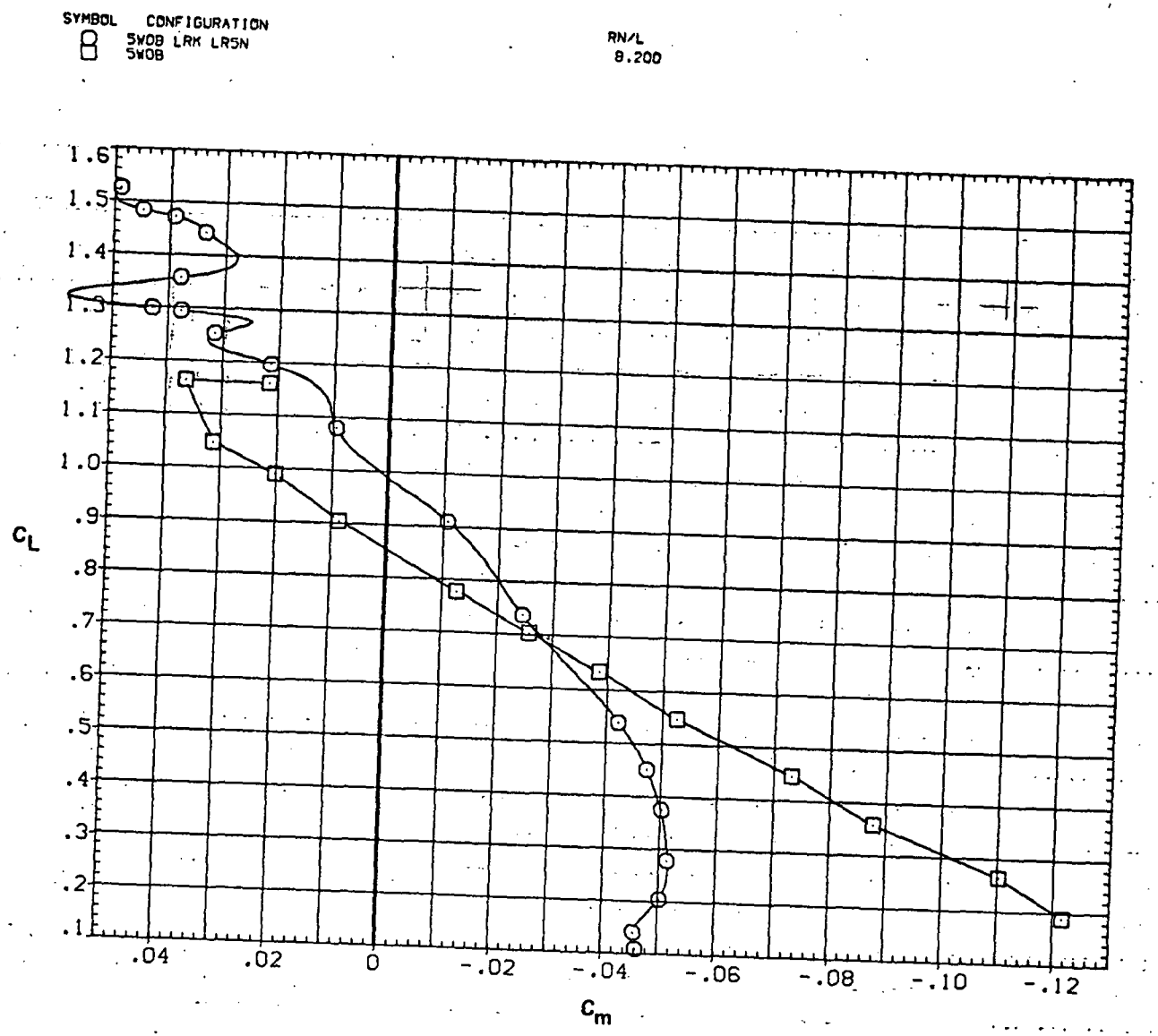

(b) C_L vs C_m

Figure 29.– Continued.

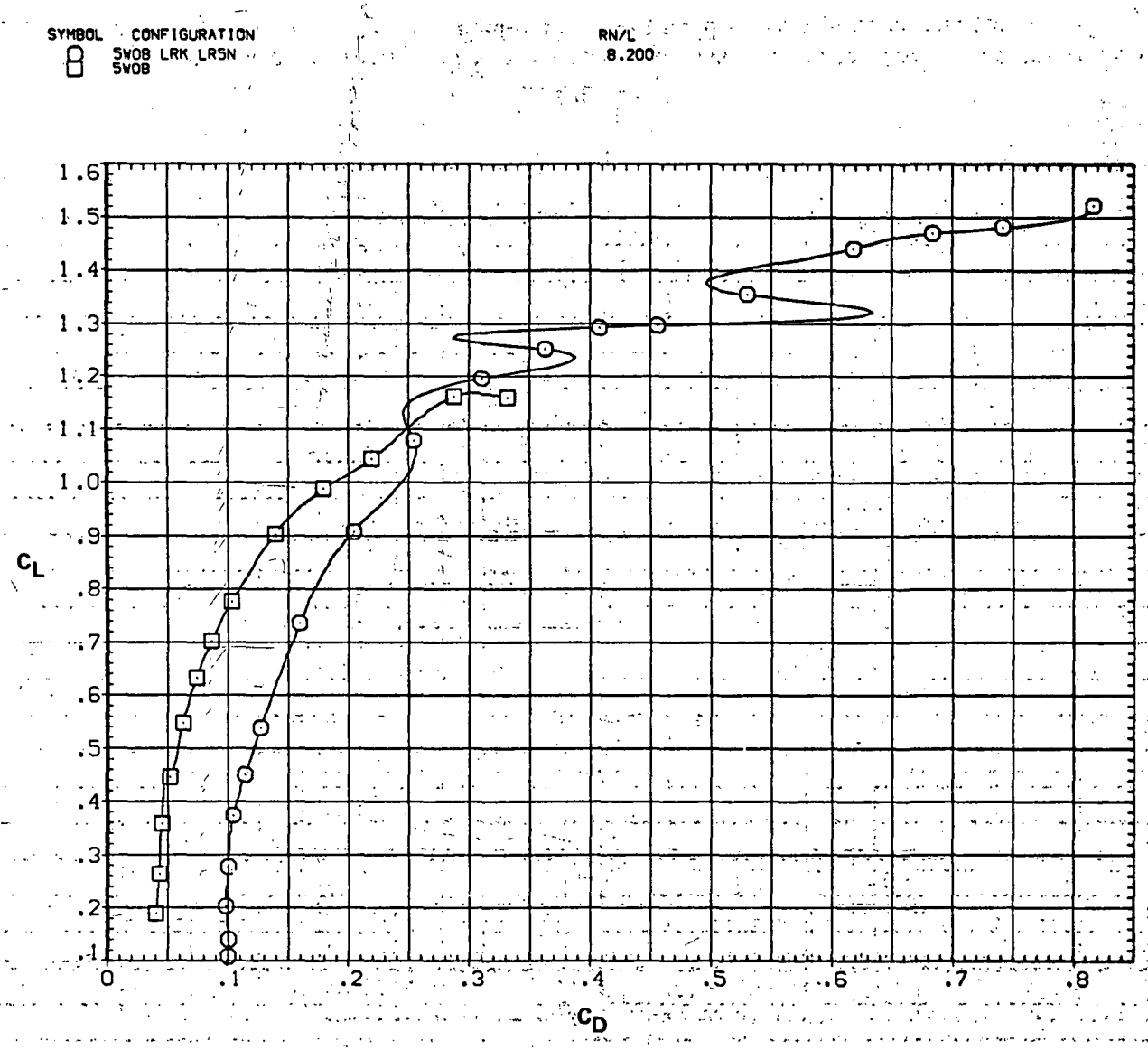

(c) C_L vs C_D

Figure 29.– Continued.

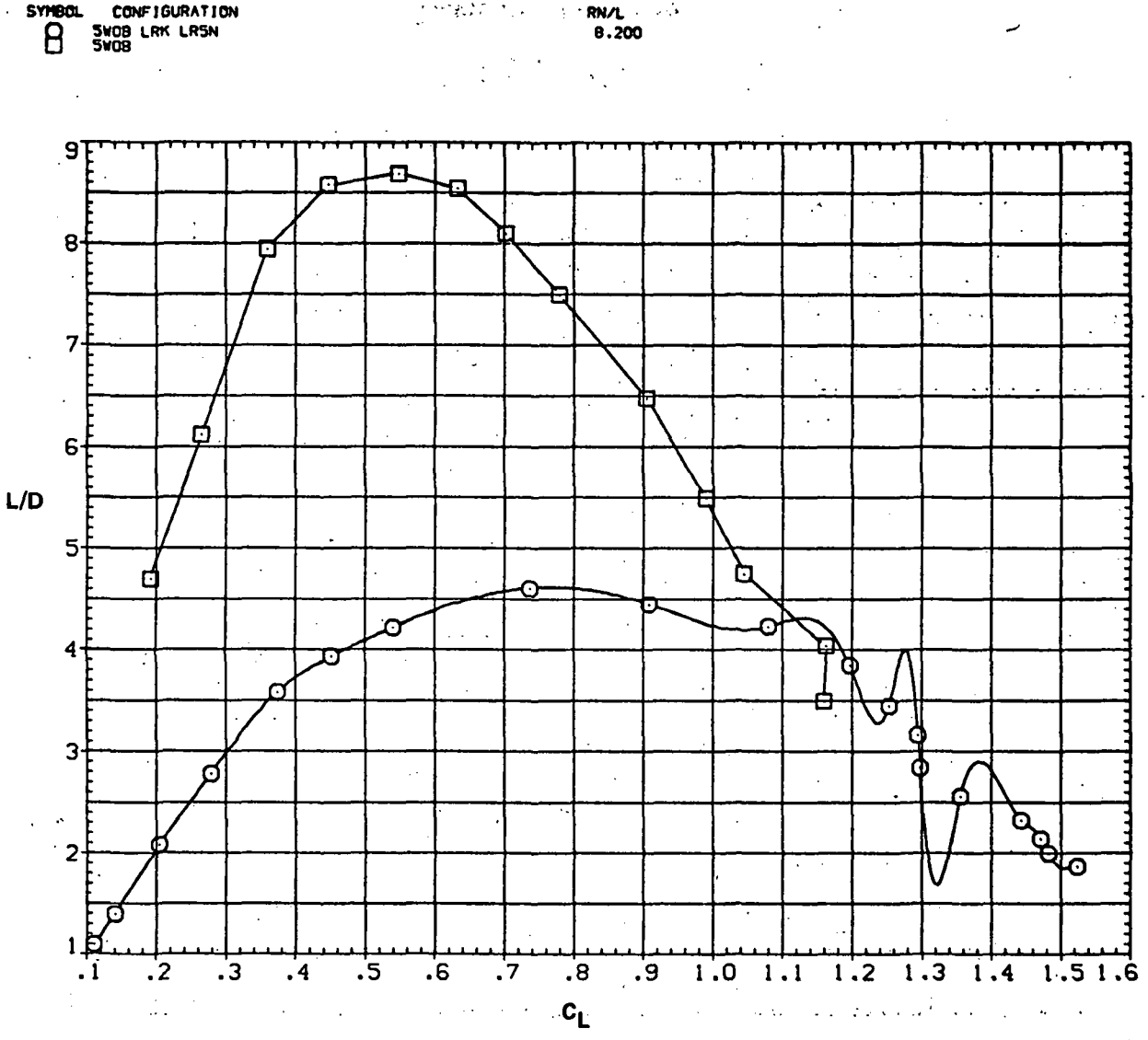

(d) L/D vs C_L

Figure 29.– Continued.

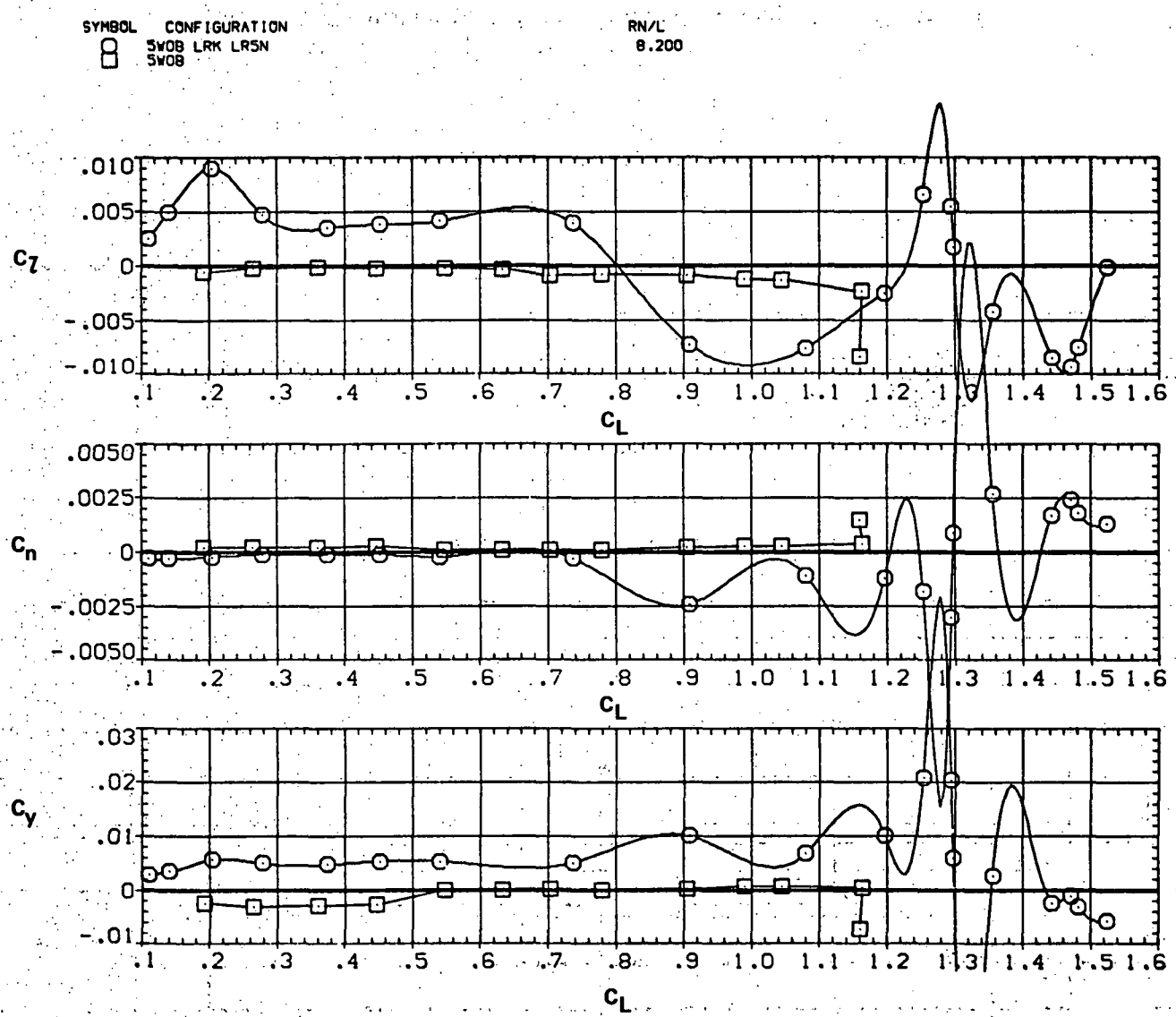

(e) C_l, C_n, and C_Y vs C_L

Figure 29.– Concluded.

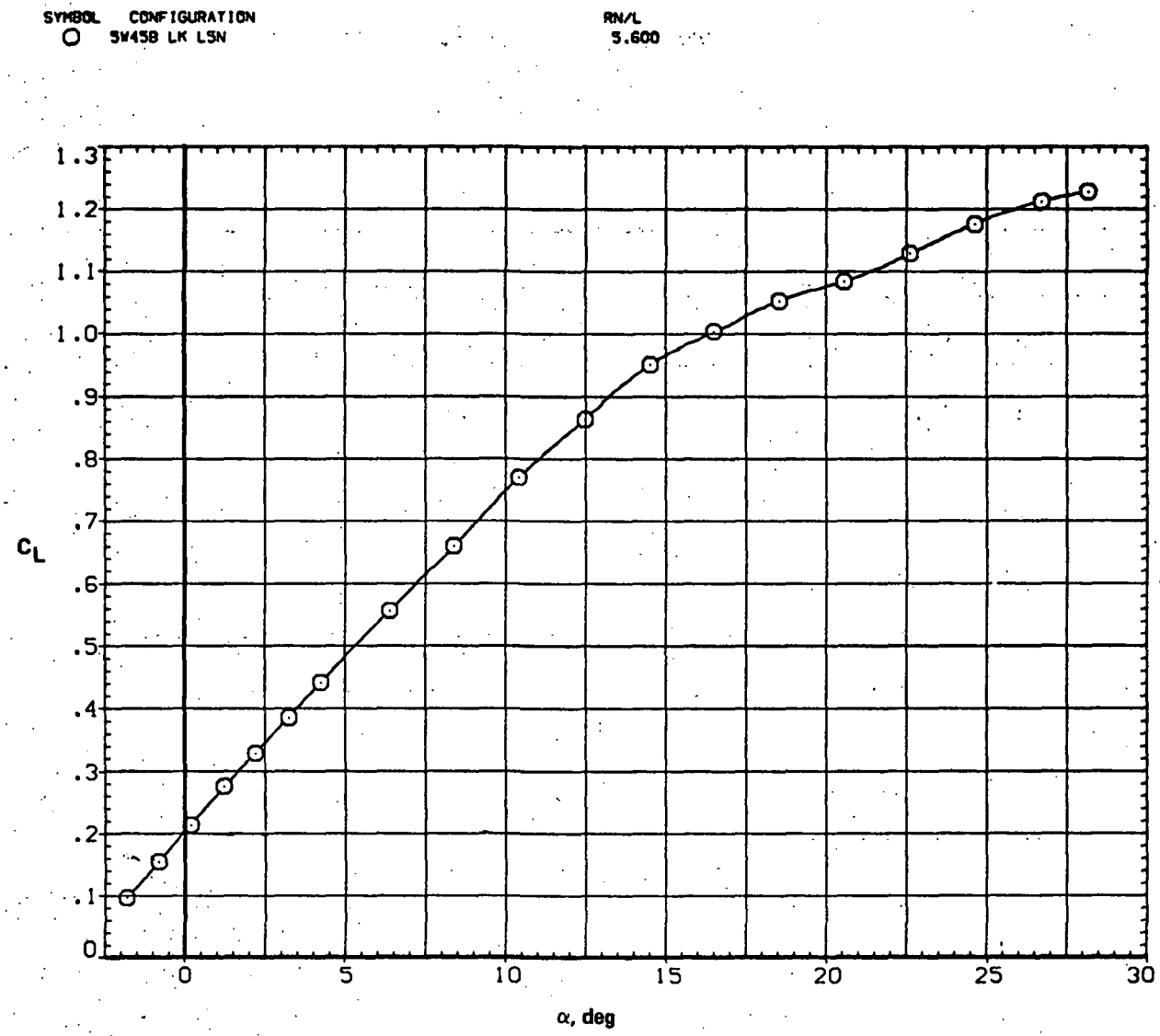

(a) C_L vs α

Figure 30.– Effect of having Krüger flaps on the downstream wing panel with a nose droop of 5° on the static longitudinal characteristics of an oblique wing: $\Lambda = 45°, M = 0.25$.

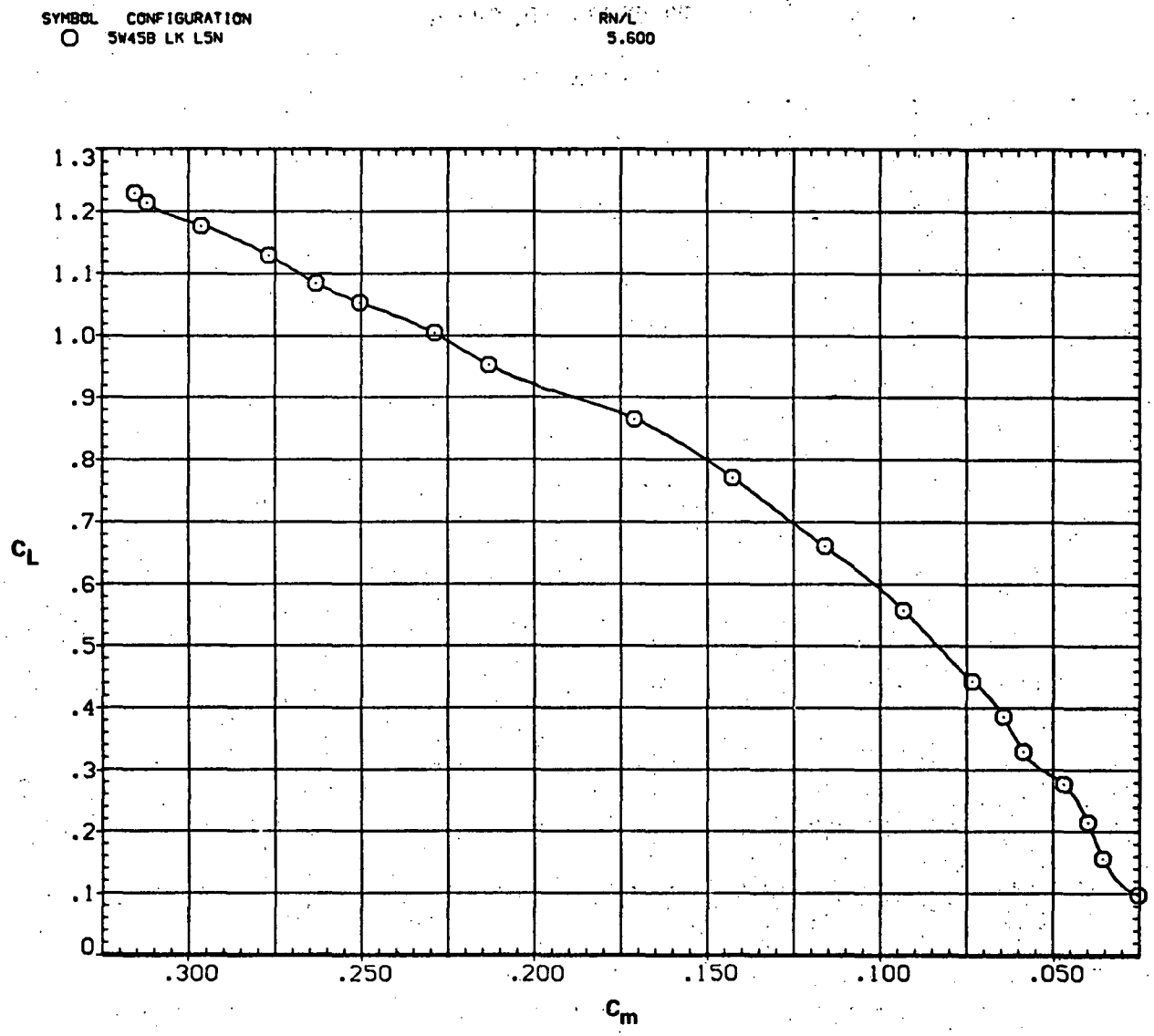

(b) C_L vs C_m

Figure 30.– Continued.

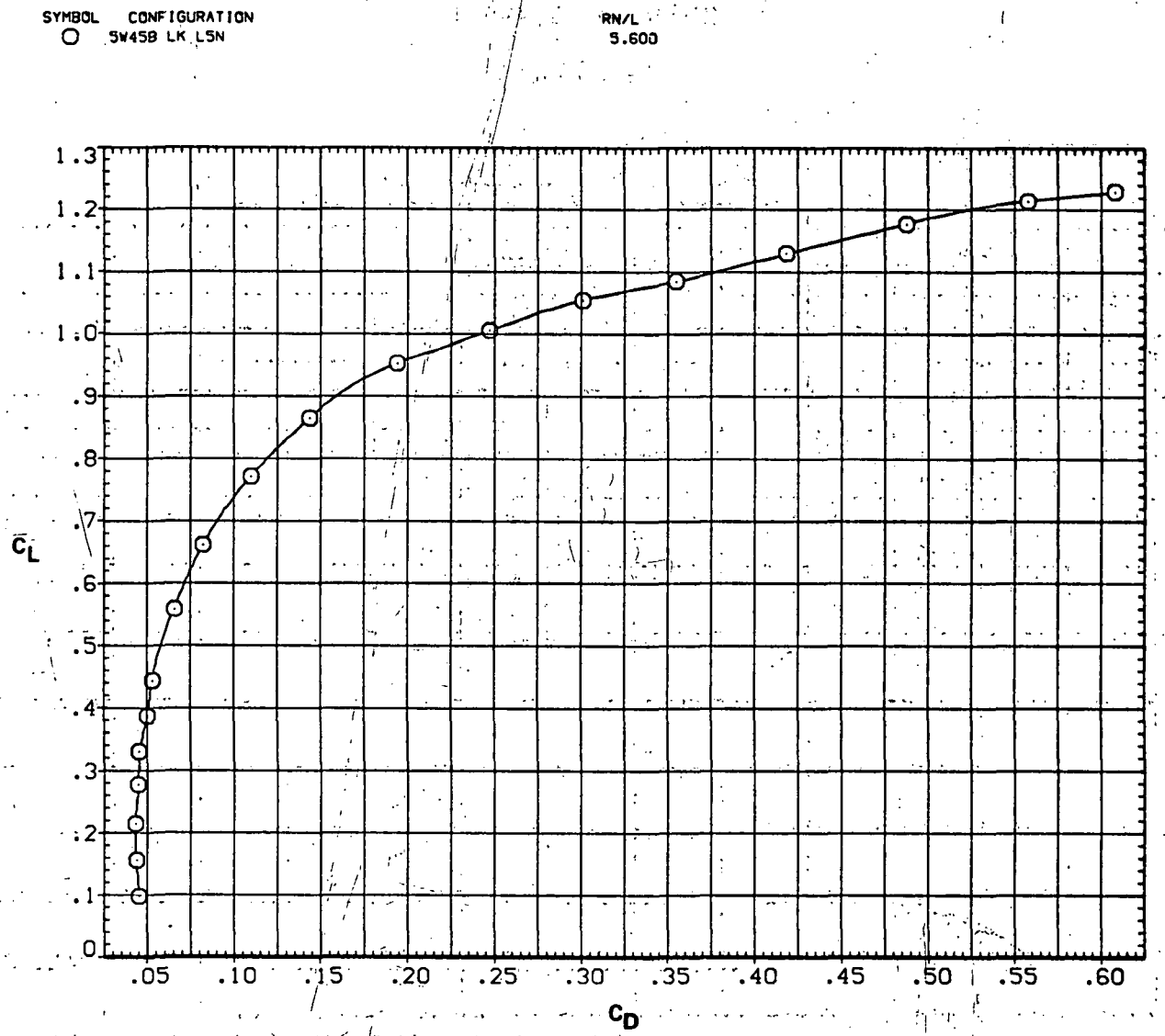

(c) C_L vs C_D

Figure 30.– Continued.

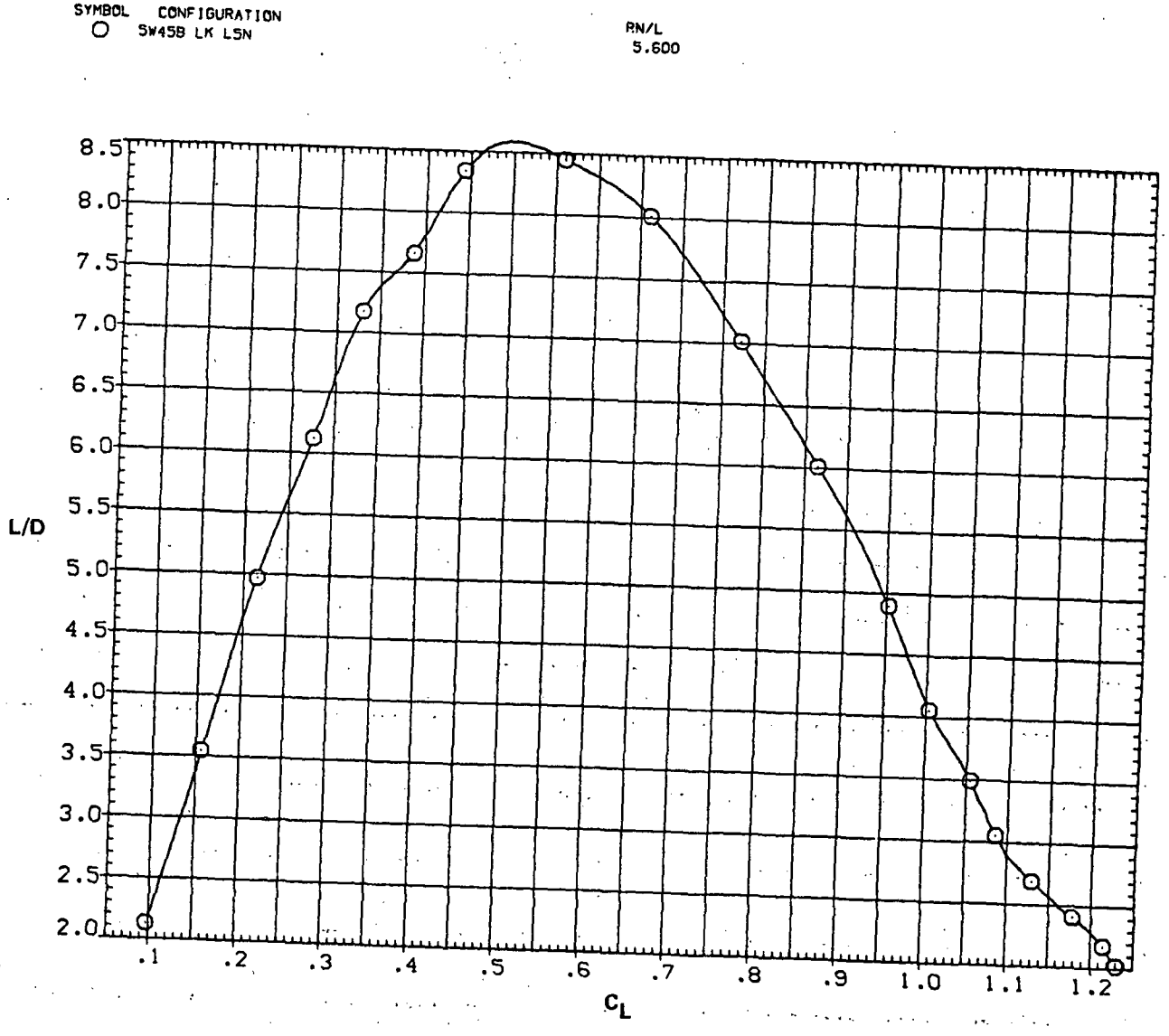

(d) L/D vs C_L

Figure 30.– Continued.

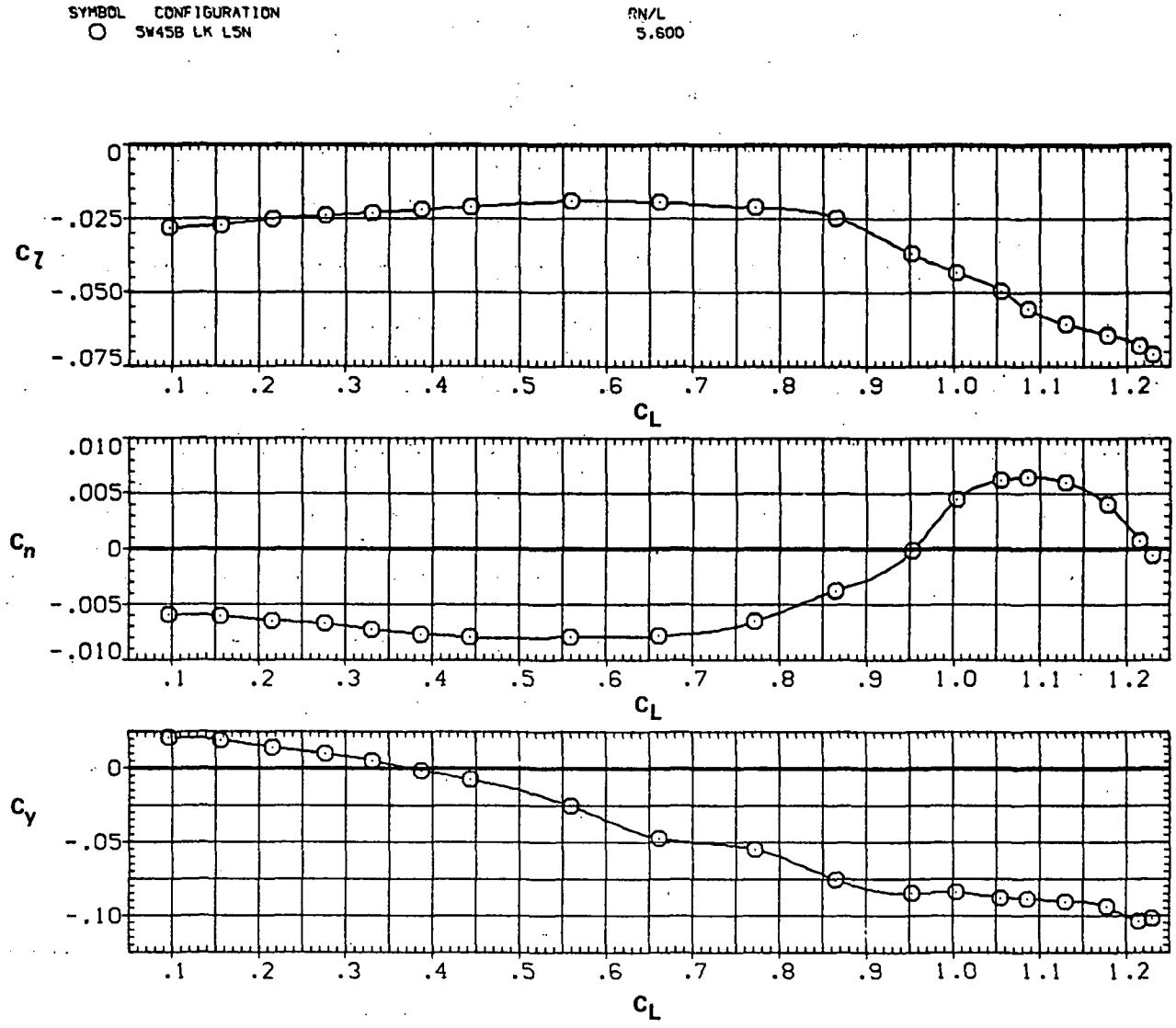

(e) C_l, C_n, and C_Y vs C_L

Figure 30.– Concluded.

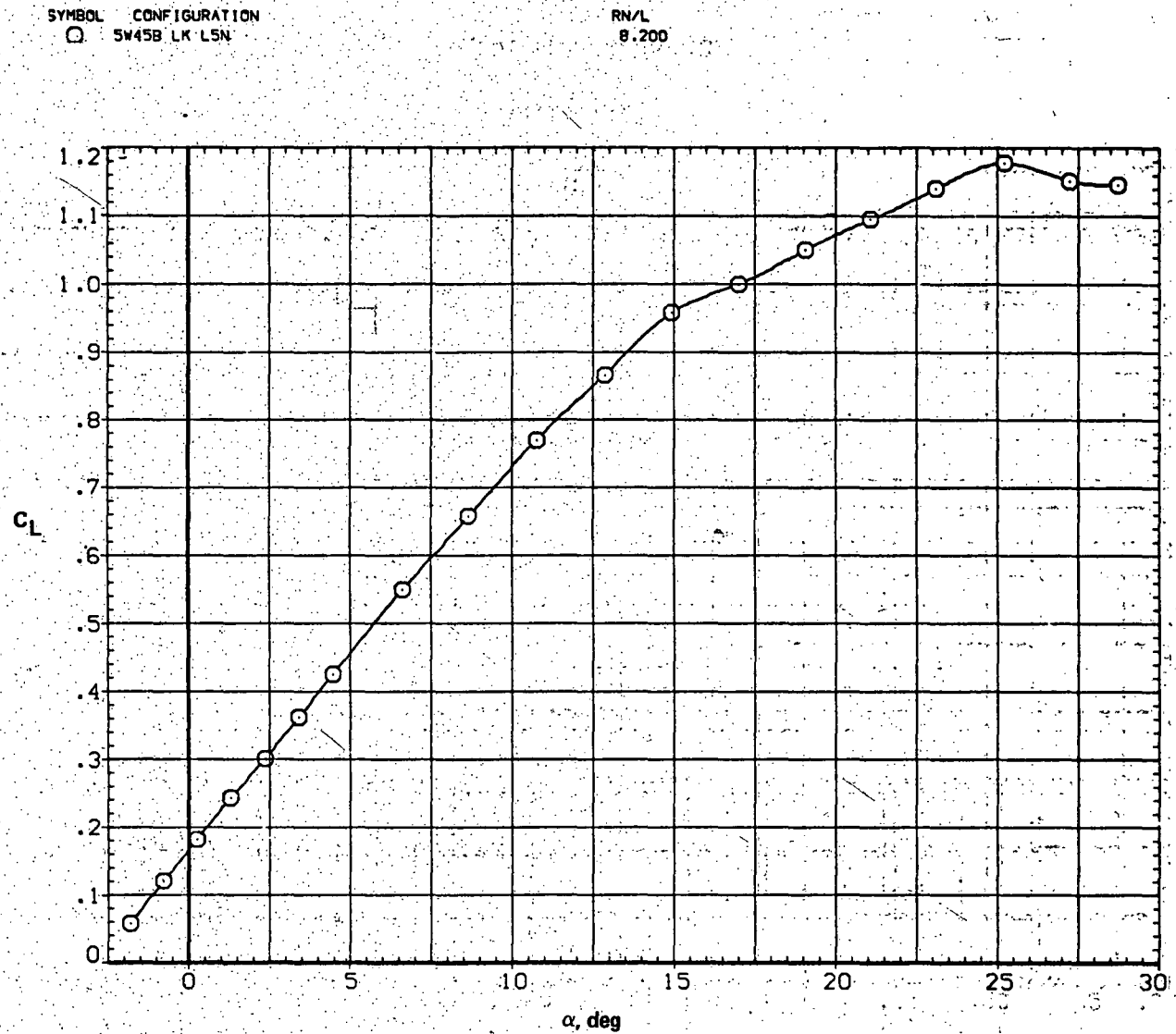

(a) C_L vs α

Figure 31.– Effect of having Krüger flaps on the downstream wing panel with a nose droop of 5° on the static longitudinal characteristics of an oblique wing: $\Lambda = 45°$, $M = 0.40$.

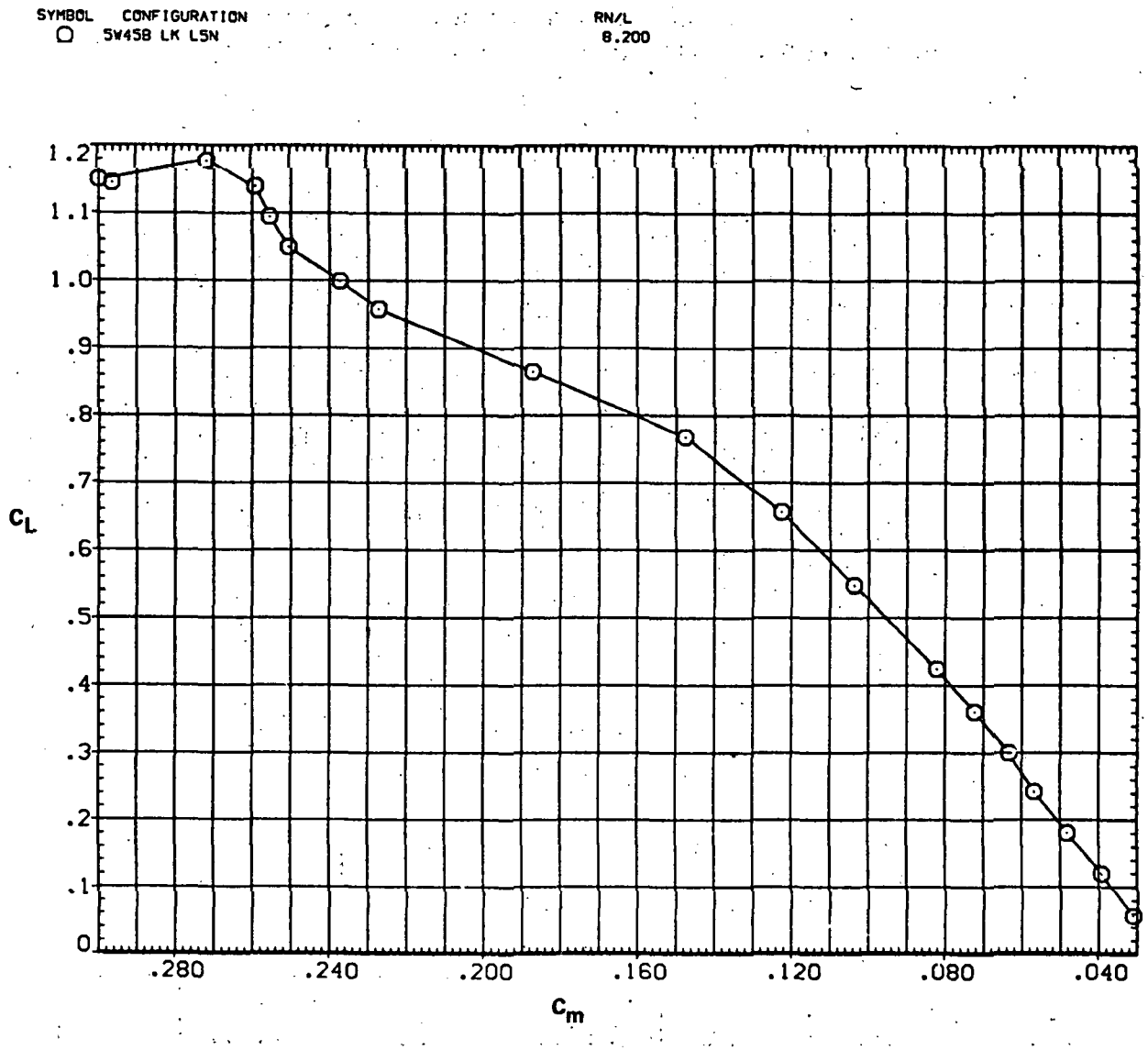

(b) C_L vs C_m

Figure 31.– Continued.

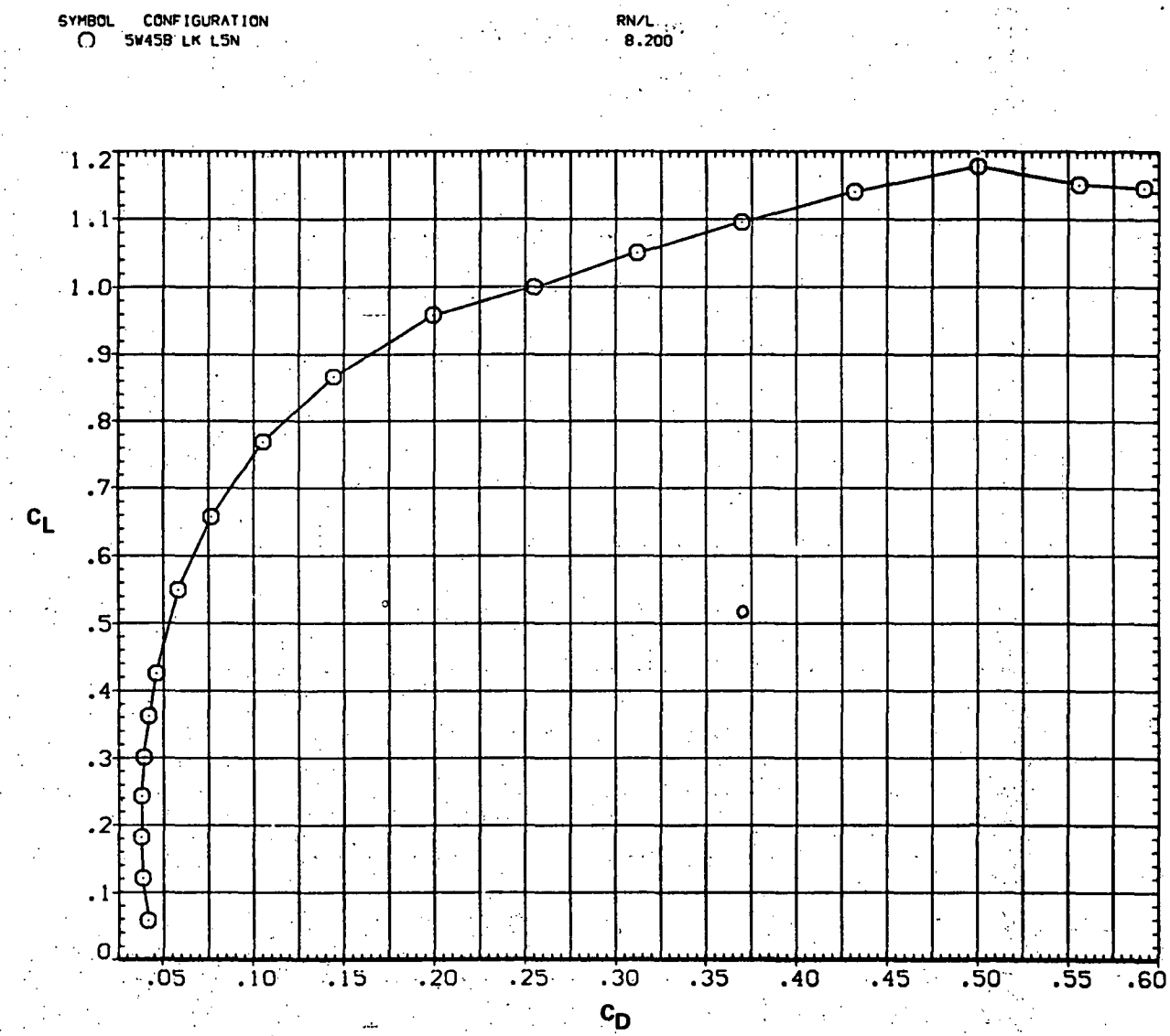

(c) C_L vs C_D

Figure 31.– Continued.

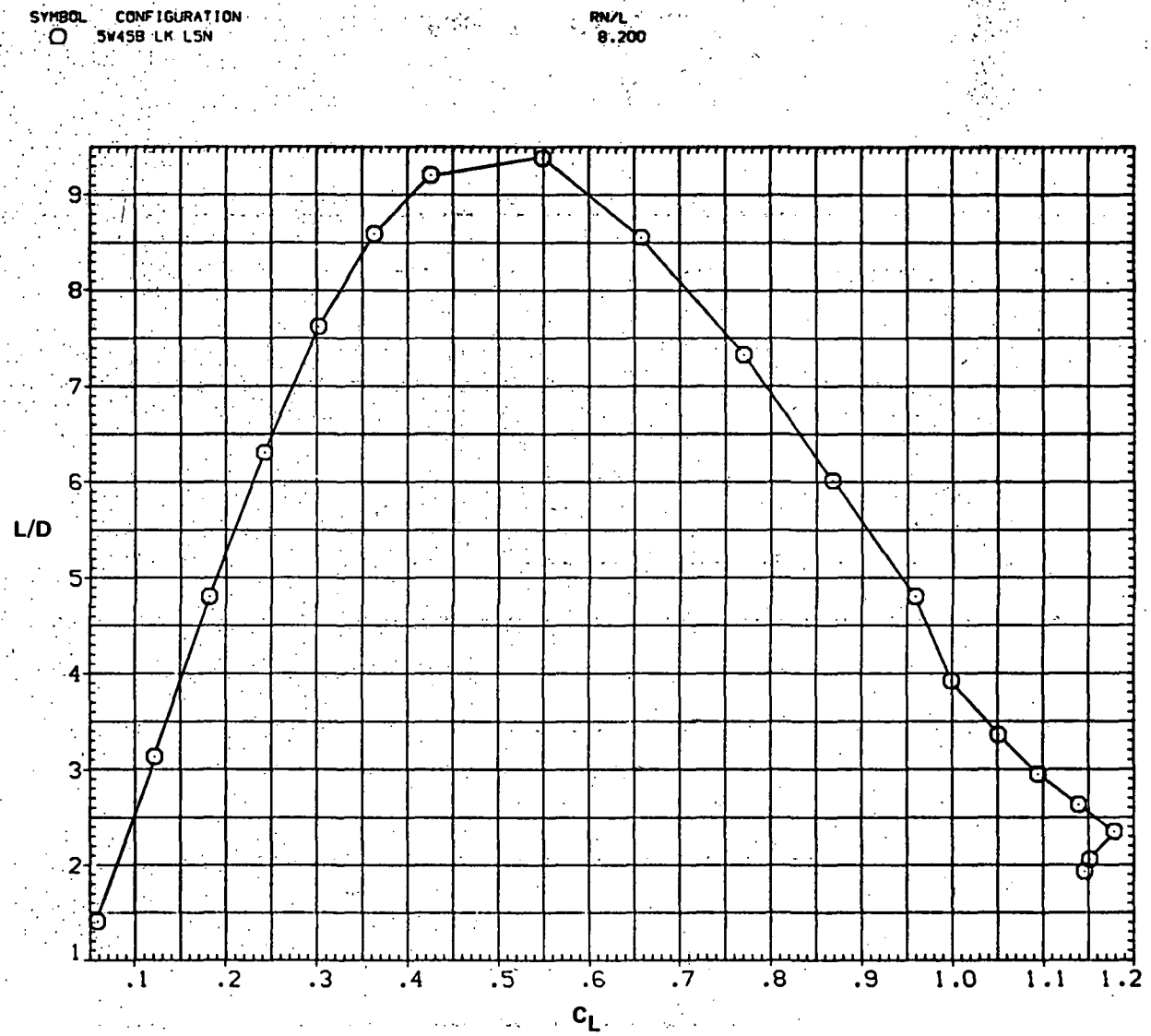

(d) L/D vs C_L

Figure 31.– Continued.

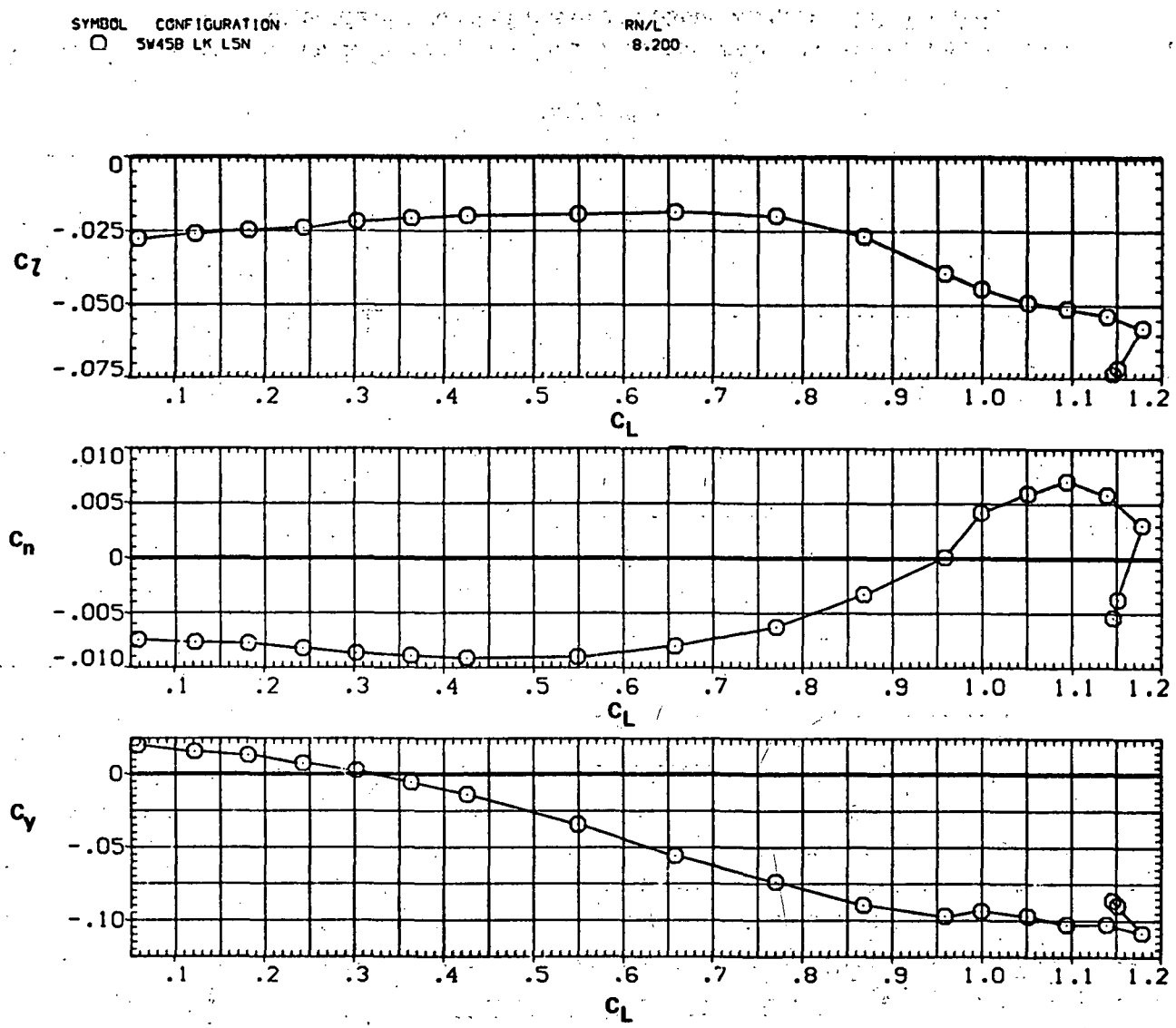

(e) C_l, C_n, and C_Y vs C_L

Figure 31.– Concluded.

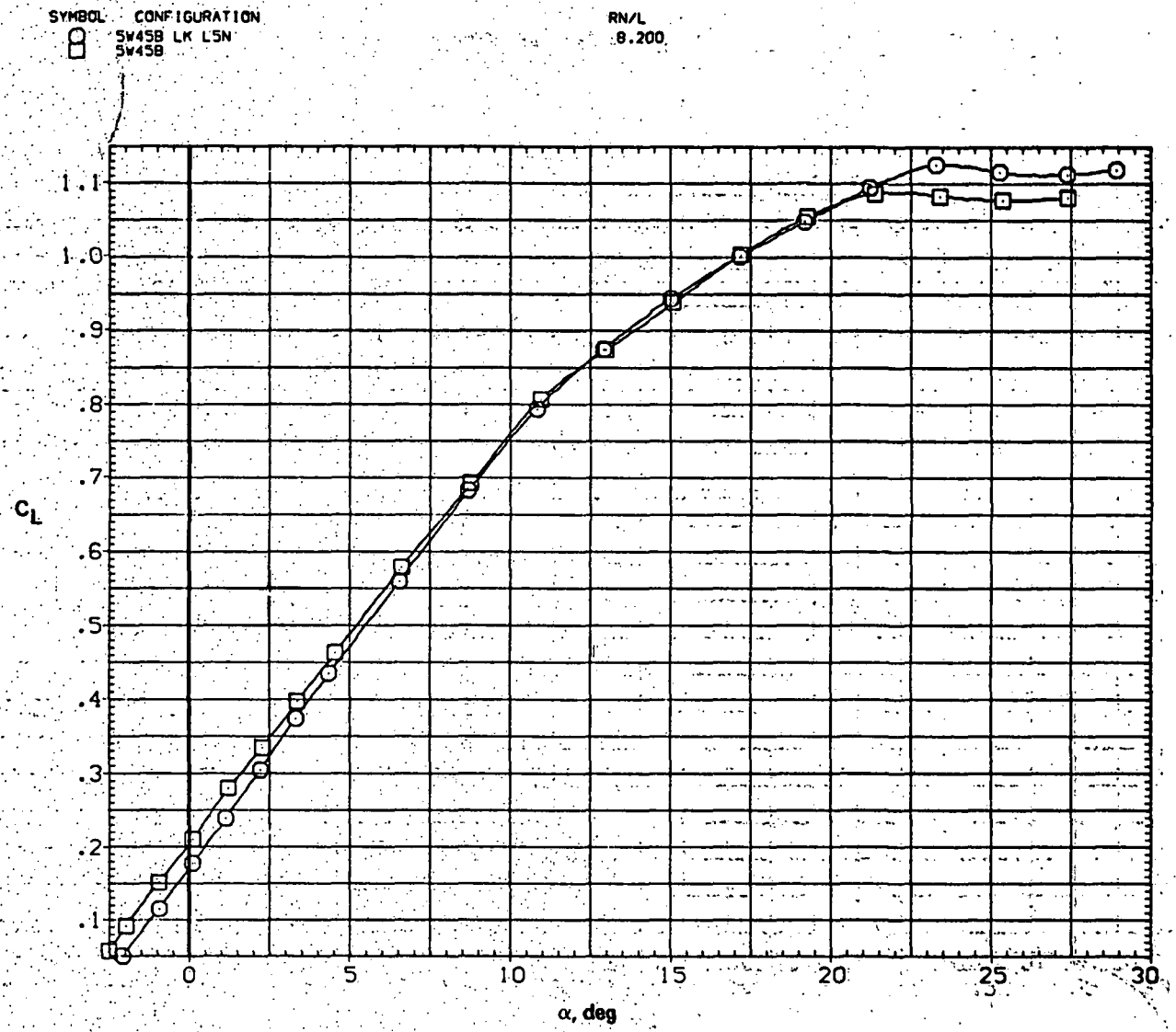

(a) C_L vs α

Figure 32.– Effect of having Krüger flaps on the downstream wing panel with a nose droop of 5° on the static longitudinal characteristics of an oblique wing: $\Lambda = 45°$, $M = 0.60$.

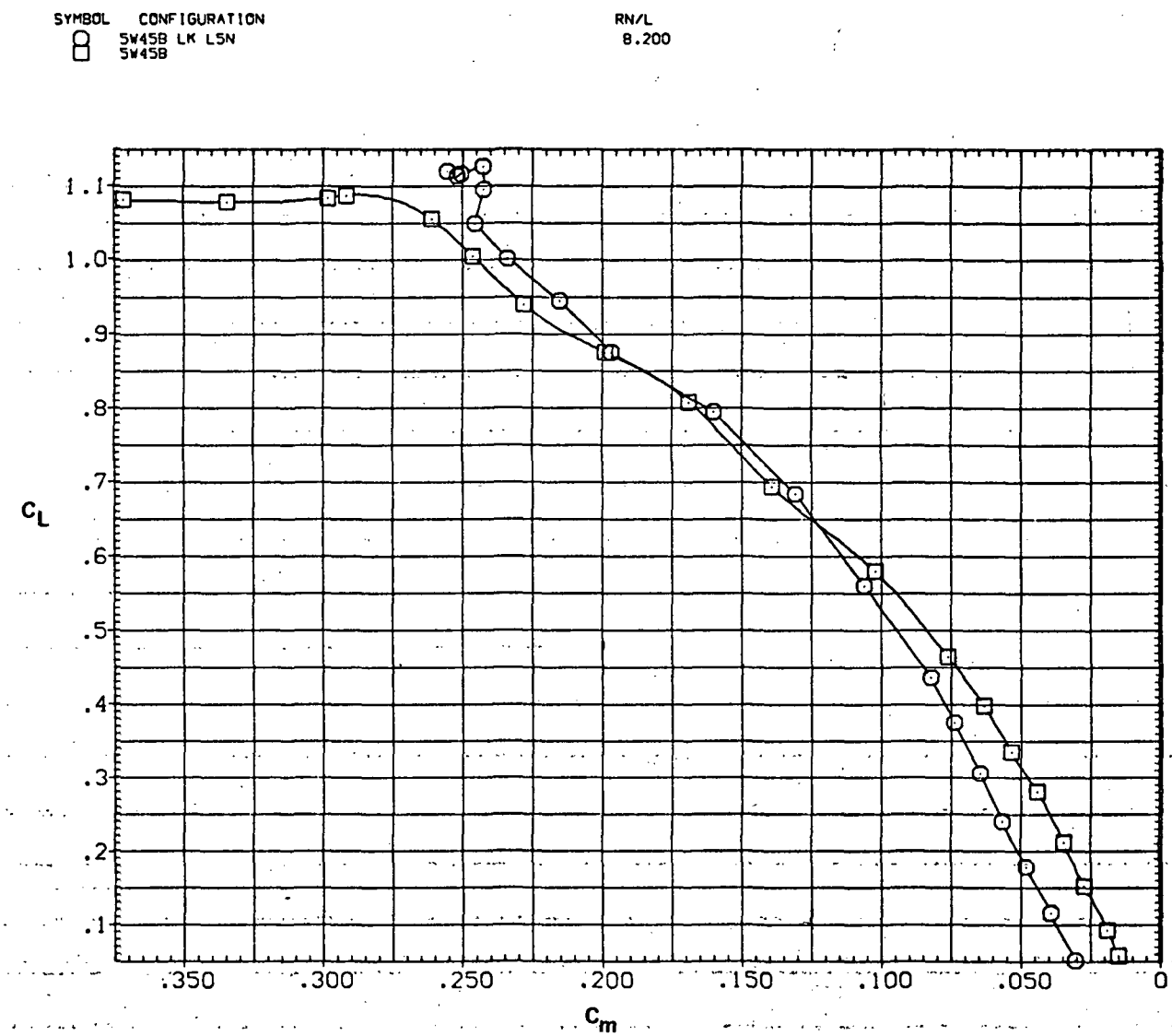

(b) C_L vs C_m

Figure 32.– Continued.

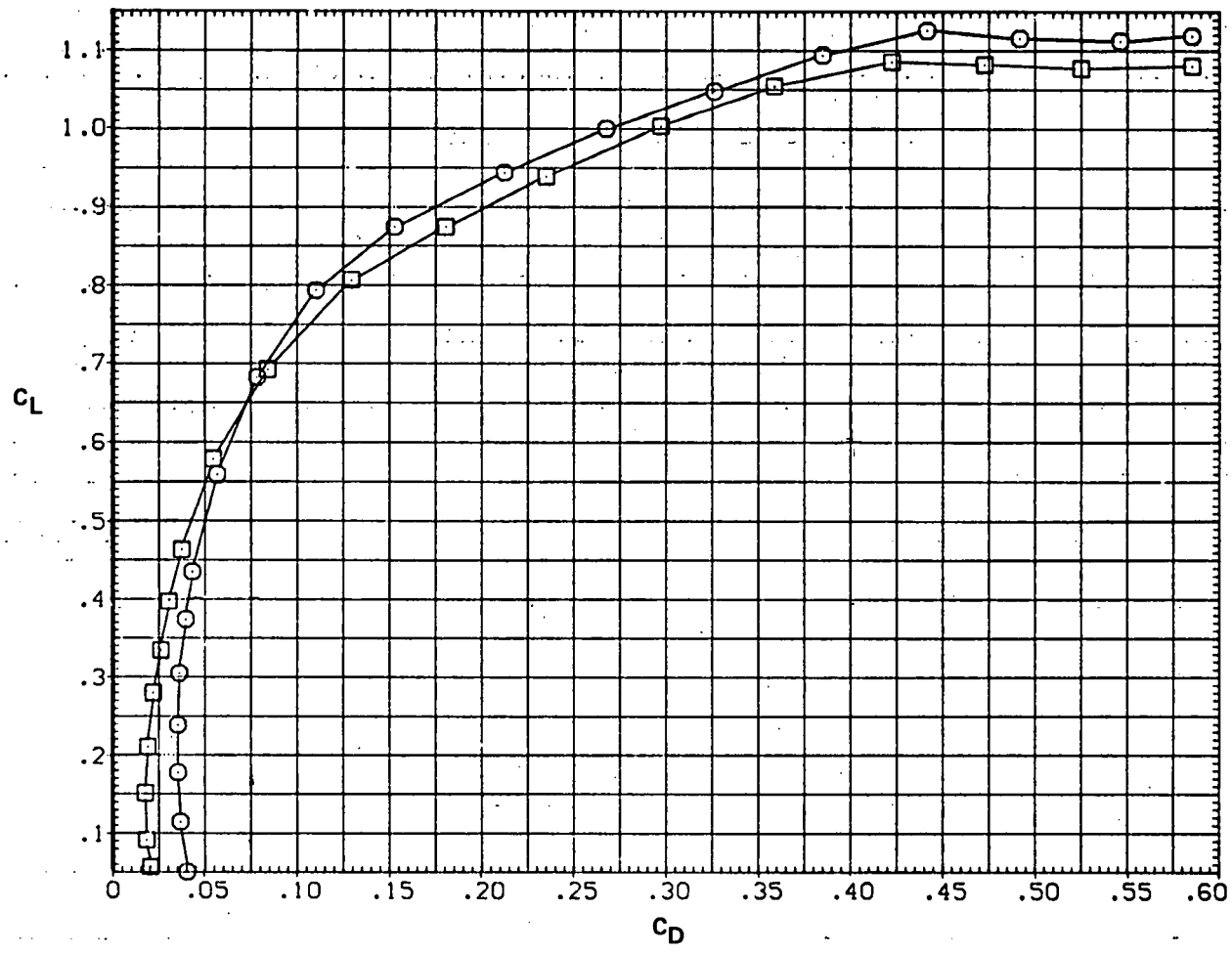

(c) C_L vs C_D

Figure 32.– Continued.

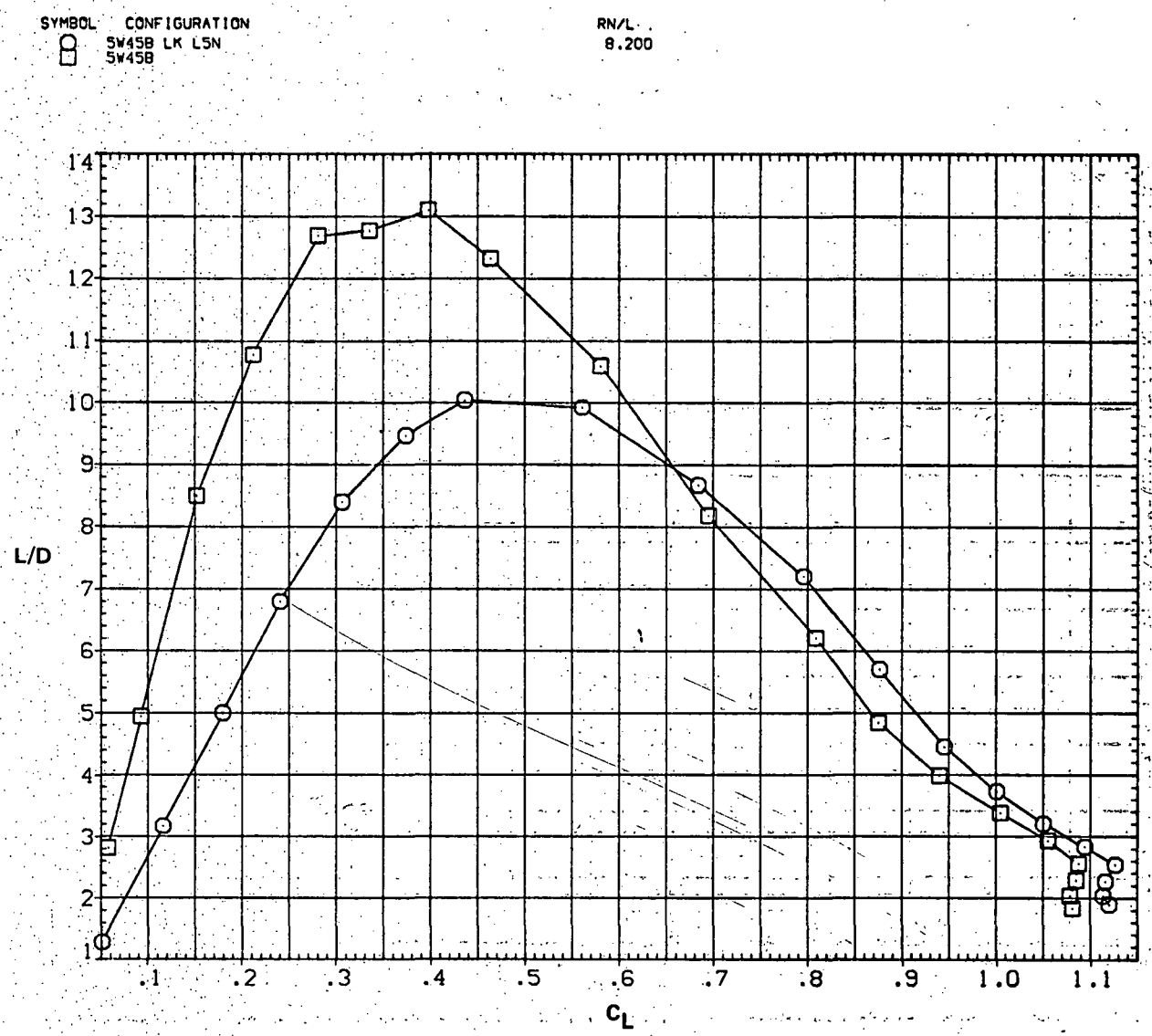

(d) L/D vs C_L

Figure 32.– Continued.

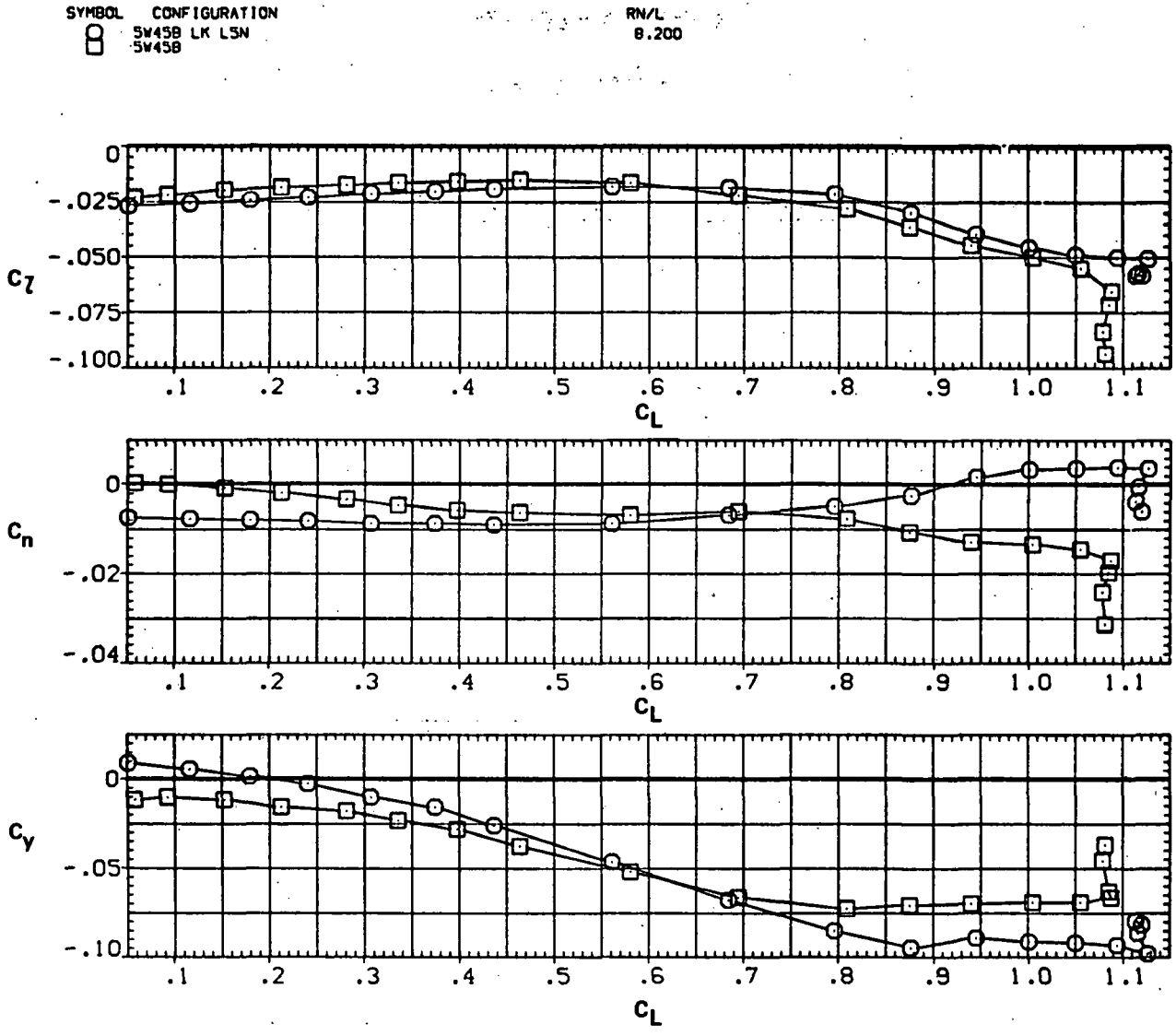

(e) C_l, C_n, and C_Y vs C_L

Figure 32.– Concluded.

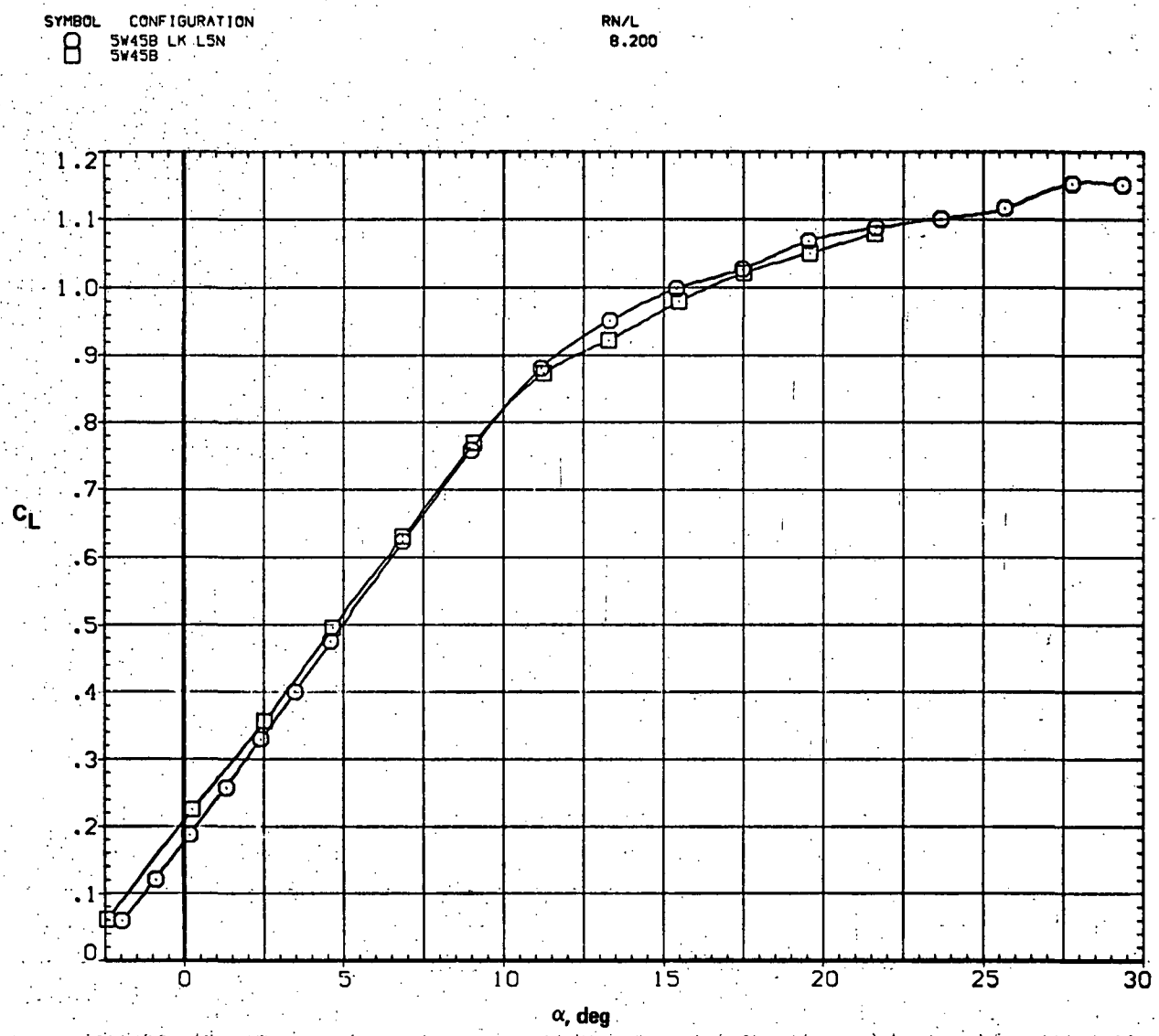

(a) C_L vs α

Figure 33.– Effect of having Krüger flaps on the downstream wing panel with a nose droop of 5° on the static longitudinal characteristics of an oblique wing: $\Lambda = 45°$, $M = 0.80$.

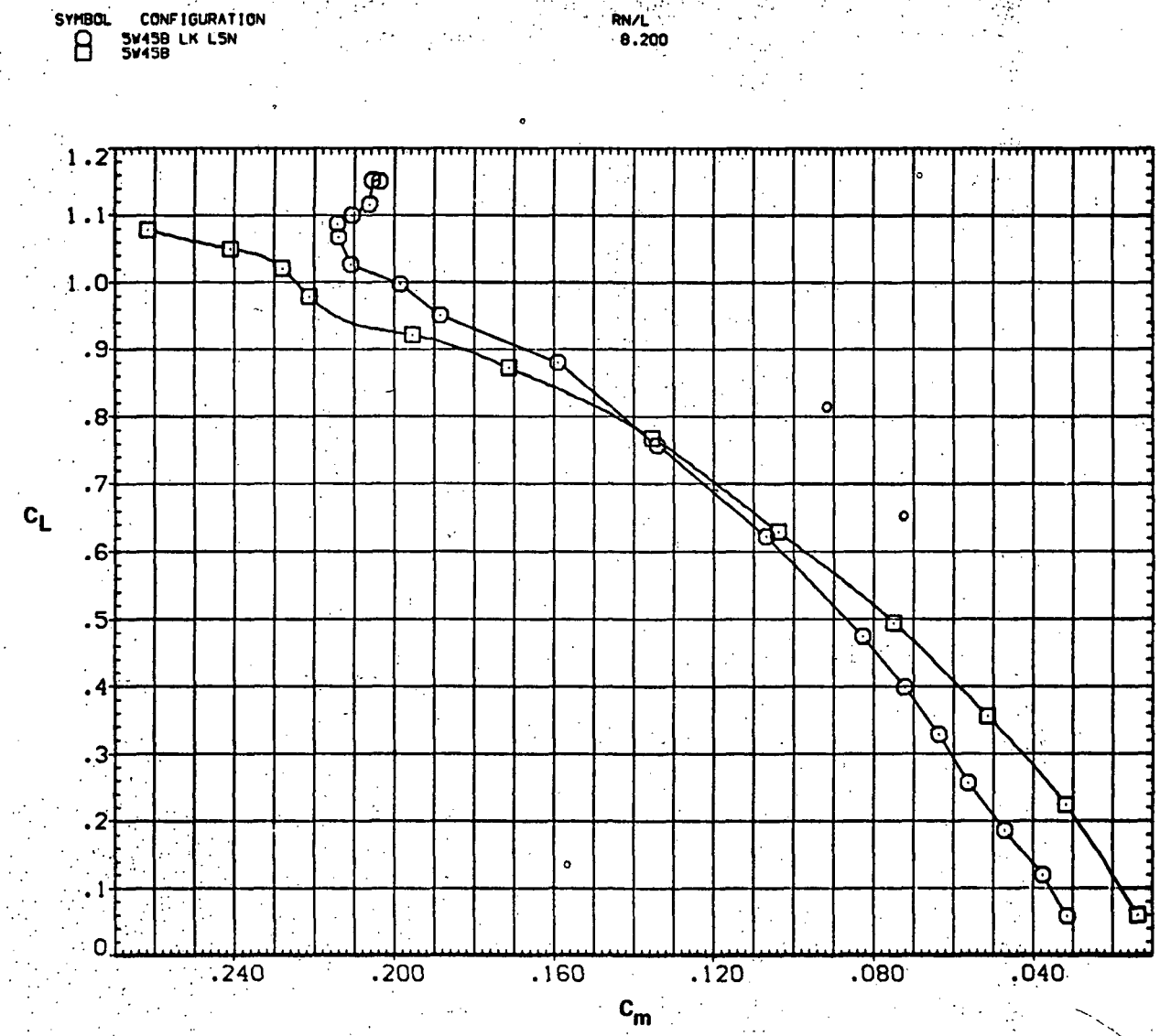

(b) C_L vs C_m

Figure 33.– Continued.

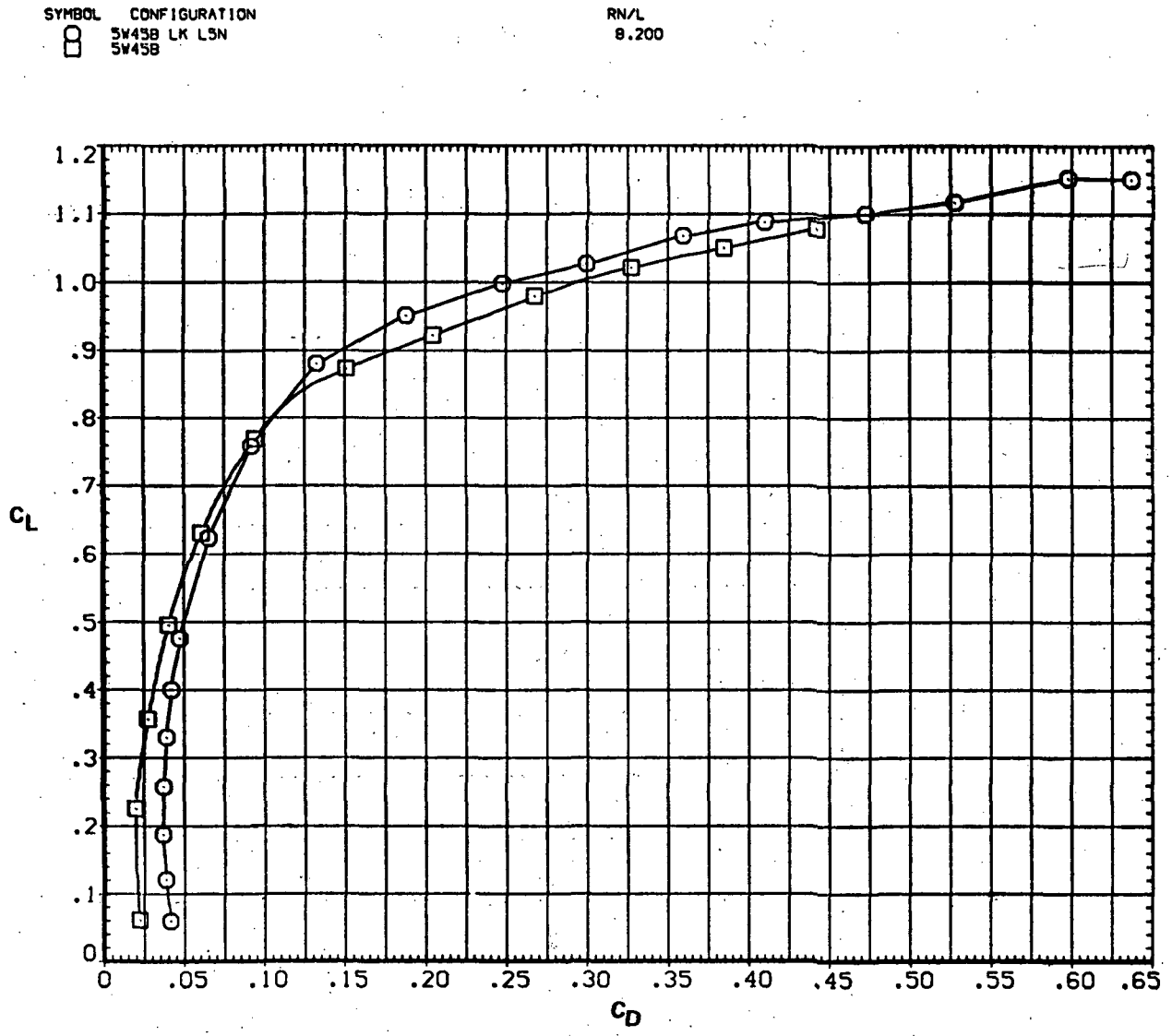

(c) C_L vs C_D

Figure 33.– Continued.

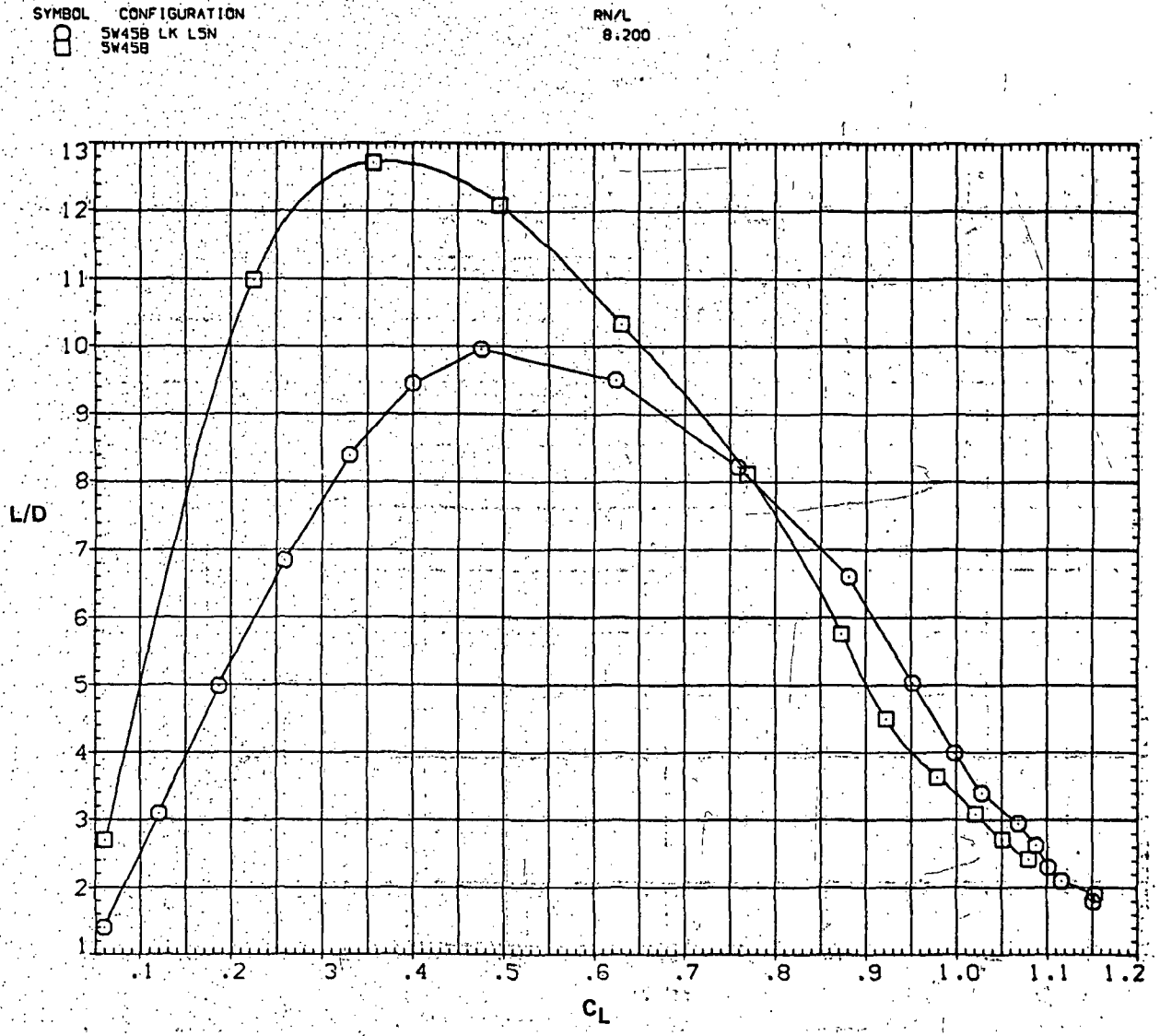

(d) L/D vs C_L

Figure 33.– Continued.

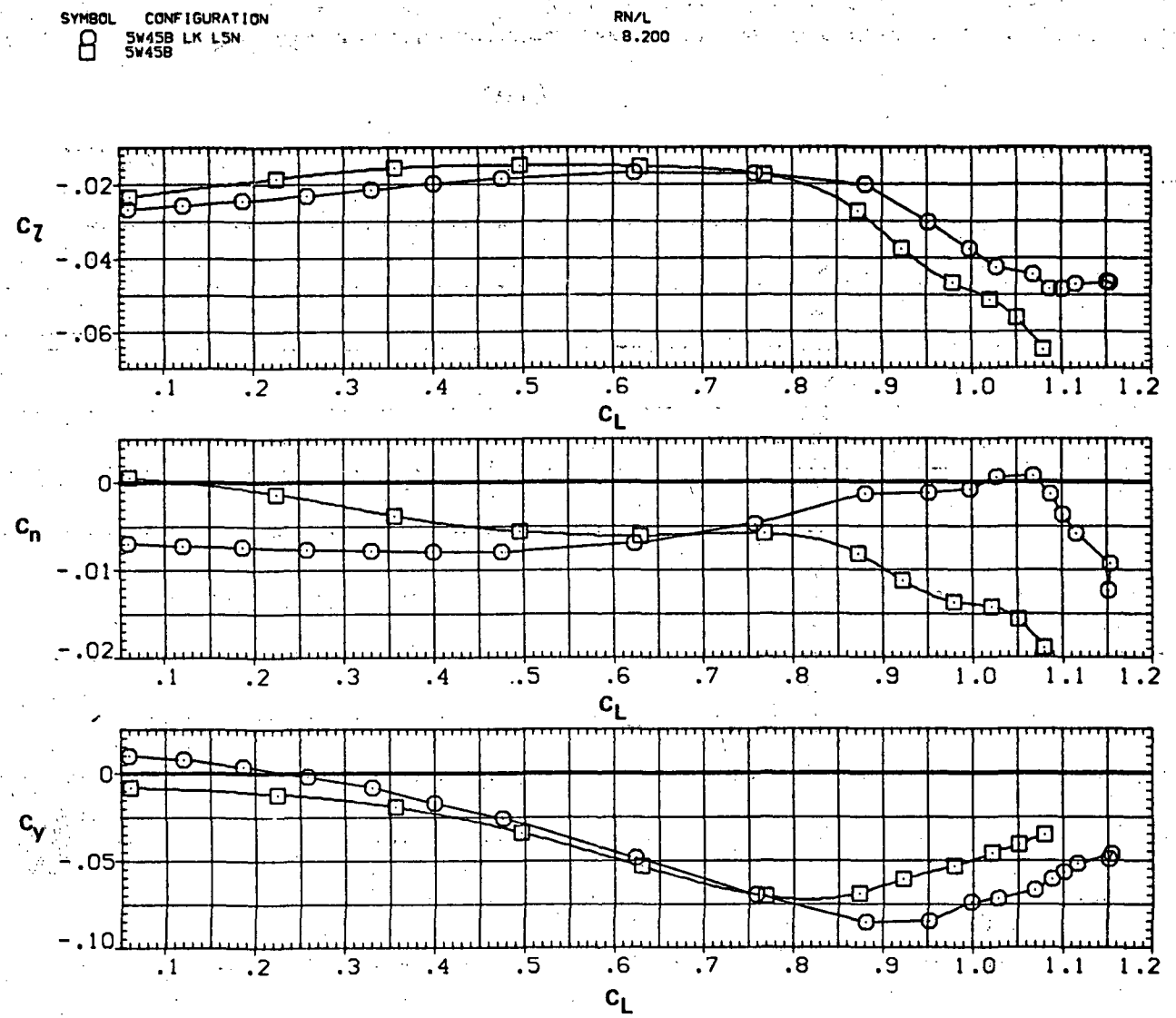

(e) C_l, C_n, and C_Y vs C_L

Figure 33.– Concluded.

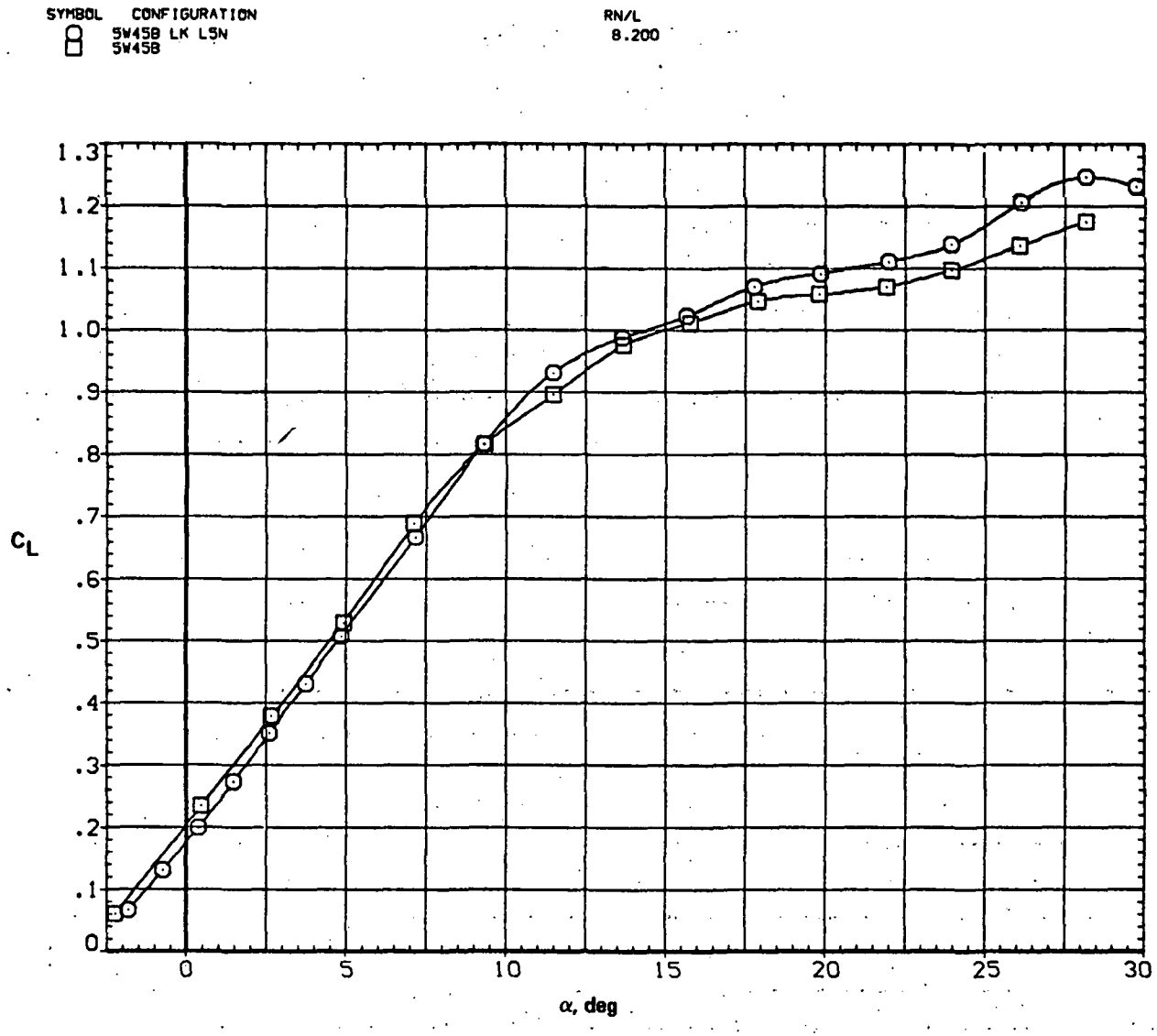

(a) C_L vs α

Figure 34.– Effect of having Krüger flaps on the downstream wing panel with a nose droop of 5° on the static longitudinal characteristics of an oblique wing: $\Lambda = 45°$, $M = 0.90$.

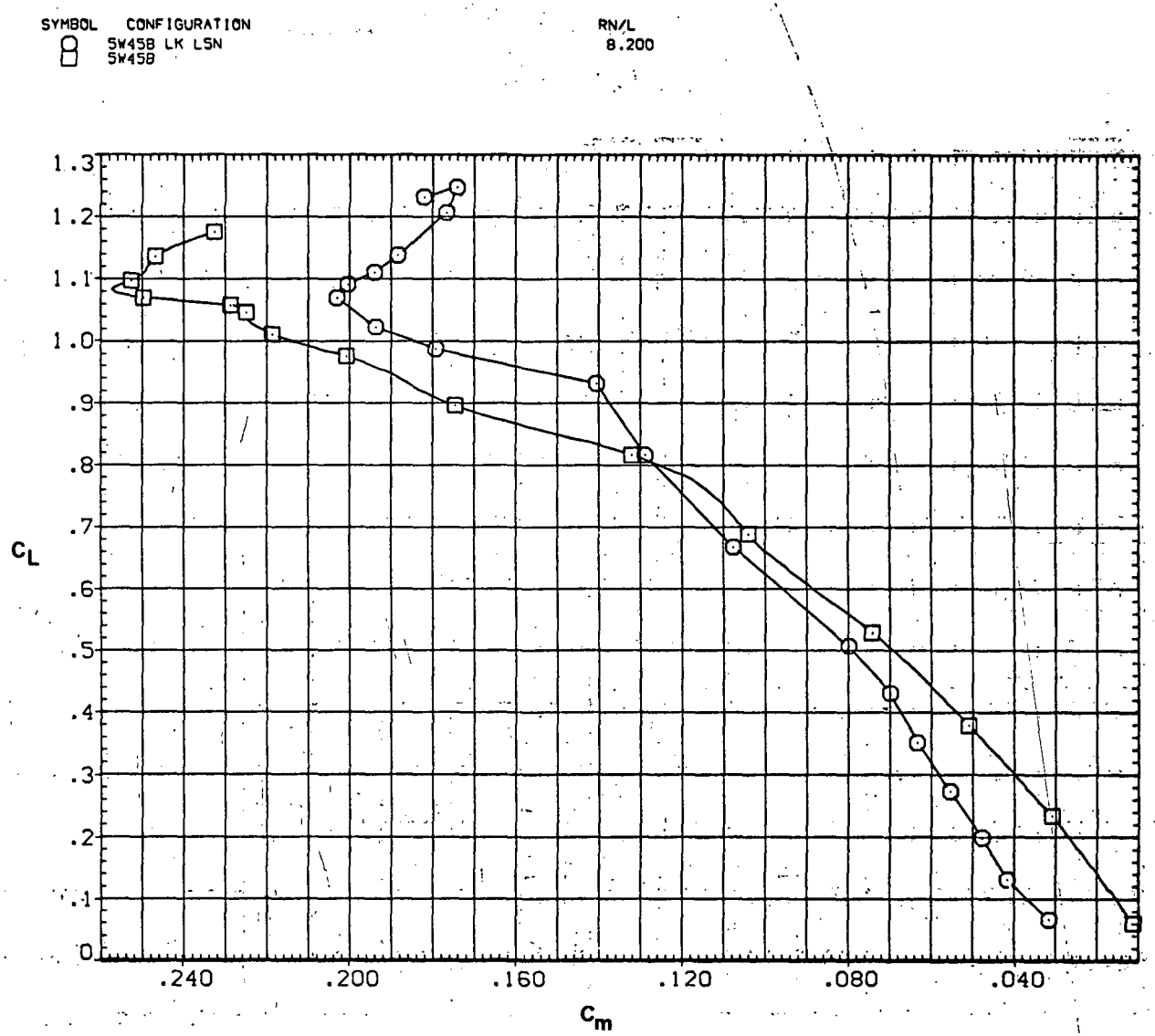

(b) C_L vs C_m

Figure 34.– Continued.

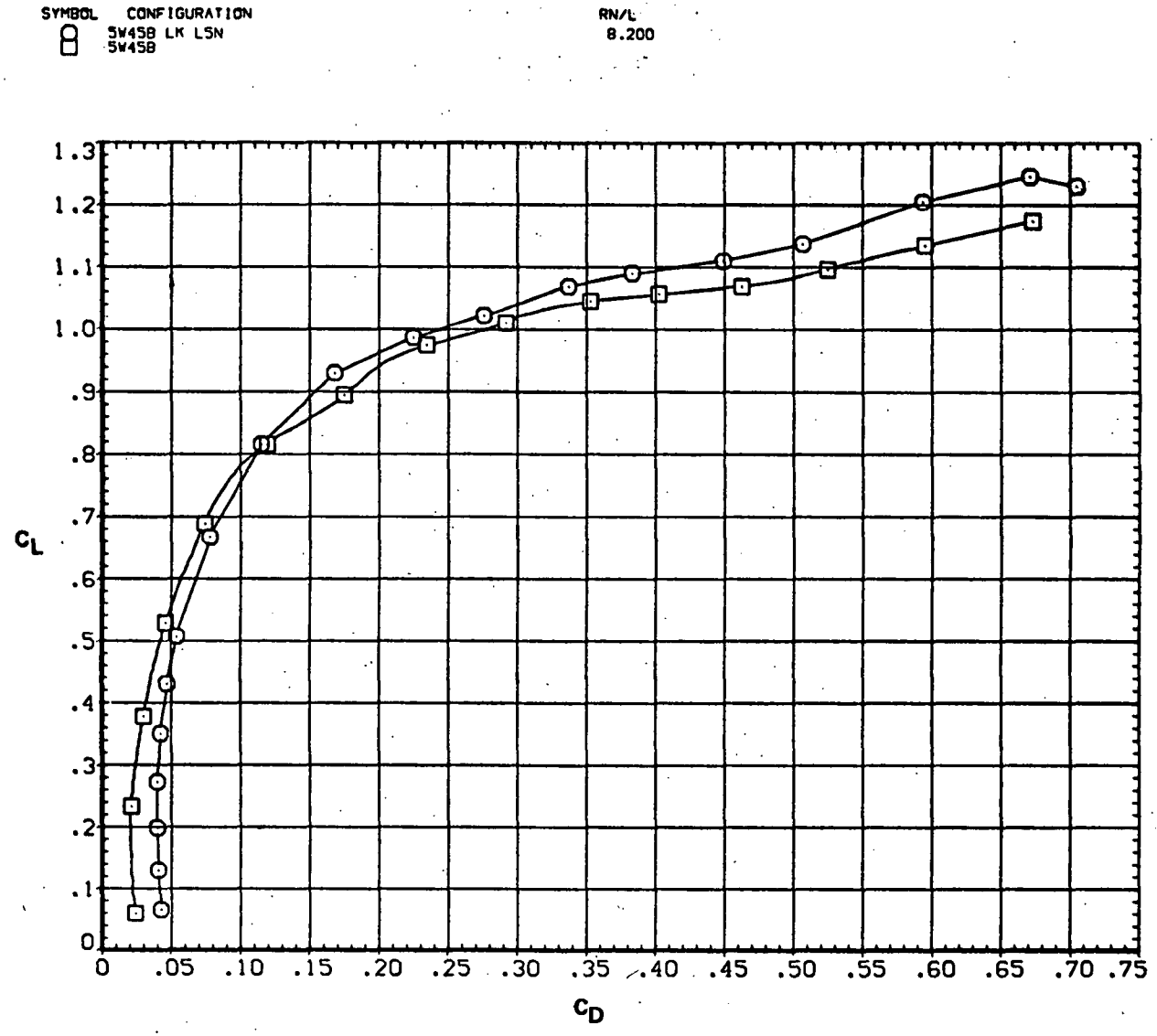

(c) C_L vs C_D

Figure 34.– Continued.

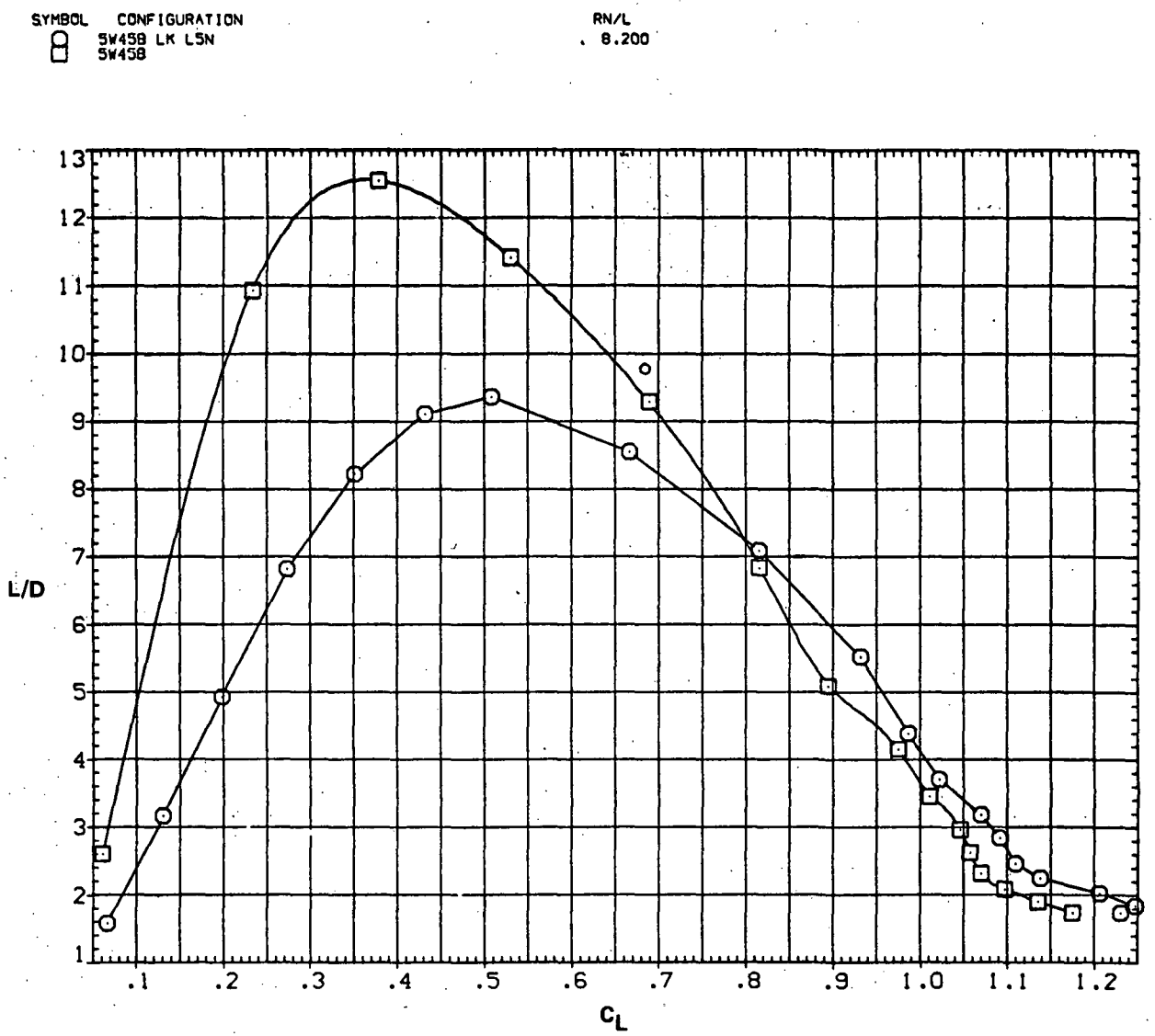

(d) L/D vs C_L

Figure 34.– Continued.

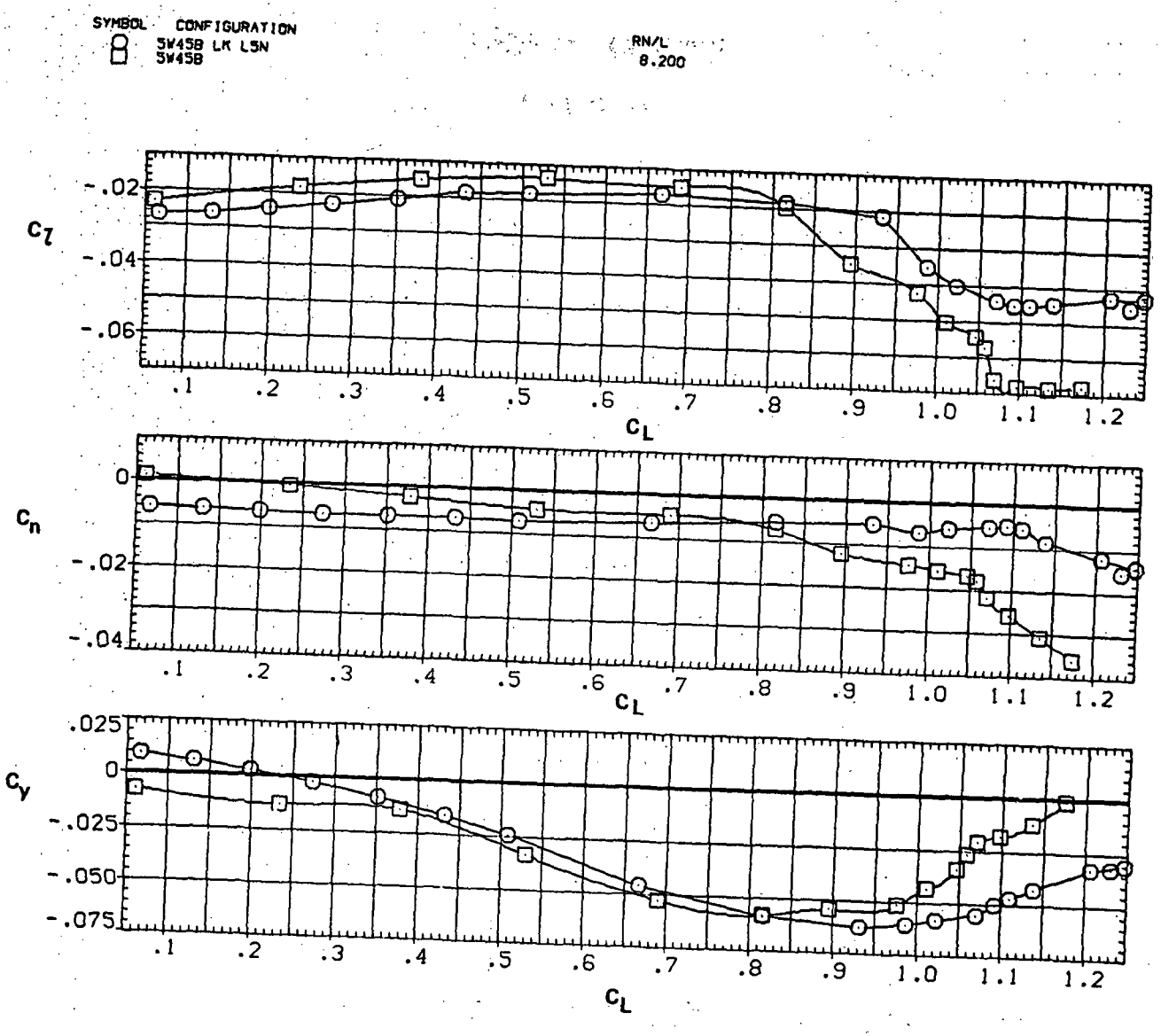

(e) C_l, C_n, and C_Y vs C_L

Figure 34.– Concluded.

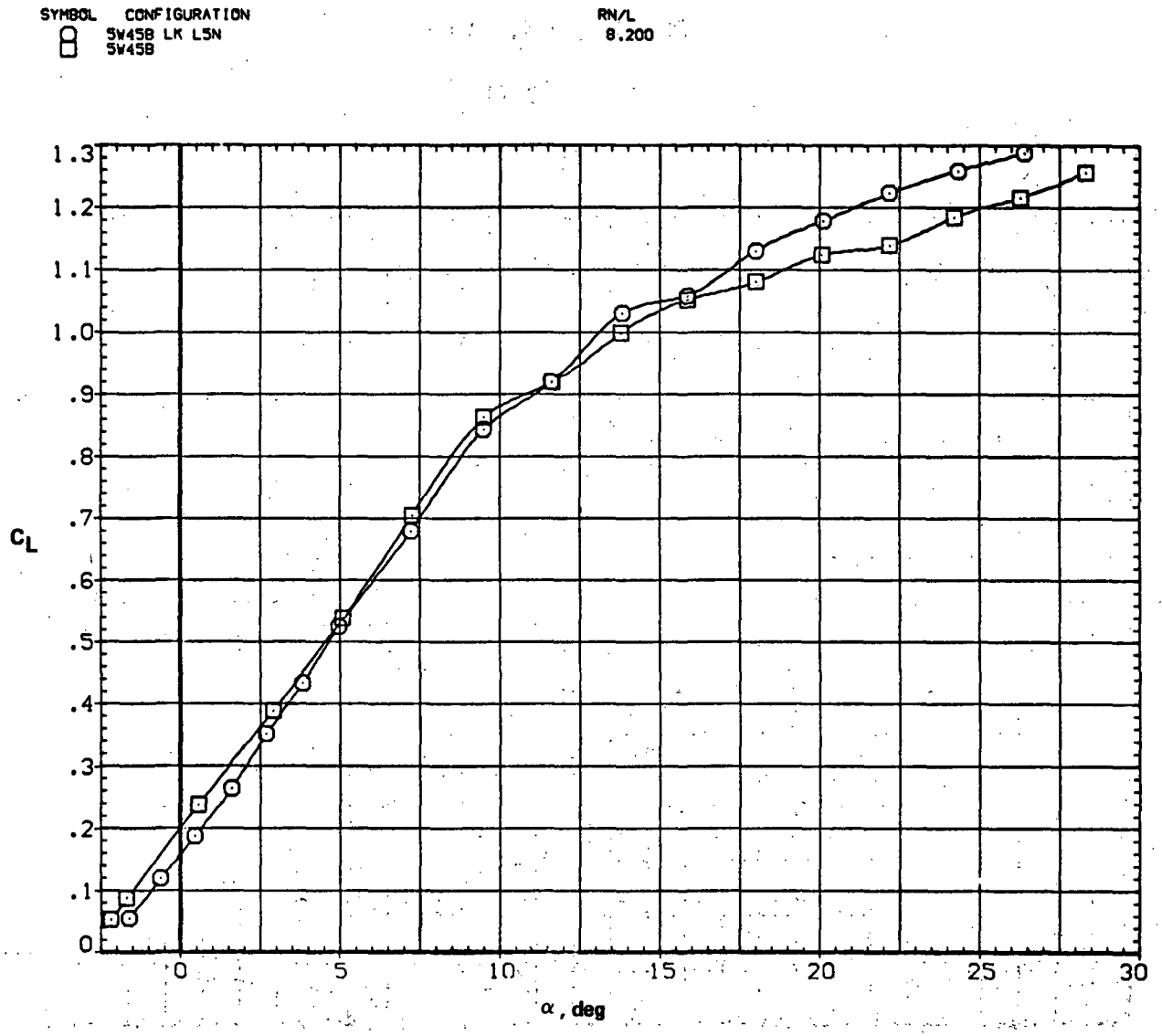

(a) C_L vs α

Figure 35.– Effect of having Krüger flaps on the downstream wing panel with a nose droop of 5° on the static longitudinal characteristics of an oblique wing: $\Lambda = 45°$, $M = 0.95$.

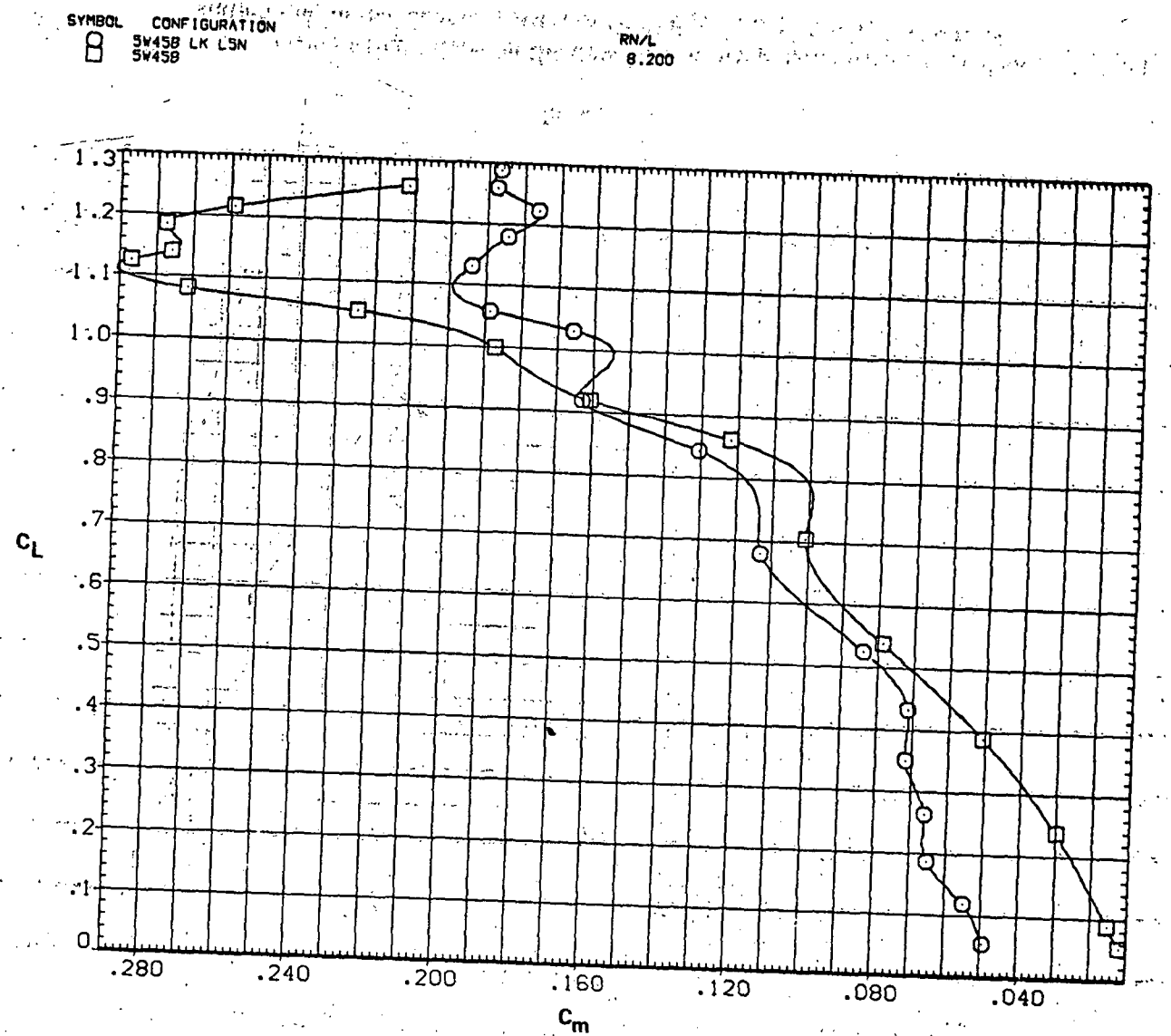

(b) C_L vs C_m

Figure 35.– Continued.

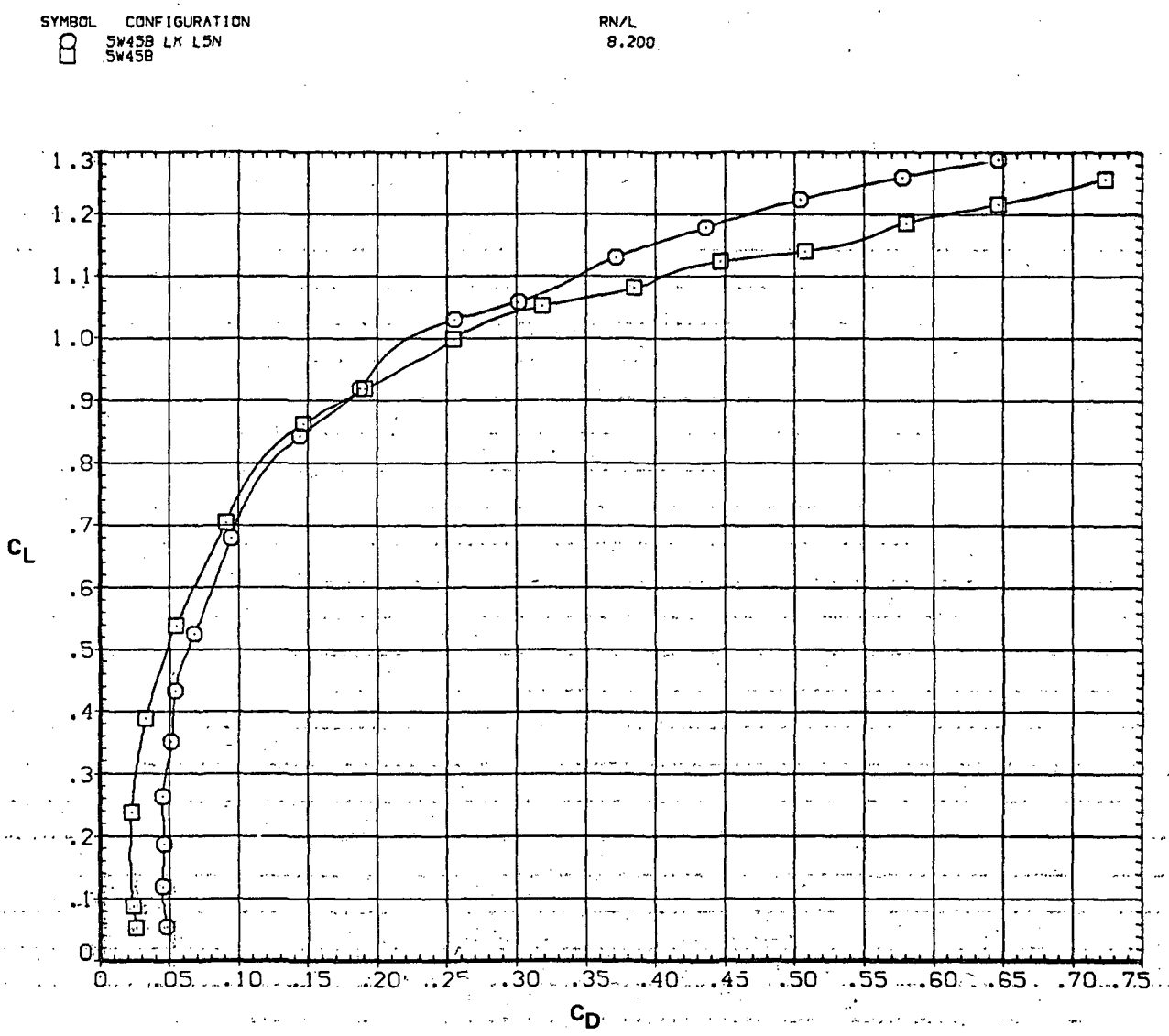

(c) C_L vs C_D

Figure 35.– Continued.

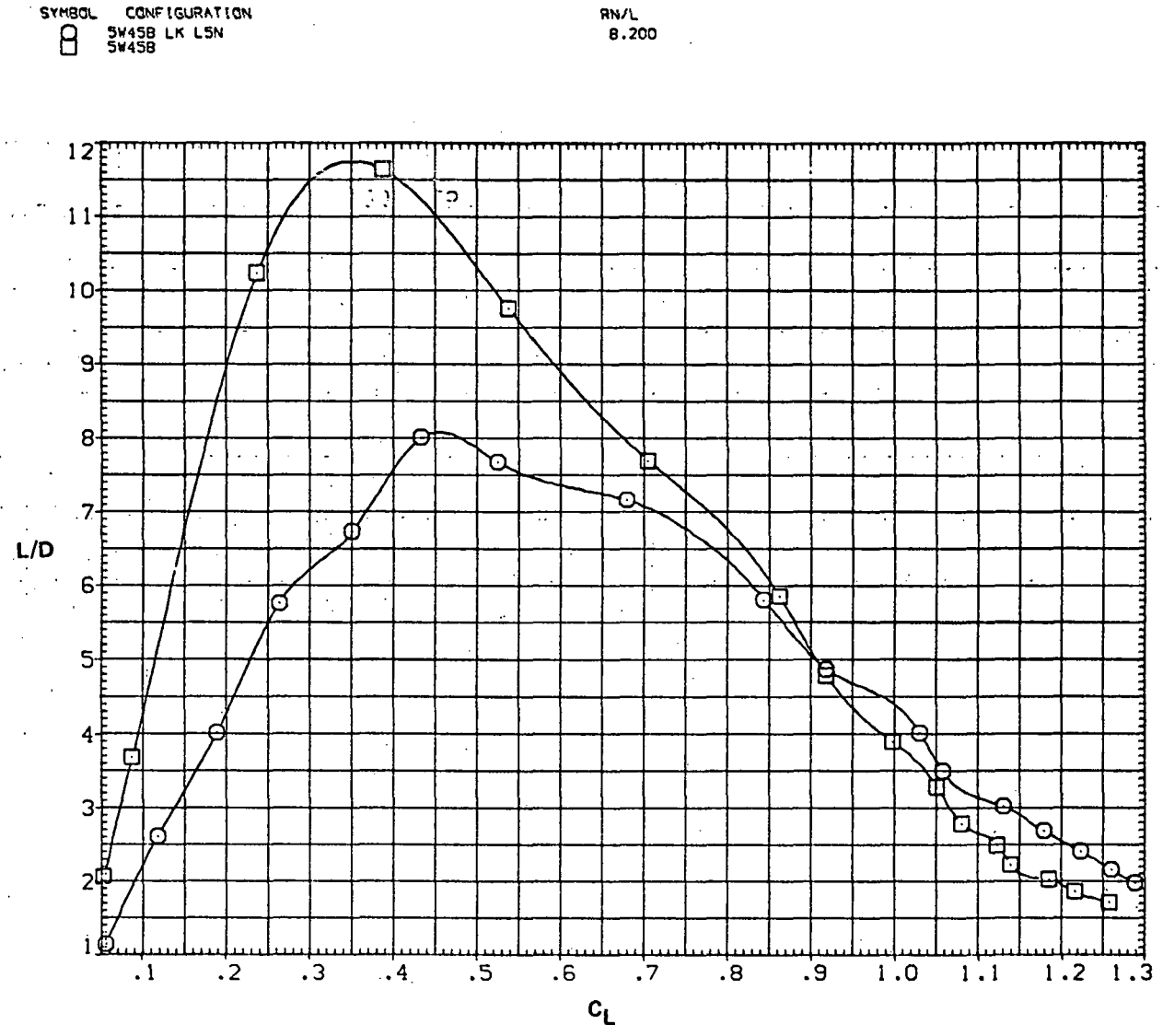

(d) L/D vs C_L

Figure 35.– Continued.

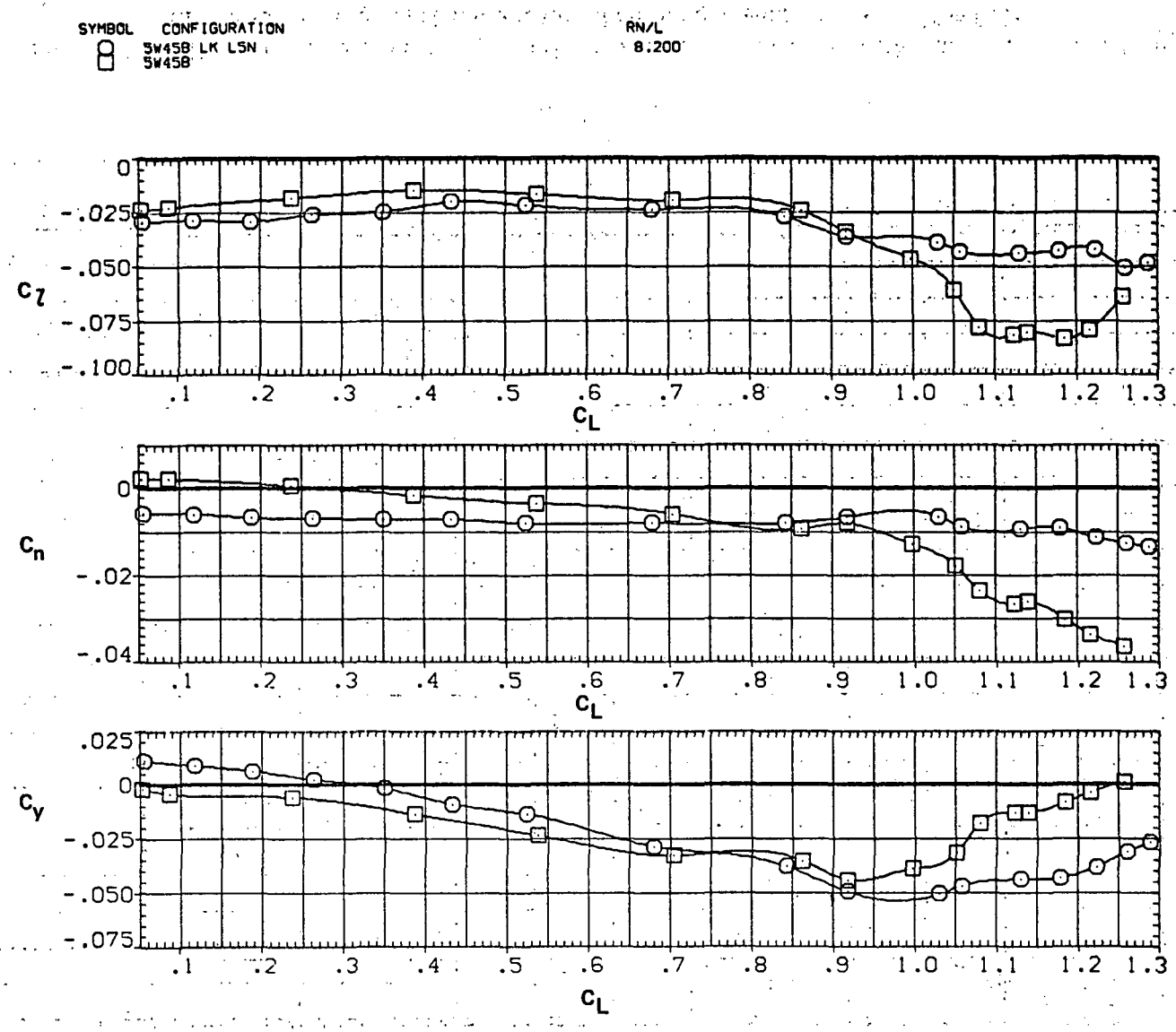

(e) C_l, C_n, and C_Y vs C_L

Figure 35.– Concluded.

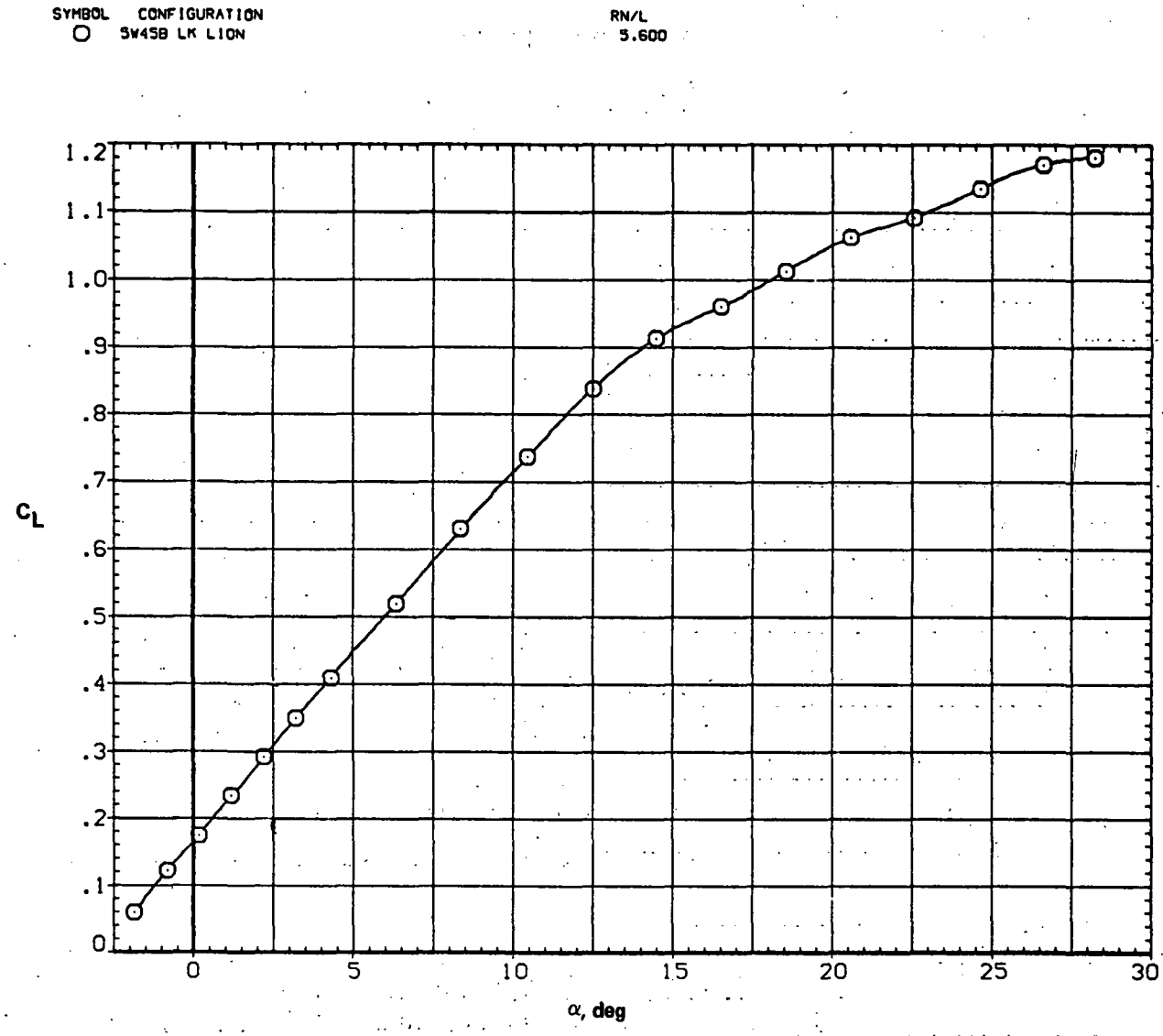

(a) C_L vs α

Figure 36.– Effect of having Krüger flaps on the downstream wing panel with a nose droop of 10° on the static longitudinal characteristics of an oblique wing: $\Lambda = 45°$, $M = 0.25$.

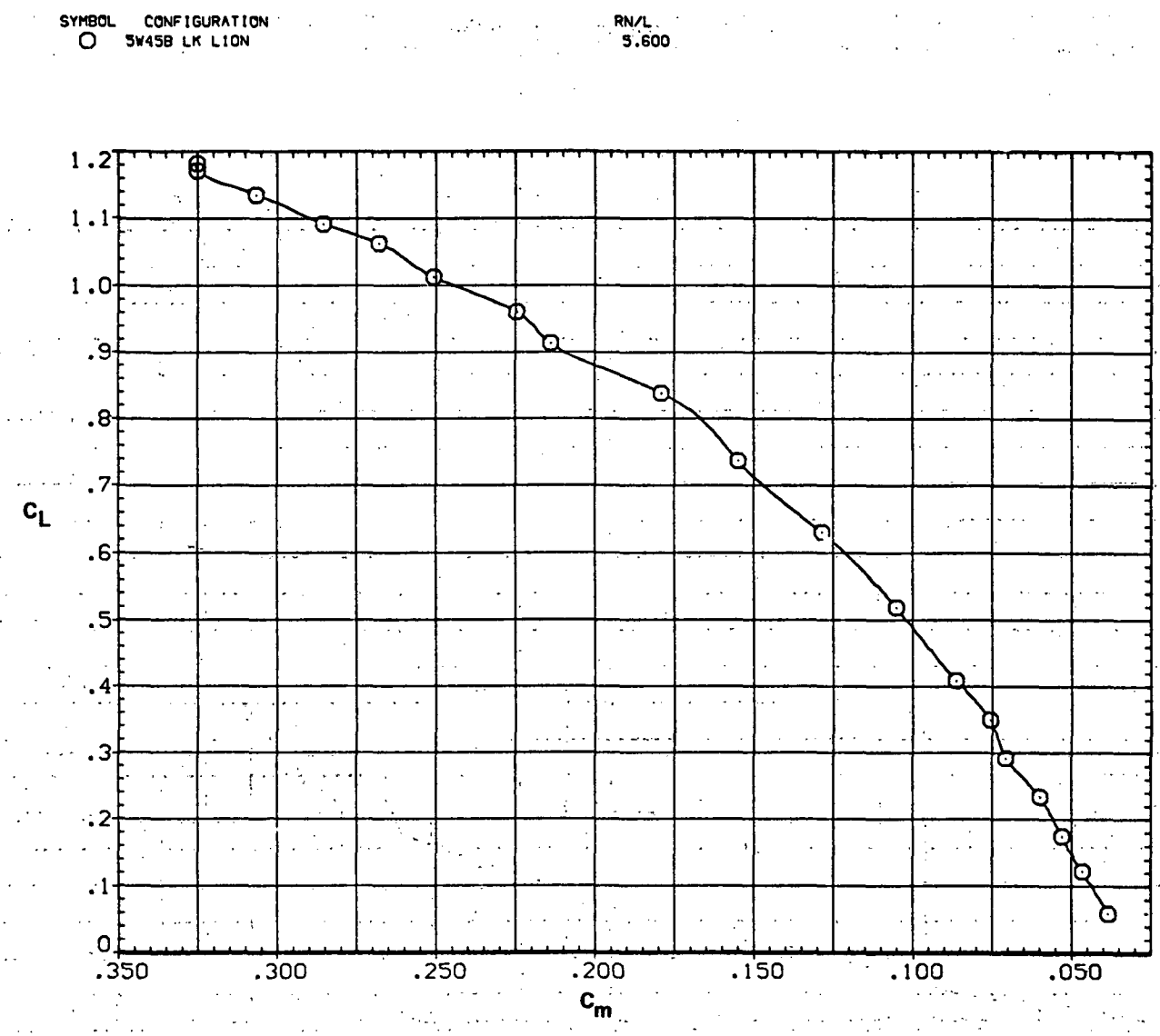

(b) C_L vs C_m

Figure 36.– Continued.

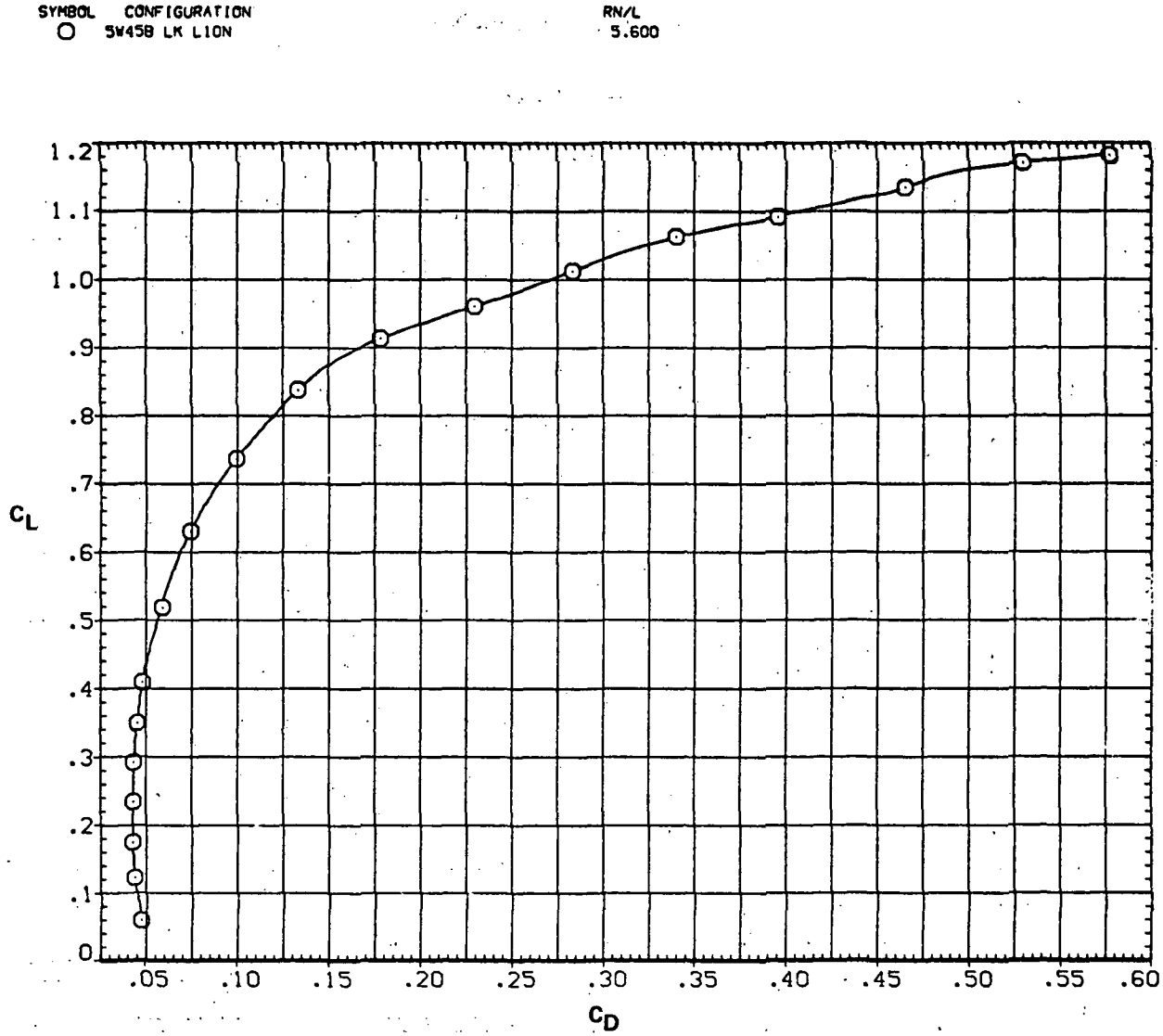

(c) C_L vs C_D

Figure 36.– Continued.

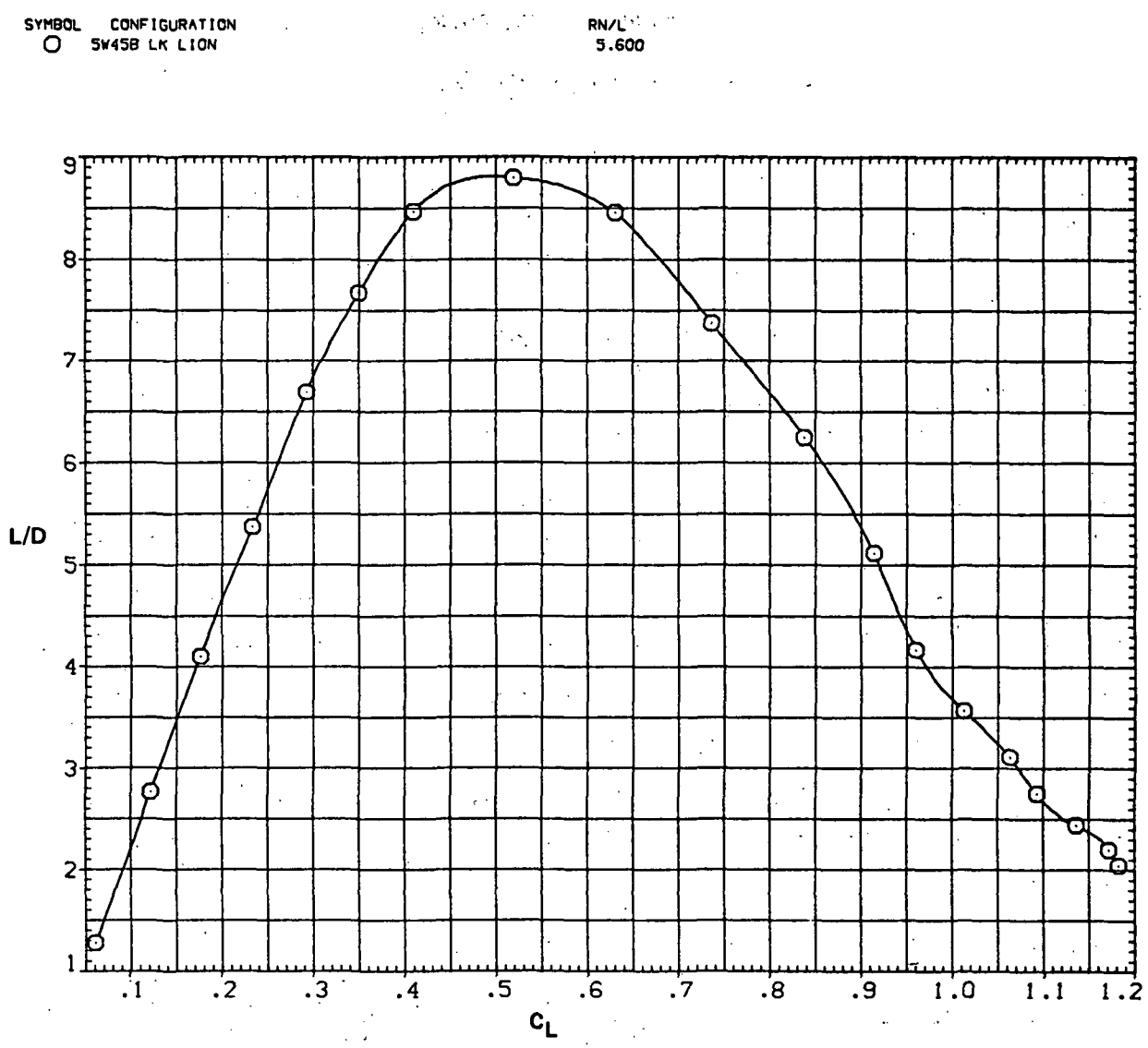

(d) L/D vs C_L

Figure 36.– Continued.

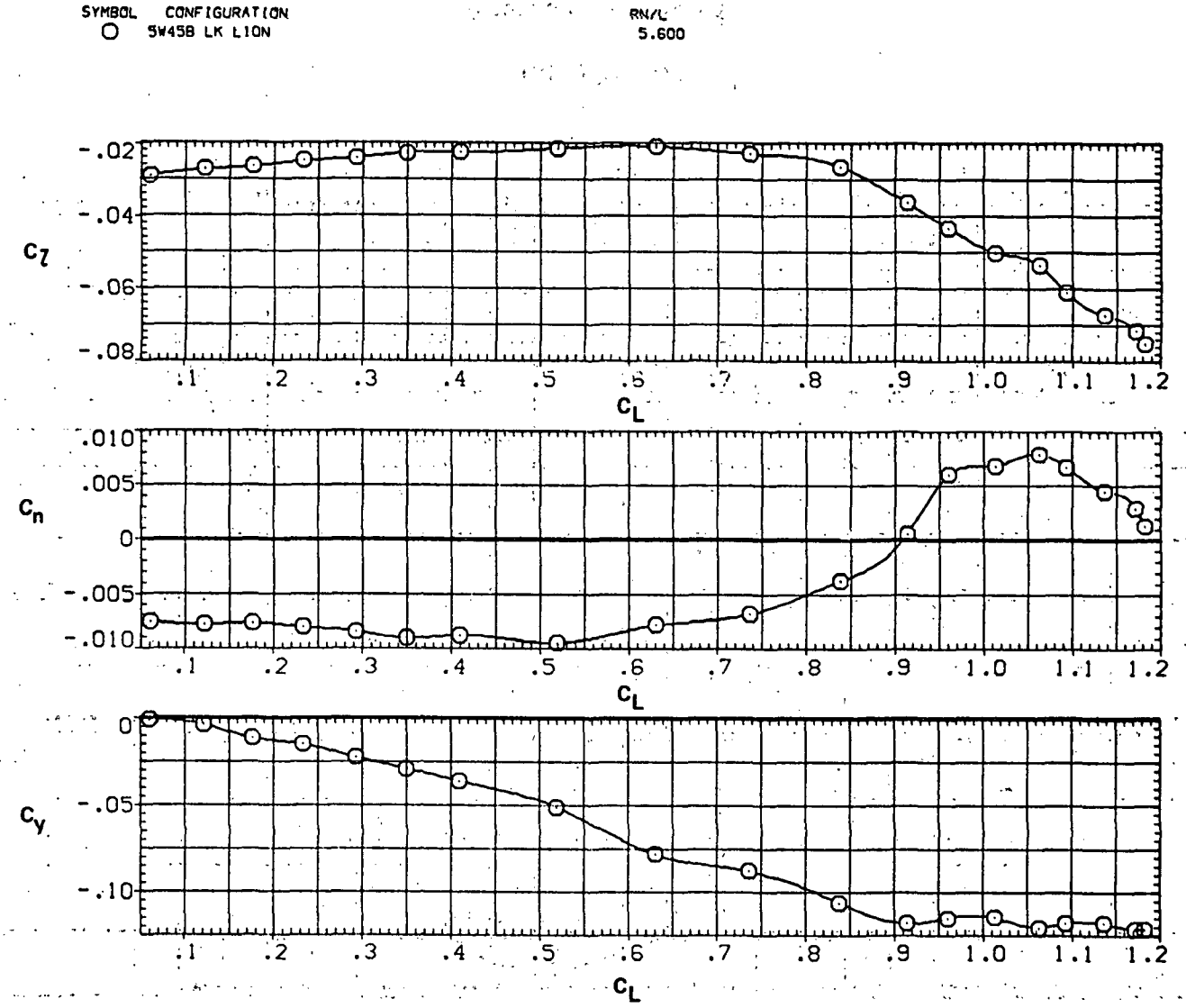

(e) C_l, C_n, and C_Y vs C_L

Figure 36.– Concluded.

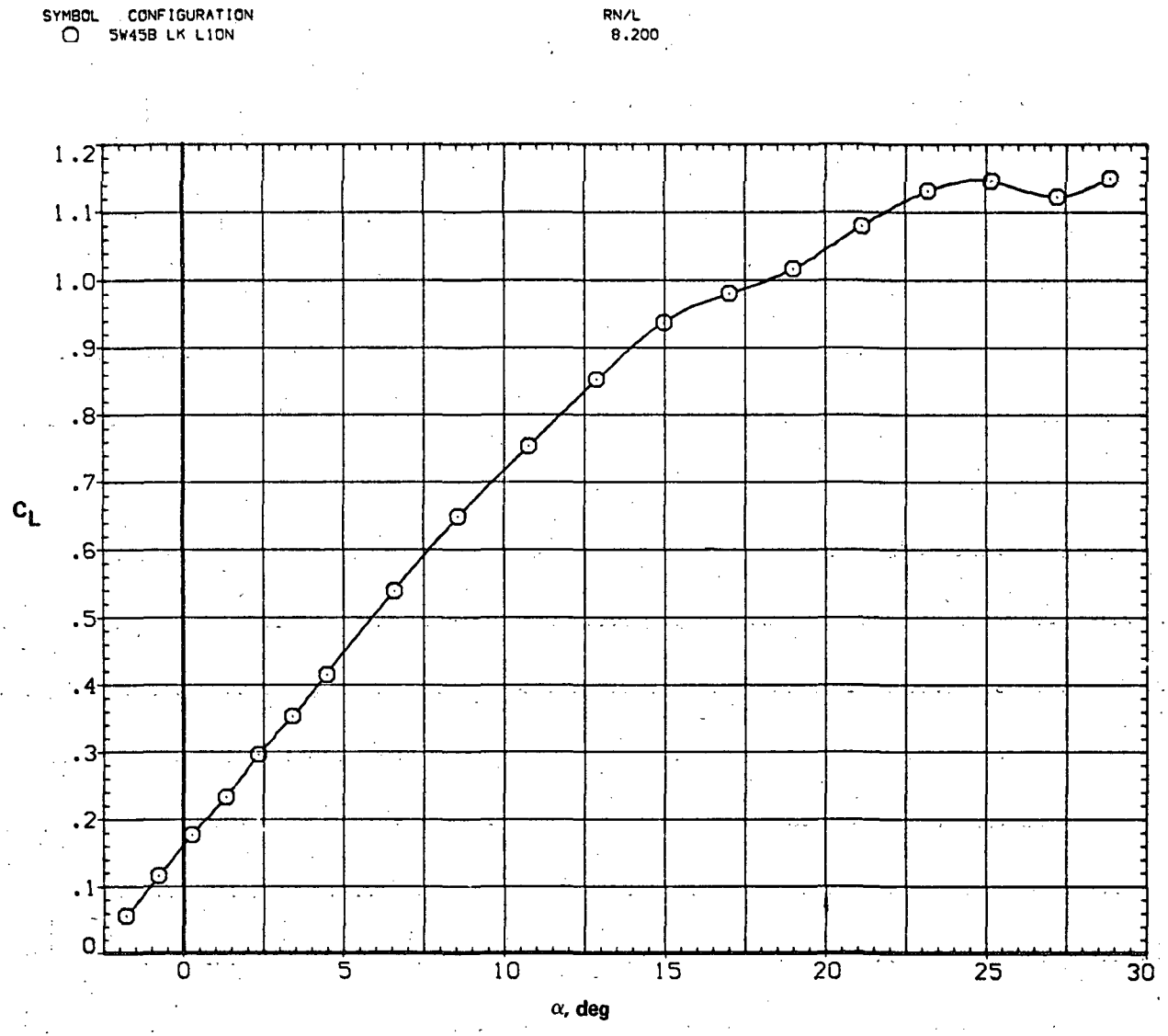

(a) C_L vs α

Figure 37.– Effect of having Krüger flaps on the downstream wing panel with a nose droop of 10° on the static longitudinal characteristics of an oblique wing: $\Lambda = 45°$, $M = 0.40$.

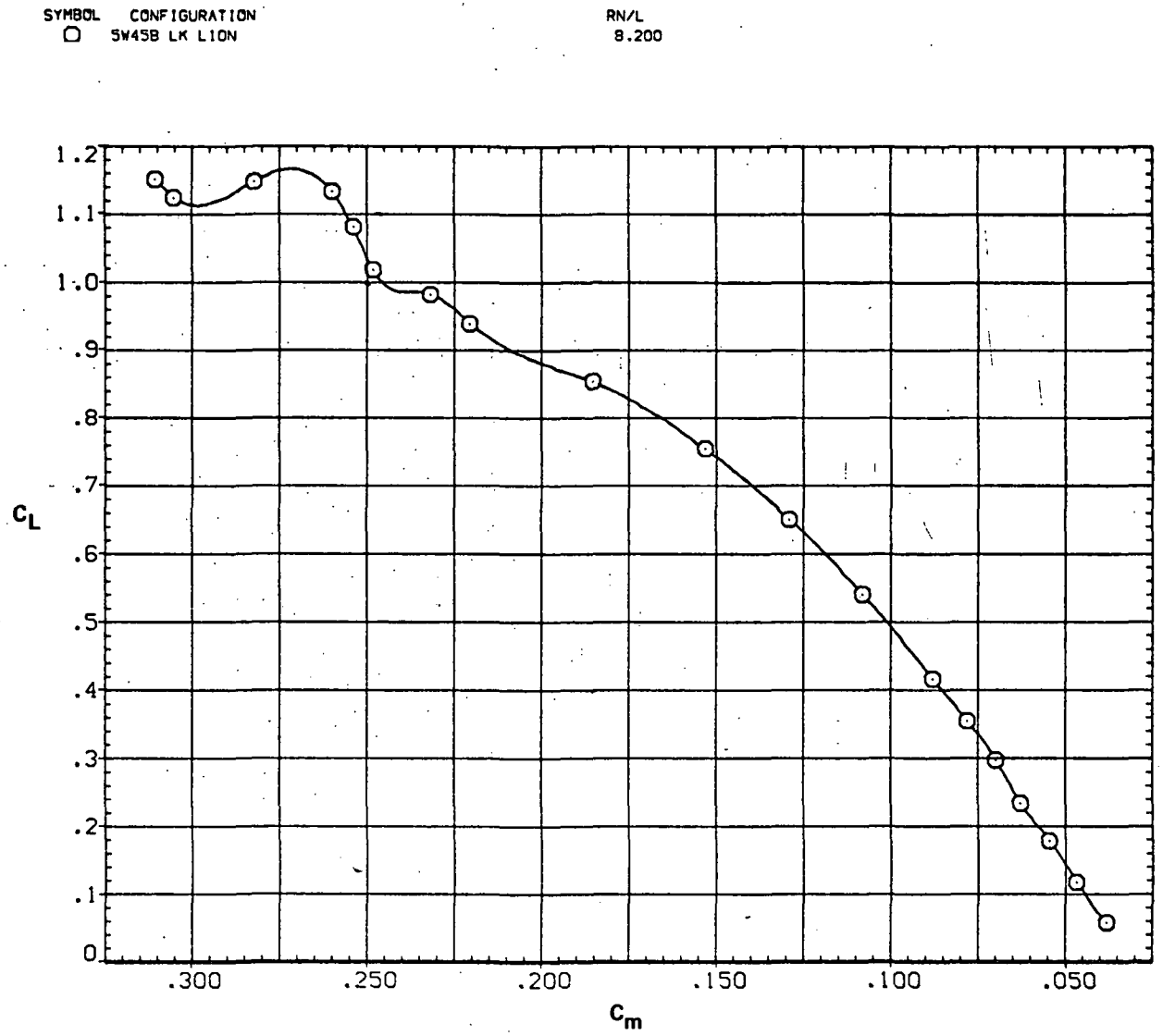

(b) C_L vs C_m

Figure 37.– Continued.

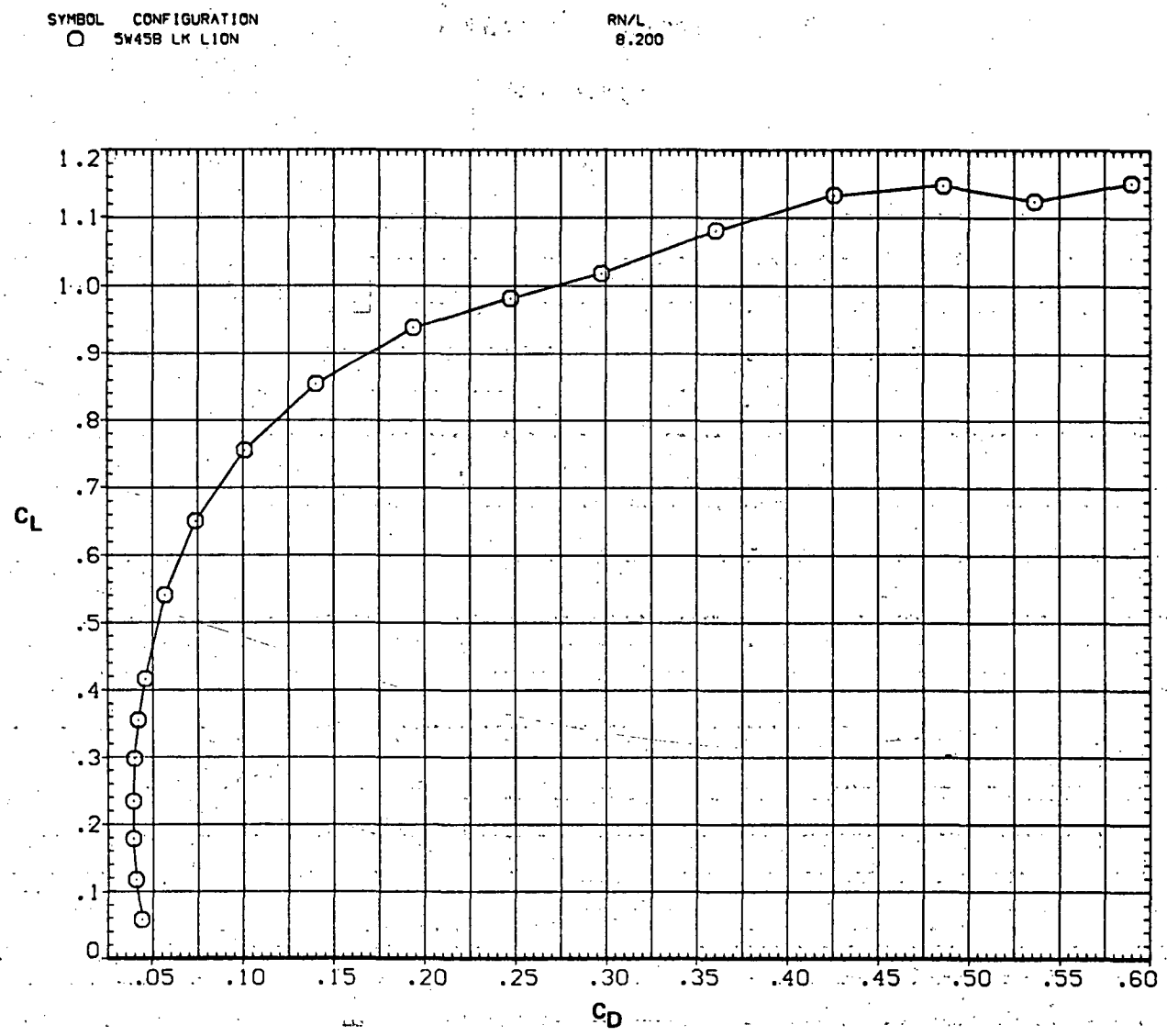

(c) C_L vs C_D

Figure 37.– Continued.

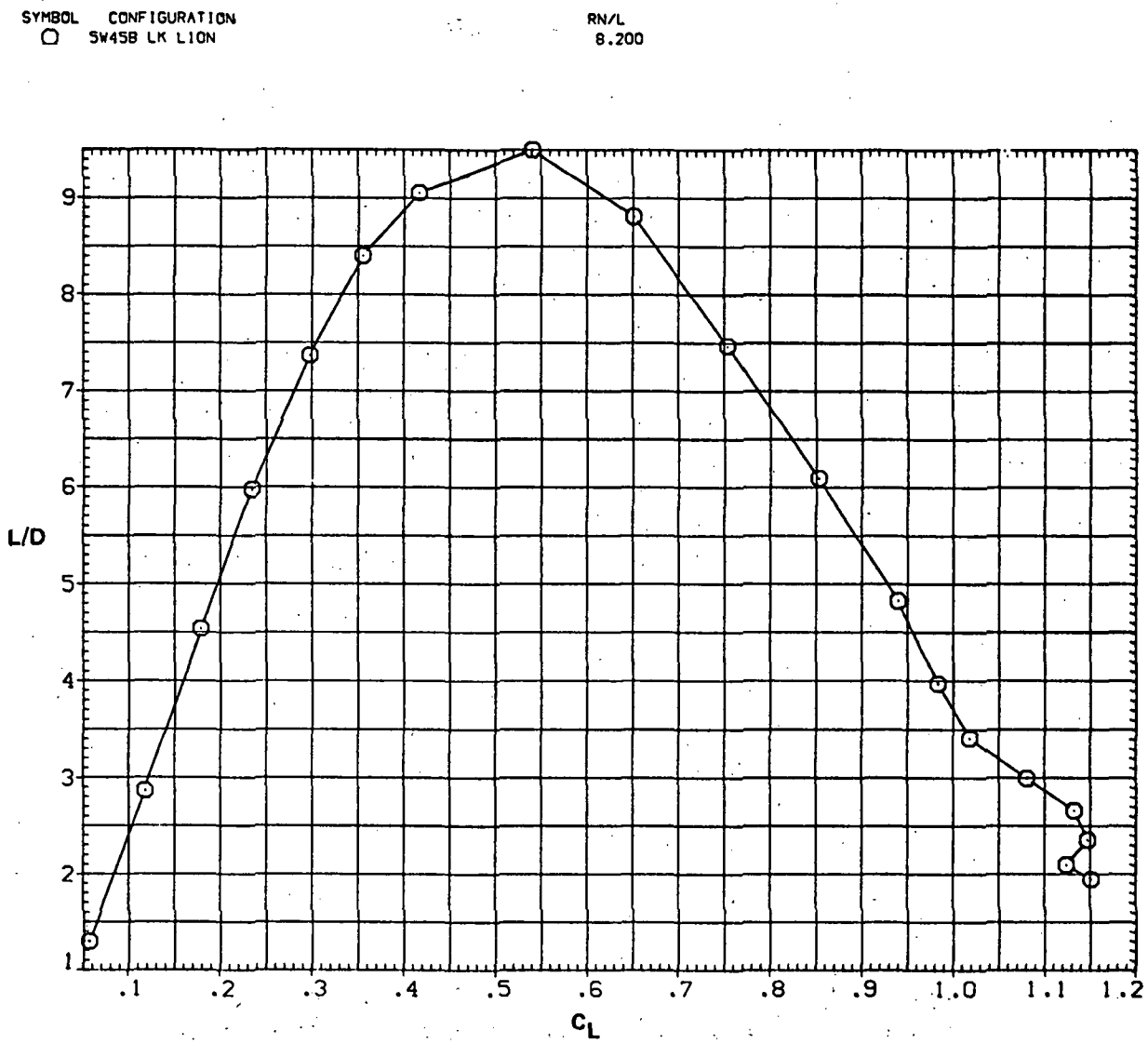

(d) L/D vs C_L

Figure 37.– Continued.

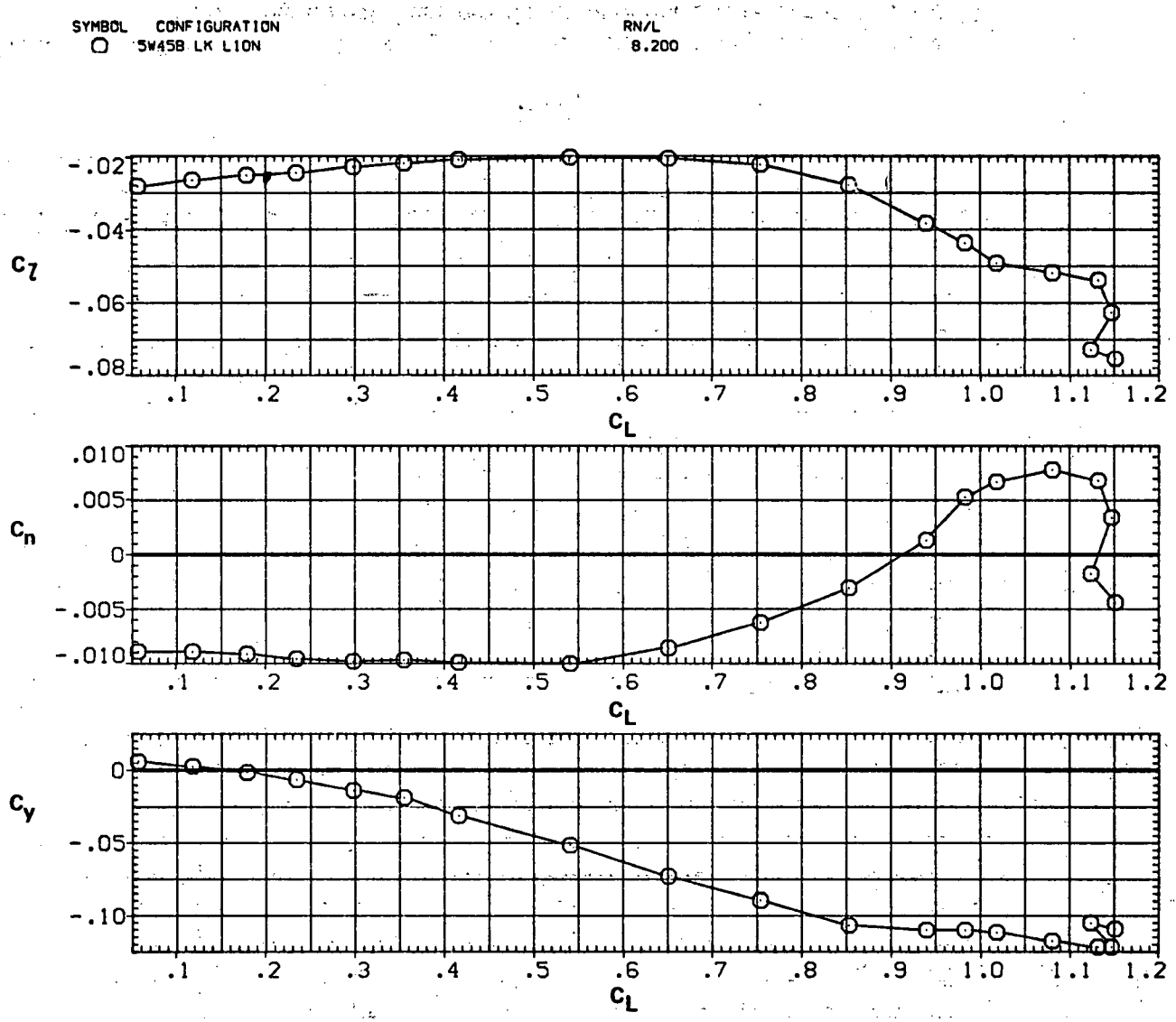

(e) C_l, C_n, and C_Y vs C_L

Figure 37.– Concluded.

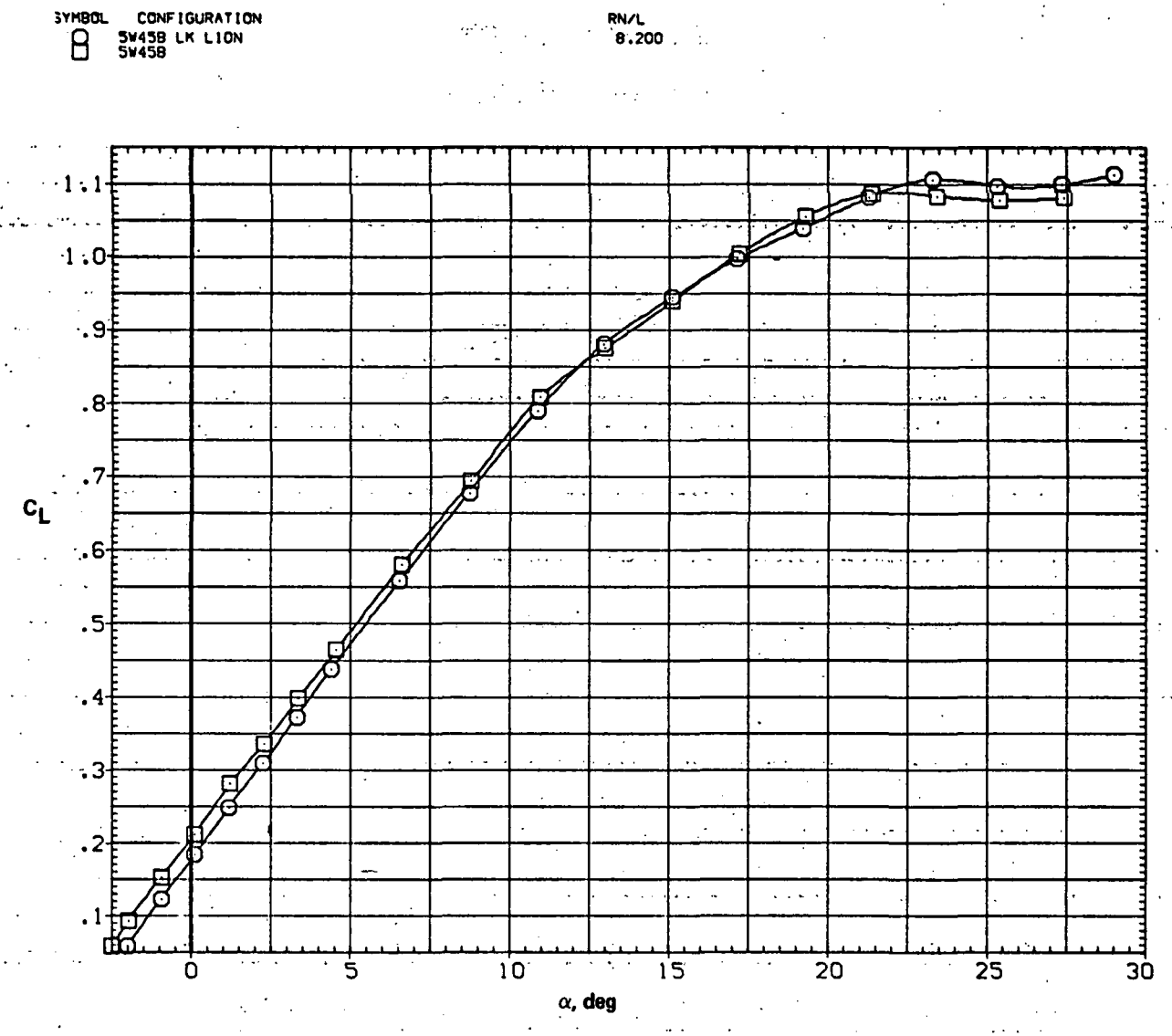

(a) C_L vs α

Figure 38.– Effect of having Krüger flaps on the downstream wing panel with a nose droop of 10° on the static longitudinal characteristics of an oblique wing: $\Lambda = 45°$, $M = 0.60$.

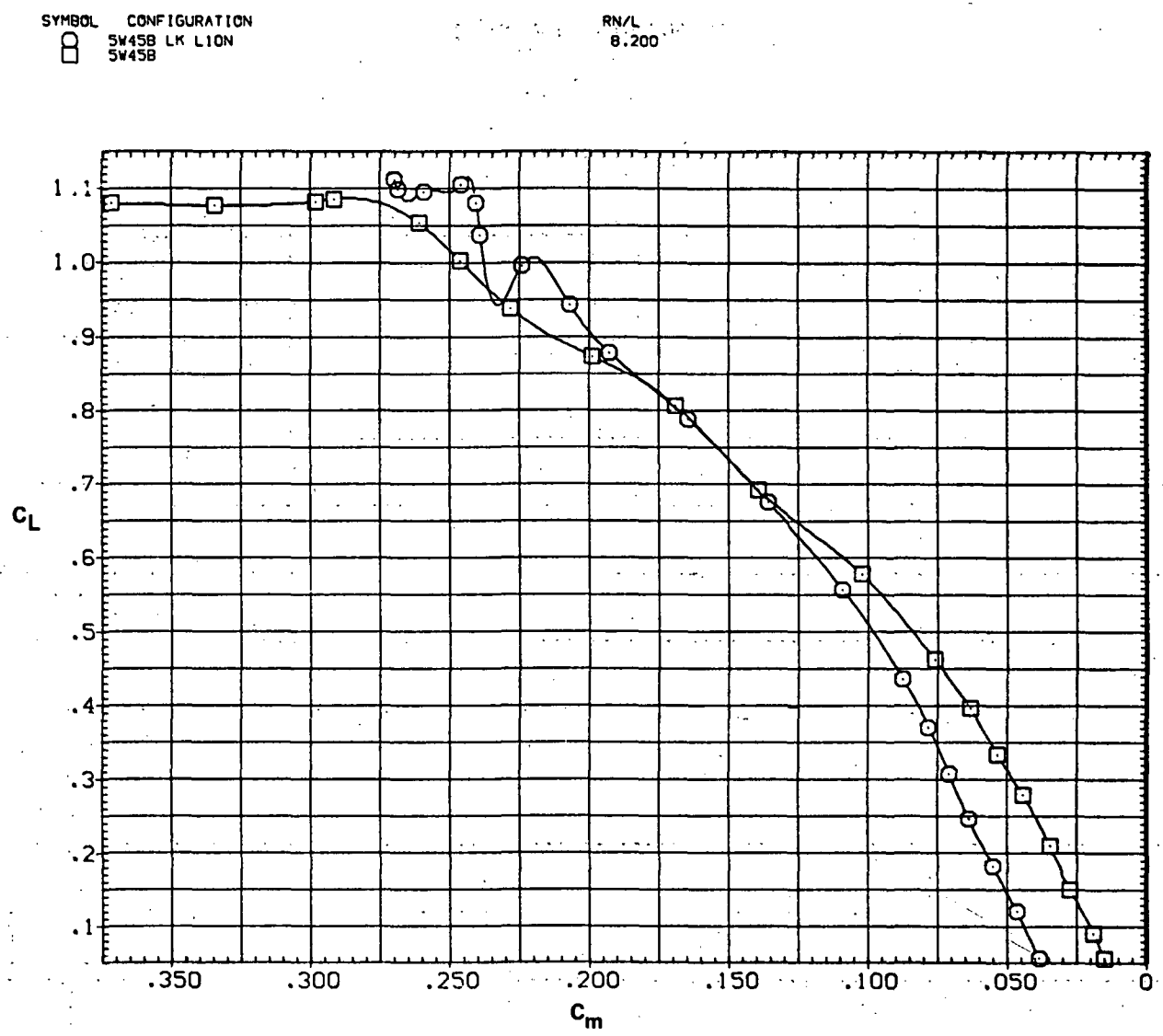

(b) C_L vs C_m .

Figure 38.– Continued.

(c) C_L vs C_D

Figure 38.– Continued.

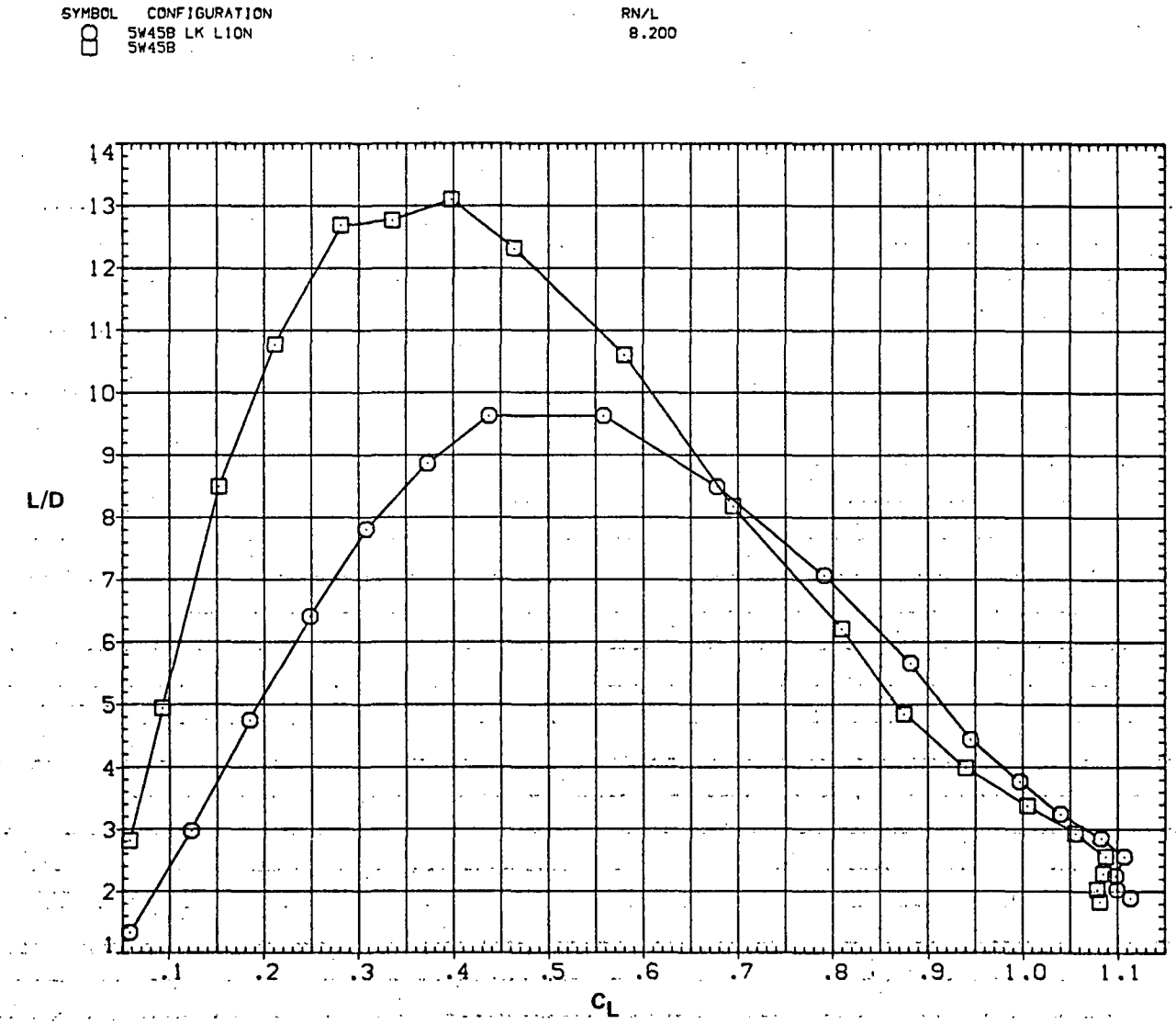

(d) L/D vs C_L

Figure 38.– Continued.

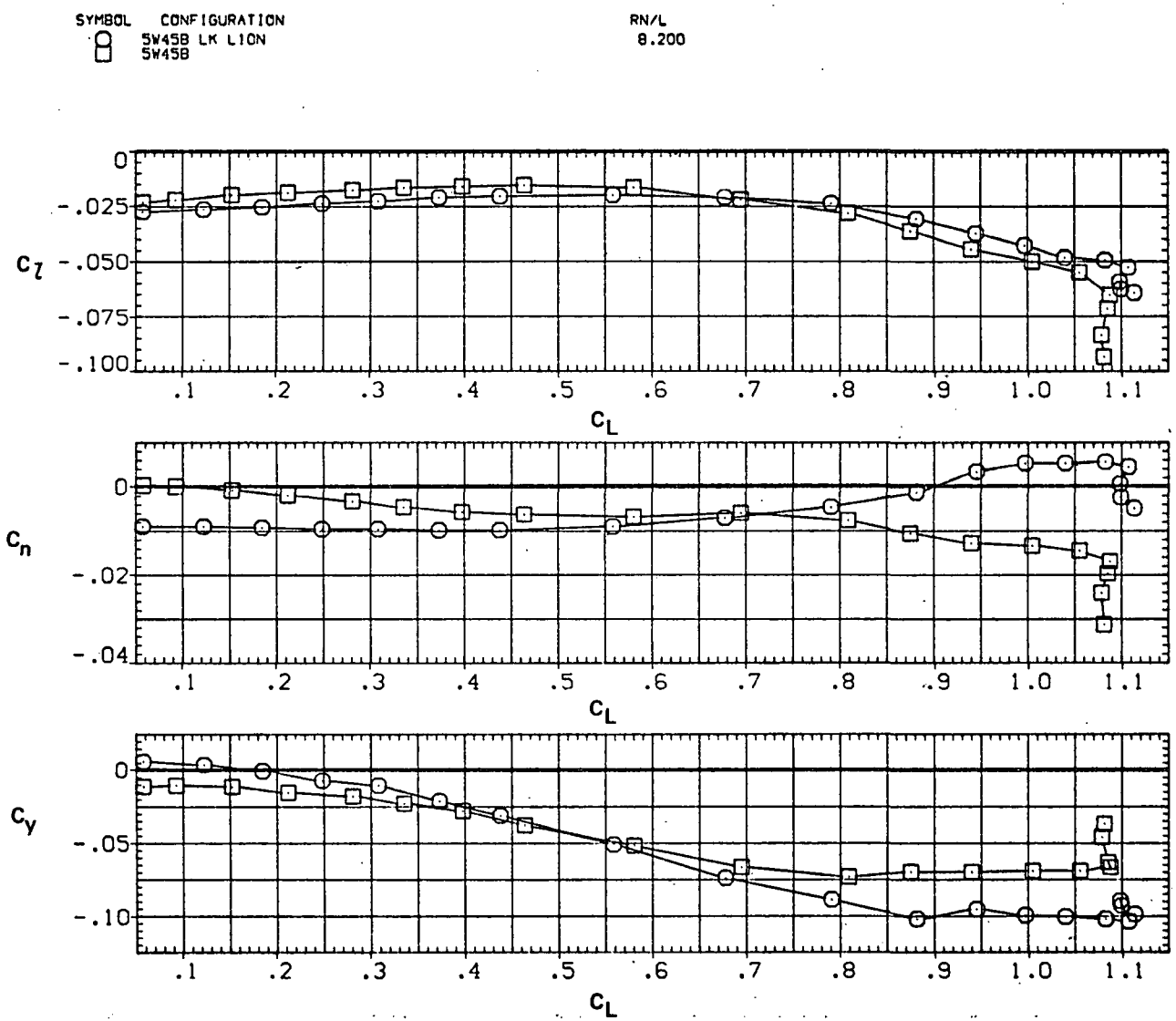

(e) C_l, C_n, and C_Y vs C_L

Figure 38.– Concluded.

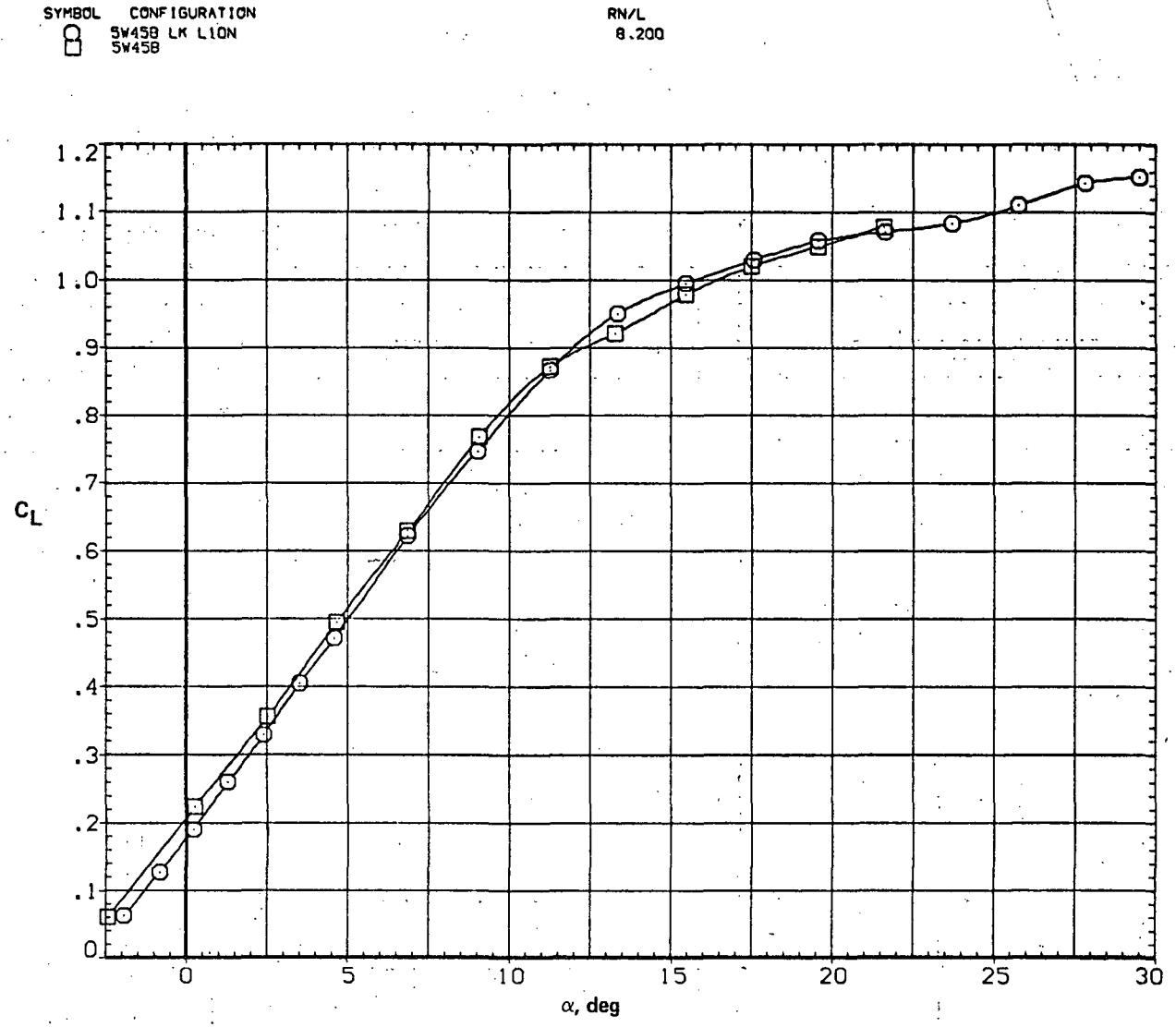

(a) C_L vs α

Figure 39.– Effect of having Krüger flaps on the downstream wing panel with a nose droop of 10° on the static longitudinal characteristics of an oblique wing: $\Lambda = 45°$, $M = 0.80$.

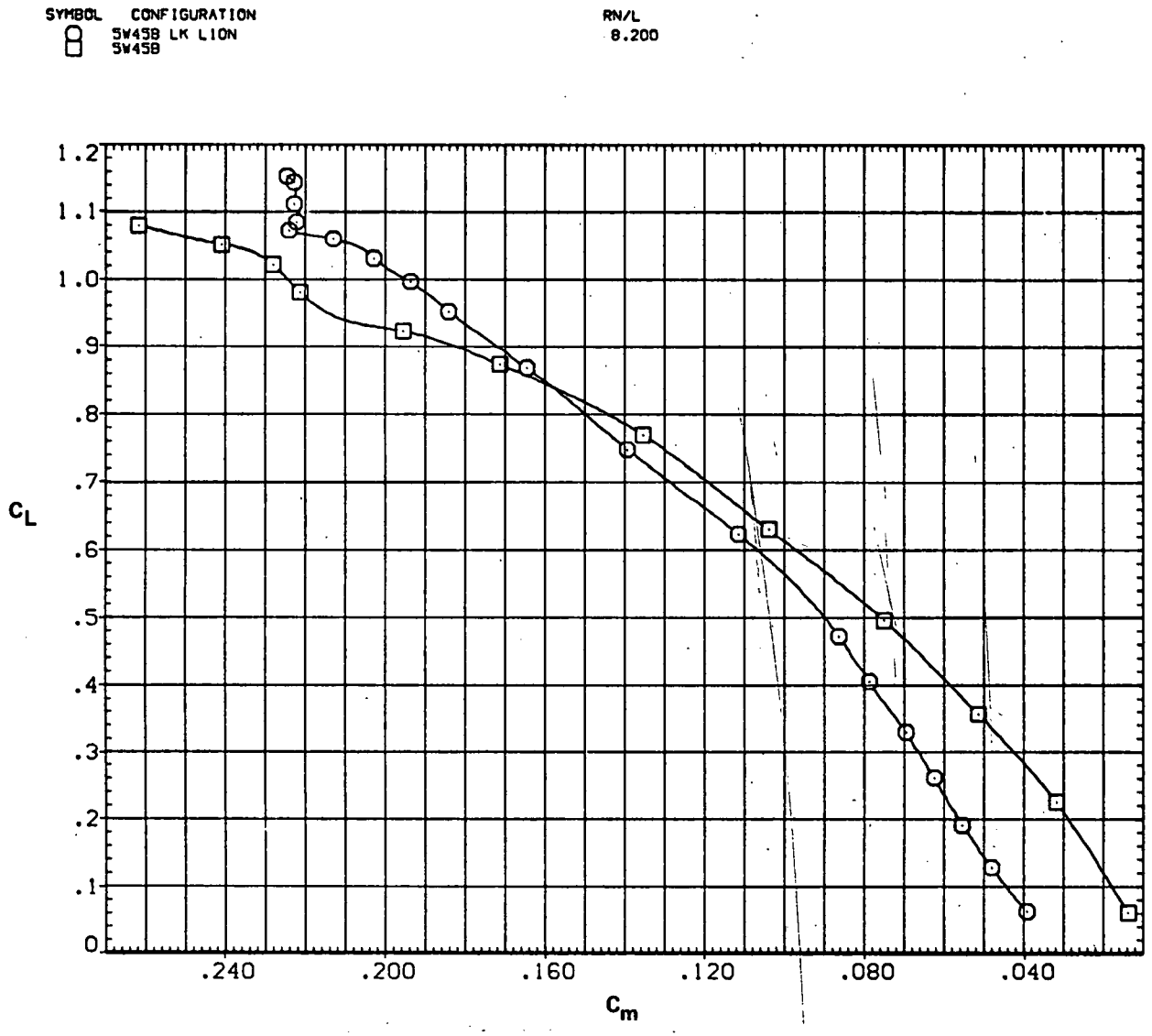

(b) C_L vs C_m

Figure 39.– Continued.

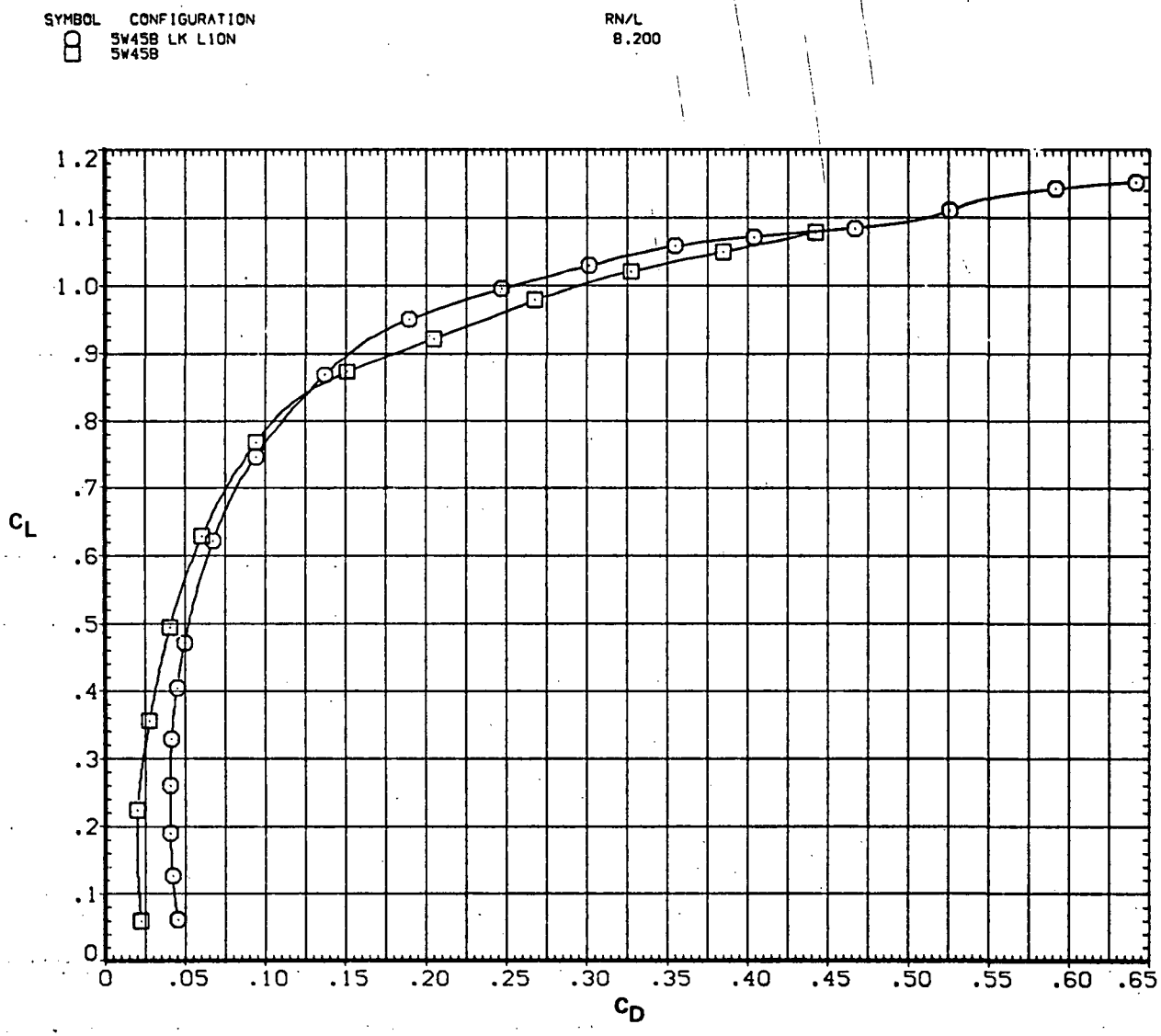

(c) C_L vs C_D

Figure 39.– Continued.

Page Intentionally Left Blank

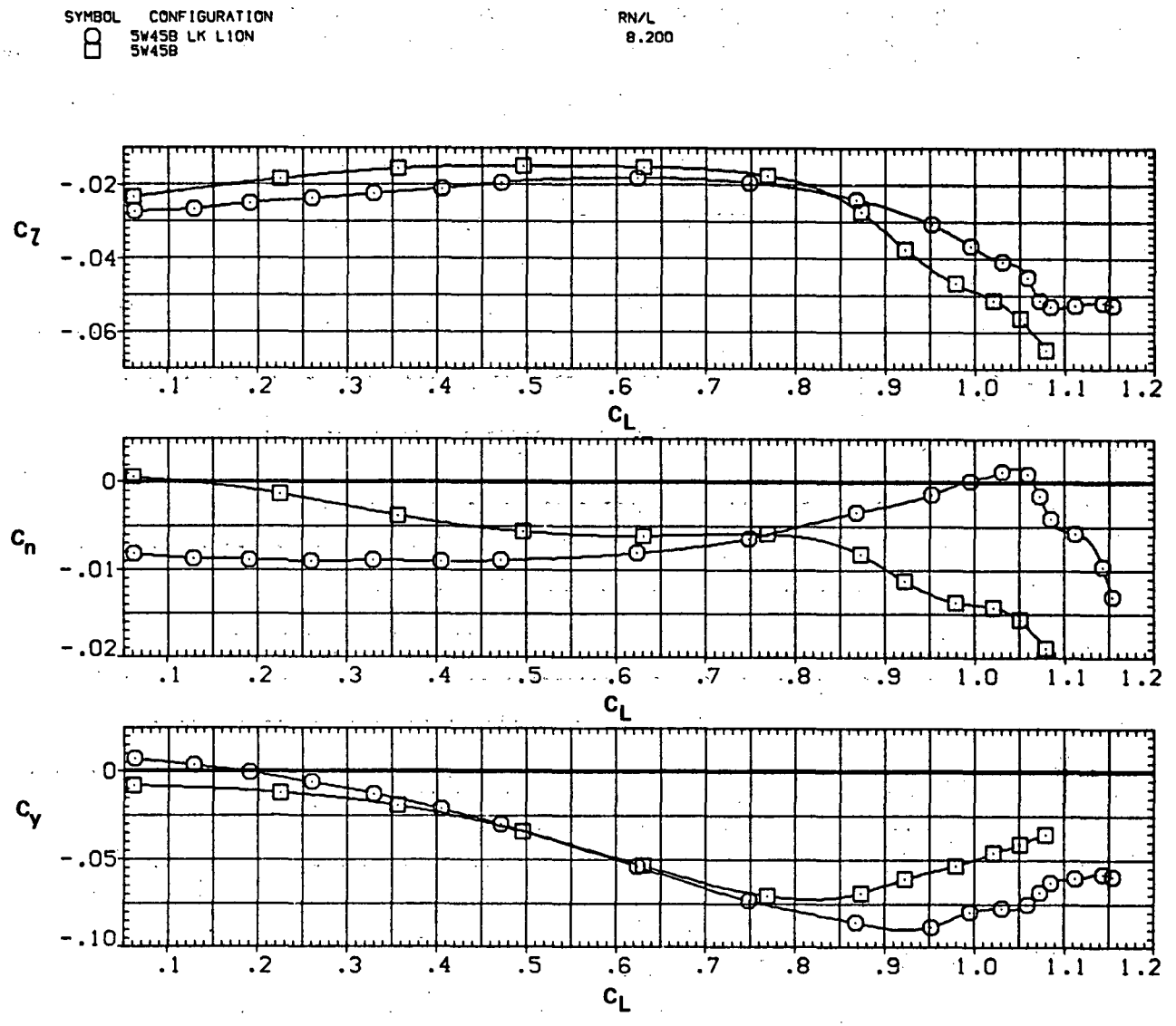

(e) C_l, C_n, and C_Y vs C_L

Figure 39.– Concluded.

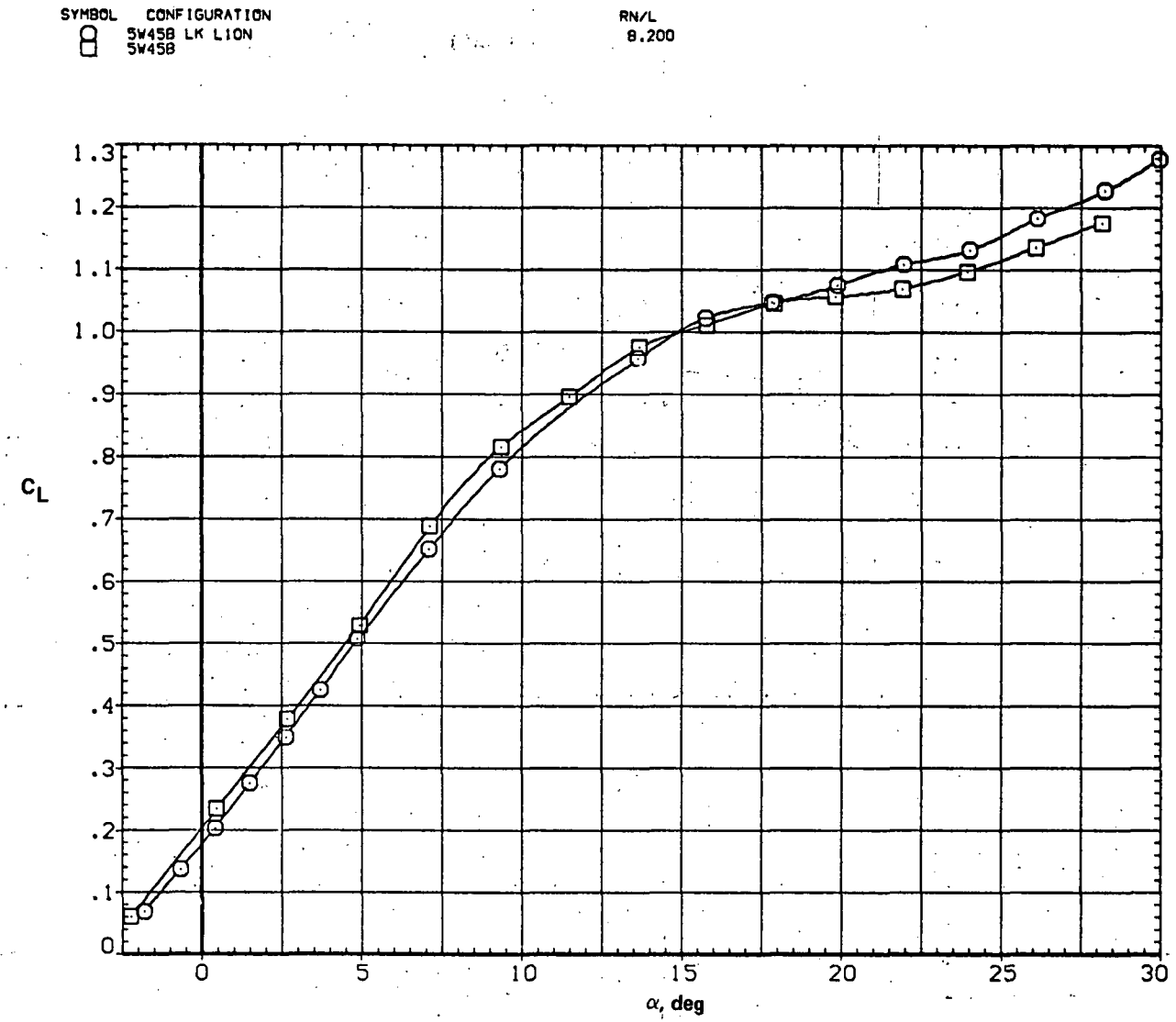

(a) C_L vs α

Figure 40.– Effect of having Krüger flaps on the downstream wing panel with a nose droop of 10° on the static longitudinal characteristics of an oblique wing: $\Lambda = 45°$, $M = 0.90$.

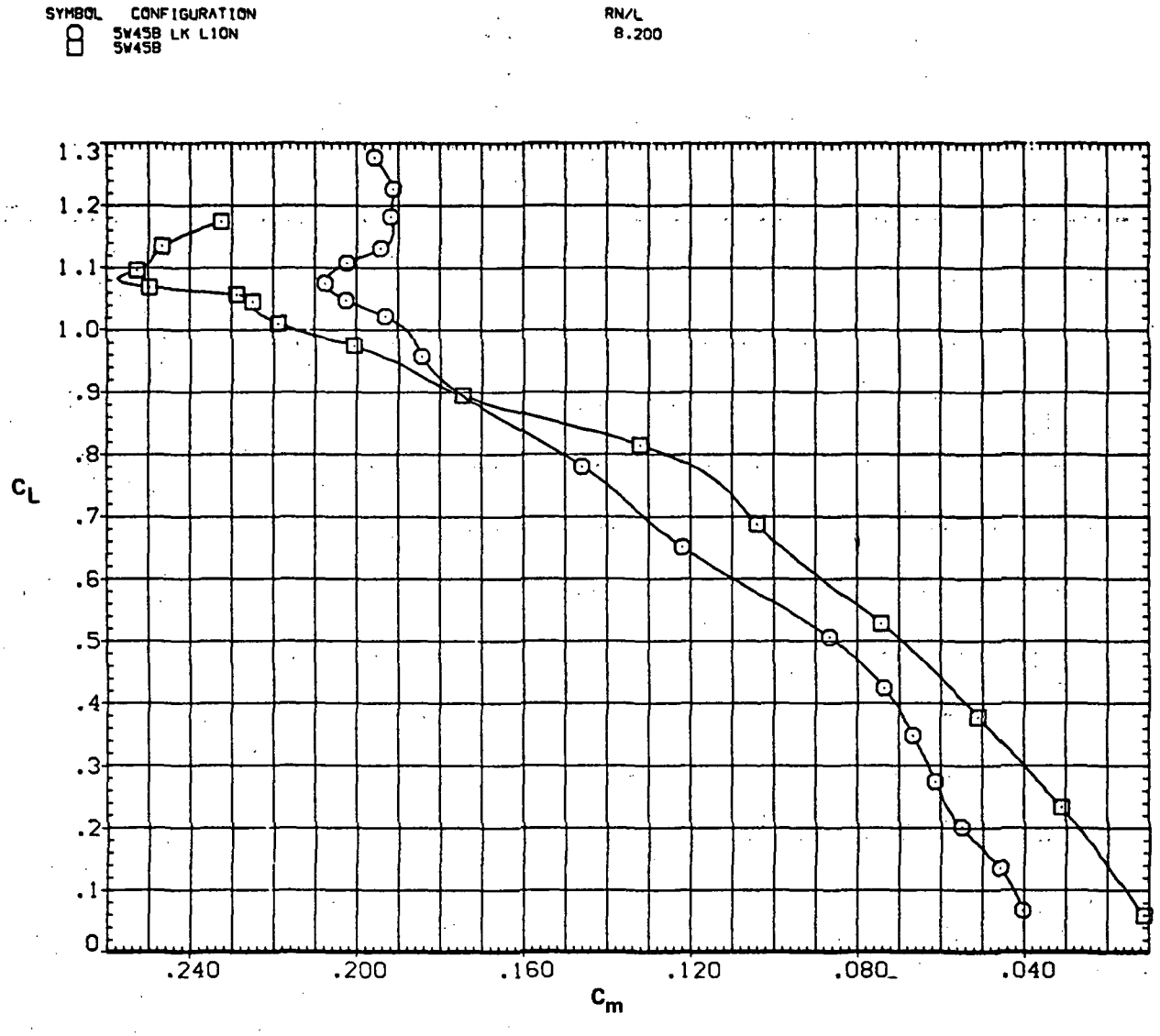

(b) C_L vs C_m

Figure 40.– Continued.

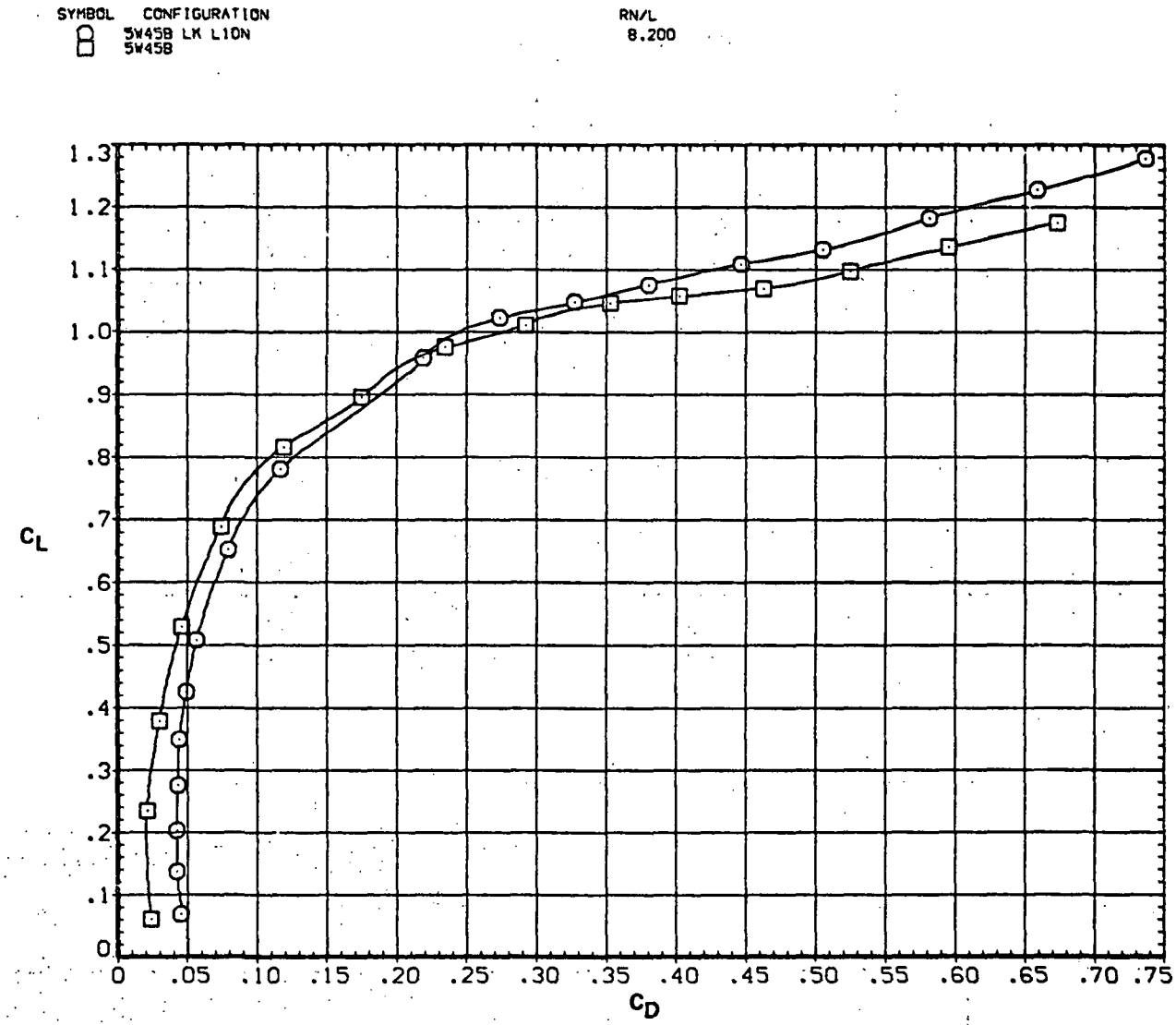

(c) C_L vs C_D

Figure 40.– Continued.

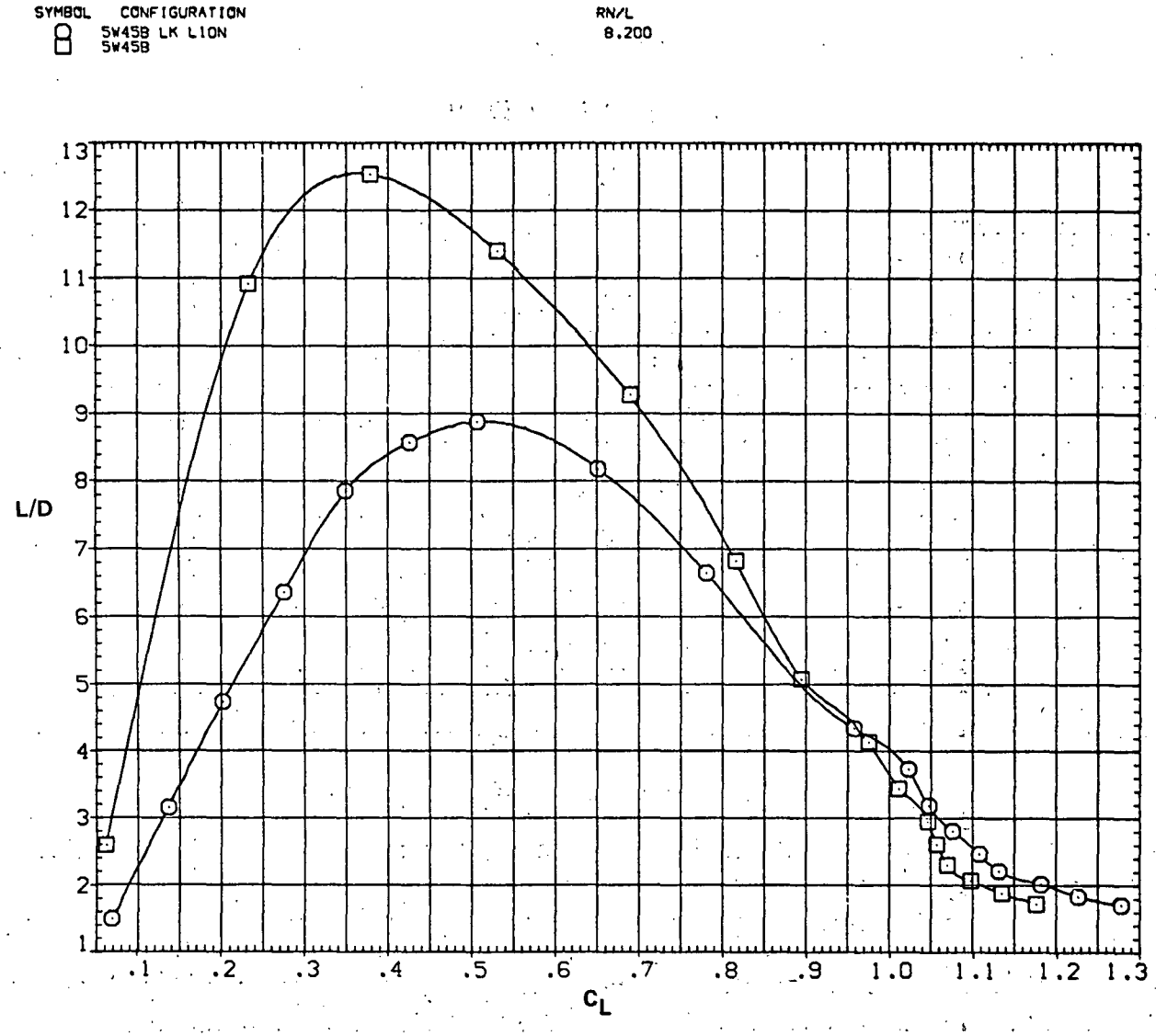

(d) L/D vs C_L

Figure 40.– Continued.

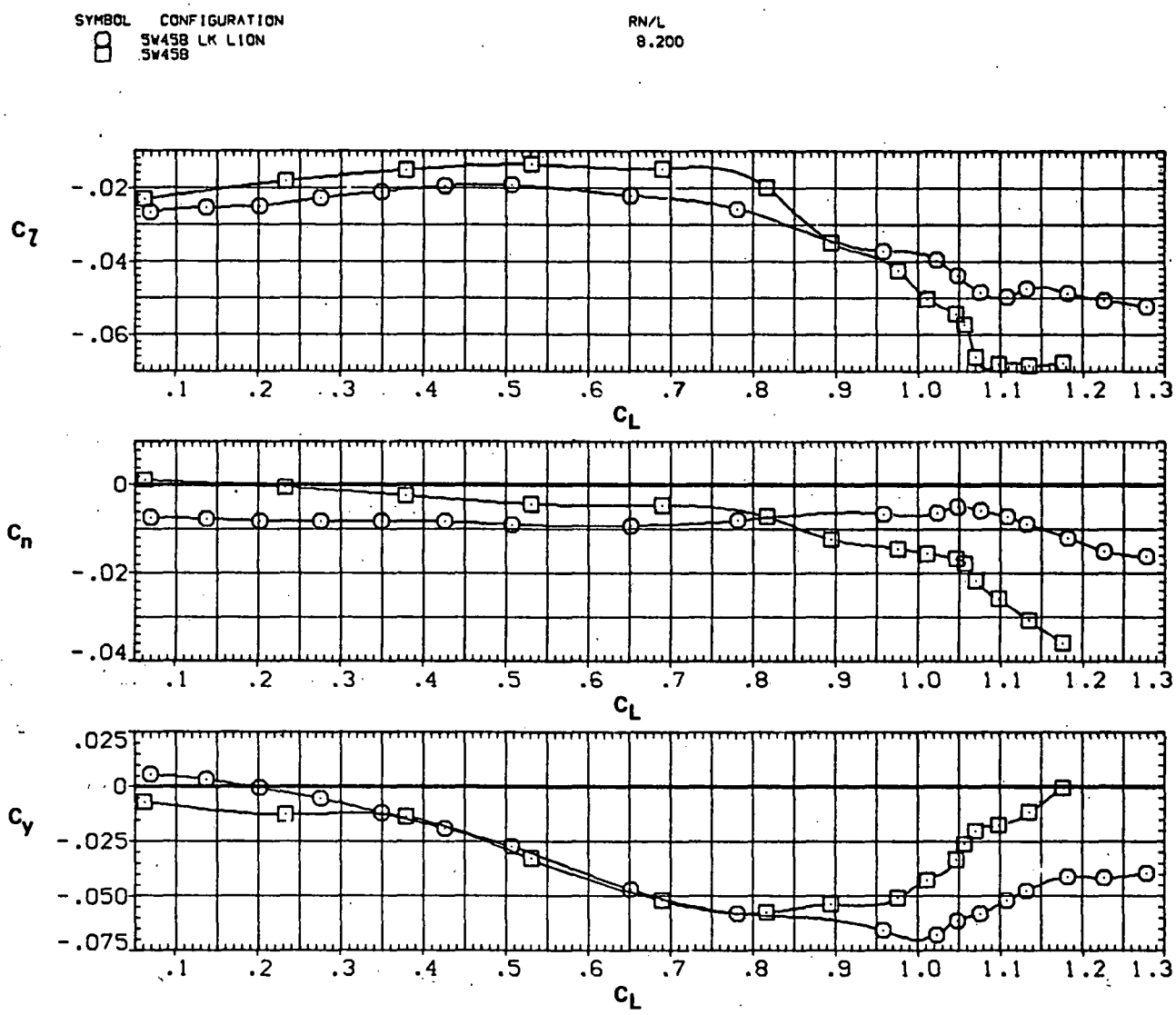

(e) C_l, C_n, and C_Y vs C_L

Figure 40.– Concluded.

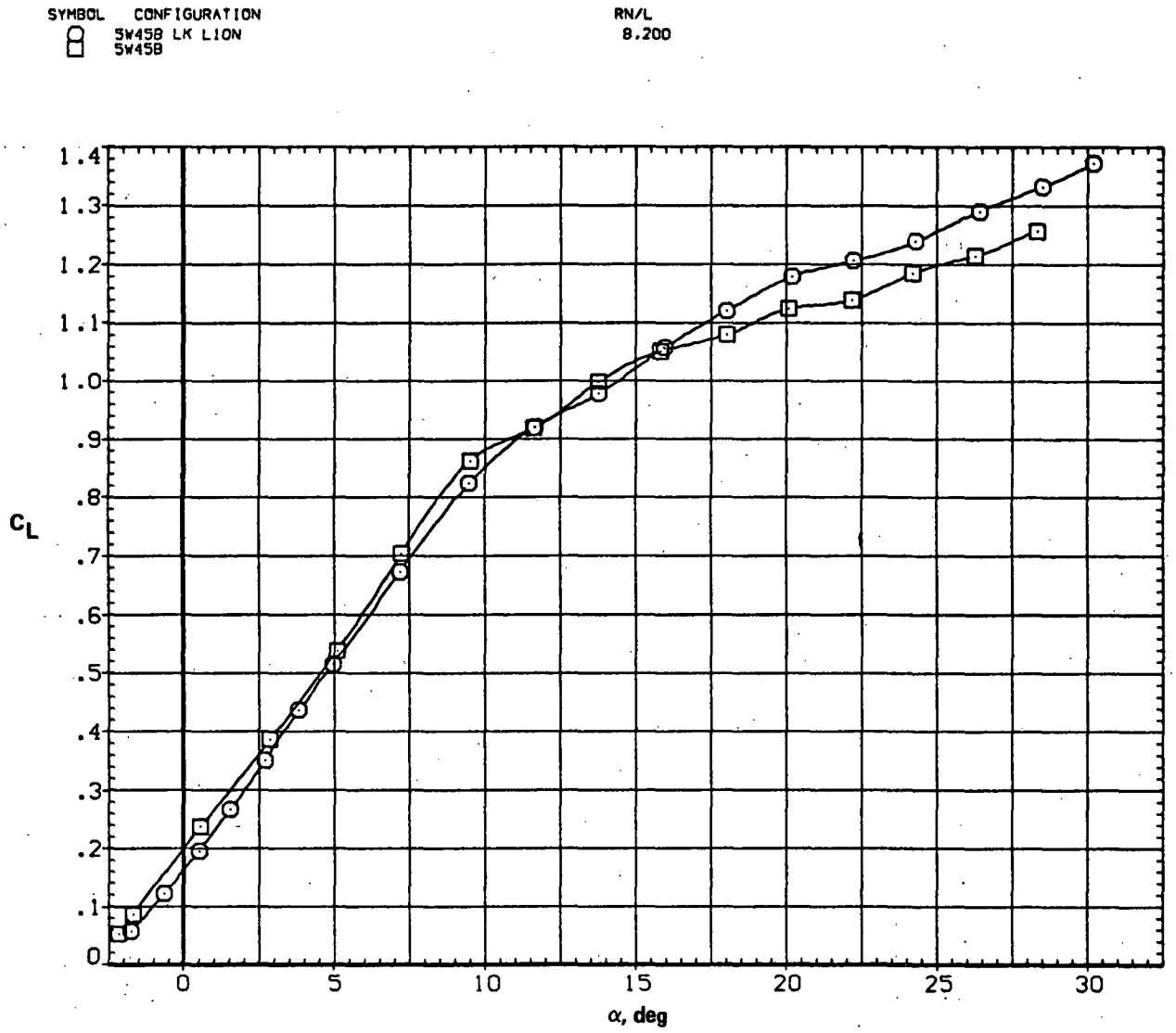

(a) C_L vs α

Figure 41.– Effect of having Krüger flaps on the downstream wing panel with a nose droop of 10° on the static longitudinal characteristics of an oblique wing: $\Lambda = 45°$, $M = 0.95$.

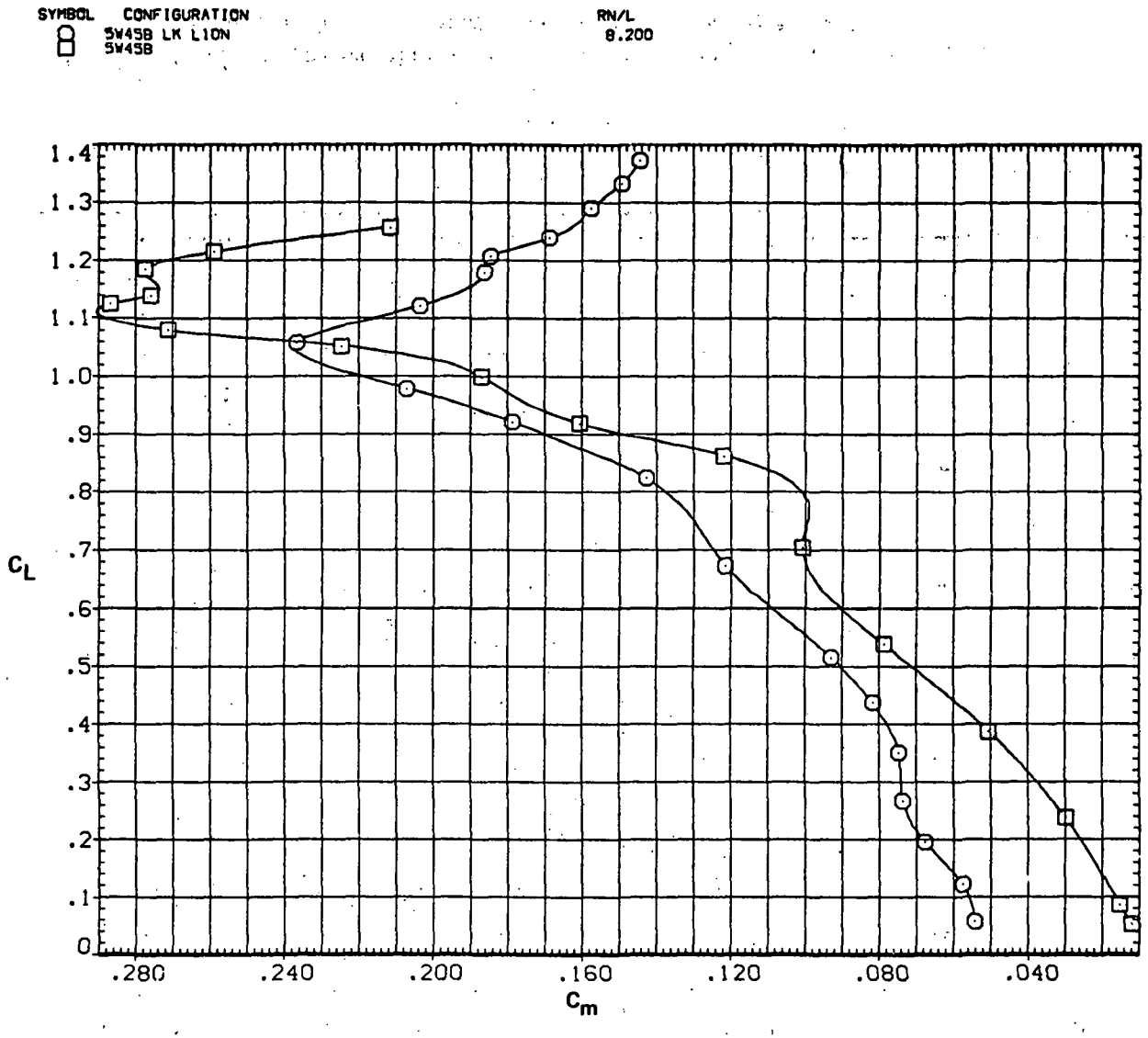

(b) C_L vs C_m

Figure 41.– Continued.

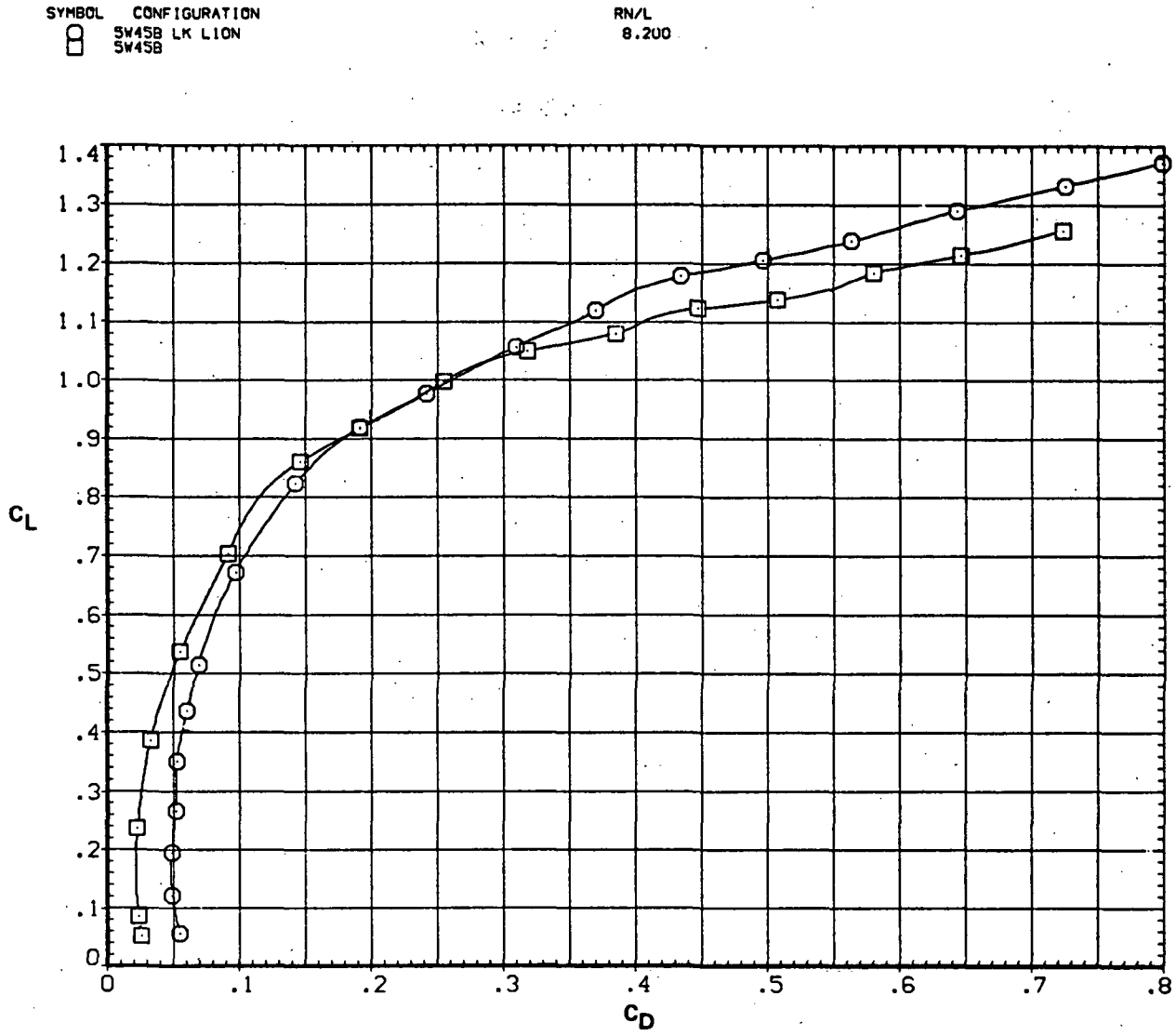

(c) C_L vs C_D

Figure 41.– Continued.

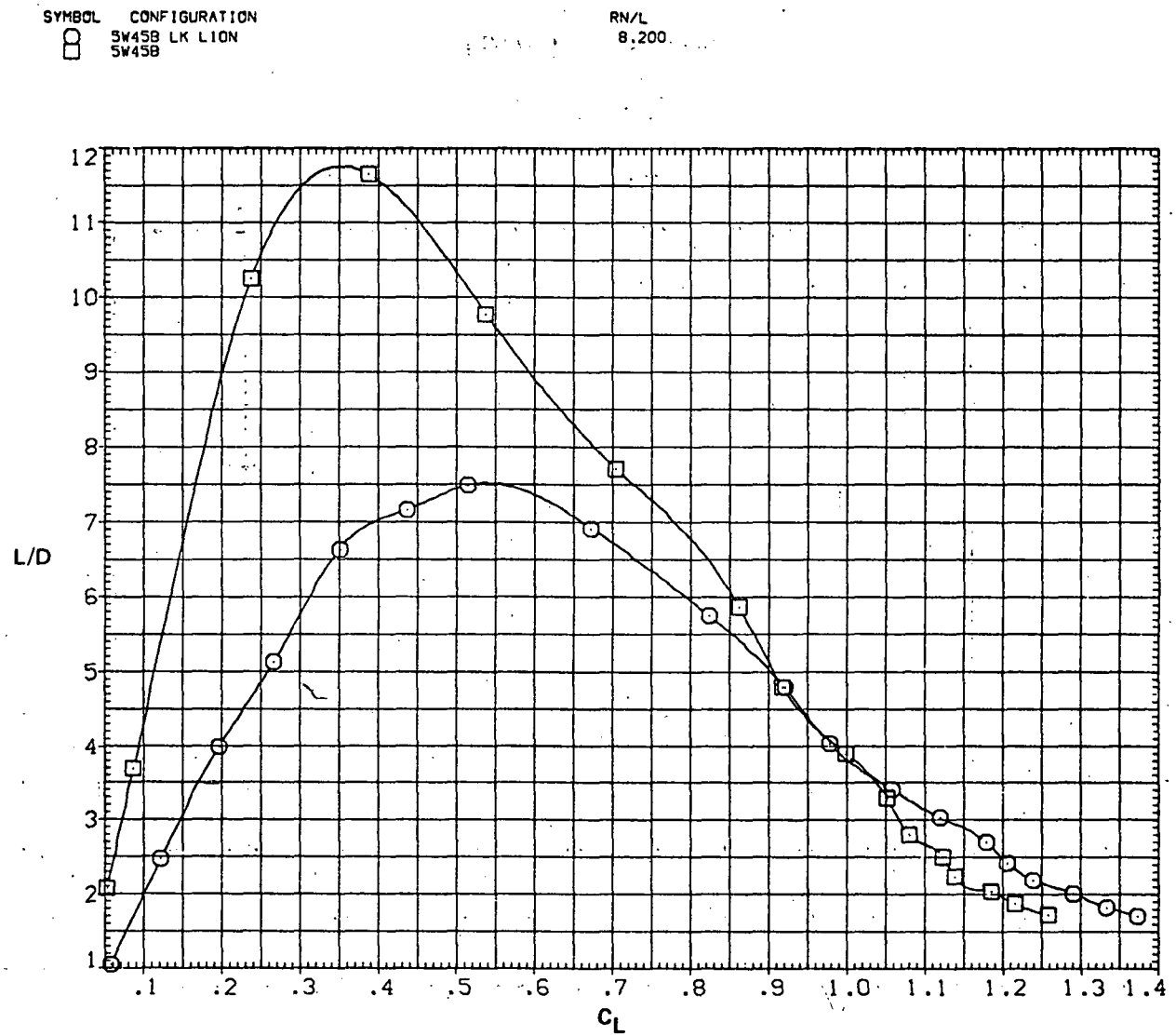

(d) L/D vs C_L

Figure 41.– Continued.

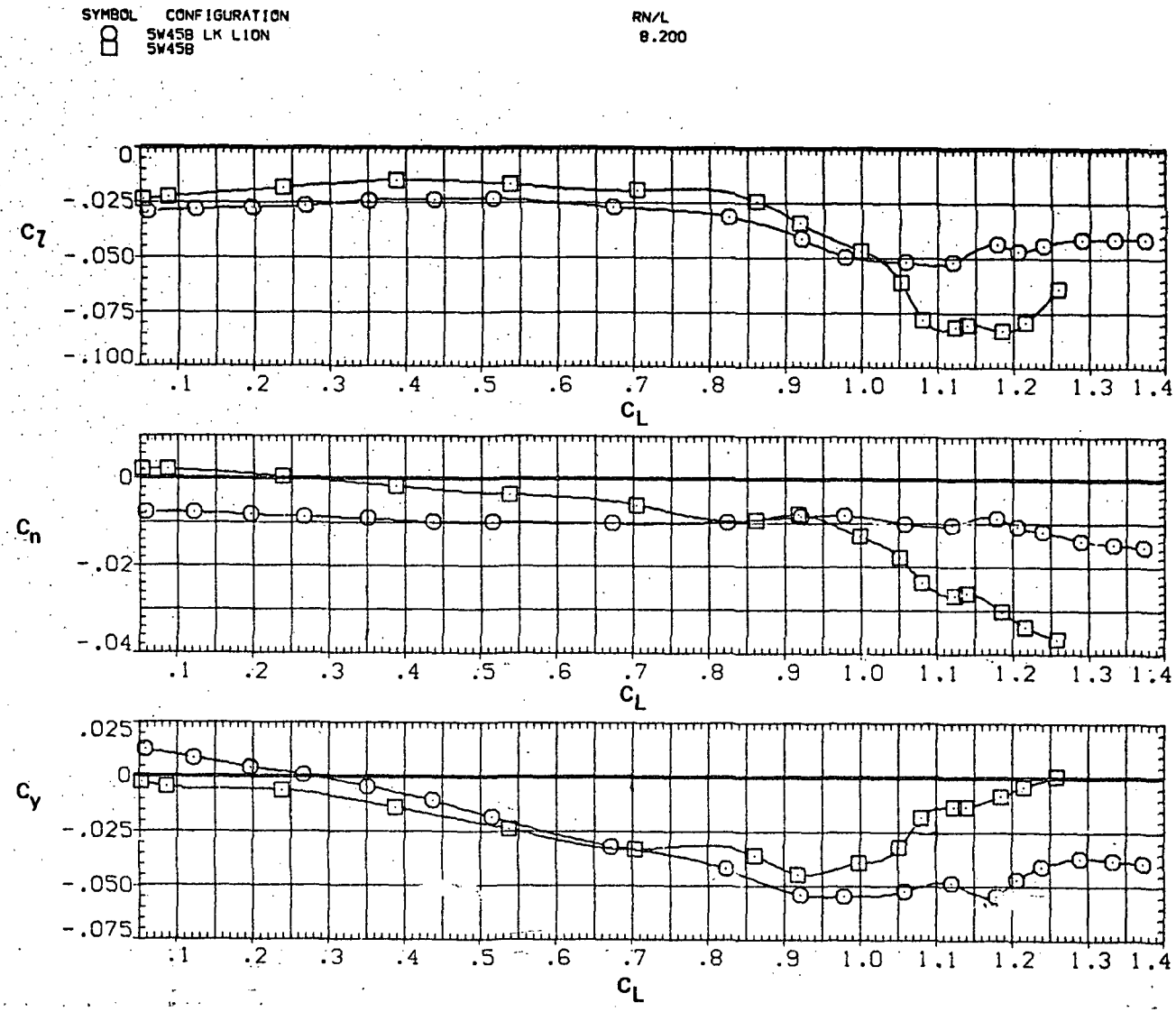

(e) C_l, C_n, and C_Y vs C_L

Figure 41.– Concluded.

NATIONAL AERONAUTICS AND SPACE ADMINISTRATION
WASHINGTON, D.C. 20546

OFFICIAL BUSINESS
PENALTY FOR PRIVATE USE $300

SPECIAL FOURTH-CLASS RATE BOOK

POSTAGE AND FEES PAID
NATIONAL AERONAUTICS AND SPACE ADMINISTRATION
451

U.S.MAIL

POSTMASTER: If Undeliverable (Section 158 Postal Manual) Do Not Return

"The aeronautical and space activities of the United States shall be conducted so as to contribute . . . to the expansion of human knowledge of phenomena in the atmosphere and space. The Administration shall provide for the widest practicable and appropriate dissemination of information concerning its activities and the results thereof."

—NATIONAL AERONAUTICS AND SPACE ACT OF 1958

NASA SCIENTIFIC AND TECHNICAL PUBLICATIONS

TECHNICAL REPORTS: Scientific and technical information considered important, complete, and a lasting contribution to existing knowledge.

TECHNICAL NOTES: Information less broad in scope but nevertheless of importance as a contribution to existing knowledge.

TECHNICAL MEMORANDUMS: Information receiving limited distribution because of preliminary data, security classification, or other reasons. Also includes conference proceedings with either limited or unlimited distribution.

CONTRACTOR REPORTS: Scientific and technical information generated under a NASA contract or grant and considered an important contribution to existing knowledge.

TECHNICAL TRANSLATIONS: Information published in a foreign language considered to merit NASA distribution in English.

SPECIAL PUBLICATIONS: Information derived from or of value to NASA activities. Publications include final reports of major projects, monographs, data compilations, handbooks, sourcebooks, and special bibliographies.

TECHNOLOGY UTILIZATION PUBLICATIONS: Information on technology used by NASA that may be of particular interest in commercial and other non-aerospace applications. Publications include Tech Briefs, Technology Utilization Reports and Technology Surveys.

Details on the availability of these publications may be obtained from:

SCIENTIFIC AND TECHNICAL INFORMATION OFFICE

NATIONAL AERONAUTICS AND SPACE ADMINISTRATION

Washington, D.C. 20546